

**Hydrogeology and Vulnerability of Karst
Systems – Examples from the Northern Alps
and the Swabian Alb**

Zur Erlangung des akademischen Grades eines
Doktors der Naturwissenschaften
an der Fakultät für Bio- und Geowissenschaften
der

Universität Karlsruhe

vorgelegte

DISSERTATION

von

Nico Goldscheider

aus Karlsruhe

Karlsruhe 2002

Tag der mündlichen Prüfung: 08. Mai 2002

Referent: Prof. Dr. H. Hötzl (Karlsruhe)

Korreferent: Prof. Dr. D. Drew (Dublin)

ABSTRACT

Groundwater from karst aquifers is among the most important drinking water resource for humanity. About one quarter of the global population is supplied by karst waters. In some alpine countries, karst water contributes 50 % to the total drinking water supply and some cities in the alpine region are almost totally dependent on karst waters. At the same time, karst aquifers are particularly vulnerable to contamination. Contaminants can easily enter the underground and are transported rapidly over large distances in the aquifer. Processes of contaminant retardation and attenuation often do not work effectively in karst systems. Therefore, karst groundwater needs special protection. A detailed knowledge of the hydrogeology of karst systems is the precondition for the development of sustainable protection schemes. Any kind of generalisation is problematic and each karst system has to be investigated individually. This is particularly important for alpine karst systems which comprise a large variety of geologic, hydrologic, climatic and topographic settings.

Within the framework of this thesis, the hydrogeology of three karst systems in the Northern Alps was investigated by means of geological and hydrogeological methods, above all tracer tests. The Hochifen-Gottesacker and the Winterstaude area are formed by relatively thin (about 100 m) karstified limestone formations which are under- and locally overlain by impervious marl. The strata are folded. Tracer tests proved that the underground drainage pattern is controlled by the stratification and, consequently, by the fold pattern: Synclines form the main flow paths, anticlines form local watersheds. Unlike that, the Alpspitze area is made of very thick (about 1000 m) limestone without interstratified impervious layers. Tracer tests proved flow paths which are largely independent of the stratification and the folds, but controlled by the base level conditions and fault tectonics.

The hydrogeological understanding of a karst system and particularly the delineation of the catchments of the karst springs is the precondition for the delineation of groundwater protection zones. However, karst areas are often very large and it is thus impossible to demand maximum protection for the entire system as the resulting land-use restrictions would not be acceptable in many cases. It is consequently essential to protect at least those areas which are especially vulnerable to contamination. This leads to the concept of groundwater vulnerability mapping which aims at a compromise between groundwater protection on the one hand and land-use on the other hand. The basics of the

concept of vulnerability mapping and a critical discussion of the existing methods is presented. Most of the methods are not applicable or lead to inconsistent results if they are applied to alpine karst systems.

Thus, a new method of groundwater vulnerability mapping with special consideration of karst aquifers was developed in co-operation with the European COST Action 620 on "vulnerability and risk mapping for the protection of carbonate (karst) aquifers". This so-called PI method classifies vulnerability on the basis of the product of two factors: The P factor indicates the protective function of the layers above the groundwater surface and the I factor (infiltration conditions) indicates the degree to which the protective cover is bypassed by lateral surface and subsurface flow which enters the aquifer at another place, e.g. via a swallow hole.

The PI method was tested and compared with other methods for the first time in the Engen area, a karst landscape in the Swabian Alb (SW Germany). Later on, the method was applied in the two alpine test sites Hochifen-Gottesacker and Winterstaude. The vulnerability map for the Winterstaude area will be used for source protection zoning for the community of Bezau.

Vulnerability maps were found to be a useful tool if the limitations of the concepts are clarified. Vulnerability maps should be made for a well defined purpose and should not be a stand-alone element but an integrated part of an overall groundwater protection scheme.

KURZFASSUNG

Grundwasser aus Karstgebieten gehört zu den wichtigsten Trinkwasserressourcen der Menschheit. Etwa ein Viertel der Weltbevölkerung wird mit Karstwasser versorgt. In einigen Alpenländern beträgt sein Anteil an der Trinkwasserversorgung etwa 50 % und manche Großstädte im Alpenraum hängen fast vollständig davon ab. Gleichzeitig sind Karstgrundwasserleiter besonders verletzlich gegenüber dem Eintrag von Schadstoffen. Diese können meist leicht in der Untergrund eindringen und sich dort rasch über weite Entfernungen ausbreiten, ohne dabei nennenswert zurückgehalten oder abgebaut zu werden. Karstgrundwasser benötigt daher einen besonderen Schutz. Die Voraussetzung für die Entwicklung von Konzepten zum nachhaltigen Grundwasserschutz ist die detaillierte Kenntnis der hydrogeologischen Verhältnisse. Dabei muss jedes Karstgebiet individuell untersucht werden; eine Verallgemeinerung ist problematisch. Dies gilt insbesondere für alpine Karstgebiete, die sich durch eine großartige geologische, hydrologische, klimatische und topographische Vielfalt auszeichnen.

Im Rahmen dieser Arbeit wurde die Hydrogeologie von drei gefalteten Karstsystemen in den nördlichen Alpen untersucht. Dabei kamen neben geologischen und hydrochemischen Methoden vor allem Markierungsversuche zum Einsatz. Die Karstgebiete *Hochifen-Gottesacker* und *Winterstauden* werden von einer bzw. zwei relativ gering mächtigen (etwa 100 m) Kalksteinformationen aufgebaut, die von stauenden Mergeln unter- und lokal auch überlagert werden. Hier konnte nachgewiesen werden, dass der unterirdische Abfluss von der Schichtung kontrolliert wird und daher den Faltenbau nachzeichnet: Synklinalen bilden die bevorzugten Fließwege, während Antiklinalen als lokale Wasserscheiden wirken. Im Gegensatz dazu besteht das Gebiet der *Alpspitze* aus einer sehr mächtigen (etwa 1000 m) Kalksteinformation ohne nennenswerte stauende Zwischenlagen. Hier wurde eine unterirdische Entwässerung unabhängig von der Schichtung und quer zum Faltenbau belegt, die hauptsächlich vom Störungsmuster und den Vorflutverhältnissen kontrolliert wird.

Das hydrogeologische Verständnis von Karstsystemen ist die Grundlage für die Ausweisung von Grundwasserschutzzonen. Karstgebiete, und auch die Einzugsgebiete einzelner Karstquellen, sind aber häufig sehr groß und es ist daher oft nicht möglich, einen optimalen Schutz für das gesamte Karstgebiet durchzusetzen, da die daraus resultierenden Landnutzungseinschränkungen meist nicht akzeptabel wären. Daher ist es notwendig, zumindest diejenigen Flächen zu schützen, die beson-

ders verletzlich (vulnerabel) gegenüber Schadstoffeinträgen sind. Dies führt zum Konzept der Vulnerabilitätskartierung, das auf einen Kompromiss zwischen Landnutzung und Grundwasserschutz abzielt. Die Grundlagen dieses Konzepts werden ausführlich erläutert und die bestehenden Methoden diskutiert. Die meisten existierenden Methoden eignen sich nicht oder nur eingeschränkt für die Anwendung im Karst.

Daher wurde in enger Zusammenarbeit mit einer europäischen Arbeitsgruppe (COST Action 620) eine neue Methode zur Vulnerabilitätskartierung entwickelt, die auch den speziellen Eigenschaften von Karstgebieten Rechnung trägt. Diese sogenannte PI-Methode berücksichtigt zwei Faktoren: Der P-Faktor (protective cover) beschreibt die Schutzfunktion der Grundwasserüberdeckung; der I-Faktor (infiltration conditions) beschreibt die Umgehung dieser Schutzfunktion durch oberflächliche Abflusskomponenten, die an anderer Stelle das Grundwasser erreichen können, beispielsweise über eine Bachschwinde.

Die PI-Methode wurde zunächst in einem Karstgebiet bei Engen in der Schwäbischen Alb getestet und mit anderen Methoden verglichen. Später wurde die Methode auch in den alpinen Karstgebieten *Hochifen-Gottesacker* und *Winterstaude* angewandt.

Vulnerabilitätskarten können Hilfsmittel zum Grundwasserschutz und zur Landnutzungsplanung sein, allerdings nur, wenn ihre Grenzen klar erkannt werden. Vulnerabilitätskarten sollten immer für einen genau definierten Zweck angefertigt werden und kein isoliertes Element, sondern integraler Bestandteil eines umfassenden Konzepts sein.

ACKNOWLEDGEMENTS

This thesis was prepared at the Department of Applied Geology at the University of Karlsruhe and supervised by Prof. Dr. H. Hötzl. First of all I want to thank him for imparting his knowledge of hydrogeology to me and for supporting me in completing this thesis with many fruitful discussions and valuable suggestions. I'm grateful also to Dr. David Drew (Trinity College Dublin) for inspiring discussions and for his good humour while correcting this thesis.

Many thanks to all my colleagues in the COST Action 620 for stimulating discussions. A special thanks to Dr. Donal Daly (Geological Survey of Ireland), Simon Neale (Environment Agency Wales) and Prof. Dr. François Zwahlen (Centre d'Hydrogéologie de Neuchâtel) for providing inspiration, and to Dr. Michael von Hoyer and Dr. Bernt Söfner (BGR Hannover) for their constructive co-operation during the *Engen* project.

I want to thank all my diploma students for the good work: Christian Tomsu, Michael Sinreich, Johanna Huth, Martin Brosemer, Nicole Umlauf, Wiebke Preußner, Kerstin Kottke, Markus Klute, Sebastian Sturm, Karina Kunoth, Maja Strathoff, Christoph Neukum, Heike Werz, Fridjof Schmidt and Nadine Göppert. With their work, they contributed considerably to this thesis and to some of my other projects and publications.

I'm grateful to the people who supported me during my extensive field work in the Alps. Tiburt Fritz and his family, Karl Keßler (Kleinwalsertal) and Fritz Rüt (Bezau) shall be acknowledged here as representatives for many others whom I can't mention here.

I want to thank all my colleagues at the University of Karlsruhe for the good and pleasant working environment during the last few years. Thanks also to all the students and friends who helped me with sampling during tracer tests.

Many thanks to the following institutions for funding parts of my work and/or travels:

- Federal Institute for Geosciences and Natural Resources (BGR), Hannover
- European Union (COST Action 620)
- Vorarlberger Naturschau, Dornbirn
- Community of Bezau

- Landeswasserbauamt Bregenz
- Raiffeisen Holding Kleinwalsertal

Many thanks to various institutions or people who supported me with practical help, suggestions, information and fruitful discussions.

Many thanks to my parents Erika and Michael Goldscheider and to my girlfriend Nadine for her essential support and understanding.

CONTENTS

Abstract	III
Kurzfassung	V
Acknowledgements	VII
Contents	IX
List of Figures	XV
List of Tables	XXI
1 Introduction	1
1.1 The significance of karst groundwater	1
1.2 Karst in the Alps	3
1.3 The purpose and structure of this thesis	4
1.4 Overview of the research and co-operation	5
2 Overview of the geology of the Alps and alpine karst systems	7
2.1 The Alps within the framework of plate tectonics	7
2.2 The tectonic-stratigraphic evolution of the Alps	8
2.2.1 Overview	8
2.2.2 The South and East Alpine facies zone	9
2.2.3 The Penninic facies zone	10
2.2.4 The Helvetic and Ultrahelvetic facies zone	11
2.2.5 The synorogenic Flysch	11
2.2.6 The late- to post-orogenic Molasse	12
2.3 Definition of alpine karst	12
2.4 Classification of alpine karst systems and distribution of karst in the Alps	13
2.4.1 Pyrenean and Canadian type of alpine karst	13
2.4.2 Plateau-like and folded alpine karst systems	13
2.4.3 The East Alpine zone	15
2.4.4 The South Alpine zone	15
2.4.5 The Penninic zone	16
2.4.6 The Helvetic zone	16
2.4.7 The Molasse zone	17
2.4.8 Overview of the three alpine test sites	17
3 Example: Hochifen-Gottesacker	18
3.1 Location, topography, climate	18
3.2 Geology	19
3.2.1 Geological framework	19
3.2.2 Stratigraphy of the Hochifen-Gottesacker area	22
3.2.2.1 Overview	22
3.2.2.2 The Cretaceous of the Helvetic Säntis nappe	22

3.2.2.3	The Ultrahelvetic and Penninic Flysch nappes	25
3.2.2.4	Quaternary deposits and rockfalls	25
3.2.3	Tectonics	26
3.2.3.1	Folds	26
3.2.3.2	Fault tectonics.....	30
3.3	Hydrogeology	31
3.3.1	Hydrogeological function of the strata	31
3.3.2	Surface and subsurface karst landforms	32
3.3.3	Hydrogeological zoning.....	34
3.4	Springs and surface waters	34
3.4.1	Overview	34
3.4.2	Eastern Hochifen-Gottesacker area	35
3.4.3	Western Hochifen-Gottesacker area	42
3.5	Hydrochemistry	45
3.5.1	Hydrochemistry and temperature as natural tracers.....	45
3.5.2	Overview on the hydrochemical analyses and results ...	45
3.5.3	Eastern Hochifen-Gottesacker area	46
3.5.4	Western Hochifen-Gottesacker area	47
3.6	Tracer tests	49
3.6.1	Earlier tracer tests.....	49
3.6.2	Overview of current tracer tests.....	49
3.6.3	Selection of the injection points and injection	50
3.6.4	Sampling.....	53
3.7	Results	53
3.7.1	Introductory remark.....	53
3.7.2	Lake Torsee and Kessleralp spring (IP11–12)	54
3.7.3	Eastern Hochifen-Gottesacker area (IP1–10)	55
3.7.4	Rockfall mass (IP8)	58
3.7.5	Western Hochifen-Gottesacker area (IP13–16)	59
3.7.6	Goldbach springs.....	61
3.8	Conclusions.....	62
3.8.1	Fold tectonics and underground drainage pattern	62
3.8.2	Hydrogeological aspects of landscape history.....	66
3.8.3	Delineation of the catchments	67
3.8.4	Hydraulic properties	70
3.8.5	Hydrogeology of the rockfall mass.....	74
4	Example: Winterstaude.....	75
4.1	Location, topography, climate	75
4.2	Geology.....	76
4.2.1	Stratigraphy.....	76
4.2.2	Tectonics	77
4.2.2.1	Overview.....	77

4.2.2.2	Folds.....	78
4.2.3	Fault tectonics	80
4.3	Hydrogeology.....	81
4.4	Springs and surface waters	82
4.5	Hydrochemistry and microbiology.....	86
4.5.1	Overview.....	86
4.5.2	Hydrochemical characteristics of the springs	86
4.5.3	Microbiology	88
4.6	Tracer tests.....	90
4.6.1	Overview.....	90
4.6.2	Selection of the injection points and the tracers, injection	90
4.6.3	Sampling.....	93
4.7	Results.....	93
4.7.1	Overview.....	93
4.7.2	Swallow hole Stonger moor (IP1).....	93
4.7.3	Karst shaft in Örla limestone (IP2)	94
4.7.4	Grebentobel stream (IP3).....	95
4.7.5	Meadow above the Kreuzboden spring (IP4)	96
4.7.6	Waste water seepage at Sonderdach (IP5)	96
4.7.7	Upper Hundsbach stream (IP6).....	97
4.7.8	Lower Hundsbach stream (IP7).....	97
4.8	Conclusions	97
4.8.1	Fold tectonics and underground drainage pattern.....	97
4.8.2	Delineation of the catchments	100
4.8.3	Hydraulic properties.....	101
5	Example: Alpspitze	102
5.1	Location, topography, climate.....	102
5.2	Geology.....	103
5.2.1	Geological framework.....	103
5.2.2	Stratigraphy	104
5.2.3	Tectonics	106
5.3	Hydrogeology.....	106
5.3.1	The Wettersteinkalk and Partnach formation.....	106
5.3.2	Raibler formation and Hauptdolomit formation.....	108
5.3.3	Quaternary deposits	108
5.3.4	Hydrogeological Zoning.....	109
5.4	Springs and surface waters	110
5.4.1	Overview.....	110
5.4.2	The Partnach river in the Reintal valley.....	110
5.4.3	The Bodenlaine stream	112
5.4.4	The Hammersbach river and the Höllental valley.....	112

5.4.5	The elevated areas	114
5.5	Hydrochemistry	115
5.6	Tracer tests	116
5.6.1	Overview	116
5.6.2	Selection of the injection points and the tracers, injections	117
5.6.3	Sampling and Analyses	118
5.6.4	Hydrologic conditions during the tracer test.....	119
5.6.5	Results with Uranine	120
5.6.6	Results with Eosine.....	124
5.6.7	Results with Naphthionate	124
5.7	Conceptual model of the karst system.....	125
6	Comparison of the three test sites – Fold Tectonics and Karst Drainage Pattern	128
6.1	Introductory remark	128
6.2	Rules of stratigraphic flow control	128
6.3	Folded alpine karst systems with high stratigraphic flow control	130
6.3.1	Influence of the base level conditions	130
6.3.2	Flow pattern in the elevated areas (zone of shallow karst).....	131
6.3.3	Flow pattern in the valleys (deep or shallow karst)	132
6.3.4	Position of the karst springs.....	133
6.3.5	Delineation of the catchments	133
6.4	Folded alpine karst systems with low stratigraphic flow control	134
7	The concept of groundwater vulnerability.....	135
7.1	Background and definitions.....	135
7.2	The origin-pathway-target model	136
7.3	Resource and source protection	137
7.4	The special situation in karst.....	138
7.5	Vulnerability and the European Water Directive	139
8	Overview and Discussion on existing methods OF Mapping Vulnerability.....	141
8.1	Classification of methods	141
8.1.1	Overview	141
8.1.2	Hydrogeological Complex and Setting Methods	141
8.1.3	Index Methods and Analogical Relations.....	142
8.1.4	Parametric System Models.....	142
8.1.5	Mathematical Models.....	143
8.1.6	Statistical Methods.....	144
8.2	Description and criticism of some basic methods.....	144

8.2.1	Introductory remark	144
8.2.2	EPIK	145
8.2.3	Discussion on the EPIK method.....	146
8.2.4	The Irish groundwater protection scheme	148
8.2.5	Discussion on the Irish system.....	150
8.2.6	The German or GLA method.....	150
8.2.7	Discussion on the GLA method.....	152
9	The PI Method	153
9.1	Background and Overview.....	153
9.2	General Concept of the PI Method	154
9.3	Protective Cover (P factor)	156
9.4	Infiltration Conditions (I factor).....	159
9.4.1	General Concept	159
9.4.2	Hydrological Basis	160
9.4.3	The I Factor	161
9.5	Construction of the Vulnerability Map	166
9.6	Modified assessment scheme for the P factor	167
9.6.1	Background	167
9.6.2	Modified assessment scheme.....	167
10	Comparative application of the PI method in the test site Engen.....	170
10.1	The test site Engen.....	170
10.1.1	Location, Topography, Climate.....	170
10.1.2	Geology	170
10.1.3	Karstification and hydrogeology.....	174
10.1.4	Soils.....	175
10.2	Application of the EPIK method	177
10.2.1	Introductory remark	177
10.2.2	Epikarst (E factor).....	177
10.2.3	Protective cover (P factor).....	177
10.2.4	Infiltration conditions (I factor)	178
10.2.5	Karst network development (K factor).....	179
10.2.6	The EPIK vulnerability map	179
10.3	Application of the GLA method	181
10.4	Application of the PI method.....	183
10.4.1	Determination of the P factor.....	183
10.4.2	Determination of the I factor	184
10.4.3	The PI vulnerability map	188
10.5	Comparison and discussion of the maps.....	188
11	Application of the PI method in the Hochifen-Gottesacker area.....	191
11.1	Overview	191
11.2	Definition of the target.....	191

11.3	Protective cover (modified P factor).....	193
11.3.1	The topsoil (layer 1)	193
11.3.2	The subsoil (layer 2)	193
11.3.3	The non-karstic bedrock (layer 3).....	193
11.3.4	The unsaturated karstic bedrock (layer 4)	195
11.3.5	Artesian pressure.....	196
11.3.6	The map of the protective cover (P map)	196
11.4	Infiltration conditions (I factor).....	197
11.4.1	Determination of the dominant flow process	197
11.4.2	Determination of the I factor	199
11.5	The PI vulnerability map.....	201
12	Application of the PI method in the Winterstaude area	203
12.1	Overview and definition of the target.....	203
12.2	Protective cover (P factor)	204
12.2.1	The topsoil (layer 1)	204
12.2.2	The subsoil (layer 2)	204
12.2.3	The non-karstic bedrock (layer 3).....	206
12.2.4	The unsaturated karstic bedrock (layer 4)	206
12.2.5	The map of the protective cover (P map)	206
12.3	Infiltration conditions	208
12.3.1	Determination of the dominant flow process	208
12.3.2	Determination of the I factor	209
12.4	The PI vulnerability map.....	209
12.5	Consequences for source protection	209
13	Conclusions, Discussion and outlook.....	212
13.1	The problem of definition	212
13.2	The problem of „intrinsic“ vulnerability	214
13.3	The COST 620 approach to intrinsic vulnerability mapping	215
13.4	Application of vulnerability maps for source and resource protection zoning	218
13.5	The COST 620 approach to specific vulnerability mapping	221
13.6	Validation of vulnerability maps.....	221
13.7	The importance/value of groundwater	222
13.8	Vulnerability maps within the framework of risk assessment.....	223
13.9	Concluding comment	224
14	References.....	225

LIST OF FIGURES

Fig. 1.1:	Carbonate rock outcrops in Europe (COST 65, 1995).....	1
Fig. 2.1:	The main facies zones of the Alps (SCHWERD 1996). Location of the test sites: 1. Hochifen-Gottesacker, 2. Winterstaude, 3. Alpspitze.....	9
Fig. 2.2:	Carbonate rock outcrops in the Alps (after BÄTZING 1997) and location of the test sites: 1. Hochifen-Gottesacker, 2. Winterstaude, 3. Alpspitze. The northern belt of karst rocks is made of the Helvetic (west) and East Alpine nappes (east), the southern belt belongs to the South Alpine zone. In the central Alps, there are some isolated karst systems (GOLDSCHIEDER et al. 2001e, Graphics: NEUKUM).	14
Fig. 3.1:	Hochifen and Gottesacker from the north. The land surface is made of Schrattekalk limestone (Helvetic zone). The Walmendinger Horn consists of Flysch (Penninic zone) and the Widderstein is made of the Hauptdolomit formation (East Alpine zone).....	18
Fig. 3.2:	Precipitation and temperature in the Breitach valley (1140 m, 1961–1990).	19
Fig. 3.3:	The Helvetic Säntis nappe in western Austria (WYSSLING 1986). Location of the Hochifen-Gottesacker and Winterstaude area.....	20
Fig. 3.4:	Geological map of the Hochifen-Gottesacker area (after ZACHER 1985).	21
Fig. 3.5:	The west face of Hochifen. Kieselkalk limestone (kf), Drusberg marl (df), transition zone (df/sk), Schrattekalk limestone (sk), Quaternary (q).....	23
Fig. 3.6:	Paleokarst in the upper Schwarzwasser valley. Cavities in Schrattekalk limestone are filled with Garschella sandstone.....	24
Fig. 3.7:	The eastern Hochifen-Gottesacker area with the Schwarzwasser valley. The Schrattekalk limestone is gently folded (folds with roman numerals).	26
Fig. 3.8:	The western margin of the Hochifen-Gottesacker area. The valley cuts through the limestone in the tight anticlines.	26
Fig. 3.9:	Block diagram of the Hochifen-Gottesacker area, view from NW. Tectonics: anticlines (roman numerals), synclines, fault pattern; stratigraphy: Palfris (pf), Kieselkalk (kf), Drusberg (df), Schrattekalk (sk), Garschella (gf), Amdener (af) formation, Quaternary deposits (q); hydrology: Kessleralp spring (Ka), Rubach (Rb) spring (WAGNER 1950, supplemented).....	27
Fig. 3.10:	Fold tectonics in the Hochifen-Gottesacker area.	28
Fig. 3.11:	Important springs (with shorthand symbol) and surface waters in the area.	36
Fig. 3.12:	The hydrograph of the Hölloch cave stream is representative for karst water flow in the trough of a plunging syncline (unpublished data A. Wolf).	36
Fig. 3.13:	Hochifen and the rockfall mass in the Schwarzwasser valley from SE; size of the blocks exaggerated, vegetation removed; Swr: Schwarzwasser river; IP: injection points of the tracer tests (see there).....	37
Fig. 3.14:	Under low water conditions, the Schwarzwasser cave is a swallow hole.	38
Fig. 3.15:	Under high water conditions, the cave becomes a spring.	38

List of Figures

Fig. 3.16:	Hydrograph of the Aubach spring during the snow melt (data: Landeswasserbauamt Bregenz; stage discharge curve not yet established).....	40
Fig. 3.17:	Hydrograph of the Aubach spring during a storm rainfall event.....	40
Fig. 3.18:	The bottom spring (Bo) in the Breitach river. a) temperature profile, b) geological view-profile, c) schematic block diagram.....	41
Fig. 3.19:	The Rubach spring (Rb).....	43
Fig. 3.20:	PIPER diagram of all springs in the Hochifen-Gottesacker area.....	46
Fig. 3.21:	Hydrochemistry and temperature of the karst springs in the Schwarzwasser valley (in rectangle) compared with the non-karstic springs in the eastern Hochifen-Gottesacker area (average values from summer 1996).....	47
Fig. 3.22:	Calcium and magnesium concentrations of the Goldbach springs and other springs in the western Gottesacker (summer 1997).....	48
Fig. 3.23:	Tracer tests in the Hochifen-Gottesacker area. Location of the injection points (IP1–16), the sampling points and the proved flow paths (simplified). Shorthand symbols and further explanations in the text.....	52
Fig. 3.24:	Eosine and Pyranine breakthrough curves at the Kessleralp spring (Ka).....	55
Fig. 3.25:	Selected breakthrough curves from different tracer tests in the eastern part of the area. The curves of the springs <i>Bü</i> and <i>Ks</i> are similar to those of <i>Au</i> and are not presented here.....	56
Fig. 3.26:	Comparison of the normalised Uranine breakthrough curves and the integrals of these curves at the four karst springs in the Schwarzwasser valley (injection IP6). Measured values and curves modelled with TRACI 95 (WERNER 1998). Further explanations in the text.....	58
Fig. 3.27:	Sulforhodamine B breakthrough curves of the upper (<i>Ru</i>) and the lower resurgence (<i>Rl</i>) below the rockfall mass. Note the different scale.....	59
Fig. 3.28:	Selected breakthrough curves from the western Hochifen-Gottesacker area. The curves in <i>La1</i> , <i>2</i> and <i>4</i> are similar to those in <i>La3</i> and are not presented here; minor traces of Sulforhodamine were detected at <i>Su</i> ; no positive results were obtained for <i>Rb</i> , <i>Gb1</i> , <i>2</i> and <i>4</i>	60
Fig. 3.29:	Integrals of the normalised Sulforhodamine breakthrough curves (injection IP 15) at different springs: regular dilution between the springs <i>Sl</i> and <i>La4</i> ; higher dilution by additional inflow at the spring <i>Gb3</i>	61
Fig. 3.30:	Generalised hydrogeological section of the Hochifen-Gottesacker area perpendicular to the fold axes. Legend for and location of the following sections.....	63
Fig. 3.31:	Generalised hydrogeological section from the Subersach valley, over the Gottesacker to the Schwarzwasser valley along the main syncline (IV/V).....	63
Fig. 3.32:	Generalised hydrogeological section of the Schwarzwasser valley under low and high water conditions.....	65
Fig. 3.33:	Schematic cross section of the Schwarzwasser valley. The lateral shift of the valley axis is a consequence of geological asymmetry and absence of erosion on the karst land surface. PDS: paleo-	

	drainage system, predicted by GOLDSCHIEDER et al. (2000c) and discovered by cavers in 2002.	67
Fig. 3.34:	a) Catchments of important springs in the Hochifen-Gottesacker area; b) detail from the western Gottesacker; (?): no direct evidence.	68
Fig. 3.35:	The measures Uranine concentrations (sampling point <i>Au</i> , injection point IP6) can be modelled perfectly with Traci 95 (WERNER 1998) by superimposing two SFDM peaks.....	72
Fig. 3.36:	Hydraulic interaction between karst conduits and the surrounding aquifer for different hydrologic conditions and the resulting breakthrough curves.....	73
Fig. 4.1:	Landscape impression of the Winterstaude area; Hochifen-Gottesacker area in the background.....	75
Fig. 4.2:	Simplified geological map of the Winterstaude area and location of the sections in Fig. 4.3.....	76
Fig. 4.3:	Geological N-S-sections of the Winterstaude area (after NEUKUM 2001 and WERZ 2001). The springs were projected into the sections. Legend and location see Fig. 4.2.....	78
Fig. 4.4:	Tectonical map of the Winterstaude area (NEUKUM 2001, GOLDSCHIEDER et al. 2001e).....	79
Fig. 4.5:	Important springs and surface waters in the Winterstaude area and groundwater contour lines of the granular aquifer in the Bezau valley floor (compiled and modified after NEUKUM 2001).....	82
Fig. 4.6:	Possible recharge mechanisms of the drainage tubes of the Kreuzboden spring; 1. infiltration from the Grebentobel stream, 2. direct infiltration of precipitation, 3. inflow from the adjacent slope, 4. inflow of karst water (WERZ 2001).....	83
Fig. 4.7:	Hydrograph of the Stuole spring (<i>St</i>) (NEUKUM 2001).....	84
Fig. 4.8:	Hydrograph of the Kressbach spring (<i>Ks</i>) (data source: <i>Landeswasserbauamt Bregenz</i> ; stage discharge curve not yet established).....	85
Fig. 4.9:	Hydrograph of the spring near the Bregenzerach (<i>Ba</i>) (NEUKUM 2001).....	86
Fig. 4.10:	PIPER-diagram of all springs in the area (data: NEUKUM 2001). Calcium and bicarbonate are dominant in most of the springs; exceptionally high contents of sulphate were found in springs which drain rockfall material.	87
Fig. 4.11:	Graphical presentation of the Ca^{2+} and Mg^{2+} concentrations of important springs in the Winterstaude area (data: NEUKUM 2001).....	88
Fig. 4.12:	Synopsis of the microbiological properties of all the springs in the area; abbreviations see text and Fig. 4.5 (data: NEUKUM 2001).	89
Fig. 4.13:	Overview of the tracer tests in the Winterstaude area. Location of the injection points (IP), sampling points (important springs with shorthand symbol) and proved flow paths (after NEUKUM 2001, GOLDSCHIEDER et al. 2001e).....	91
Fig. 4.14:	Breakthrough curves for Eosine (injection IP1), Sulforhodamine (IP2) and Uranine (IP5) at the Stuole (<i>St</i>) and the neighbouring Bleile spring (<i>Bl</i>).	95
Fig. 4.15:	Breakthrough curves for Naphthionate (IP3) and Pyranine (IP4) at the Kreuzboden spring.....	96
Fig. 4.16:	Schematic hydrogeological block diagram of the Winterstaude area. Location of the injection points (IP1–IP7), the springs (with	

List of Figures

	shorthand symbol) and the proved flow paths (NEUKUM 2001, slightly modified).....	98
Fig. 5.1:	View from the Alpspitze to the Zugspitze.	102
Fig. 5.2:	Precipitation and air temperature in Garmisch-Partenkirchen (GAP) (719 m) and on the summit of the Zugspitze (2959 m). Data from the period 1961–1990.....	103
Fig. 5.3:	Simplified geological map of the Alpspitze area (after MILLER 1962). Quaternary deposits outside the main valleys are not shown.....	104
Fig. 5.4:	View from the east on Mt. Alpspitze and the karstified cirque around the hidden lake Stuibensee. IP1: injection point of the tracer test.	107
Fig. 5.5:	Springs, surface waters and important locations in the Alpspitze area.	109
Fig. 5.6:	Hydrograph of the Partnachursprung (<i>Pu</i>) (data: ENDRES 1997).	110
Fig. 5.7:	Schematic hydrogeological section of the rockfalls in the Reintal valley (modified after BROSEMER 1999, out of scale, length 2 km).	111
Fig. 5.8:	The Klammsquelle (<i>gorge spring, Kl</i>) discharges from a karst conduit in Wettersteinkalk limestone, around 30 m above the water course level.	114
Fig. 5.9:	PIPER diagram of all the springs in the area.	116
Fig. 5.10:	Overview of the tracer tests in the Wettersteingebirge; location of the injection points (IP), the sampling points and the proved flow paths.	117
Fig. 5.11:	Uranine breakthrough curve in the river up- and downstream from the Klammsquelle (gorge spring, <i>Kl</i>).	120
Fig. 5.12:	Comparison of the Uranine breakthrough curves of the springs <i>He</i> and <i>Rg</i> at the entrance of the Höllental gorge.	122
Fig. 5.13:	Uranine breakthrough curves of the spring S3 and the collectors S1–3 and S2–3.	123
Fig. 5.14:	Schematic hydrogeological section of the upper Höllental valley with the Naphthionate injection point (IP3) and the breakthrough curve of the Hammersbach spring (<i>Ha</i>). The granular aquifer formed by the rockfall mass and the alluvial plain collects the seeping surface water and the karst groundwater and is drained by the spring <i>Ha</i>	125
Fig. 5.15:	Schematic graphical presentation of important factors controlling the hydrogeology of the Alpspitze area: steep topography, significant surface runoff during storm rainfall, large thickness of the karstifiable limestone, thick unsaturated zone, lack of low permeability layers, no significant stratigraphic flow control, underground flow crossing the folds.....	126
Fig. 6.1:	Illustration of the three rules of stratigraphic flow control.....	129
Fig. 6.2:	Schematic illustration of the relation between fold tectonics, base level conditions, surface and underground drainage pattern in an alpine karst system with strong stratigraphic flow control. In the zone of shallow karst, synclines form the main flow paths; in the zone of deep karst, flow across the folds is possible.	131
Fig. 7.1:	The origin-pathway-target model for vulnerability assessment.	136
Fig. 8.1:	Hypothetical example for an inconsistent vulnerability assessment when EPIK is applied strictly. The delineation as protection zone S3 would be insufficient in the described case.	148
Fig. 8.2:	Illustration of the Irish groundwater protection scheme. The vulnerability map can be used both for source and resource	

	protection zoning (GSI 1999). Explanation of the abbreviations in the text.....	149
Fig. 8.3:	Illustration of the GLA concept (HÖLTING et al. 1995) to assess the protective function of the layers above the groundwater surface: 1. topsoil, 2. subsoil, 3. unsaturated bedrock (a. non-karstic, b. karstic). 151	
Fig. 9.1:	Illustration of the PI method: The P factor takes into account the effectiveness of the protective cover (1. topsoil, 2. subsoil, 3. non-karstic bedrock, 4. unsaturated karstic bedrock). The I factor expresses the degree to which the protective cover is bypassed by lateral surface and subsurface flow, especially within the catchments of sinking streams.....	155
Fig. 9.2:	Simplified flow chart for the PI method.....	155
Fig. 9.3:	Determination of the P factor (modified after HÖLTING et al. 1995).....	157
Fig. 9.4:	Epikarst and protective function: a) The unsaturated karstic bedrock may provide a protective function if the epikarst is slightly developed so that water storage is the dominant process. b) Concentration of flow in a highly developed epikarst decreases the protective function.....	158
Fig. 9.5:	Determination of the I factor. If it is impossible to distinguish six different flow processes, it is sufficient to distinguish between infiltration (white), subsurface (light grey) and surface flow (dark grey). In this case, the bold numbers can be used to determine the I' factor (2 nd step).....	162
Fig. 9.6:	Determination of the predominant flow process as a function of the saturated hydraulic conductivity and the depth to low permeability layers. If it is not possible to distinguish all six processes, it is often sufficient to differentiate between infiltration, subsurface and surface flow. This can be done on the basis of direct field observations and geological data.....	163
Fig. 9.7:	Topographic sketch and geological profile illustrating the five different zones of the „surface catchment map“ in the order of decreasing risk: a) sinking stream with 10 m buffer, b) 100 m buffer, c) catchment of sinking stream, d) rest of the area draining into the karst, e) area draining out of the karst. The arrows indicate lateral (sub)surface flow.....	165
Fig. 9.8:	Determination of the “modified” P factor (after DALY et al. 2000b). Grey colours symbolise the limitation of Darcy's law and the K value. 169	
Fig. 10.1:	Overview of the Engen area (data base: LGRB 1999).....	171
Fig. 10.2:	Geology of the Engen area (data: LGRB 1999, nomenclature GLA 1995).....	173
Fig. 10.3:	Hydrogeological profile of the Danube-Aach system (SCHREINER 1992, new stratigraphic nomenclature GLA 1995).....	174
Fig. 10.4:	Soil map of the Engen area (data: LGRB 1999, German nomenclature).....	176
Fig. 10.5:	EPIK vulnerability map of the Engen area.....	180
Fig. 10.6:	Map of the protective function of the layers above the groundwater surface (“vulnerability map”) after the GLA method (Dickel et al. 1993a, b; LGRB 1999).....	181
Fig. 10.7:	Map of the protective cover (P map) after the PI method.....	183

List of Figures

Fig. 10.8:	Determination of the dominant flow process by intersecting the coverage <i>depth to low permeability layers</i> with the coverage <i>topsoil permeability</i>	185
Fig. 10.9:	Determination of the I map (showing the degree to which the protective cover is bypassed) by intersecting the I' map (intensity of lateral flow) and the surface catchment map (sinking streams and their catchments).....	187
Fig. 10.10:	PI vulnerability map of the Engen area.....	189
Fig. 11.1:	Overview of the Hochifen-Gottesacker area. The groundwater in the karst aquifer was taken as the target for vulnerability mapping. In three areas, the groundwater in a local granular aquifer was taken as the target. The upper Subersach valley is not part of the karst system. However, river water infiltrates into the aquifer 2 and reaches the karst spring <i>Gb3</i>	192
Fig. 11.2:	Protective function of the topsoil, subsoil, non-karstic bedrock and unsaturated karst bedrock; artesian pressure in the aquifer.....	194
Fig. 11.3:	The P map of the Hochifen-Gottesacker area (after KUNOTH 2000).....	196
Fig. 11.4:	Map of the dominant flow process (after STRATHOFF 2000).....	198
Fig. 11.5:	Surface catchment map of the Hochifen-Gottesacker area.....	199
Fig. 11.6:	The I map shows the degree to which the protective cover is bypassed by lateral (sub)surface flow which enters the karst aquifer at another point.....	200
Fig. 11.7:	PI vulnerability map of the Hochifen-Gottesacker area.....	202
Fig. 12.1:	Bedrock geology map of the Winterstaude area (after Werz 2001). There are two interacting karst aquifers – Örfli and Schrattekalk limestone. The target for vulnerability mapping is the groundwater in the respective uppermost aquifer. The granular aquifer of the valley floor and the southern strip of the area was not considered for vulnerability mapping.....	203
Fig. 12.2:	Protective function of the topsoil, the subsoil, the non-karstic bedrock and the unsaturated karst (modified after Werz 2001).....	205
Fig. 12.3:	The vulnerability map was made by intersecting the P and the I map.....	207
Fig. 12.4:	The catchment of the Kreuzboden spring is identical to the surface catchment of the Grebentobel stream. It can be subdivided in an inner (low permeability formations, frequent surface runoff) and outer zone (high permeability formations, rare surface runoff) (after WERZ 2001).....	210
Fig. 13.1:	Conceptual model of the European Approach (DALY et al. 2002; Graphics: N. Goldscheider).....	216
Fig. 13.2:	Creation of resource and source vulnerability maps by a combination of the factors O, C, P and K (after Daly et al. 2002).....	219
Fig. 13.3:	The Irish groundwater protection scheme provides an example of how vulnerability maps can be used as a basis for resource and source protection. The scheme is not restricted on karst but applicable for all types of aquifers, in this case a sand/gravel aquifer (modified after GSI 1999). The PI method and the COST 620 concept follows this logic but uses a slightly different nomenclature.....	220
Fig. 13.4:	Vulnerability by itself is not a sufficient criterion for protection zoning. Thus, the Irish groundwater protection schemes additionally take into account the value/importance of the groundwater.....	222

LIST OF TABLES

Tab. 3.1:	Overview of the important springs in geographical order and decreasing altitude. The term <i>complex</i> is used for proved interaction between different aquifer types and for disputable situations; explanations in the text.	35
Tab. 3.2:	Suggested classification for estavelles; detailed explanation see GOLDSCHIEDER et al. (1999b).	39
Tab. 3.3:	Overview of the injections in the Hochifen-Gottesacker area.	50
Tab. 3.4:	Overview of tracer test results in the Hochifen-Gottesacker area. The time of maximum concentration t_m and normalised maximum concentration c/M is given for each proved connection. White box: sampled spring; grey: not sampled; + indirect evidence for connection, no breakthrough curve; - no connection; * only the time of first visible detection is given by SPÖCKER 1961; **curve shows no clear maximum.	54
Tab. 3.5:	Groundwater flow velocities in the Hochifen-Gottesacker area.	70
Tab. 3.6:	Determination of hydraulic properties of the karst aquifer on the basis of the tracer test IP6. Dispersivities and transit times were calculated by modelling the breakthrough curves with Traci 95 (Werner 1998).	72
Tab. 3.7:	Hydrogeological characteristics of the rockfall mass compared with a typical karst and a typical granular aquifer.	74
Tab. 4.1:	Overview of the tracer injection points in the Winterstaude area.	91
Tab. 4.2:	Overview of the tracer test results in the Winterstaude area for the important sampling points. The time of maximum concentration (t_m), normalised maximum concentration (c/M) and recovery rate (%) is given for each proved connection. White box: spring was analysed for the respective tracer; grey: not analysed, no connection (clear hydrogeological evidence); + connection proved with charcoal bags; - no connection.	94
Tab. 9.1:	Legend for the vulnerability map, the P and the I map.	166
Tab. 10.1:	Comparison of the different classification schemes for the protective cover after the PI and the GLA method.	190
Tab. 13.1:	suggested COST 620 classification of carbonate aquifers (modified after DALY et al. 2002).	217

1 INTRODUCTION

1.1 The significance of karst groundwater

Groundwater from karst aquifers is among the most important resources of drinking water for the growing population of the world. Carbonate rock outcrops, of which a large part is karstified, cover about 7–12 % of the planet's dry, ice-free land and about 25 % of the global population is supplied by karst waters (FORD & WILLIAMS 1989, DREW & HÖTZL 1999). In Europe, carbonate terrains occupy 35 % of the land-surface (Fig. 1.1) and a significant portion of the drinking water supply is abstracted from karst aquifers. In some European countries, karst water contributes 50 % to the total drinking water supply and in many regions, it is the only available fresh water resource (COST 65, 1995).



Fig. 1.1: Carbonate rock outcrops in Europe (COST 65, 1995).

At the same time, karst aquifers are particularly vulnerable to contamination: Due to thin soils, point recharge in dolines, shafts and swallow holes, as well as concentration of flow in the epikarst and vadose zone, contaminants can easily reach the groundwater, where they are transported rapidly in karstic conduits over large distances (HÖTZL 1996). As the residence time of contaminants in the system is often short and their interaction with the aquifer is limited, many processes of contaminant attenuation like filtration and adsorption, as well as chemical and microbiological decay often do not work effectively in karst systems.

As karst areas are both important for drinking water supply and vulnerable to contamination, they need special protection (DREW & HÖTZL 1999). However, protection zoning for karst is more complicated than for granular aquifers: Karst systems are highly heterogeneous; karst catchments may cover large areas (often more than 100 km²) and karst groundwater is characterised by high flow velocities (10–500 m/h). If the same criteria of groundwater protection that are applied for granular aquifers (e.g. 50-day-line of travel time) were used for karst aquifers, the protection zones would consequently cover enormous areas. From the point of view of drinking water protection, this would be sensible. However, from the practical point of view, it is impossible to demand maximum protection for large areas, because the resulting land-use restrictions would not be acceptable in many cases.

As a consequence, it is essential to protect at least those areas within a karst system where contaminants can easily reach the groundwater (SCHLOZ 1994). This leads to the concept of groundwater vulnerability that is not restricted to karst, but is most relevant and most complicated when applied to karst areas. The fundamental concept of groundwater vulnerability is that some areas are more vulnerable to contamination than others (VRBA & ZAPOROZEC 1994). Thus, it is the ultimate goal of a vulnerability map to show up areas of different vulnerability. Vulnerability maps can be used for land-use planning at different scales and especially for the delineation of source and resource protection zones (GSI 1999). The delineation of protection zones on the basis of a vulnerability map aims at a compromise between drinking water protection on the one hand and land-use on the other hand: In the highly vulnerable zones, drinking water protection is the priority and land-use has to be restricted, while land-use of some types can be accepted in the less vulnerable zones.

Thus, it is necessary to define objective and applicable criteria to mapping the vulnerability of groundwater to contamination. However, due

the special characteristics and the high variability of karst systems, such criteria are difficult to determine. For that reason, the COST Action 620 was set up by the Directorate General for Science, Research and Development of the European Commission. The objective of COST 620 is to propose an approach to „vulnerability and risk mapping for the protection of carbonate (karst) aquifers“.

1.2 Karst in the Alps

Large parts of the Alps are formed of carbonate rocks. Most of them are karstified and contain significant groundwater resources. Thus, karst water contributes essentially to the total drinking water supply in the alpine countries, e.g. 50 % in Austria, 50 % in Slovenia and 15 % in Switzerland (COST 65, 1995). Vienna, Salzburg, Innsbruck, Grenoble and several other big cities are supplied with drinking water from alpine karst systems. Thus, the detailed hydrogeological understanding of alpine karst systems forms a precondition for developing concepts for the sustainable protection and use of alpine karst water resources (KRÁLIK 2001). Alpine karst waters are often characterised by a good hydrochemical quality, while the microbial quality is often endangered by agricultural activities (COXON 1999) and tourism (ZOJER 1999).

At the same time, alpine karst systems are an interesting object of study from the scientific point of view (ZÖTL 1974). The hydrogeological characteristics of alpine karst systems are mainly influenced by the geology: that is the stratigraphy (lithology and thickness of the strata), the tectonics (folds and faults) and the landscape history. All these controlling factors are highly variable in the Alps: Most of the karst rocks in the Alps are of Mesozoic age, but there are also karstified Tertiary and Palaeozoic rocks. Limestone and dolomite are the predominant karstifiable rocks in the Alps, but some areas are made of marble, calcareous sandstone and conglomerate, gypsum, anhydrite or salt. The thickness of the karst aquifers ranges between a few metres and several kilometres. Alpine karst systems are plateau-like or folded and most often intensively cut by all kinds of faults and fractures. The landscape history includes several phases of folding and thrusting, uplift and erosion, glaciation and deglaciation. The age of karstification ranges between Mesozoic (paleokarst) and recent.

Last but not least, there is a great variability in altitude, topography and climate: Many of the high and prominent summits in the Alps are formed of karst rocks (e.g. Ortler, 3899 m) but karstified limestone was also proved by drillings at several kilometres depth below the Alps.

Karst rocks form some of the highest and steepest rock faces in the Alps (e.g. the north face of Eiger, 3870 m) but also some large plateaux with gentle topography (e.g. the Dachstein plateau). The climate is influenced by Atlantic, Mediterranean and continental elements. Thus, the total annual precipitation ranges between around 600 and 4500 mm per year. Both the temperature and the proportion of snow strongly depend on the altitude. Perennial snow fields and glaciers are frequent in the highest alpine karst systems.

Due to the described variability of geology, topography and climate, each alpine karst system has its individual character. Hydrogeological research in alpine karst system often leads to surprising results and allows new insights in the complex relation between the controlling factors and the resulting hydrogeological characteristics.

1.3 The purpose and structure of this thesis

This thesis is both a contribution to the development of an approach to mapping karst groundwater vulnerability within the framework of the European COST Action 620 and a contribution to the regional hydrogeology of alpine karst systems.

Chapters 2–6 of this thesis deal with the hydrogeology of alpine karst systems. An overview on the geology of the Alps and the distribution of karst is given. The three test sites that were studied within the framework of this thesis are presented – Hochifen-Gottesacker, Winterstaude and Alpspitze. The geology, hydrogeology and hydrology of these test sites are described and the results of the hydrochemical investigations and the numerous tracer tests are discussed in detail. The last section is an attempt to describe how the stratigraphy, the base level conditions, the fault and fold tectonics control the underground drainage pattern of folded alpine karst systems.

The chapters 7–13 are a contribution to the ongoing COST Action 620 on vulnerability and risk mapping for the protection of carbonate (karst) aquifers. The concept of groundwater vulnerability is presented and an overview on existing methods is given. The PI method of mapping groundwater vulnerability which was developed within the framework of this thesis is described in detail. The method was firstly applied in the Engen area in the south-western Swabian Alb. Later on, it was modified on the suggestions of COST 620 and applied in two of the alpine test sites. The last chapter gives a critical discussion of the concept of groundwater vulnerability, as well as an outlook on future challenges.

1.4 Overview of the research and co-operation

This thesis was prepared at the Department of Applied Geology at the University of Karlsruhe (AGK) and supervised by Prof. Dr. H. Hötzl. It is not the result of one single research project but rather a „conglomerate“ of various small applied and research activities that were funded by different institutions. Some steps of the research were financed by the AGK. Fourteen diploma theses were carried out within the framework of this thesis from which eleven contribute directly or indirectly to this thesis while the other three dealt with different projects.

The first step of the research was the hydrogeological investigation of the eastern Hochifen-Gottesacker area within the diploma thesis of the author (GOLDSCHIEDER 1997). The other parts of the area were later on investigated by HUTH (1998), SINREICH (1998) and TOMSU (1998) within their diploma theses. Many tracer tests have been carried out in the area. Several brief or detailed papers on the various aspects of hydrogeology, landscape history and groundwater protection of the Hochifen-Gottesacker area were published together with various co-authors (see references). During the research activities in this area, the risk potential of an organic waste disposal site was assessed and protection zones for several karst springs were delineated. These parts of the research were funded by the Raiffeisen Holding Kleinwalsertal and the Landeswasserbauamt Bregenz respectively.

The field work in the area of Mt. Alpspitze was done by BROSEMER (1998) and UMLAUF (1998) within their diploma theses. The results were published together (GOLDSCHIEDER et al. 1999a).

The research in the Winterstaude area was carried out in order to develop a concept for sustainable drinking water supply and protection for the community of Bezau. However, the project is also a contribution to the regional hydrogeology of the state of Vorarlberg. Thus, the work was funded by the community of Bezau and by the Vorarlberger Naturschau. NEUKUM (2001) and WERZ (2001) contributed to this project within their diploma theses. The results were published together (GOLDSCHIEDER et al. 2001d, e).

The PI method of mapping groundwater vulnerability is a contribution to the COST Action 620. It was worked out by GOLDSCHIEDER et al. (2000a, b) and first applied in a test site in the Swabian Alb by STURM (1999) and KLUTE (2000) within their diploma theses. Both of them contributed to the development of the method. This project was funded by the German Federal Institute for Geosciences and Natural Re-

sources (BGR) and carried out in close co-operation with BGR and the Geological Survey of Baden-Württemberg (LGRB).

Later on, the PI method was slightly modified according to suggestions given by COST 620. KUNOTH (2000) and STRATHOFF (2000) applied this modified PI method in the alpine karst system Hochifen-Gottesacker and WERZ (2001) applied it in the Winterstaude area. All of them contributed to the further development of the method.

The karstification and hydrogeology of carbonate conglomerates in the sub-alpine Molasse zone was investigated within the framework of the diploma thesis of GÖPPERT (2002).

2 OVERVIEW OF THE GEOLOGY OF THE ALPS AND ALPINE KARST SYSTEMS

2.1 The Alps within the framework of plate tectonics

The Alps are a part of the Alpine belt which marks the collision zone between the African and the Eurasian plates (COWARD & DIETRICH 1989). It extends from Gibraltar to the Middle East; further east it passes into the Himalayan belt which results from the collision between India (Indo-Australian Plate) and Eurasia (WINDLEY 1995). The evolution and structure of the Alpine belt is complicated as it evolved over a period of 200 Ma by the continuous motion and interaction of a complex mosaic of plates and microplates. Many continental margins, mid-ocean ridges, island arcs and back-arc basins have been created and subsequently destroyed during the evolution of the Alpine belt.

The development of the entire Mediterranean region and the Alpine fold belt was controlled by the opening of the central and North Atlantic and the resulting movement of the African plate relative to the European (correct: Eurasian) plate (TRÜMPY 1985). The relatively simple movement of the two large lithospheric plates led to complex motions of the intervening microplates (FRISCH 1981).

In the late Permian and Triassic, all continents were unified in the super-continent Pangaea. In the eastern part of Pangaea, the wedge-shaped Tethys ocean separated the northern (Eurasia) from the southern land-masses (Africa, Arabia, India, Australia, Antarctica). The western end of the Tethys was located between SE Europe and NE Africa. Thus, the Permian is continental or shallow-marine in West Europe. Evaporites started forming in the late Permian. During the Triassic, extensive and thick carbonate platforms formed on the continental margins of the Tethys. In the surrounding of the future North Atlantic, the formation of grabens and the related volcanism started in the Permian and Triassic, indicating the break-up of Pangaea (SCHÖNENBERG & NEUGEBAUER 1997).

The opening of the central Atlantic ocean between North Africa and America started in the Middle Jurassic, while Europe was still jointed to North America. Consequently, Africa was moving eastward relative to Europe. This left-lateral movement led to the formation and rotation of microplates and allowed the creation of oceanic basins. The Penninic

ocean that formed between Europe and the Adriatic microplate was of major importance for the development of the Alps.

During the Cretaceous, the opening of the Atlantic advanced further towards the north and the creation of the North Atlantic ocean started in the Upper Cretaceous. As the North Atlantic opened with a faster rate than the central Atlantic, Europe was moving eastward relative to Africa. This overall right-lateral movement led to E-W compression in the oceanic basins of the western Tethys region and caused the closure of the southern Penninic ocean and, subsequently, a first collision between the Adriatic microplate and the European continental margin in the Upper Cretaceous (early-alpine orogenesis).

Since the Eocene, the central and the North Atlantic have opened at a similar rate. At the same time, the African plate was generally moving northwards. Consequently, the lateral movements between the two large lithospheric plates decreased while significant N-S compression started and led to a series of orogenies in the entire Mediterranean region. The Alps were formed by the stepwise collision of the Adriatic microplate in the south and the European plate in the north (late-alpine orogenesis). The Adriatic plate acted as the overriding upper plate, the European plate was the subducting lower plate and the intervening remnant of the Penninic ocean was closed.

2.2 The tectonic-stratigraphic evolution of the Alps

2.2.1 Overview

The Alps can be subdivided into different main tectonic-stratigraphic facies zones: the South Alpine, the East Alpine (Austro-Alpine), the Penninic and the Helvetic zone (Fig. 2.1). Synorogenic Flysch sediments are present within all the main zones and late- to post-orogenic Molasse foreland basins formed north and south of the Alps. However, the latter is rather the northern foreland basin of the Apennines (SCHÖNENBERG & NEUGEBAUER 1997, TRÜMPY 1985).

The Alps are an asymmetric orogene: The Helvetic, Penninic and East Alpine units were transported as large thrust sheets (nappes) in northern direction. The East Alpine nappes were thrust on top of the Penninic nappes and both were thrust on top of the Helvetic nappes. The nappes consist both of the sedimentary cover and the crystalline, pre-Alpine basement. During the last stage of orogenesis, folding and thrusting affected even the southern margin of the Molasse basin north

of the Alps. Due to the northward movement of the nappes, most of the thrusts and folds are north-verging. In contrast to that, the South Alpine zone is characterised by south-verging structures and can consequently be described as an extension of the Dinarides. The two parts of the Alps are separated from each other by a first order tectonic boundary, the Periadriatic (Insubric) line (SCHMID et al. 1989). Plutonic bodies intruded along that line during the Paleogene.

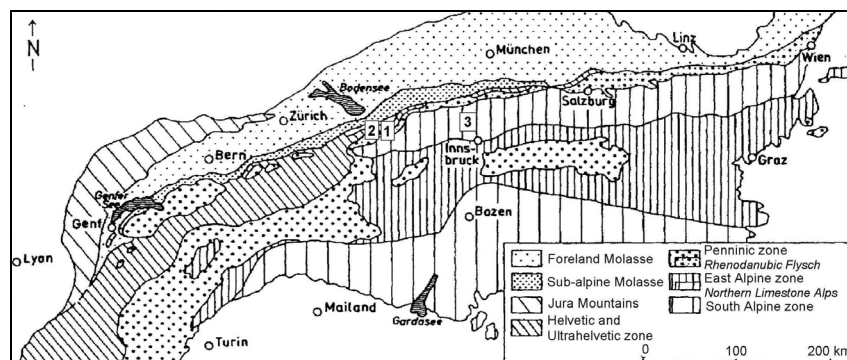


Fig. 2.1: The main facies zones of the Alps (SCHWERD 1996). Location of the test sites: 1. Hochfien-Gottesacker, 2. Winterstaude, 3. Alpspitze.

The following sections provide a brief overview on Alpine geology by describing the development and structure of the main tectonic-stratigraphic units in a simplified way.

2.2.2 The South and East Alpine facies zone

Tectonically, the north-verging East Alpine zone belongs to the main body of the Alps from which the south-verging South Alpine zone is separated by the Periadriatic line. However, close analogies in basement petrography and sedimentary sequence prove that the two zones originate from the southern margin of Tethys and form a unity in terms of paleogeography and stratigraphy (LAUBSCHER 1989). The development of the sedimentary facies is closely related to the tectonic evolution of the Adriatic microplate.

In the Permian and Lower Triassic, the Adriatic microplate was part of Pangaea. Continental red-bed sediments (Verrucano) were deposited and extensive acid volcanites were erupted. Marine sediments formed locally in the South Alpine zone.

During the Triassic, the South and East Alpine were flooded by the Tethys and extensive carbonate platforms with reefs were forming. Up to 4000 m of sediments were deposited on the subsiding passive continental margins (PREY 1978). The marine „Alpine Triassic“ differs significantly from the mostly continental „Germanic Triassic“.

Since the late Triassic and during the Jurassic, the South Penninic ocean had been opening. The carbonate platforms broke down and a mosaic of blocks was formed. Up to 4000 m thick sediments were deposited in the quickly subsiding grabens, while sedimentation stopped on the horsts. During the Upper Jurassic and Lower Cretaceous, the South Penninic ocean was further expanding and deep marine, pelagic sediments (e.g. radiolarites) were deposited.

In the Lower Cretaceous, the relative movement between the African and European plate reversed and the oceanic basins came under compression. This early-alpine orogenesis led to the formation of a significant topography, so that sub-marine landslides (olistostromes) took place. Between the Upper Cretaceous and the Eocene, basins were subsiding and filled with sediments of the „Gosau“ facies. During the Gosau sedimentation, the East Alpine was uplifted and formed the front of the upper plate, while the South Alpine subsided and was partly covered with Flysch sediments.

2.2.3 The Penninic facies zone

The Penninic nappes form large parts of the Western Alps and outcrop in tectonic windows under the East Alpine nappes in the central Eastern Alps. The Penninic zone is highly heterogeneous and can be subdivided into three (sub)-zones (SCHÖNENBERG & NEUGEBAUER 1997): The southern zone is the South Penninic ocean (Piemontais trough). The middle zone (Briançonnais) consists of thinned continental crust that was under shallow water or locally above the sea-level in the Jurassic, but subsided rapidly during the Upper Cretaceous. The northern zone (Valais) is a deep oceanic trough.

Consequently, there are all kinds of continental, shallow- and deep-marine sediments, as well as remnants of oceanic crust (ophiolites) within the Penninic zone. Carbonate platforms formed locally in the middle Penninic zone during the Jurassic. Large parts of the Penninic zone underwent a regional metamorphism after subduction.

2.2.4 The Helvetic and Ultrahelvetic facies zone

The Helvetic nappes form the outer zone of the French and Swiss Alps, as well as parts of West Austria. Further to the east, a narrow and discontinuous strip of Helvetic rocks follows the northern margin of the Northern Limestone Alps (SCHÖNENBERG & NEUGEBAUER 1997).

The Helvetic sedimentary rocks were formed on the crystalline basement of the European plate. During the Permian, up to 1000 m of continental red-bed sediments (Verrucano) were locally deposited in extensional basins. The Triassic of the Helvetic zone still shows the typical characteristics of the „Germanic“ facies.

During the Jurassic, the Penninic ocean was forming and the Helvetic zone became the passive continental margin south of Europe. Thus, the Jurassic and Cretaceous sediments are neritic, relatively thin and full of hiatus' in the northern Helvetic zone. Towards the south, the sediments become more bathyal, thick and complete. Significant limestone formations were deposited in the Jurassic and Cretaceous.

The sedimentary rocks of the Ultrahelvetic facies zone formed on the continental slope between the Helvetic continental margin and the southward bordering Penninic deep sea troughs. Tectonically, the Ultrahelvetic nappes form a narrow, discontinuous imbricate zone.

2.2.5 The synorogenic Flysch

During the alpine orogenesis, extensive synorogenic sediments were deposited. These so-called Flysch sediments formed from the early Cretaceous to the Lower Oligocene and consist of marine shaly formations, characterised by the presence of intercalations of sandstone and impure limestone beds (HOMEWOOD & CARON 1982). Deep-marine turbidity currents contributed to the transport of the Flysch sediments.

In plate tectonic terms, Flysch sedimentation takes place in three different environments: 1. in extensional basins; 2. in deep-sea fans; 3. in active trenches bordering island arcs if subduction rates are low or if the sediment supply rate is high. The third possibility is the classical model of Alpine Flysch formation (DEWEY et al. 1973).

Flysch sediments were deposited in all the facies zones of the Alps. As the orogenic activity progressed successively from south to north, the Flysch sedimentation progressed northward as well. In the East Alpine and Penninic zone, Flysch formation started in the Lower Cretaceous

and lasted until the Eocene; in the Helvetic and Ultrahelvetic zone, it took place between the Upper Cretaceous and the Lower Oligocene.

2.2.6 The late- to post-orogenic Molasse

The Molasse basin North of the Alps formed during the last phase of the orogenesis in the Oligo- and Miocene. The tectonic activity reached the Helvetic zone which was overridden by the Penninic and East Alpine nappes. The Alps were rising up and a foreland basin was forming along their northern margin. Up to 5000 m of sediments were deposited in the simultaneously subsiding basin. Extremely coarse grained conglomerates were deposited in alluvial fans at the northern margin of the Alps. These conglomerates are rich of limestone and dolomite components. Both the thickness of the formations and the grain size of the sediments decrease with increasing distance from the Alps. Several phases of marine, brackish and freshwater sedimentation can be distinguished.

Tectonically, the Molasse basin can be subdivided in two main zones: The southern zone is the sub-alpine Molasse which was affected by tectonic activity, folded and overridden by the Alpine nappes. The northern zone is the foreland Molasse which is not folded.

2.3 Definition of alpine karst

Before defining the term *alpine karst*, it is useful, to explain the origin of the name the *Alps* and the various meanings of the adjective *alpine*.

The term *Alp* or *Alm* comes from the pre-roman time. The alemmanic term *Alp* is used in Switzerland and the West Austrian state of Vorarlberg, while the bajuvarian term *Alm* is used in Bavaria and Austria. An *Alp* or *Alm* is a cattle pasture in the mountains above the forest-line. These mountain pastures are traditional, typical and significant in the Alps, and so the entire mountain range was named after this type of land-use (BÄTZING 1997).

The adjective *alpine* is used in a wide sense for almost everything that has something to do with the Alps or with any kind of high mountains. In geography and vegetation science, the term *alpine* is used in a more strict sense for the zone between the forest-line and the snow-line. Thus, the term *alpine karst* can be defined in three different ways:

1. karst in high mountain areas;
2. karst in the Alps;

3. karst in the alpine zone (height level), that is between the forest- and the snow-line.

As karst systems in high mountain areas all over the world show some similar characteristics (but also significant differences!), the first definition is considered to be widely applicable. In the literature, the term *alpine karst* is used for high mountain karst systems in general, e.g. for karst in the Canadian Rocky Mountains (SMART 1983), in the Spanish Picos de Europa (FERNANDEZ-GIBERT et al. 2000) and, of course, in the Alps (e.g. AUDRA 1994). This thesis uses the first definition but deals with karst systems in the Alps only.

The third definition is applicable in terms of karst geomorphology because there is a close relation between the height level and the exokarst landforms (e.g. WILHELMY 1992). However, the definition is not applicable in term of hydrogeology as the hydrologic borders of karst systems do generally not coincide with the forest- and the snow-line.

2.4 Classification of alpine karst systems and distribution of karst in the Alps

2.4.1 Pyrenean and Canadian type of alpine karst

FORD & WILLIAMS (1989) suggest to distinguish between a *Pyrenean type* and a *Canadian type* of alpine karst system dependent on the ice-karst relationship. The first type is present if the glaciers were confined to the cirques and upper valleys so that meltwater could discharge underground into lower karst valleys that were ice-free, i.e. the karst inputs are glaciated but not the outputs. This condition prevailed in most of the Pyrenees and Picos de Europa, the Caucasus, the US Rocky Mountains, as well as in parts of the Southern and Eastern Alps.

The Canadian type is present if the glacier occupied all valleys and extended in the foreland of the mountain ranges, far beyond the output spring. This ice-karst relationship predominates in the Canadian Rocky Mountains and in large parts of the Northern, Western and central Alps.

2.4.2 Plateau-like and folded alpine karst systems

The hydrogeological characteristics of alpine karst systems are strongly influenced by their geological structure. Due to the high variability of the stratigraphic, tectonic and climatic conditions and due to the complex landscape history, each alpine karst system has to be considered as an

individual case, so that any generalisation and simplification is problematic (TRIMMEL 1998). However, it is possible to distinguish between at least two main types in terms of their geological structure: plateau-like and folded alpine karst systems (HÖTZL 1992).

Plateau-like karst systems are frequent in the central and eastern section of the Northern Limestone Alps which belong to the East Alpine zone (ZÖTL 1961), as well as in the Dolomiten mountain range which belongs to the South Alpine zone (BORSATO et al. 1995).

Folded alpine karst systems are frequent in the zone of the Helvetic nappes, that is in the northern Swiss Alps (BÖGLI & HARUM 1981, LEIBUNDGUT 1995) and in Western Austria. Folded karst systems also predominate in the western section of the Northern Limestone Alps (ORTH 1992). There are transitions between folded and plateau-like systems, and some folded systems show a plateau-like morphology, e.g. the Gottesacker „Plateau“ which is presented in this thesis.

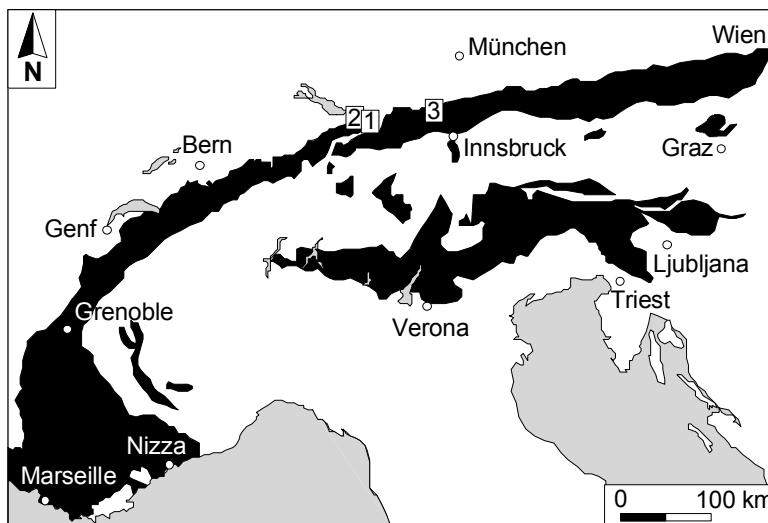


Fig. 2.2: Carbonate rock outcrops in the Alps (after BÄTZING 1997) and location of the test sites: 1. Hochifien-Gottesacker, 2. Winterstaude, 3. Alpspitze. The northern belt of karst rocks is made of the Helvetic (west) and East Alpine nappes (east), the southern belt belongs to the South Alpine zone. In the central Alps, there are some isolated karst systems (GOLDSCHIEDER et al. 2001e, Graphics: NEUKUM).

Karstifiable rocks are present within all the main tectonic-stratigraphic units of the Alps. The most extensive karst systems are formed by the

Mesozoic carbonate rocks of the South Alpine, East Alpine and Helvetic nappes. In the following sections, the distribution of karst systems in the Alps will be described for each of the main tectonic-stratigraphic units (Fig. 2.2). A detailed reference list for alpine karst systems in Austria was recently presented by KRÁLIK (2001).

2.4.3 The East Alpine zone

Extensive Triassic carbonate platforms with a total thickness of up to 4000 m are characteristic of the East Alpine zone. The two most significant carbonate formations are the Wettersteinkalk (Ladinian) and the Dachsteinkalk limestone (Norian), both up to more than 1000 m thick. The ten longest caves of Austria are developed in the Dachsteinkalk limestone (TRIMMEL 1998). Other relevant karstifiable formations are the up to 2000 m thick Hauptdolomit and the overlying 400 m thick Plattenkalk limestone (both Norian).

These formations comprise large parts of the Northern Limestone Alps, a mountain range of 500 km length and 50 km width which extends from the Alpine Rhine valley to Vienna. The mountain range can be subdivided in three sections: The western section is characterised by karst systems made of folded Hauptdolomit, Plattenkalk and Wettersteinkalk limestone, e.g. the Wettersteingebirge (see chapter 5 of this thesis). The central section is dominated by large plateau-like karst massifs formed of Dachsteinkalk limestone, e.g. the famous Dachstein Plateau (BAUER 1989) and the Tennengebirge Plateau (TOUSSAINT 1971). Plateau-like karst massifs which are formed by Wettersteinkalk limestone are typical for the eastern section, e.g. the Schneebergalpen (MAURIN & ZÖTL 1959).

Even though the Austrian Central Alps south of the Northern Limestone Alps mainly consist of crystalline rocks, some karstifiable carbonate formations are present. In the so-called graywacke zone, there are prominent caves in Palaeozoic iron-ore-bearing metamorphic limestone (TRIMMEL 1998). The Lurbach System near Graz (Austria) is made of thick and extremely karstifiable Paleozoic limestone. The area was investigated in great detail by BEHRENS et al. (1992).

2.4.4 The South Alpine zone

Triassic carbonate rocks form the most significant karst systems in the South Alpine zone which extends from Lugano to Ljubljana. Most of the prominent summits and plateau-like karst massifs in the Dolomites in

South Tyrol (North Italy) are made of the 1000 m thick Schlern dolomite (Ladinian) and the 600 m Dachstein dolomite (Norian), equivalents to the formations in the East Alpine zone. Karst systems in the Dolomites were recently described by BORSATO et al. (1995).

2.4.5 The Penninic zone

On the central Penninic shallow water threshold (Briançonnais), carbonate platforms formed locally during the Jurassic. The Sulzfluh limestone (Malm) forms some large karst systems, above all the karst plateau of Mount Sulzfluh on the Swiss-Austrian border (KRIEG 1988). Most other parts of the Penninic zone are made of non-karstifiable metamorphic rocks, predominantly schist.

2.4.6 The Helvetic zone

The Helvetic facies zone is characterised by an interstratification of limestone and marl formations that formed on the southern passive continental margin of Europe during the Jurassic and Cretaceous. The limestone formations are often intensively karstified and act as aquifers, while the marls formations act as aquicludes. The thickness of each of the formations often ranges between tens and a few hundreds of metres – significantly less than the carbonate formations in the South and East Alpine zone. The most important, thick and laterally extensive limestone formations are the up to 400 m thick Quintnerkalk (Oxfordian-Tithonian) and the up to 150 m thick Schrattekalk limestone (Barremian-Aptian) (BÖGLI & HARUM 1981).

Large parts of the Northern Swiss and the Western Austrian Alps consist of the Helvetic nappes: Berner Alps, Glarner Alps, Säntis Alps and Bregenzerwald mountains. Further to the east, the Helvetic nappes outcrop as a narrow and discontinuous stripe at the northern margin of the Northern Limestone Alps. In all of the mentioned areas, there are famous alpine karst systems, of which some have been investigated in great detail, e.g. the Muotatal area in central Switzerland (BÖGLI & HARUM 1981, YEANNIN et al. 1995) and the Säntis/Alpstein area in eastern Switzerland (LEIBUNDGUT 1995). Some of the most prominent caves in the world formed in the Schrattekalk limestone: The 182.5 km long Hölloch is number four and the 140.0 km long Siebenhengste-Hohgant-Höhlensystem is currently number seven in the list of the world's longest caves.

2.4.7 The Molasse zone

The Molasse zone is not commonly known as a karst landscape. However, within the large alluvial fans that formed in the Molasse basin during the Oligo- and Miocene near the northern margin of the Alps, there are thick, extensive and extremely coarse-grained conglomerates („Nagelfluh“) that mostly consist of carbonate components. Dolines, swallow holes and karrenfields are frequent on conglomerate outcrops (SCHOLZ & STROHMENGER 1999). GÖPPERT (2002) investigated the hydrogeology of an alpine karst system in the Molasse zone by means of tracer tests and proved underground flow velocities of up to 270 m/h and flow paths of up to 8 km length. On an area of 12 km², she mapped around 200 dolines, two small poljes, two estavelles and a karst spring with a discharge rate up to 400 L/s.

2.4.8 Overview of the three alpine test sites

The three test sites that are presented in this thesis belong to the type of folded alpine karst systems (Fig. 2.1 and Fig. 2.2). The Hochifen-Gottesacker area is situated in the Northern Alps at the border between the German state Bavaria (Allgäuer Alps) and the Austrian state Vorarlberg (Bregenzerwald Mountains). The Winterstaude is a part of the West Austrian Bregenzerwald Mountains. These two karst systems belong to the Helvetic zone and mainly consist of Cretaceous Schratenkalk limestone. The area around Mt. Alpspitze in the South Bavarian Wettersteingebirge mountain range is a part of the Northern Limestone Alps and is predominantly made of Triassic Wettersteinkalk limestone.

3 EXAMPLE: HOCHIFEN-GOTTESACKER

3.1 Location, topography, climate

The Hochifen-Gottesacker area is situated in the Northern Alps at the border between the German state Bavaria (Allgäuer Alps) and the Austrian state Vorarlberg (Bregenzerwald Mountains). The 2230 m high Mt. Hochifen (also called *Hoher Ifen*) is the highest summit. The northward bordering Gottesacker (*field of god, graveyard*) covers an area of about 10 km² and is one of the most spectacular alpine karst landscapes (Fig. 3.1). The total size of the investigated area is 72 km².

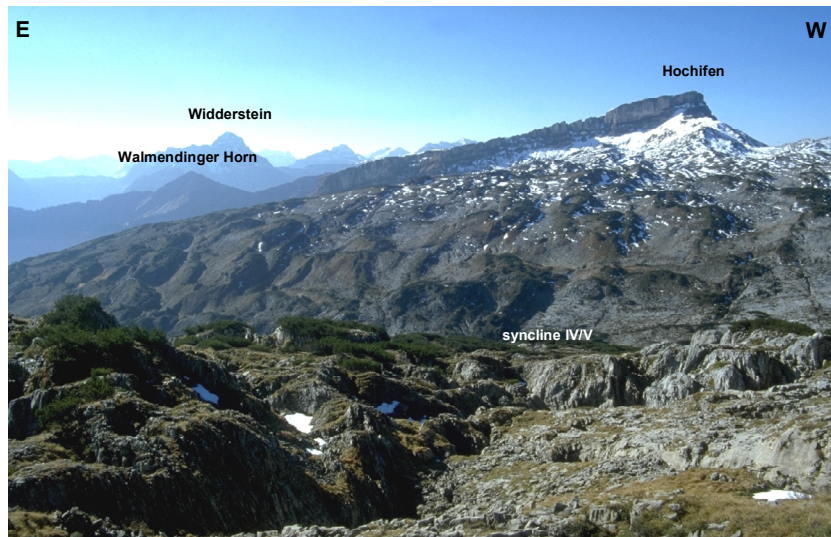


Fig. 3.1: Hochifen and Gottesacker from the north. The land surface is made of Schratenkalk limestone (Helvetic zone). The Walmendinger Horn consists of Flysch (Penninic zone) and the Widderstein is made of the Hauptdolomit formation (East Alpine zone).

Towards the east and the south, the karstified rocks plunge under the Flysch nappes along the bordering Schwarzwasser valley which consequently forms a clear tectonic boundary. However, the mountain ridge made of Flysch to the south of the valley drains by surface runoff into the karst aquifer so that the hydrologic boundary of the system is formed by the crest of that ridge. To the west of the area, the Subersach valley separates the Hochifen-Gottesacker area from the west-

ward bordering karst systems. To the north, the bordering valleys form a clear tectonic, topographic and hydrologic border.

There is no weather station in the area, but in the eastward bordering Breitach valley in an altitude of 1140 m (Fig. 3.2). There, the mean annual precipitation (1961–1990) is 1836 mm with a major maximum in June-August and a second maximum in December-January. The minimum precipitation occurs in October and in February-April respectively. The precipitation in the elevated parts of the area is assumed to be higher. The mean annual air temperature at 1140 m is 5.7 °C. In the Alps, the vertical temperature gradient is about 0.6 K/100 m, and so a mean temperature of 0 °C has to be expected at 2100 m.

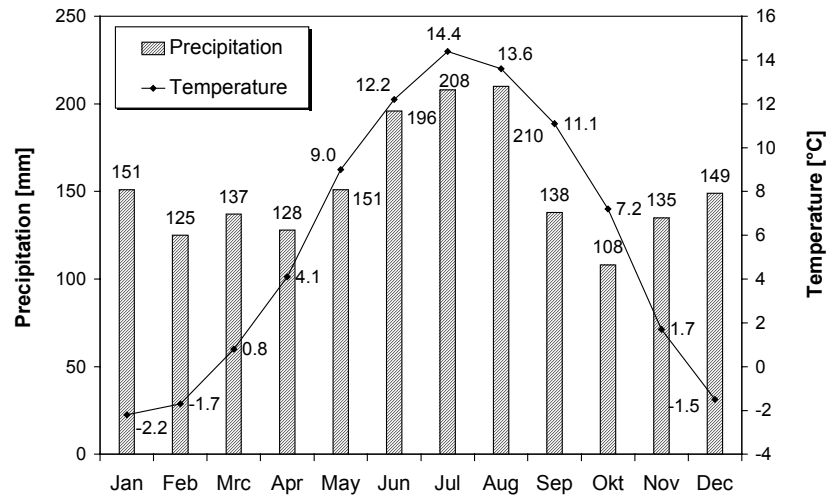


Fig. 3.2: Precipitation and temperature in the Breitach valley (1140 m, 1961–1990).

3.2 Geology

3.2.1 Geological framework

The Alps of Vorarlberg (Bregenzerwald) and SW Bavaria (Allgäuer Alps) are characterised by an extraordinary geological diversity. From north to south, the following four main tectonic-stratigraphic units of the Alps are present within a distance of around 20 km: the Molasse zone, the Helvetic, Penninic and East Alpine nappes. These units were formed side by side and were thrust on top of each other during the

alpine orogenesis. The units which formed furthest to the south, are now the highest nappes (SCHOLZ 1995).

The Molasse zone is the lowest tectonic-stratigraphic unit and forms the northern part of the Allgäuer Alps and Bregenzerwald Mountains.

The Helvetic nappes are tectonically in a higher position and are situated further to the south. They predominantly consist of Jurassic and Cretaceous sedimentary rocks. The Säntis nappe, named after the 2502 m high Mt. Säntis in the Switzerland, is the largest thrust sheet within the Helvetic nappe system (Fig. 3.3).

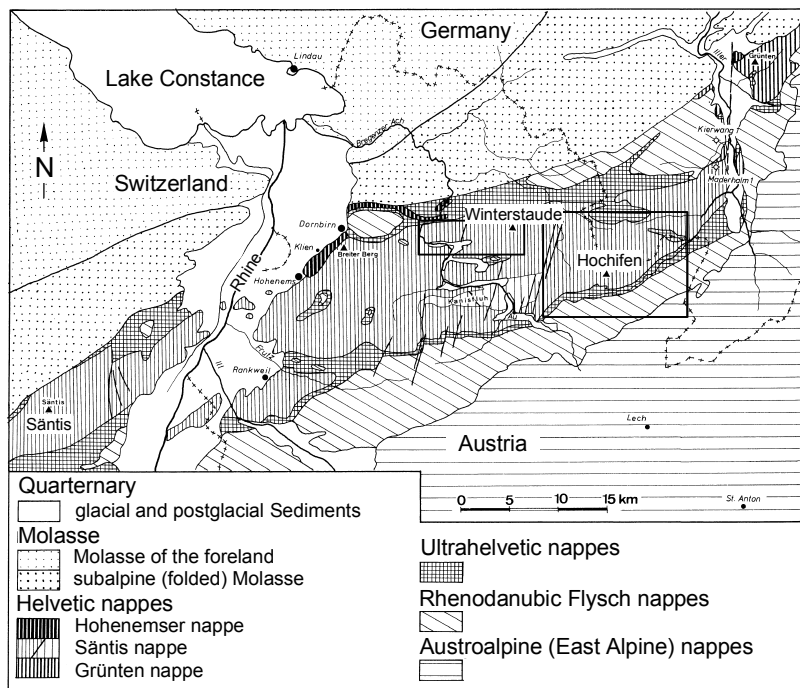


Fig. 3.3: The Helvetic Säntis nappe in western Austria (WYSSLING 1986). Location of the Hochifen-Gottesacker and Winterstaude area.

The Rhenodanubic Flysch belongs to the Penninic nappes. It formed during the Cretaceous and Paleogene. The Flysch consists of clayey sandstone and forms steep mountain ridges of up to about 2000 m, often overgrown by grass (Fig. 3.1). Between the Helvetic and Penninic nappes, there is a narrow imbricate zone of Ultrahelvetic nappes.

In large parts of western Austria, the Flysch is eroded so that the Helvetic Säntis nappe outcrops and forms a large tectonic half window (RICHTER 1984, WYSSLING 1986). To the north, south and east, the Helvetic strata plunge under the surrounding Flysch nappes. The Hochifen-Gottesacker area is both a culmination of fold axes and an anticlinorium at the eastern section of this half window.

The East Alpine nappes are the highest unit of the Alps. They mainly consist of Mesozoic sedimentary rocks and form large parts of the Northern Limestone Alps. In the Allgäuer Alps, the up to 1000 m thick Norian Hauptdolomit formation forms almost all the prominent, about 2500 m high summits of the central mountain range (Fig. 3.1).

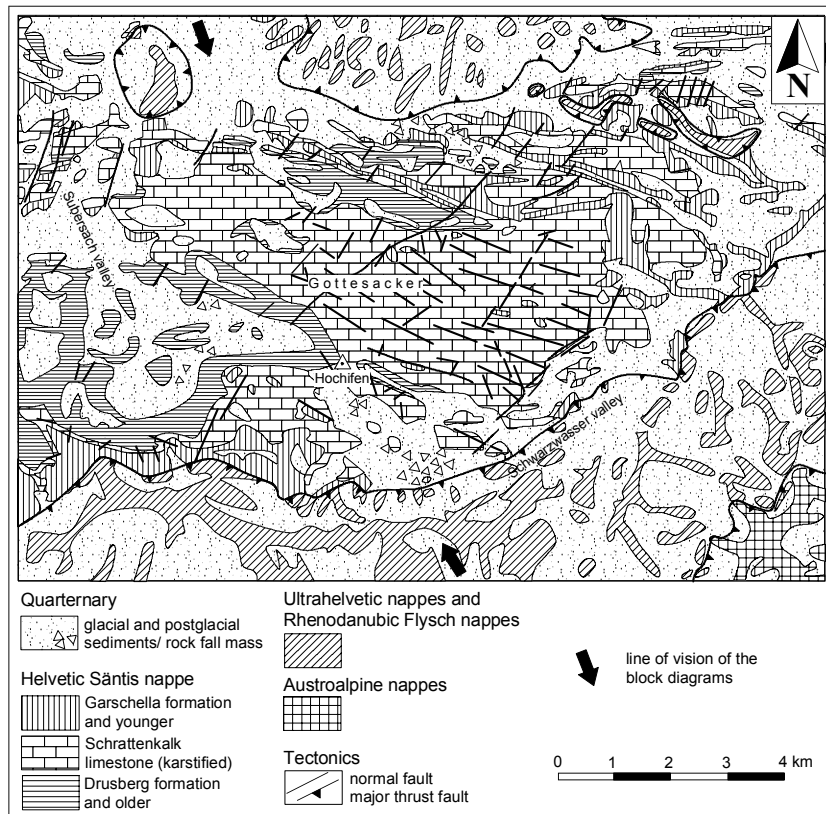


Fig. 3.4: Geological map of the Hochifen-Gottesacker area (after ZACHER 1985).

3.2.2 Stratigraphy of the Hochifen-Gottesacker area

3.2.2.1 Overview

The entire Hochifen-Gottesacker area is formed by Cretaceous sedimentary rocks of the Helvetic Säntis nappe. The southward bordering mountain range consists of Cretaceous and Tertiary formations of the Ultrahelvetic and Penninic Flysch nappes and the valleys are frequently covered by Quaternary deposits (Fig. 3.4).

Most of the formations are highly diachronous so that the lithostratigraphic mapping units (the formations) are not consistent with the chronostratigraphic classification (the stages). The stratigraphic description and above all the values for the thickness are valid for the area of investigation only but not for the entire Helvetic zone. For a short and clear way of expression, the term 'formation' will often be replaced by a characteristic rock type in the following, e.g. 'Schrattenkalk limestone' instead of 'limestone of the Schrattekalk formation'.

3.2.2.2 The Cretaceous of the Helvetic Säntis nappe

Large parts of the Alps in Vorarlberg are formed by the Helvetic Säntis nappe. In the Hochifen-Gottesacker area, sedimentary rocks form Berriasian to Maastrichtian outcrop. The Helvetic sequence is characterised by an interstratification of limestone, marl and sandstone of each several tens to hundreds of meters.

The oldest relevant rocks belong to the Palfris formation (Berriasian to Valanginian) which consists of marl and thin bedded marly limestone. As the base of this formation does not outcrop, only the minimum thickness of about 30 m can be assessed. The Kieselkalk formation (Hauterivian) is up to 60 m thick and consists of limestone which contains quartz sand, layers of chert nodules and relics of siliceous sponges. The Kieselkalk limestone often forms prominent vertical rock faces. The Drusberg formation (Barremian to Aptian) is up to 250 m thick and consists of a well bedded, monotonous interstratification of marl and marly limestone. The Drusberg marl and the older formations outcrop in the western part of the area, above all in the cores of eroded anticlines. At the west face of Mt. Hochifen, all the formations from the Palfris marl to the Schrattekalk limestone outcrop (Fig. 3.5).

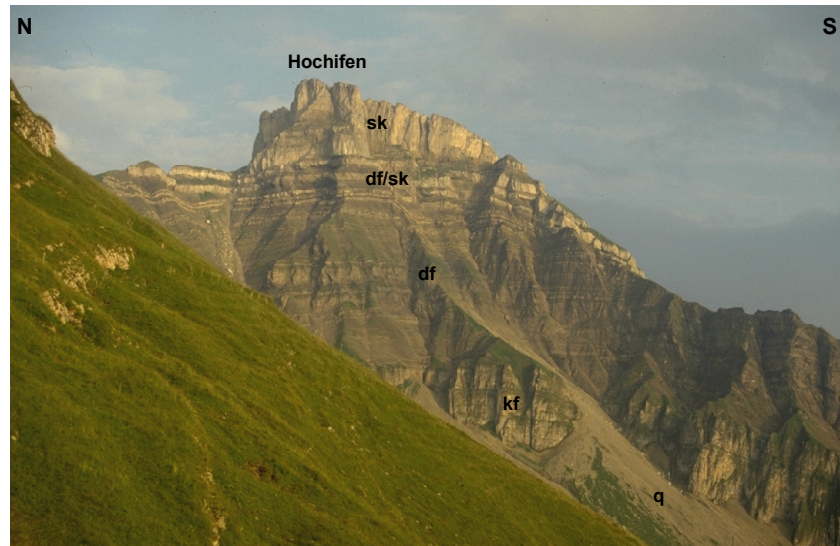


Fig. 3.5: The west face of Hochifen. Kieselkalk limestone (kf), Drusberg marl (df), transition zone (df/sk), Schrattenkalk limestone (sk), Quaternary (q).

The limestone of the Schrattenkalk formation (Barremian-Aptian) is the most prominent rock of the Helvetic zone (SCHWERD 1996). It is a pure limestone (97 % of CaCO_3) consisting of arenitic, moderately rounded detritus of fossils such as bivalves, corals and sponges, as well as the mega-foraminifere *Orbitolina* (WAGNER 1950, ZACHER 1973, BOLLINGER 1988, SCHOLZ 1995). To the south of the Hochifen-Gottesacker area, the Schrattenkalk formation is about 125 m thick, towards the north its thickness decreases at about 75 m. It forms the entire surface of the Gottesacker, the summit of Mt. Hochifen (Fig. 3.1), as well as the gorges in the Schwarzwasser and Breitach valley.

At the northern margin of the Gottesacker, the boundary between the Drusberg marl and the Schrattenkalk limestone is sharp and clear. At the southern margin, the thickness, number and purity of the interstratified limestone banks within the Drusberg marl increases towards the top of the formation until the Schrattenkalk facies is reached (Fig. 3.5). Further to the south, in the upper section of the Schwarzwasser valley, it is not possible to tell the Schrattenkalk from the Drusberg formation as there are more than 100 m of interstratification of marl and limestone banks of each several meters thickness.

The Garschella formation (Aptian to Cenomanian) is highly diachronous and characterised by significant lateral changes of facies. It consists of several members with a total thickness between a few dm and 70 m (FÖLLMI & OUWEHAND 1987). In the Hochifen-Gottesacker area, the formation is up to about 8 m thick but missing locally. It mostly consists of thick-bedded glauconitic quartz sandstone with siliceous or calcareous cement. In the upper section of the Schwarzwasser valley, karst cavities in the Schrattenkalk limestone are filled with glauconitic sandstone (Fig. 3.6). These paleokarst features indicate that the sandstone was deposited transgressively on a karstified land surface (SINREICH 2000). The overlying Seewerkalk formation (Turonian to Santonian) consists of up to 50 m of thin-bedded limestone which is missing in large parts of the Hochifen-Gottesacker area.

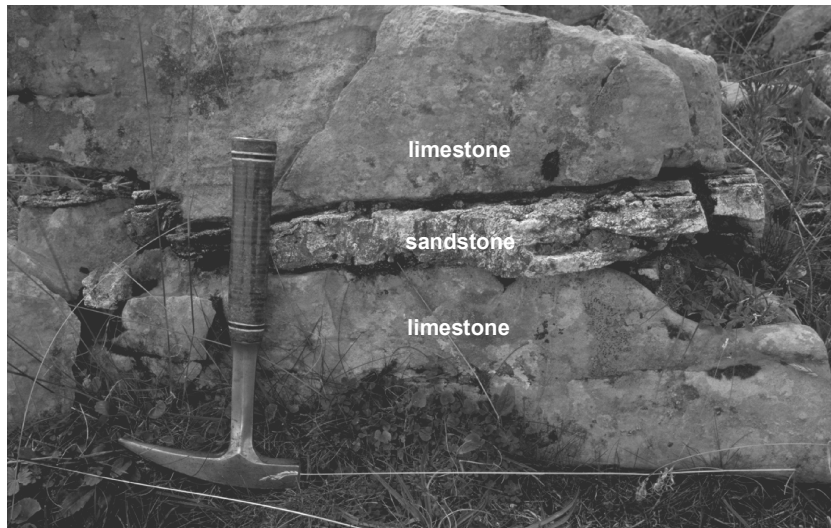


Fig. 3.6: Paleokarst in the upper Schwarzwasser valley. Cavities in Schrattenkalk limestone are filled with Garschella sandstone.

The diachronous Amdener formation (Santonian to Campanian) consists of up to 250 m of monotonous, sandy-silty marl with intensive cleavage. The overlying Wang formation consists of marl as well but is more sandy and glauconit-bearing than the Amdener marl (HÖPFNER 1970). The total thickness is about 200 m (SCHWERD 1996) but less than 100 m outcrop in the area of investigation (SINREICH 1998). The Garschella and the younger formations are preserved in the cores of synclines and in a narrow zone along the valleys.

3.2.2.3 The Ultrahelvetic and Penninic Flysch nappes

A zone of multiple imbricates, consisting of isolated wedges, is located between the Helvetic nappes and the Rhenodanubic Flysch. In the Allgäuer Alps and in Vorarlberg, this zone is represented by the Ultrahelvetic Liebensteiner nappe and the Feuerstätter Flysch nappe (SCHWERD 1996). Along the Schwarzwasser valley, a narrow zone of highly disturbed heterogeneous sedimentary formations (Cenomanian–Eocene) outcrops, consisting of limestone, marl, sand- and claystone.

The Rhenodanubic Flysch nappe belongs to the Penninic nappes, though its paleogeographic position is still disputable (SCHOLZ 1995). The sedimentary rock formations of the Rhenodanubic Flysch form the mountain range on the southern side of the Schwarzwasser valley: The Ofterschwanger formation (Albian to Cenomanian) is between 200 and 300 m thick and consists of clayey-marley sediments with some banks of sandstone and limestone; the Reiselberger formation (Cenomanian to Turonian) is up to 500 m thick and consists of thick-bedded turbiditic sandstone rich of biotite and rock fragments; the Piesenkopf formation (Turonian to Coniacian) is up to 250 m thick and consists of a thin-bedded interstratification between marl and limestone.

3.2.2.4 Quaternary deposits and rockfalls

The Schwarzwasser valley and the Subersach valley are covered with widespread moraines which locally include clayey sediments from glacial lakes. Steep slopes are often covered with scree. Rock fall material, consisting of large blocks, is frequent below rock faces of the Schrattekalk limestone. In the wide and gentle section of the valleys, alluvial sediments were deposited.

Several rockfalls and rock slide-avalanches occurred after the deglaciation, the most important one from the southern slope of Mt. Hochifen which is formed by the southern limb of an anticline. Here, the Schrattekalk limestone dips about 25 to 30° southwards and is underlain by the Drusberg marl which acted as a lubricating surface. The landslide came to rest in the upper Schwarzwasser valley and forms a block field of 1 km² consisting of Schrattekalk debris and blocks up to the size of a house. The volume of the rockfall mass is estimated between 7.2 (SCHMIDT-THOMÉ 1960) and 10 millions of m³ (WAGNER 1950). As the river loses all its sediment load at this obstacle, a large alluvial plain formed upstream from the rockfall mass.

3.2.3 Tectonics

3.2.3.1 Folds

As the sedimentary sequence of the Helvetic zone is characterised by an interstratification of competent limestone (Kieselkalk and Schratenkalk formations) and incompetent marl (Drusberg and Amdener formation), polyharmonic flexural-shear folds are the predominant fold type (EISBACHER 1996). The Schratenkalk limestone forms north-verging folds with wavelengths between 1 and 2 km and amplitudes of up to 800 m while high order folds can be observed locally in the Drusberg marl (GOLDSCHIEDER 1997).



Fig. 3.7: The eastern Hochifen-Gottesacker area with the Schwarzwasser valley. The Schratenkalk limestone is gently folded (folds with roman numerals).



Fig. 3.8: The western margin of the Hochifen-Gottesacker area. The valley cuts through the limestone in the tight anticlines.

Within the Säntis nappe, the folds generally trend W-E. To the west of the area, the fold axes form a depression in the Subersach valley and

rise to a culmination on the top of the Hochifen-Gottesacker area. Here, the fold axes turn in ESE to SE direction and plunge under the Flysch nappes along the Schwarzwasser valley. The Hochifen-Gottesacker area is both a culmination and an anticlinorium.

The degree of tectonic constriction increases from east to west, so that the folds are open at the eastern and close at the western border of the area. Consequently, gently folded Schrattekalk limestone is preserved along the entire Schwarzwasser valley (Fig. 3.7), while the Subersach valley cuts through the limestone in the tight anticlines (Fig. 3.8).

As anticlines often form ridges while synclines often form valleys, the folds can easily be recognised in the field (Fig. 3.9). However, there are impressive examples of relief inversion. When the Schrattekalk limestone is removed in an anticline, the underlying formations are eroded quickly so that deep valleys form, surrounded by steep rock faces of Schrattekalk limestone.

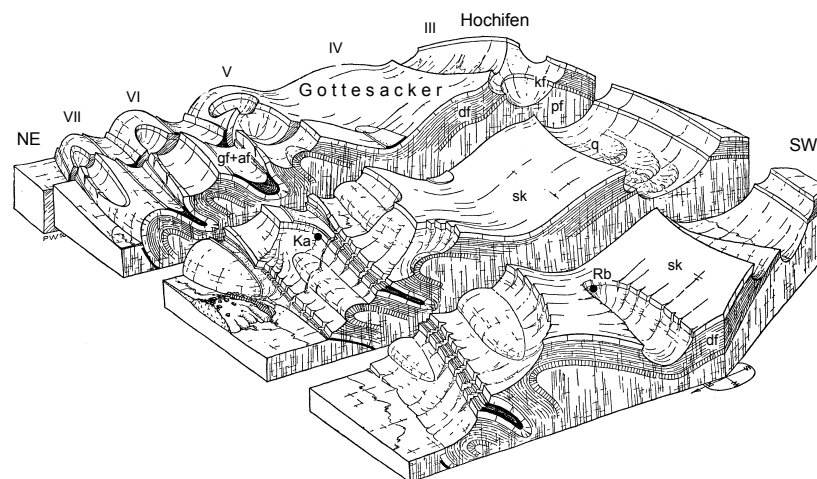


Fig. 3.9: Block diagram of the Hochifen-Gottesacker area, view from NW. Tectonics: anticlines (roman numerals), synclines, fault pattern; stratigraphy: Palfris (pf), Kieselkalk (kf), Drusberg (df), Schrattekalk (sk), Garschella (gf), Amdener (af) formation, Quaternary deposits (q); hydrology: Kessleralp spring (Ka), Rubach (Rb) spring (WAGNER 1950, supplemented).

WAGNER (1950) describes eleven fold trains in the eastern section of the Säntis nappe; six anticlines and five synclines are situated in the Hochifen-Gottesacker area (Fig. 3.10). In the following, the anticlines

3.2 Geology

are numbered from S to N in roman numerals; the synclines are numbered by combining the numerals of the bordering anticlines.

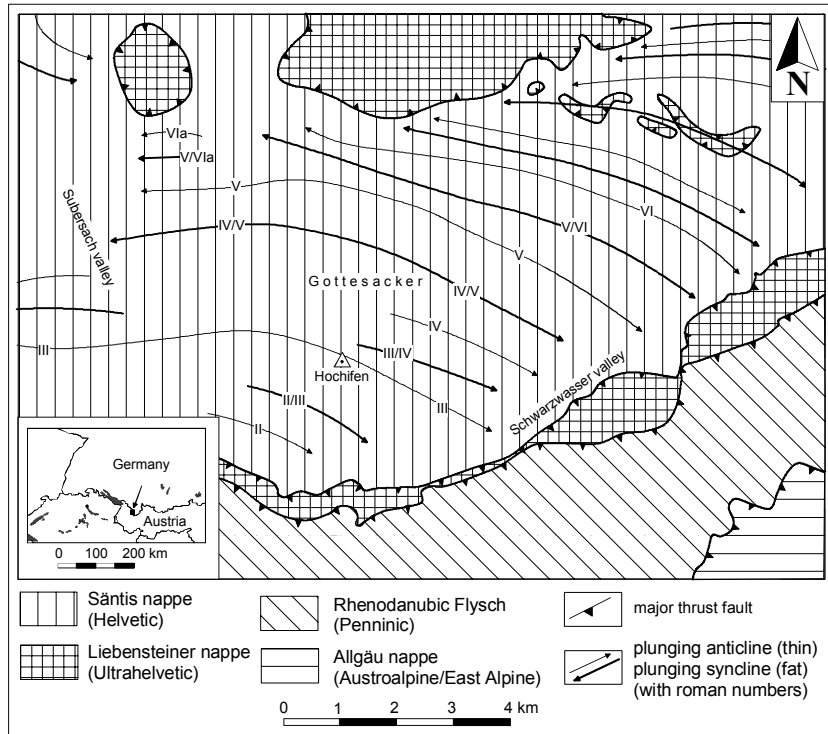


Fig. 3.10: Fold tectonics in the Hochfifen-Gottesacker area.

The western section of the anticline VI is eroded along its crest so that the Schratenkalk limestone form a series of rock faces of about 100 m height and 6 km length, while the older formations outcrop along the core of the anticline. The fold axis culminates in its middle section and plunges in ESE direction under the Breitach valley where the limestone is covered by younger rocks. However, the Breitach gorge cuts the limestone at the crest of the anticline. The short anticline VIa in the western part of the area is not a prolongation of the anticline VI but an independent structure.

The southward bordering syncline V/VI forms the Mahdtal valley in its eastern section, culminates in the middle section, forms a valley in the western section and breaks off in a vertical rock face. Along the core of

the syncline and in the lower section of the Mahdtal valley, the limestone is covered by younger formations. The short syncline V/V1a in the western part of the area is an independent structure.

The anticline V begins in the Subersach valley (W), rises to an axial culmination at the northern margin of the Gottesacker and plunges in ESE direction under the Schwarzwasser valley (E) where the river cuts a deep gorge into the Schrattekalk limestone. In the eastern and western section of the anticline, the limestone is preserved forming rounded mountain ridges. In the middle section, it is deeply eroded along the crest of the anticline so that the older formation outcrop along two valleys (relief inversion). The vertical, 100 m high and 5 km long series of rock faces at the southern margin of this erosional window are formed by the southern limb of the anticline, while the northern limb forms a wall-like landform.

The syncline IV/V culminates in the centre of the Gottesacker, forms large dry valleys on both sides of the culmination and plunges in ESE and W direction under the bordering Schwarzwasser and Subersach valley respectively. In the eastern section of the syncline, the Schrattekalk limestone is preserved and outcrops on the entire surface. In the western section, it is locally eroded so that the Drusberg formation outcrops in an erosional window which is surrounded by rock faces of the Schrattekalk limestone (Fig. 3.9).

The anticline IV forms the southern part of the Gottesacker. However, it is an independent structure east of the culmination only, while it unifies with the southward bordering anticline III further to the west. Thus, the syncline III/IV exists in the eastern part of the Gottesacker only and forms a dry valley there. A large normal fault runs parallel to this valley.

The anticline III culminates at the summit of Mt. Hochifen and plunges in ESE direction under the Schwarzwasser valley. Towards the west, it unifies with the northward bordering anticline IV. This anticline is an excellent example for relief inversion (SCHMIDT-THOMÉ 1960). Along the crest of the anticline, the Schrattekalk limestone is eroded removed so that valleys formed by fluvial and glacial erosion. To the west of Mt. Hochifen, the entire stratigraphy from the Palfris to the Schrattekalk formation outcrops in a 600 m deep valley (Fig. 3.9). The eastward prolongation of that valley is a cirque (Ifenmulde) north-east of Mt. Hochifen. The summit of Mt. Hochifen is formed by a remnant of the southern limb of the anticline.

Both the syncline II/III and the southward bordering anticline II are only about 2 km long. Their eastern sections form the landscape south of Mt. Hochifen in the upper Schwarzwasser valley. The interstratification between Drusberg marl and Schrattekalk limestone outcrops at the land surface. The fold axes plunge in ESE direction under the large rockfall mass which fell from Mt. Hochifen (Fig. 3.13). The western sections of the folds are eroded. The southern limb of the anticline II is covered with the rocks of the Garschella, Amdener and Wang formation. South of this anticline, the Helvetic Säntis nappe plunges under the Ultrahelvetic and Penninic Flysch nappes.

3.2.3.2 Fault tectonics

The Hochifen-Gottesacker area is intensively cut by a network of faults (Fig. 3.4), most of them with minor displacement. Within the competent Schrattekalk limestone, the fault surfaces are sub-vertical and clearly visible as they often form fault scarps. Within the under- and overlying incompetent formations, the deformation is rather penetrative so that the fault tectonics is less clearly developed. The faults belong to two main systems: SW-NE trending faults (short: NE faults) and SE-NW trending faults (short: NW faults).

The NE faults trend 40 to 50° (CRAMER 1959) and are left-lateral strike-slip faults with a significant extension component. Three important NE fault zones cross the area:

- A branch of the 'Ostergunten fault zone' (OBERHAUSER 1951) follows the Subersach valley with a horizontal displacement of about 1 km.
- The 'big fault' (WAGNER 1950, CRAMER 1959) follows the culmination line on top of the Gottesacker and is clearly visible as it cuts through the anticlines V, VI and VII (Fig. 3.9). The displacement of this fault is about 120 m.
- The 'Schwarzwasser fault zone' (GOLDSCHIEDER 1997) runs parallel to the Schwarzwasser valley and forms a series of vertical rock faces at the left (NW) side of the valley, as well as a line of dolines and dry valleys below these rock faces.

The fold pattern is different on both sides of these NE major faults, indicating that the faulting started before the end of the folding (RICHTER 1984). Due to the extension component normal to the sub-vertical fault surface, open fissures formed and were filled with reddish calcite veins of up to 12 m width (WAGNER 1950).

The NW faults trend 120 to 130° (CRAMER 1959) and are normal faults with right-lateral strike-slip displacement. As the NW faults displace the NE faults, the former are clearly younger than the latter. The NW faults have no extension component and are consequently closed. However, they are often enlarged by corrosion and form karst corridors (bogaz) or lines of dolines. A significant NW fault runs parallel to the syncline III/IV and forms a fault scarp of 40 to 60 m (GOLDSCHIEDER 1997).

Other fault directions can be observed locally. The most significant are S-N, W-E, WSW-ENE and SSE-NNW (WAGNER 1950, CRAMER 1959).

3.3 Hydrogeology

3.3.1 Hydrogeological function of the strata

The hydrogeology of the Hochifen-Gottesacker area is characterised by a karst aquifer of about 100 m thickness which is underlain and, locally, overlain by lowly permeable layers.

The Palfris and Kieselkalk formation outcrop only locally and play no significant role in the hydrogeology of the area. The Palfris marl is characterised by low permeability. The Kieselkalk formation consists of impure, siliceous limestone and is slightly karstifiable. In the Muotatal area in central Switzerland, the Kieselkalk is well karstified in its upper part and only fractured and slightly karstified in its lower part (BÖGLI & HARUM 1981).

The Drusberg formation mostly consists of marl, acts as an aquiclude and forms the base of karstification below the overlying Schrattenkalk limestone. The underground karst water flow takes place near the base of the Schrattenkalk limestone on top of the Drusberg marl or within the karstified limestone banks in the upper part of the Drusberg formation.

The Schrattenkalk formation consists of a competent pure limestone (97 % of CaCO₃) without significant matrix (intergranular) porosity. The limestone is intensively cut by faults and fractures which have been locally reactivated by mass movements. The Schrattenkalk limestone is extremely karstifiable and forms a karst major aquifer which is characterised by high flow velocities, short residence times and fast hydraulic reactions to hydrologic events. There is no surface runoff but all the discharge takes place underground. According to BÖGLI & HARUM (1981), this limestone is the major karst rock in the Helvetic zone.

The transition zone between the Schrattekalk and Drusberg formation consists of an interstratification between marl and limestone banks of each several meters thickness. The limestone banks form thin karst aquifers which correspond to each other via faults and fractures. They show similar characteristics as the Schrattekalk karst aquifer (SINREICH 1998, GOLDSCHIEDER & HÖTZL 2000).

The Garschella sandstone and, above all, the Amdener marl are lowly permeable and form an aquiclude on top of the karst aquifer. The Amdener marl always drains by surface runoff and often forms the underground of wetlands and highmoor bogs. However, in other parts of the Helvetiv zone, some members of the Garschella formation are made of karstifiable rocks and form a hydrogeological unity with the Schrattekalk limestone (BÖGLI & HARUM 1981).

The Flysch formations consist of an interstratification of claystone, impure sandstone, marl and thin-bedded limestone. They are characterised by a low permeability and frequently drain by surface runoff.

The composition and permeability of the Quaternary deposits is highly variable. Permeable glacial sediments cover large parts of the Schwarzwasser valley. However, they contain no significant groundwater because they are underlain by karstified limestone, so that infiltrating water percolates through the granular material and infiltrates into the karst aquifer. Locally, the karst surface is sealed by clayey ground moraine, so that moors have been formed.

A granular aquifer of local importance formed in moraine, scree and rockfall material on top of the Drusberg marl in the cirque 'Ifenmulde' NE of Mt. Hochifen. In the Subersach valley a significant groundwater body is developed in glacial and alluvial sediments which cover the plunging syncline IV/V, that is the so-called 'Iferwies' granular aquifer.

Even though that the large rockfall mass in the upper section of the Schwarzwasser valley is strictly speaking a granular aquifer, it shows remarkable hydrologic similarities to a karst aquifer: high flow velocity, short residence time, fast reactions on hydrologic events and lack of surface runoff (SINREICH et al. 2002).

3.3.2 Surface and subsurface karst landforms

The Hochifen-Gottesacker area is the largest and most impressive karst landscape within the Alps of Vorarlberg and SW Bavaria (Fig. 3.1). Due to its large variety of karst landforms and the vegetation, it is considered to be of 'international importance' (BROGGI 1987). The exo-

karst landforms were described by ECKERT (1902), WAGNER (1950), CRAMER (1959), SCHMIDT-THOMÉ (1960), ROSENDAHL & GRUNER (1995), GOLDSCHIEDER (1997) and ROSENDAHL (2000). There are numerous publications on the caves. The most recent and comprehensive overview was given by FUMY et al. (2000).

The elevated part of the Gottesacker is a large, bare karren field. Deep and sharp-edged klufkarren are predominant, frequently decorated by small rillenkarren. Free karren are characteristic for the outcrops of bedding planes, especially in less fractured zones. The type of free karren is controlled by the gradient: Meandering karren develop on gentle gradients ($< 5^\circ$), rinnenkarren on moderate gradients ($5\text{--}40^\circ$), rillenkarren on steep gradients ($> 40^\circ$). The lower parts of the Gottesacker are covered with shallow, patchy rendzina soil and overgrown with coniferous forest. Large outcrops of round karren without soil are frequent and prove young erosion, because this type of karren forms below the soil only (CRAMER 1959).

The fault directions are of major importance for the pattern of karstification. Especially the NW faults are often followed by lines of dolines and shafts – although the NW faults have no significant extensional component. Frequently, the dolines and shafts are so close to each other, that they unify and form corridors (bogaz) of hundreds of meters length and several meters depth and width. Natural bridges which cross the corridors prove that the NW faults were originally closed. The NE faults are filled with reddish calcite veins which are less karstifiable and consequently form linear, dam-like structures. They are called 'red lines' (WAGNER 1950) and are often used as footpaths.

The area is rich in caves: 24 caves of more than 50 m length are known (FUMY et al. 2000). The largest one is the 5.3 km long Hölloch in the Mahdtal valley which must not be mixed up with the 182.5 km long Hölloch in the Swiss Alps, the fourth longest cave in the world. However, both caves formed in the same limestone formation.

The caves consists of vertical shafts of up to 80 m and passages parallel to the bedding, frequently close to the base of the Schraffenkalk limestone. Many caves follow approximately the troughs of the synclines. In detail, the cave plans are controlled by the fault directions and the bedding (GOLDSCHIEDER et al. 2000c). The Schwarzwasser cave – named after the valley where it is located – is the most interesting object from the hydrological point of view, because it acts as an estavelle (GOLDSCHIEDER et al. 1999b).

3.3.3 Hydrogeological zoning

In the Hochifen-Gottesacker area, the base of the Schrattekalk limestone forms the base of karstification, while the surrounding rivers act as receiving channels and form the base level of the system. Consequently, all the elevated parts of the area belong to the zone of shallow karst as was defined by BÖGLI (1978). The characteristic of the Schwarzwasser valley is ambivalent in terms of hydrogeological zoning: On the one hand, the base of the karst aquifer is below the valley floor (deep karst?). On the other hand, in large parts of the valley, the base of the karst aquifer is above the springs which discharge the aquifer (shallow karst?). Clear deep karst is present in the lowest section of the valley and in the Schrattekalk aquifer below the Flysch mountains.

Large parts of the area are formed by outcrops of karstified Schrattekalk limestone and thus belong to the zone of open karst. Along the valleys, the karst aquifer is locally covered by non-karstifiable deposits. The zone of covered karst can be subdivided into the zone of buried karst, where the aquifer is overlain by deposits which are younger than the karstification (rockfall masses, moraines) and in the zone of subterranean karst, where the aquifer is covered by formations which are older than the karstification (but younger than the limestone).

In the entire zone of open karst, as well as in large parts of the zone of covered karst, the groundwater is unconfined. Confined conditions are present locally, where the karst aquifer is covered by impervious formations in the core of synclines plunging under the valley floor. An artesian system of local importance was proved in the lower section of the Schwarzwasser valley, where the syncline V/VI plunges under the base level (GOLDSCHIEDER 1997).

3.4 Springs and surface waters

3.4.1 Overview

The Hochifen-Gottesacker area is located at the European or continental watershed between the River Rhine and the Danube. The eastern part of the area is tributary to the Danube (via Schwarzwasser river, Breitach and Iller), the western part is tributary to the Rhine (via Subersach river, Bregenzerach and Lake Constance). An overview of the relevant springs in the area is presented in Tab. 3.1 and Fig. 3.11.

Tab. 3.1: Overview of the important springs in geographical order and decreasing altitude. The term *complex* is used for proved interaction between different aquifer types and for disputable situations; explanations in the text.

area	name of the spring	symbol	altitude [m.a.s.l.]	discharge [l/s]	type of aquifer
South and East	upper resurgence	Ru	1280	0-2500	rockfall
	lower resurgence	Rl	1280	6-70	rockfall
	estavelle	Ev	1120	-500 to 4000	karst
	Aubach spring	Au	1080	0-6000	karst
	Bürgermeister spring	Bü	1040	40	karst
	Kesselschwand spring	Ks	1050	15	karst
	Sägebach spring	Sb	1035	150-2000	karst
	bottom spring	Bo	980	200	karst
North	Kessleralp spring	Ka	1440	10-60	karst
West	Rubach spring	Rb	1600	10-200	karst
	Rubach lake spring	Ls	1490	30-50	complex
	Schneckenlochbach spring	Sl	1220	10-1000	karst
	Laublisbach spring 1	La1	1070	3-20	karst
	Laublisbach spring 2	La2	1040	1-4	karst
	Laublisbach spring 3	La3	1025	5-50	complex
	Laublisbach spring 4	La4	1025	5	complex
	Goldbach spring 1	Gb1	1010	42-82	complex
	Goldbach spring 2	Gb2	990	4-56	granular
	Goldbach spring 3	Gb3	990	70-246	karst
	Goldbach spring 4	Gb4	980	4-151	granular
spring near Subersach river	Su	960	15-46	karst	

3.4.2 Eastern Hochifen-Gottesacker area

The eastern part of the Gottesacker drains underground. In the northward bordering Mahd tal valley, the underground flow can be observed directly in the turbulent stream of the Hölloch cave (Fig. 3.12). The lower section of the valley is formed by the impervious Garschella and Amdener formation and drains by surface runoff.

At the southern margin of the Gottesacker, east of Mt. Hochifen, several small springs drain the granular aquifer in the Ifenmulde cirque. However, the water seeps underground after a short distance. One of the springs is used for the drinking water supply of a mountain hut.

3.4 Springs and surface waters

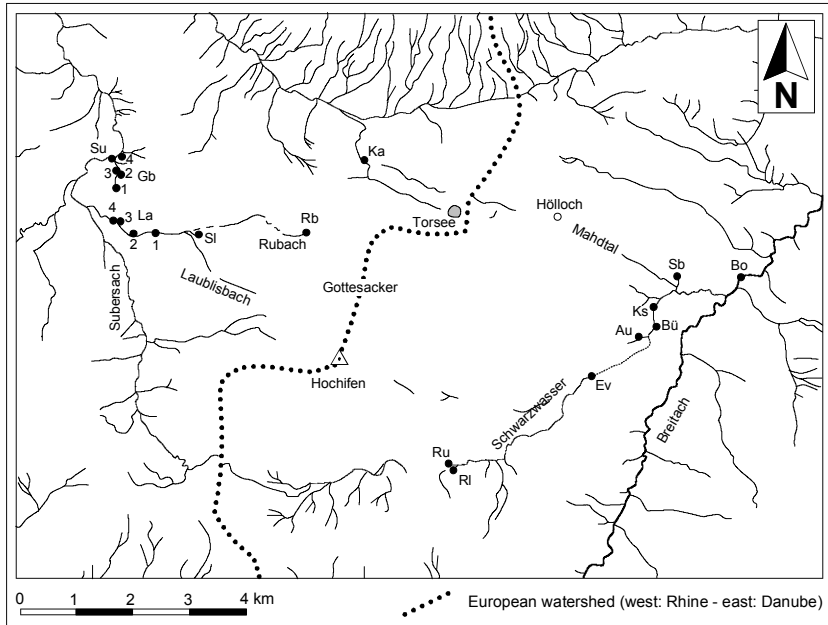


Fig. 3.11: Important springs (with shorthand symbol) and surface waters in the area.

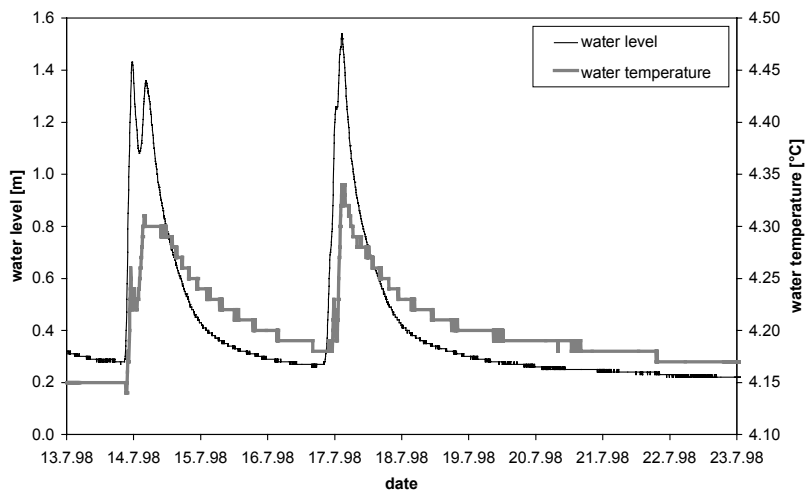


Fig. 3.12: The hydrograph of the Höllloch cave stream is representative for karst water flow in the trough of a plunging syncline (unpublished data A. Wolf).

In the Schwarzwasser valley, the karstified limestone plunges under the Flysch nappes in southern and eastern direction. This geological asymmetry leads to a hydrological asymmetry: The Flysch mountains at the SE (right) side of the valley are predominantly drained by surface runoff, while the karst area at the NW (left) side is drained underground. Therefore the Schwarzwasser river is supplemented by many tributaries from the right side of the valley but no tributaries from the left side. Consequently, there are two flow systems in the valley: the surface river that drains the right side of the valley and the underground karst water flow (GOLDSCHIEDER & HÖTZL 2000).

The valley is characterised by a change of gorges and wide valley floors. The gorges are situated in the anticlines where the river cuts the limestone, while the valley floors are located in the synclines, where sandstone and marl outcrop, covered by young sediments.

The Schwarzwasser river has its source at the European watershed and belongs to the catchment of the Danube. In an altitude of 1340 m, it sinks via swallow holes in the rockfall mass which precipitated from Mt. Hochifen and caused obstruction in the valley. Below the rockfall, there are two neighbouring groups of springs at 1280 m: The upper one is the resurgence (*Ru*) of the Schwarzwasser river, while the lower one is the resurgence (*Ri*) of several small streams from the Flysch mountains (Fig. 3.13) (SINREICH 1998).

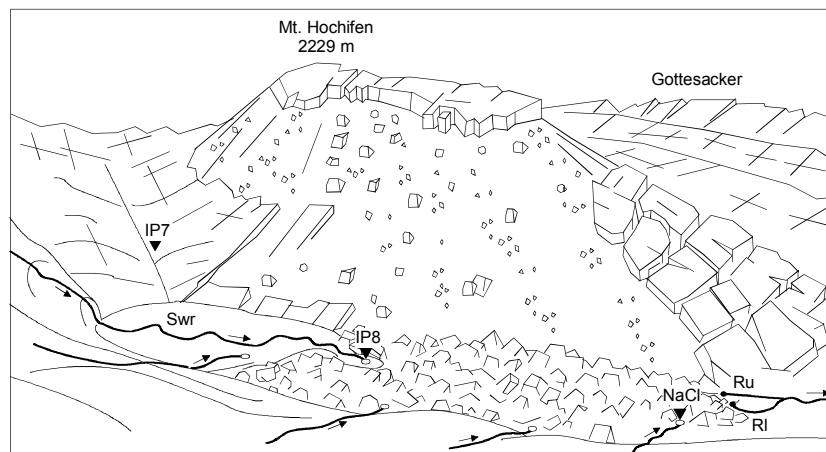


Fig. 3.13: Hochifen and the rockfall mass in the Schwarzwasser valley from SE; size of the blocks exaggerated, vegetation removed; Swr: Schwarzwasser river; IP: injection points of the tracer tests (see there).

3.4 Springs and surface waters



Fig. 3.14: Under low water conditions, the Schwarzwasser cave is a swallow hole.



Fig. 3.15: Under high water conditions, the cave becomes a spring.

In the middle section of the valley, the anticline IV plunges under the valley, so that the karstified limestone outcrops and is cut by the river, forming a gorge. Under low water conditions, the river sinks in the entrance of the Schwarzwasser cave which is situated in this gorge at

1120 m (Fig. 3.14). Under high water conditions, the cave entrance acts as a spring. Consequently, the cave is an estavelle (shorthand symbol: *Ev*), probably the largest in the Alps (Fig. 3.15). The highest observed discharge is about 4 m³/s and the highest sink rate about 0.5 m³/s. The cave connects the surface river with the underground karst water flow. According to the definition suggested by GOLDSCHIEDER et al. (1999b), it is an active, normal estavelle (Tab. 3.2).

Tab. 3.2: Suggested classification for estavelles; detailed explanation see GOLDSCHIEDER et al. (1999b).

suggested term	driving force	high water function	low water function	reference (example)
active or normal estavelle	variation of hydraulic head in the aquifer	(bottom) spring	swallow hole	Goldscheider et al. 1999b
passive or inverse estavelle	variation of water level in the receiving channel	swallow hole	(bottom) spring	Spöcker 1950
submarine estavelle	variation of freshwater pressure	freshwater spring	sea water swallow hole	Kuscer & Kuscer 1964

About 1 km downstream, the river receives inflow from the Aubach spring (*Au*) which is located at 1080 m in a gorge that follows a SWS-ENE trending fault. The spring comprises several outlets, discharges up to about 6 m³/s and dries up in long periods without recharge.

In the year 2000, the *Landeswasserbauamt Bregenz* installed a measuring point at the Aubach spring. The electrical conductivity, water temperature, turbidity and water level are measured each 15 minutes. The stage discharge curve is not yet established, and so it is impossible to calculate the discharge on the basis of the measured values. As the measuring point is 200 m downstream from the highest outlet of the spring, the air temperature influences the water temperature.

During snow melt, the spring shows characteristic daily variations: The minimum discharge (water level) occurs before midday and coincides with the maximum water temperature, turbidity and electrical conductivity. The highest discharge takes place during the late evening and coincides with decreasing temperature, minimum conductivity and turbidity (Fig. 3.16). A storm rainfall event during summer causes a sudden increase of the discharge rate. The maximum discharge rate coincides with the minimum temperature and conductivity. The turbidity first de-

3.4 Springs and surface waters

creases due to dilution and then increases due to the transport of sediments in the karst network (Fig. 3.17).

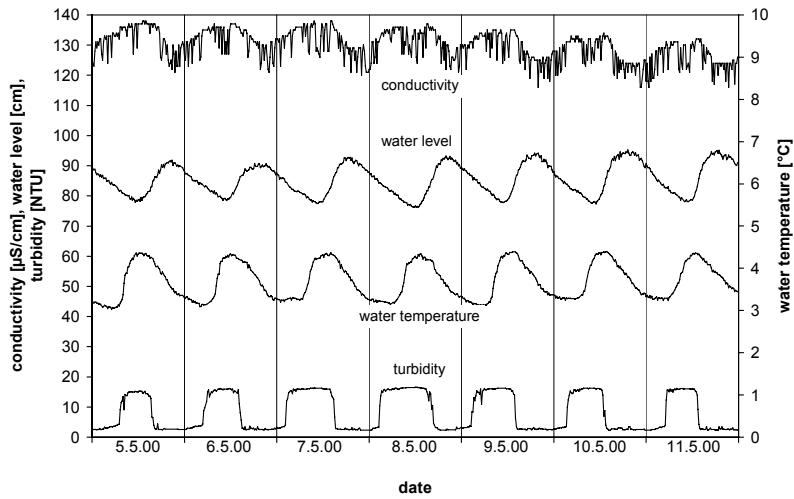


Fig. 3.16: Hydrograph of the Aubach spring during the snow melt (data: Landeswasserbauamt Bregenz; stage discharge curve not yet established).

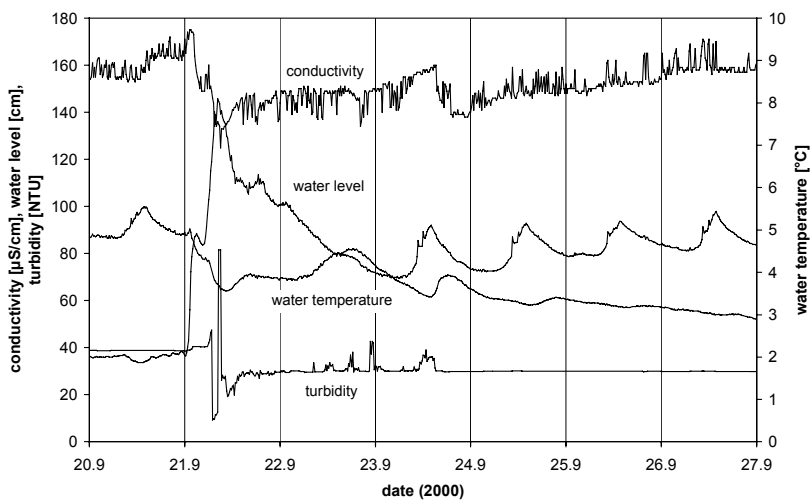


Fig. 3.17: Hydrograph of the Aubach spring during a storm rainfall event.

In the gorge below the confluence of the Schwarzwasser river and the Aubach stream, there are two permanent karst springs: The Bürgermeister spring (*Bü*) at 1050 m altitude and the Kesselschwand spring (*Ks*) at 1040 m discharge nearly constantly about 40 and 15 l/s respectively. The springs *Au*, *Bü* and *Ks* are located in the anticline V.

Below these springs, the limestone is covered by the low permeable younger strata in the core of the syncline V/VI which forms the Mahdtal valley. At 1035 m altitude, these strata are eroded locally along a normal fault, so that the karst aquifer outcrops in a low topographic position. This is the location of the Sägebach spring (*Sb*) that discharges between 150 and about 2000 l/s. Earlier authors assumed that the Mahdtal valley is the only catchment of *Sb* (WAGNER 1950, CRAMER 1959, SPÖCKER 1961). However, under low water conditions, the discharge of *Sb* is significantly higher than the total discharge of the Schwarzwasser river upstream from *Sb* (about 55 l/s) even though that the Schwarzwasser valley is much larger than the Mahdtal valley. Thus, GOLDSCHIEDER (1997) concluded that the catchment of *Sb* must include the Schwarzwasser valley.

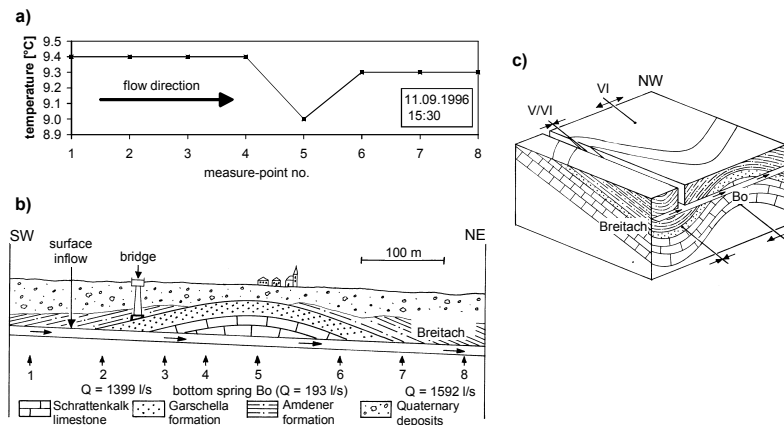


Fig. 3.18: The bottom spring (Bo) in the Breitach river. a) temperature profile, b) geological view-profile, c) schematic block diagram.

Below the confluence of the Schwarzwasser river and the Breitach river, the limestone outcrops again in the anticline VI. Here, it was possible to detect an anomaly in temperature and electrical conductivity indicating the upwelling of cold karst water (Fig. 3.18). By measuring the discharge of the river above (1399 l/s) and below (1592 l/s) this

anomaly using the salt-dilution method, the discharge rate of this invisible bottom spring (*Bo*) was determined: 193 l/s under low to medium water conditions. As the spring is the lowest (980 m) and probably the youngest outlet, the Breitach river forms the base level of the karst system (GOLDSCHIEDER & HÖTZL 2000). Further development of the karst system will increase the discharge rate of this lowest spring, while the significance of higher springs will decrease.

Beside these karst springs, there are several small springs in the Schwarzwasser valley and the Mahdtal valley which are discharged from small granular aquifers consisting of Quaternary deposits and from bogs (described in detail by GOLDSCHIEDER 1997). However, the spring water usually sinks underground before reaching the river.

3.4.3 Western Hochifen-Gottesacker area

The western Gottesacker is mainly formed by the syncline IV/V. Locally, the karstified Schratenkalk limestone is eroded in the trough of the syncline so that the Drusberg marl outcrops in an erosional window, surrounded by limestone rock faces. The valley floor is covered with alluvial sediments (gravel).

The Rubach spring (*Rb*, 1600 m) is situated at the upper edge of this erosional window, in the trough of the plunging syncline IV/V and near the base of the karst aquifer (in a limestone bank between marl beds). The spring discharges from a fault which has probably been reactivated by mass movements due to the adjacent deep erosional window (Fig. 3.19). The discharge rate ranges between about 10 and 200 l/s. The 870 m long Rubach cave is adjacent to the spring. Its sub-horizontal 2-D network (controlled by the syncline, the faults and the bedding) is typical for confined flow in thin beds of soluble rocks between impervious beds (sandwich) (WHITE 1969). After storm rainfall, the cave floods within 10 minutes (FUMY et al. 2000).

Under low water conditions, the spring water seeps into gravel covering the valley floor and sinks into a karstified limestone bank in the Drusberg formation. Downstream from the alluvial plain, the water comes out again in the Rubach lake springs (*Ls*) at 1490 m and flows out of the erosional window. As soon as the stream reaches the limestone, it sinks underground at different locations, dependent on the hydrologic conditions. During high water, there is a continuous stream from *Rb* to the Subersach river.



Fig. 3.19: The Rubach spring (Rb).

The Schneckenlochbach spring (*S*) is located at 1220 m, near the trough of syncline IV/V, directly below the 2010 m long Schneckenloch cave. The discharge ranges between about 10 and 1000 l/s (TOMSU 1998, WAGNER 1950). It is the main outlet of the western Gottesacker and forms a local base level of the karst system. The spring water unifies with two other streams, forming the Laublisbach stream. The stream flows through a gorge that follows the syncline and cuts down close to the base of the limestone. Only a small amount of water seeps underground so that the stream hardly ever dries up.

Four springs are located near the lower section of the Laublisbach stream where the syncline plunges under an alluvial plain in the Subersach valley. *La1* at 1070 m altitude (3–20 l/s) and *La2* at 1040 m (1–4 l/s) discharge from the karst aquifer, near the base of the overlying sandstone; *La3* (5–50 l/s) and *La4* (5 l/s) are discharged from gravel at the bank of the stream at 1025 m. Under low water conditions, all the water seeps into the Iferwies granular aquifer (TOMSU 1998).

About 1 km to the north, the Subersach valley cuts through the Schratenkalk limestone in the anticline V, allowing an impressive view of the fold. This is the location of the three Goldbach springs which fed a short but significant stream. It has its source in Goldbach spring 1

(*Gb1*) at 1010 m which discharges 42–82 l/s from scree and block material; *Gb2* is located at the right side of the stream at 990 m and discharges 4–56 l/s; *Gb3* is situated opposite and discharges 70–246 l/s from karst conduits. The Goldbach stream follows a branch of the Ostergunten fault zone. Two other relevant groups of springs are located next to the stream: A karst spring at the Subersach river (*Su*) discharges 15–46 l/s; the Goldbach spring 4 (*Gb4*) – which is not tributary to the Goldbach stream – consists of about 10 outlets with a total discharge of 4–151 l/s (TOMSU 1998)

The Subersach river has its source at the European watershed between Rhine and Danube and belongs to the catchment of the Rhine. As the karstified limestone is deeply eroded in the upper section of the valley, it is not a part of the karst system. However, there are hydrologic interactions between the karst aquifer and the river: On the one hand, the river acts as a receiving channel for the karst waters and forms the base level of the system. On the other hand, the river loses 42 to 137 l/s of water by influent flow into the Iferwies granular aquifer which interacts with the karst aquifer in the plunging syncline IV/V (TOMSU 1998, GOLDSCHIEDER & HÖTZL 2000).

In the high valleys to the north of the Gottesacker, the strata are intensively folded so that the karstified limestone is eroded along the anticlines and covered by overlaying impervious formations along the synclines. Thus, there is both a surface river network and underground karst water flow. The only significant karst spring in this area is the Kessleralp spring (*Ka*) which is situated in an overhanging rock face at 1440 m and discharges 10–60 l/s out of a karst conduit (HUTH 1998).

The intermittent Lake Torsee is located near the European watershed on Drusberg marl. It is recharged by several small springs at the base of scree slopes and discharged via swallow holes in the Schratenkalk limestone. The lake is situated both at the culmination line of the fold axes and on the 'big fault' (WAGNER 1950). As the eastern block is relatively subsided, CRAMER (1959) assumes that the lake discharges to the east (towards the Danube), even though that it is located west of the surface watershed.

3.5 Hydrochemistry

3.5.1 Hydrochemistry and temperature as natural tracers

The hydrochemical properties of spring waters can be used as natural (environmental) tracers. Natural tracers allow conclusions to be drawn on the characteristics of the aquifer. They indicate mixing between different types of water (e.g. groundwater and surface water) and give indications as to underground flow paths (KASS 1992).

The calcite saturation index SI (DIN 38404 1993) indicates whether the water is under-saturated ($SI < 0$), or over-saturated ($SI > 0$) with calcite. Under-saturation indicates a low water–rock interaction, that is a short residence time and a small specific contact surface. Over-saturation indicates intensive water–rock interaction. In karst systems with a well developed active conduit network, the spring water is often under-saturated with calcite and consequently aggressive (DREYBRODT 2000).

The water temperature is easy to measure and gives valuable information: The temperature of a spring which is discharged from an aquifer with a high depth to water table, is almost constant and identical to the mean annual air temperature of the place. Vice versa, high temperature variations allow to conclude on a shallow depth to water table and/or on the influence of surface water (MATTHEß 1994). In mountainous areas, the mean annual air temperature decreases with increasing altitude; the gradient is 0.6 K/100 m (HÄCKEL 1993). Thus, the temperature of spring water allows to conclude on the altitude of the catchment.

3.5.2 Overview on the hydrochemical analyses and results

All springs of the Hochifen-Gottesacker area were investigated in summer and autumn 1996 and 1997 under different hydrologic conditions. In winter, most of the springs are inaccessible. Temperature, conductivity, oxygen, pH-value and buffer capacity were measured at place while the inorganic cations and anions were analysed in the lab (GOLDSCHIEDER 1997, HUTH 1998, SINREICH 1998).

All spring waters are low mineralised: HCO_3^{2-} (30–287 mg/l) and Ca^{2+} (8.8–83 mg/l) are the dominant ions (Fig. 3.20); SO_4^{2-} (0.0–29 mg/l) and Mg^{2+} (0.1–8.1 mg/l) are significant for some springs but absent in other springs; the concentrations of Na^+ , K^+ , NO_3^- and Cl^- are generally low; Fe^{2+} , Mn^{2+} , CO_3^{2-} , PO_4^{3-} and NH_4^+ is below the limit of detection or

insignificant in most of the springs; the spring water is rich of dissolved oxygen (5.3–15.0 mg/l).

All the karst springs in the Hochifen-Gottesacker area and the resurgence which drains the rockfall mass in the Schwarzwasser valley are under-saturated with calcite ($-0.9 < SI < -0.1$) which indicates short residence times and limited rock–water interaction. Most of the small springs which drain local granular aquifers (scree slopes) are also under-saturated. Some of the small springs which discharge from moraine are slightly over-saturated ($0.0 < SI < 0.5$) which proves a more intensive rock–water interaction.

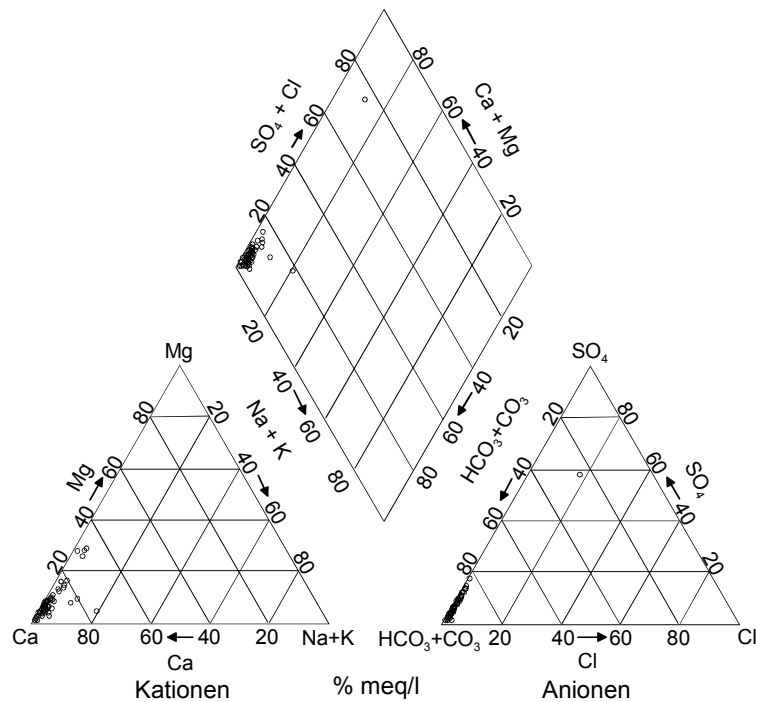


Fig. 3.20: PIPER diagram of all springs in the Hochifen-Gottesacker area.

3.5.3 Eastern Hochifen-Gottesacker area

The hydrochemical properties of the various small springs which discharge from local granular aquifers (moraine, scree slopes, rockfall material) show some variability, while the properties of the four karst

springs in the Schwarzwasser valley (*Au*, *Bü*, *Ks*, *Sb*) are almost identical (Fig. 3.21). This hydrochemical similarity indicates that the karst springs discharge from the same groundwater body.

In summer and autumn, most of the small springs show highly variable temperatures which are significantly above the average annual air temperature of the respective altitude. These springs drain shallow aquifers (rock debris underlain by impervious rocks) or are influenced by surface waters. Unlike that, the temperatures of the four karst springs (5.3–5.5 °C) are almost identical and about 0.5–1.0 K lower than the average annual air temperature of the respective altitude (Fig. 3.21). This is an evidence that these springs drain the same aquifer which gets inflow from a catchment of high altitude: from the Gottesacker.

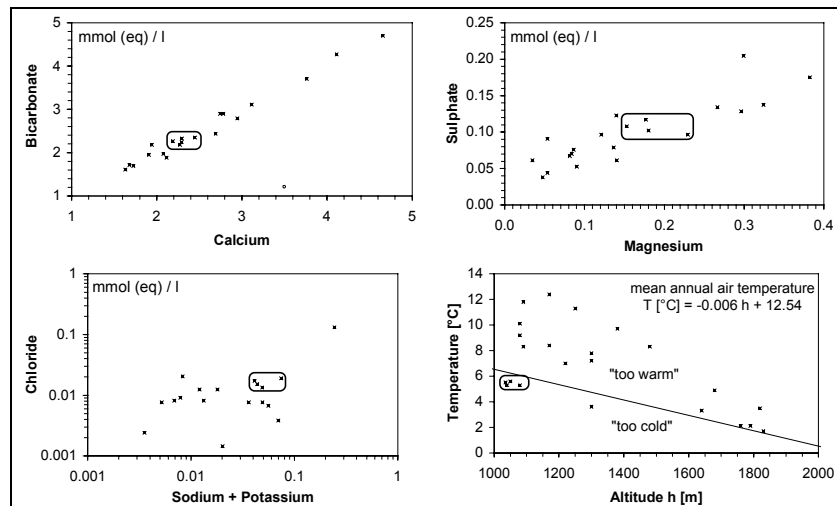


Fig. 3.21: Hydrochemistry and temperature of the karst springs in the Schwarzwasser valley (in rectangle) compared with the non-karstic springs in the eastern Hochifen-Gottesacker area (average values from summer 1996).

3.5.4 Western Hochifen-Gottesacker area

The main goal of the hydrochemical investigations in the western part of the area was to obtain detailed information on the catchments of the Goldbach springs, especially on the springs 1 and 3 which are relevant for future drinking water supply.

The springs within the syncline IV/V of the western Gottesacker are characterised by low concentrations of Ca^{2+} and Mg^{2+} which increase with decreasing altitude, that is with increasing temperature and travel time in the karst aquifer ($Rb < SI < La1-4$). The characteristics of the Goldbach springs 1 and 3 are significantly different: *Gb1* shows nearly constant concentrations with the highest Mg^{2+} and the lowest Ca^{2+} content of all springs; *Gb3* shows high Ca^{2+} and medium Mg^{2+} concentrations which are highly variable; high Ca^{2+} and medium Mg^{2+} concentration were proved in the Subersach river as well (Fig. 3.22).

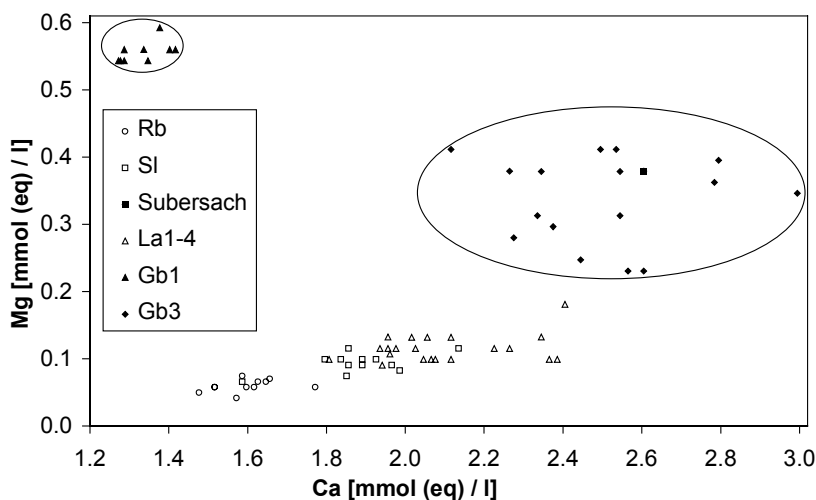


Fig. 3.22: Calcium and magnesium concentrations of the Goldbach springs and other springs in the western Gottesacker (summer 1997).

The hydrochemical properties prove that the water of Goldbach spring 1 is neither karst groundwater, nor water from the Subersach river, nor is it a mixture between these two types of water. Consequently, it must originate from a different aquifer with an independent catchment, probably from the forested mountain ridge east of the spring which is characterised by mass movements. The relatively high contents of Mg^{2+} , together with the low discharge variations and the good microbial quality of the spring indicate a significantly longer residence time compared to the other karst springs in the area.

The water of Goldbach spring 3 can be explained as a mixture between karst groundwater, water from the Subersach river and, possibly, water from the catchment of Goldbach spring 1.

The water temperature of the Goldbach springs (*Gb1–4*) and the springs at the lower section of the Laublisbach stream (*La1–4*) were measured in August, October and December 1997. The large temperature variations of up to 6.2 K in the springs *La1*, 3 and 4 and *Gb3* indicate the influence of surface water from the Laublisbach stream and from the Subersach river respectively. The low variations of less than 0.5 K in *La2* and *Gb1*, 2 and 4 prove that there is no significant influence of surface water.

3.6 Tracer tests

3.6.1 Earlier tracer tests

Tracer tests with Uranine in 1949 and 1955 proved the hydraulic connection between the Hölloch cave in the Mahdtal valley (injection point IP1) and the Sägebach spring (*Sb*) while the tracer did not reach the Aubach spring (*Au*) (SPÖCKER 1961). The springs *Bü* and *Ks* were not sampled and the bottom spring (*Bo*) was not yet known. WAGNER (1950) and KRIEG (1969) carried out tracer tests in order to prove local hydraulic connections in caves.

3.6.2 Overview of current tracer tests

Within the framework of this thesis, the following tracer tests were carried out in the Hochifen-Gottesacker area (Tab. 3.3, Fig. 3.23):

- September 1996: eastern Gottesacker and Schwarzwasser valley; two injection points (IP2, IP3); medium to high water conditions (GOLDSCHIEDER 1997, 1998a).
- August 1997: Schwarzwasser valley; three injection points (IP4–IP6); medium to low water conditions (GOLDSCHIEDER 1998b, 2000).
- September 1997: entire area with Subersach and Schwarzwasser valley, rockfall mass; ten injection points (IP7–IP16); sudden change from low to high water conditions (TOMSU 1998, SINREICH 1998, GOLDSCHIEDER & HÖTZL 1999, 2000).

The purpose of these tracer tests was to determine the underground flow paths, to delineate the catchment areas of the springs, to locate

3.6 Tracer tests

the European watershed more precisely, to characterise the hydraulic properties of the aquifer and to obtain information about the mechanisms of contaminant transport.

The fluorescent dyes Uranine, Eosine, Sulforhodamine B, Naphthionate and Pyranine were used as tracers. Altogether, 1320 water samples and 94 charcoal bags were taken and analysed in the lab in Karlsruhe using the Synchronous-Scan-Method. Up to five different tracers were analysed in each sample (see BEHRENS 1982, KÄSS 1992).

Tab. 3.3: Overview of the injections in the Hochifen-Gottesacker area.

no.	description	date	tracer	mass [kg]	flushing water
IP1	Hölloch cave (3 injections, see Spöcker 1961)	1949/55	Uranine	1.8-10	-
IP2	sewage shaft "Ifen 2000", Gottesacker south	20.09.96	Uranine	4.80	10 m ³
IP3	ponor doline "am Geißbühl"	20.09.96	Eosine	5.00	-
IP4	Ladstatt cave shaft (filled with waste)	14.08.97	Sulforh.	0.70	1 m ³
IP5	karst shaft near Ladstatt cave	14.08.97	Eosine	0.60	1 m ³
IP6	Schwarzwasser cave (estavelle)	14.08.97	Uranine	0.20	-
IP7	swallow hole "Iferflucht"	11.09.97	Eosine	5.84	-
IP8	sink of the Schwarzwasser river into the rockfall	12.09.97	Sulforh.	3.00	-
IP9	central Gottesacker east of culmination line	12.09.97	Uranine	1.00	400 l
IP10	central Gottesacker west of culmination line	12.09.97	Uranine	2.00	400 l
IP11	swallow hole lake Torsee	12.09.97	Pyranine	3.70	-
IP12	swallow hole near "Bestlesgund-Alp"	12.09.97	Eosine	0.37	-
IP13	karst shaft near "Wasenkopf"	12.09.97	Eosine	4.00	800 l
IP14	upper swallow hole of the Rubach stream	12.09.97	Pyranine	2.00	-
IP15	lower swallow hole of the Rubach stream	12.09.97	Sulforh.	3.00	-
IP16	confluence Rubach-Laublisbach	12.09.97	Napht.	3.45	-

SINREICH (1998) carried out some small tracer tests with salt (NaCl) in order to prove local hydraulic connections in the upper Schwarzwasser valley and the rockfall mass. In October 2000, a comparative tracer test was carried out within the framework of an ATH programme. Ten substances were injected simultaneously in the Schwarzwasser cave under low water conditions: the fluorescent dyes Naphthionate, Pyranine, Uranine and Sulforhodamine B; three different salts with Lithium, Strontium and Bromide as ionic tracers; killed bacteria and fluorescent microspheres in red and green as particle tracers. The results were described by GOLDSCHIEDER et al. (2001b) but are not relevant here.

3.6.3 Selection of the injection points and injection

In order to get a comprehensive picture of the underground flow pattern of the entire karst system, at least one injection point was selected in each syncline both east and west of the culmination line (Fig. 3.23).

The additional aim of the injections in the central Gottesacker (IP9-10) and in the swallow hole that takes the outflow from Lake Torsee (IP11) was the localisation of the European watershed.

The injections in the Schwarzwasser valley (IP6, IP3, IP7) were carried out in order to check the function of the karst aquifer in the valley as a hydraulically connected collector for all the karst and surface waters of the eastern part of the area. The hydraulic properties of the rockfall mass in the upper section of the valley should be characterised by the injection in the sink of the Schwarzwasser river (IP8).

One tracer was injected in the sewage shaft of the ski station 'Ifen 2000' (IP2) in order to determine the influence of waste water on the springs of the granular aquifer 'Ifenmulde' and the springs in the Schwarzwasser valley. The injections IP4 and IP5 should check which of the springs are potentially endangered by sewage water from the Ladstatt cave shaft that was filled with waste before 1975 (see GOLDSCHEIDER 1998b, 2000).

3.6 Tracer tests

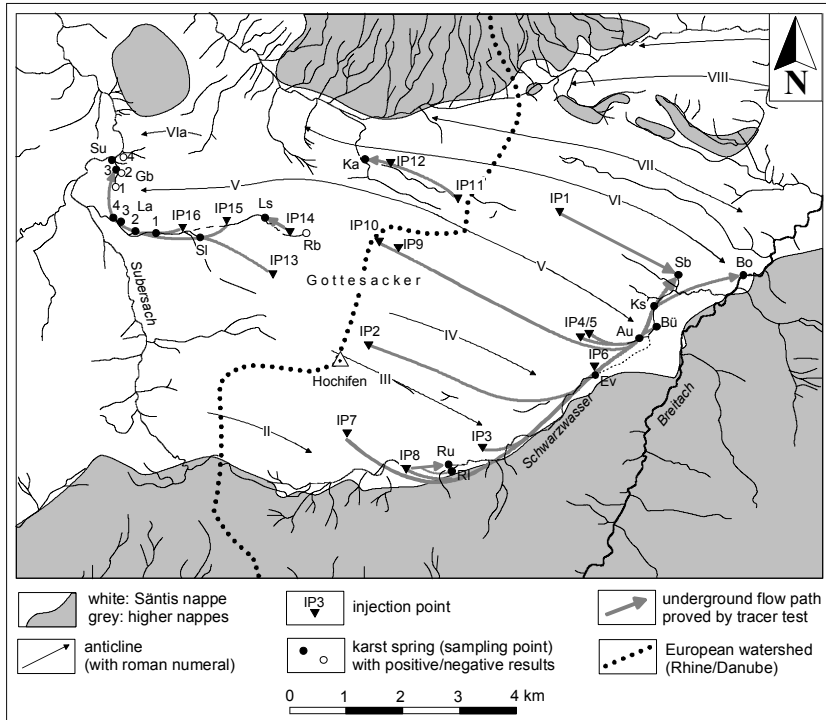


Fig. 3.23: Tracer tests in the Hochifen-Gottesacker area. Location of the injection points (IP1–16), the sampling points and the proved flow paths (simplified). Shorthand symbols and further explanations in the text.

In the western part of the area, four injection points are located within the syncline IV/V that forms the western Gottesacker: IP15 is located in the trough of the syncline; IP13 on its southern limb; IP14 is the sink of a stream into a karstified limestone bank within the Drusberg marl. Another tracer was injected in the confluence of the Laublisbach and the Rubach streams (IP16) in order to check if the springs in the valley, and especially the Goldbach springs, receive inflow from seeping and sinking surface water.

If possible, the tracers were injected in swallow holes, ponor dolines or sinking streams so that flushing water was not necessary. For the injection in the sewage shaft (IP2), 10 m³ of flushing water from the septic tank of the ski station were used. The fire brigade provided each 1000 L of water for the injections in the Ladstatt cave and the neighbouring shaft (IP4, 5). For the injections on the central (IP9, 10)

and western Gottesacker (IP13), two tanks of each 800 l were transported by an helicopter.

3.6.4 Sampling

After the injections, all springs in the area were observed for up to 60 days (Fig. 3.23). Water samples in 50 ml brown glass bottles were taken manually or with automatic samplers at all important springs where tracers were expected to appear, while charcoal bags were installed in the other springs. For the tests in September 1996 and August 1997, only the springs in the eastern part of the area and the Schwarzwasser valley were observed. In September 1997, samples were taken in the entire Hochifen-Gottesacker area and in the Hölloch cave stream.

Water samples were taken directly downstream from the estavelle (*Ev*), while charcoal bags were installed at six different points in the Schwarzwasser river upstream from the estavelle. As the bottom spring (*Bo*) discharges directly into the Breitach river which acts as a receiving channel for all the other karst springs as well, it is difficult to prove a possible appearance of tracers at this spring. Consequently, water samples were taken in the Breitach river upstream from, downstream from and directly at the assumed spring.

3.7 Results

3.7.1 Introductory remark

The results of the three multi tracer tests are described in geographical-hydrological order and not in chronological order. For instance, it is sensible to describe all the result from the Schwarzwasser valley (which forms a unity) in one section, even though the results were produced within three different time periods. An overview of the results is given in Fig. 3.23 and Tab. 3.4.

3.7 Results

Tab. 3.4: Overview of tracer test results in the Hochifen-Gottesacker area. The time of maximum concentration t_m and normalised maximum concentration c/M is given for each proved connection. White box: sampled spring; grey: not sampled; + indirect evidence for connection, no breakthrough curve; - no connection; * only the time of first visible detection is given by SPÖCKER 1961; **curve shows no clear maximum.

area ↓	spring no.	South and East										North		West				t_m c/M
		IP1*	IP2	IP3	IP4	IP5	IP6	IP7	IP8	IP9+10	IP11	IP12	IP13	IP14	IP15	IP16		
South and East	Ru		-	-				-	11 121									h 10^6m^{-3}
	Rl		-	-				-	36 0.85									h 10^6m^{-3}
	Ev		17 17	23 6.0			= IP6	75 3.5	38 6.1	-								h 10^6m^{-3}
	Au	-	20 11	25 3.1	81 0.36	32 3.5	12 70	97 5.9	45 2.6	33 4.4	-							h 10^6m^{-3}
	Bü		22 8.2	31 2.6	81 0.35	33 3.3	13 68	97 5.9	45 2.5	32 6.6	-							h 10^6m^{-3}
	Ks				81 0.33	37 3.2	15 61	97 5.4	46 2.1	35 3.4	-							h 10^6m^{-3}
	Sb	61*	33 2.5	44 1.0	107 0.31	56 2.5	31 31	111 3.5	55 0.85	42 0.55	-							h 10^6m^{-3}
	Bo		+	+	+	+	+	+	+	+								
North	Ka									29 48	11 4452						h 10^6m^{-3}	
West	Rb									-				-				
	Ls									-				22 52				h 10^6m^{-3}
	Sl									-			30 47	24 16	4 2980			h 10^6m^{-3}
	La1									-			33 0.53	26 2.6	12 393	6 910		h 10^6m^{-3}
	La2									-			** 0.15	40 0.09	25 4.2	21 32		h 10^6m^{-3}
	La3									-			38 23	24 0.975	19 70	11 164		h 10^6m^{-3}
	La4									-			33 0.63	28 0.335	17 41	13 102		h 10^6m^{-3}
	Gb1									-			-	-	-	-		
	Gb2									-			-	-	-	-		
	Gb3									-			46 0.08	+	22 0.57	18 3.3		h 10^6m^{-3}
	Gb4									-			-	-	-	-		
	Su									-			+	+	76 0.04	+		h 10^6m^{-3}

3.7.2 Lake Torsee and Kessleralp spring (IP11–12)

The Pyranine which was injected in the swallow holes of Lake Torsee (IP11) was not detected in the Hölloch cave and in the springs in the Schwarzwasser valley. It reached the spring Ka about 27 h after the injection. Obviously, the Lake Torsee discharges in a westerly direction towards the catchment of the river Rhine. The results prove that the

underground and the surface watershed are identical here, contrary to the assumption of CRAMER (1959). The Eosine that was injected in a swallow hole (IP12) in the trough of the syncline V/V1 reached the spring *Ka* after 10 h (Fig. 3.24). Thus, the catchment of this spring consists of the western section of this syncline and the Lake Torsee.

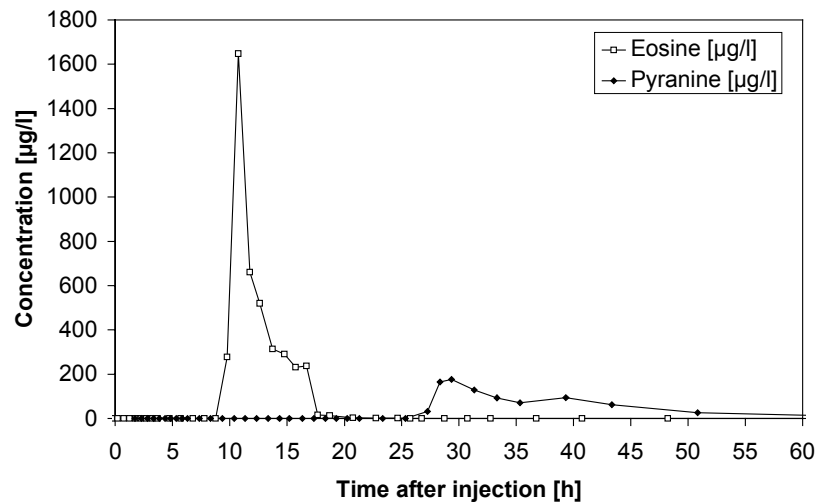


Fig. 3.24: Eosine and Pyranine breakthrough curves at the Kessleralp spring (*Ka*).

3.7.3 Eastern Hochifen-Gottesacker area (IP1–10)

The Uranine which was injected in the central Gottesacker 100 m to the east (IP9) and 100 m to the west (IP10) of the culmination line reached the Aubach spring (*Au*) about 31 h after the injection and later on the four karst springs in the Schwarzwasser valley (*Bü*, *Ks*, *Sb*). No trace of Uranine was detected in any of the springs in the western part of the area. The results prove that the underground watershed is at least 100 m west of the culmination line here. No trace of Uranine was detected in the estavelle (*Ev*). Thus, the underground karst water flow in the syncline IV/V reaches the collector in the Schwarzwasser valley upstream from the Aubach spring but downstream from the estavelle.

The Uranine which was injected in the sewage shaft at the southern margin of the Gottesacker (IP2) first reached the estavelle after 14 h and then, 17-27 h after the injection, the four karst springs in the

3.7 Results

Schwarzwasser valley. Thus, the syncline III/IV belongs to the catchment of the estavelle and the four springs.

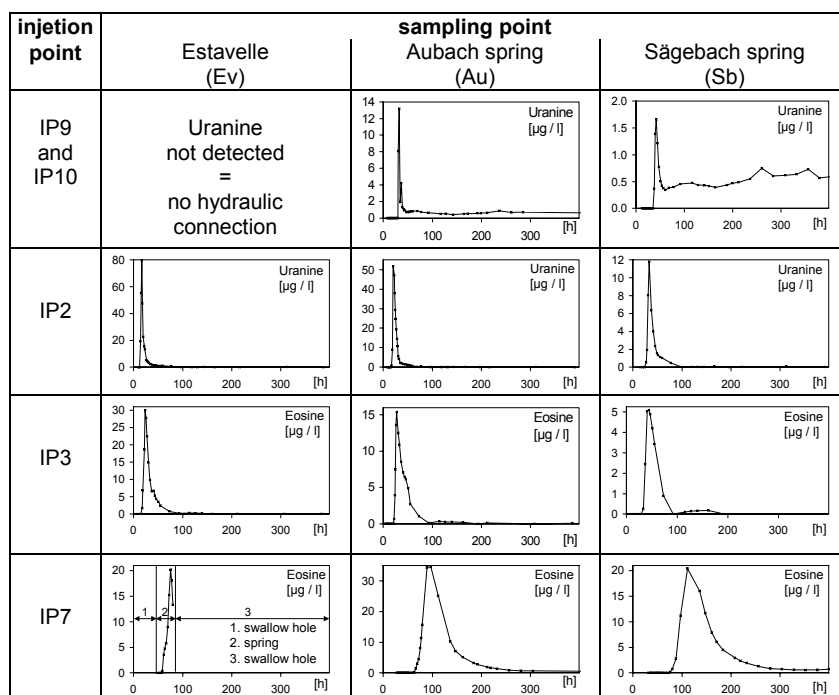


Fig. 3.25: Selected breakthrough curves from different tracer tests in the eastern part of the area. The curves of the springs *Bü* and *Ks* are similar to those of *Au* and are not presented here.

The Eosine which was injected in a doline (IP3) in the Schwarzwasser valley reached the estavelle and the four karst springs after 23–44 h. Nine days after the injection, the concentration in the Breitach river was 0.01 µg/l upstream from the bottom spring (*Bo*), 0.07 µg/l directly at and 0.05 µg/l downstream from the spring. This is the evidence that the bottom spring discharges groundwater from the Schwarzwasser valley into the Breitach river. Thus, the bottom spring at 980 m is the lowest direct outlet and forms the base level of the system.

The Eosine that was injected in a swallow hole (IP7) in the upper section of the valley – upstream from the rockfall mass – reached the estavelle and the four karst springs after 59–76 h. This is the evidence that there is a hydraulically connected karst aquifer in the entire valley which is discharged by the estavelle, the four karst springs and the

bottom spring. Minor traces of Eosine were detected in two water samples taken at the resurgence (*Ru*) during a flood wave. Possibly, karst water rises up into the rockfall mass under high water conditions.

No trace of the dyes that were injected in IP2, 3 and 7 were detected in the Schwarzwasser river upstream from the estavelle. This result proves that the river gets no inflow from the karst system on the left (NW) side of the valley but is exclusively fed by tributaries from the Flysch mountains on the right (SE) side and from the rockfall mass (except for extreme high water).

The Uranine which was injected under low water conditions in the Schwarzwasser cave (IP6) reached the springs *Au*, *Bü*, *Ks* and *Sb* after 7–9 h and 22 h respectively. This is the evidence that the cave connects the surface river with the underground karst aquifer which is drained by these four springs. This tracer test and all the other injections in the eastern part of the Hochifen-Gottesacker area prove that the groundwater from the Schwarzwasser valley flows under the Mahdtal valley and rises up to the Sägebach spring (*Sb*) which is situated at the opposite side of the valley. The earlier tracer injections in the Hölloch cave (IP1, SPÖCKER 1961) proved that the Sägebach spring gets additional inflow from the Mahdtal valley.

The mixing relation of water from the Mahdtal valley and from the Schwarzwasser valley in the Sägebach spring can be quantified using the integrals of the normalised breakthrough curves: Springs that are fed by the same underground flow without any additional inflow might show tracer breakthrough curves with a different shape. However, the area below the curves (the integral) must be equal, independent from the discharge rate of the spring and the distance to the injection point. In case of additional inflow from another catchment, all concentrations are diluted so that the integral is reduced according to the proportion of inflow. Consequently, it is possible to calculate the proportion of additional inflow by comparing the integrals of the breakthrough curves (GOLDSCHIEDER 1998b).

The mixing calculation with the integrals of the normalised Uranine breakthrough curves of the injection IP6 showed that the Sägebach spring (*Sb*) gets 80 % of its water from the Schwarzwasser valley and 20 % from the Mahdtal valley (Fig. 3.26). However, this relation is only representative for the given low water conditions.

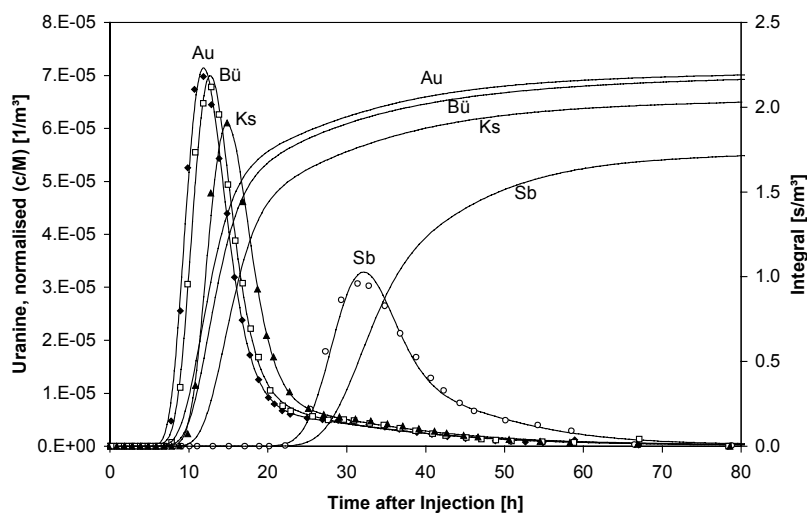


Fig. 3.26: Comparison of the normalised Uranine breakthrough curves and the integrals of these curves at the four karst springs in the Schwarzwasser valley (injection IP6). Measured values and curves modelled with TRACI 95 (WERNER 1998). Further explanations in the text.

The tracers that were injected in the Ladstatt cave (IP4) and the neighbouring karst shaft (IP5) reached the four springs in the Schwarzwasser valley within a few days, proving that the waste that had been dumped into the cave is potentially endangering the water quality of these springs. Further details of this experiment are presented by GOLDSCHIEDER (1998b, 2000).

3.7.4 Rockfall mass (IP8)

The Sulforhodamine was injected in the sink of the Schwarzwasser river into the rockfall mass under low water conditions. It reached the upper resurgence (*Ru*) after 8 h, the maximum concentration was 362 µg/l. Initially, it was not detected in the directly neighbouring spring *Rl*. About 12 h after the injection, a storm rainfall led to increasing discharge rates. At about the time of maximum discharge, 31 h after the injection, a breakthrough of Sulforhodamine was observed at the lower resurgence (*Rl*). However, the maximum concentration was only 2.6 µg/l (Fig. 3.27). A portion of the Sulforhodamine seeped into the karst aquifer and reached the estavelle and the springs in the lower section of the valley. SINREICH (1998) injected salt in a stream from the

Flysch mountains that sinks into the southern margin of the rockfall mass. The electrical conductivity was increasing in *Rl* but not in *Ru*.

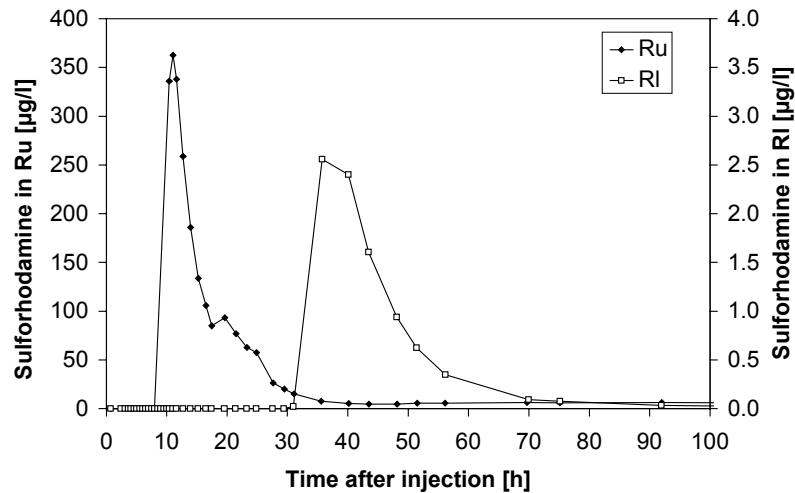


Fig. 3.27: Sulforhodamine B breakthrough curves of the upper (*Ru*) and the lower resurgence (*Rl*) below the rockfall mass. Note the different scale.

Putting all these results together, it is evident, that *Ru* is the main resurgence of the sinking Schwarzwasser river, while *Rl* is the resurgence of some small sinking streams from the Flysch mountains. There is a hydraulic barrier between the two springs but the water from the Schwarzwasser river can overflow this barrier and reach *Rl* under high water conditions. A portion of the groundwater in the rockfall mass seeps into the underlying karst aquifer.

3.7.5 Western Hochifen-Gottesacker area (IP13–16)

No trace of the Uranine that was injected in the central Gottesacker (IP10) reached the Rubach spring (*Rb*) or any other springs in the western part of the area, because the tracer was obviously transported towards the Schwarzwasser valley.

The Pyranine that was injected in the sink of the Rubach stream (IP14) reappeared 20 h later in springs at the little lake 500 m downstream (*Ls*). The relatively high flow velocity of 25 m/h is strong evidence that the sinking water flows into a karstified limestone bank within the Drus-

berg formation and not in the alluvial plain which covers the valley floor. Further downstream, the water sinks underground again in a swallow hole (IP15).

All the tracers that were injected in the western Gottesacker, reached the Schneckenlochbach spring (*S*) after a short time: Sulforhodamine was detected 2.8 h after the injection in the sink of the swallow hole IP15; Pyranine reached the spring after 22 h and Eosine arrived 30 h after the injection in the karst shaft IP13 (Fig. 3.28). These results prove that this spring drains the entire western Gottesacker area.

The three tracers mentioned above and the Naphthionate reached the four springs at the lower section of the Laublisbach stream (*La1–4*), proving that the four springs discharge water from the western Gottesacker. The positive results for Naphthionate show that the springs receive seeping surface water from the Laublisbach stream.

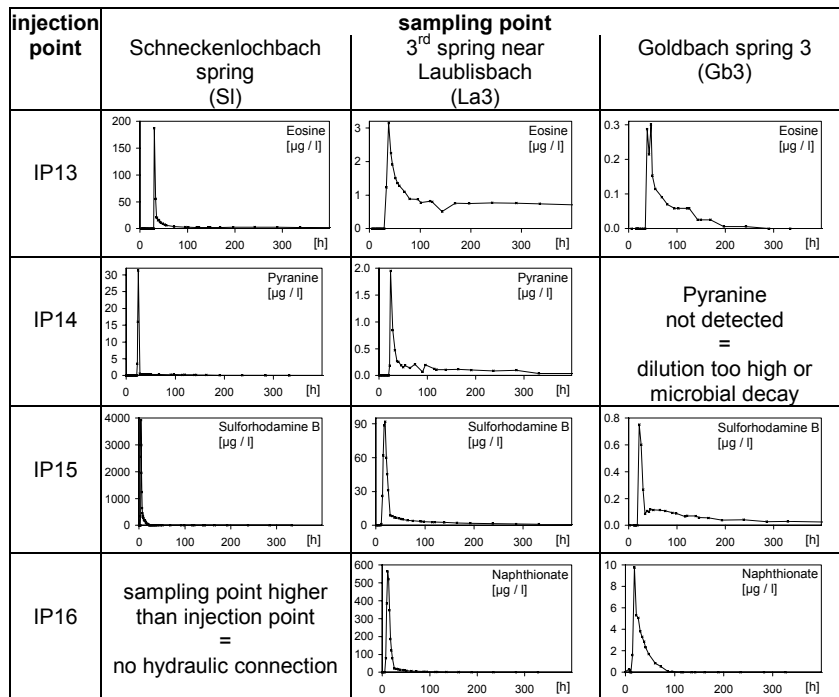


Fig. 3.28: Selected breakthrough curves from the western Hochifen-Gottesacker area. The curves in *La1*, 2 and 4 are similar to those in *La3* and are not presented here; minor traces of Sulforhodamine were detected at *Su*; no positive results were obtained for *Rb*, *Gb1*, 2 and 4.

3.7.6 Goldbach springs

The Goldbach springs (*Gb1–4*) are the most complicated springs of the area and require a detailed discussion of the tracer tests results.

In Goldbach spring 3, Naphthionate, Sulforhodamine and Eosine arrived 14, 22 and 38 h after the injection. The respective maximum concentration of 9.8, 0.75 and 0.30 $\mu\text{g/l}$ was reached quickly after the first detection (Fig. 3.28). The results show that the entire western Gottesacker belongs to the catchment of this spring. Pyranine was not detected. However, water that contains Pyranine reached the injection points for Sulforhodamine and Naphthionate (IP 15, 16). As these tracers reached the spring, the negative results for Pyranine must be due to high dilution or microbial decay. There are examples for the decay of Pyranine in karst groundwater (e.g. GOLDSCHIEDER et al. 2001b, c).

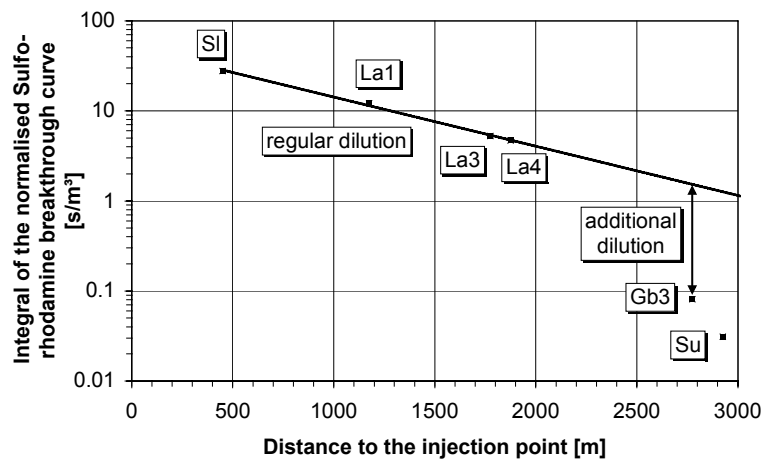


Fig. 3.29: Integrals of the normalised Sulforhodamine breakthrough curves (injection IP 15) at different springs: regular dilution between the springs *SI* and *La4*; higher dilution by additional inflow at the spring *Gb3*.

The concentrations in Goldbach spring 3 are significantly lower than in the other springs. The proportion of karst water from the western Gottesacker in this spring can be quantified by mixing calculations with the integrals of the breakthrough curves (see section 3.7.3): Within the western Gottesacker, the integrals of the breakthrough curves decrease exponentially from *SI* to *La1–4* dependent on the length of the flow path (Fig. 3.29). This effect can be explained by regular dilution in

the aquifer. At Goldbach spring 3, the integral is 17 times lower than it could be expected by regular dilution. Thus, only 6 % (1:17) of its water comes from the western Gottesacker during the given hydrologic conditions while the rest must originate from another catchment, that is the Iferwies granular aquifer.

The 'Iferwies' granular aquifer is recharged by the following mechanisms: diffuse infiltration of rain and melting water (visible), seeping water from the Laublisbach stream (visible), influent flow of the Subersach river (proved by flow measurements) and upwelling of karst water from the plunging syncline IV/V (proved by tracer tests). A branch of the 'Ostergunten' strike-slip fault drains the granular aquifer and connects it with the Goldbach spring 3.

None of the tracers were detected at Goldbach spring 1. Thus, the karst aquifer in the western Gottesacker, the 'Iferwies' granular aquifer, the Subersach river and the Laublisbach stream cannot be part of its catchment. Furthermore, there are significant hydrochemical differences between the spring and these waters. The catchment of *Gb1* is probably the slope and mountain ridge east of the spring, which is characterised by mass movements.

The tracers did not reach Goldbach spring 2 and 4 as well. Thus, the spring 2 is not connected with the neighbouring spring 3 but fed by a local granular aquifer or by water from the catchment of spring 1. Spring 4 is completely independent from the other springs and discharges the bordering scree slope which is underlain by Amdener marl.

Minor traces of Sulforhodamine were detected in the karst spring at the Subersach river (*Su*). A salt tracer test proved that this spring receives seeping water from the Goldbach stream.

3.8 Conclusions

3.8.1 Fold tectonics and underground drainage pattern

The underground drainage pattern of the alpine karst system Hochifen-Gottesacker is mainly controlled by the stratification, the fold tectonics and the base level conditions.

The Schrattealk limestone forms the karst aquifer. It is underlain and locally overlain by impervious marl and sandstone aquicludes. Compared with the topographic differences in altitude (about 1000 m), the karst aquifer is relatively thin (about 100 m). The underground flow is

parallel to the stratification. The presence of stratigraphic flow control is a precondition for the effectiveness of the folds as tectonic flow control.

In the elevated parts of the area, the base of the karst aquifer is high above the level of the surrounding valleys (shallow karst), so that the underground flow takes place near the base of the aquifer. Consequently, the water flows towards the troughs of the plunging synclines which form the main underground flow paths (Fig. 3.30). ORTH (1984) calls this phenomenon 'structure conform karst drainage'. The anticlines form local watersheds and the culmination line of the fold axes forms a part of the European watershed between Rhine and Danube (Fig. 3.31). The watershed and the crest line locally differ up to 100 m.

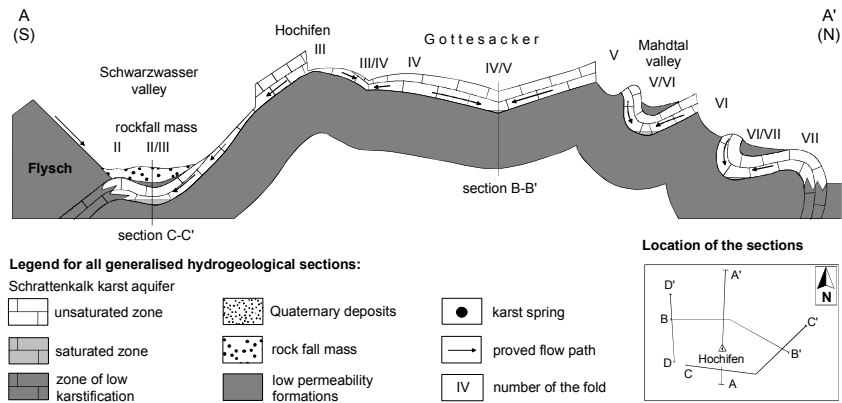


Fig. 3.30: Generalised hydrogeological section of the Hochifen-Gottesacker area perpendicular to the fold axes. Legend for and location of the following sections.

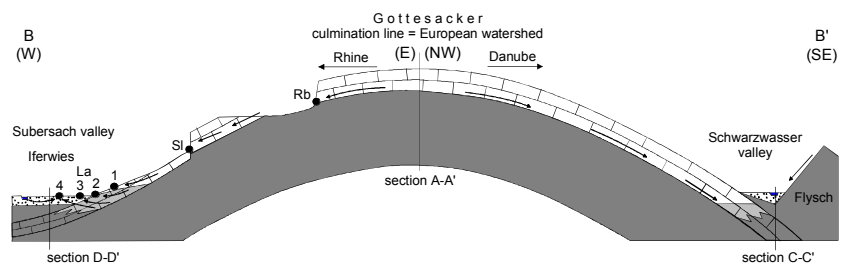


Fig. 3.31: Generalised hydrogeological section from the Subersach valley, over the Gottesacker to the Schwarzwasser valley along the main syncline (IV/V).

In the central Gottesacker area, the strata are gently folded. The karstified limestone forms the land surface and the drainage is exclusively underground. In the northward bordering high valleys, the folds are closer so that the limestone is eroded along the anticlines and covered along the synclines (Fig. 3.30). Consequently, there is surface runoff and underground karst water flow which both follow the fold axes.

The plunging synclines are drained by valleys which run across the folds (Fig. 3.31). The south- and eastward bordering Schwarzwasser valley follows the main thrust of the Flysch over the Helvetic Säntis nappe while the westward bordering Subersach valley follows a major strike-slip fault zone and an axial depression.

The degree of tectonic constriction increases from east to west so that the strata are gently folded in the Schwarzwasser valley while the folds are closer in the Subersach valley. This structural difference influences the underground drainage pattern.

In the Schwarzwasser valley, gently folded Schrätenkalk limestone is preserved along the entire valley and forms a hydraulically connected karst aquifer which collects the karst waters from the left (NW) side of the valley and the surface waters from the Flysch area on the right (SE) side. The underground flow runs across the folds and follows the axis of the valley (Fig. 3.32). Thus, the synclines lose their function as the main flow paths and the anticlines are no obstacle for the karst groundwater flow along the valley.

The aquifer is drained by several karst springs in the middle and lower section of the valley. Their hydrologic characteristics depend on their topographic position within the valley: In the upper section of the valley, there are no significant karst springs. In the middle section, there is the estavelle (*Ev*). In the lower section of the valley, there are the intermittent Aubach spring (*Au*) and, further downstream, three permanent karst springs (*Bü*, *Ks*, *Sb*). The bottom spring (*Bo*) in the Breitach river is the lowest and youngest outlet of the system with a probably nearly constant discharge rate. Continued development of the underground karst network will increase the discharge rate of this spring. The karst springs are either located in the anticlines (*Ev*, *Au*, *Bü*, *Ks*, *Bo*) where the rivers cut the limestone, or on fault-controlled limestone outcrops (*Sb*). All springs discharge from the same aquifer and show similar hydrochemical properties.

3.8.2 Hydrogeological aspects of landscape history

The two main driving forces of alpine landscape history are the regional uplift of the mountain range since the Miocene which caused fast erosion and relative deepening of the base levels, and the repeated Pleistocene glaciations. The glaciers formed wide main valleys with hanging valleys high above the regional base level. Deep gorges have been forming in the hanging valleys by backward erosion (SCHOLZ 1995).

The consequences of these processes on the hydrogeology of alpine karst systems can be exemplified by the Hochifien-Gottesacker area. All the active karst springs in the area are situated in late- to postglacial gorges. The permanent deepening of the base level is reflected by the fact that the youngest springs are situated in the lowest position while the older springs are situated higher up in the valley. The discharge variations of the springs increase with increasing altitude. The highest (and oldest) springs act as high water outlet before they become inactive. In the Mahdtal valley, it was possible to detect an inactive spring outlet in an altitude of 1240 m, more than 200 m above the active Sägebach spring (GOLDSCHIEDER et al. 2000c).

Almost the entire land surface of the Gottesacker is formed by karstified Schrätenkalk limestone, though the formation is thin (100 m) compared to the dimensions of the landscape (1300 m difference in altitude). This spatial overrepresentation of limestone outcrops can be explained by landscape evolution: For as long as the limestone is covered by marl, there is surface runoff and erosion. As soon as the surface of the limestone gets exposed, the drainage shifts underground and surface erosion stops. When the limestone is finally removed by complete dissolution or by rockfalls, surface erosion starts again. Thus, the land surface formed of marl or sandstone is always young and quickly evolving, while the karst surface represents a standstill in landscape history. Karstification protects the limestone from being eroded.

An interesting consequence of this process can be observed in the Schwarzwasser valley, where the limestone strata plunge under the Flysch along the valley axis (Fig. 3.33). The NW side of the valley is formed by karstified limestone, while the SE side consists of Flysch. Thus, there is almost no erosion on the NW but permanent erosion on the SE side of the valley. The slope gradients are much steeper on the SE side. As a consequence, the valley axis is shifting to the SE while it is deepening, and the underground drainage system is laterally shifting as well. The active underground system is situated close to the Flysch boundary, while there are remains of older drainage systems on the left

side of the valley, e.g. dry valleys, aligned dolines and inactive spring outlets. The existence of significant paleo-drainage systems parallel to the recent flow system and above the level of the Schwarzwasser valley floor was predicted by GOLDSCHIEDER et al. (2000c). In winter 2001/2002 cavers discovered the predicted galleries. Details will be published later.

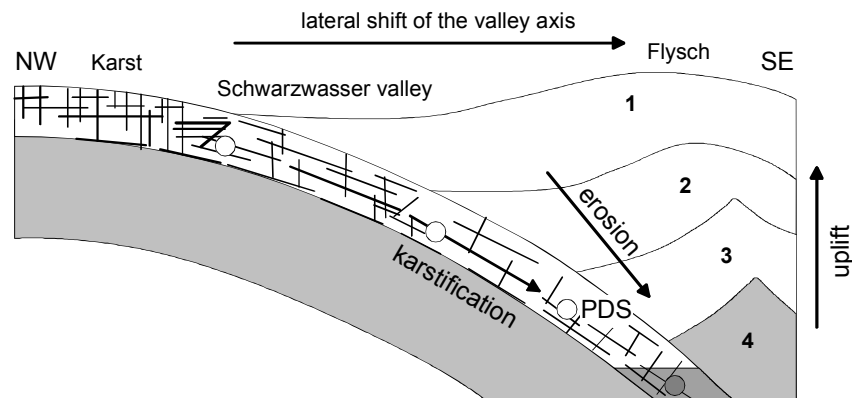


Fig. 3.33: Schematic cross section of the Schwarzwasser valley. The lateral shift of the valley axis is a consequence of geological asymmetry and absence of erosion on the karst land surface. PDS: paleo-drainage system, predicted by GOLDSCHIEDER et al. (2000c) and discovered by cavers in 2002.

3.8.3 Delineation of the catchments

As there is both a strong stratigraphic and tectonic flow control, it is possible to delineate the catchments of the springs much more precisely, than it is possible with most other karst systems (Fig. 3.34). The catchments were delineated on the basis of geological and hydrological information; most of them were proved by tracer tests.

The eastern Hochifen-Gottesacker area forms a large, connected catchment. Under low water conditions, when the estavelle is a swallow hole, the catchment includes the Flysch mountains on the right (SE) side of the Schwarzwasser valley. The large catchment is subdivided into sub-catchments by the crests of the anticlines:

- The bottom spring (*Bo*) and the Sägebach spring (*Sb*) drain the entire catchment.

3.8 Conclusions

- The springs *Au*, *Bü* and *Ks* drain the entire area without the Mahdtal valley.
- When the estavelle (*Ev*) functions as a spring, it drains the Schwarzwasser valley upstream from the estavelle and the southern part of the Gottesacker (syncline III/IV).

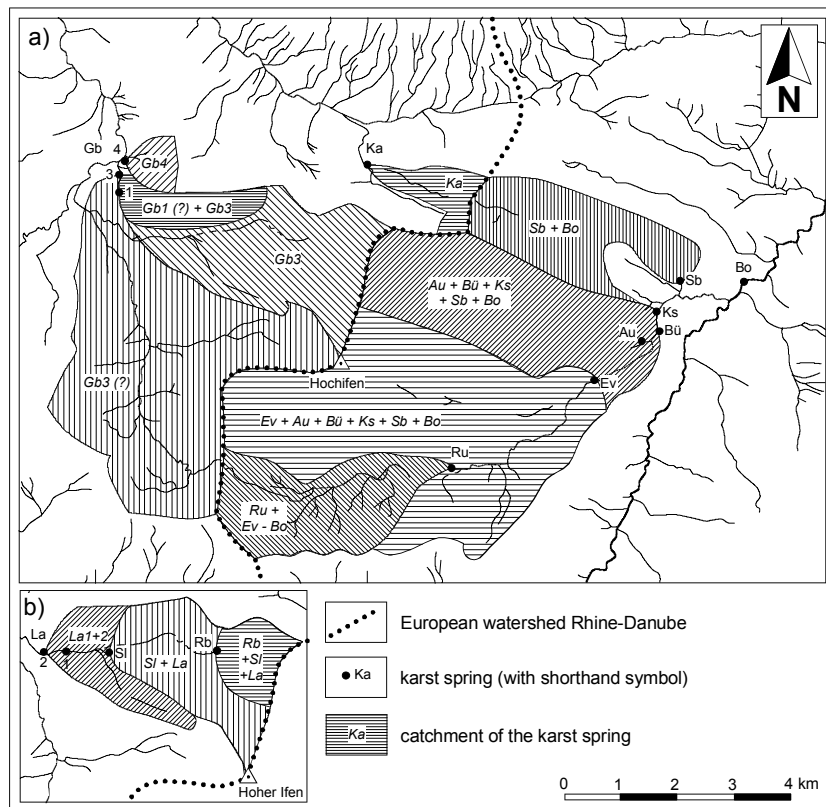


Fig. 3.34: a) Catchments of important springs in the Hochifen-Gottesacker area; b) detail from the western Gottesacker; (?): no direct evidence.

In the western part of the area, the syncline IV/V forms the main catchment that is divided in several sub-catchments with a complex internal structure:

- The upper section of the syncline is drained by the Rubach spring (*Rb*) (evident because of the hydrogeological situation but not checked by tracer tests).
- The Schneckenlochbach spring (*Sl*) drains the upper and middle section of the syncline. The water from the upper section does not reach the spring directly but is first discharged by *Rb* and later on sinks in the karst aquifer again.
- The springs at the lower section of the Laublisbach stream (*La1–4*) receive water from the entire syncline as well as seeping water from the Laublisbach stream.
- The Goldbach spring 3 (*Gb3*) receives water from the entire western Gottesacker (proved by tracer tests) and, probably, from the Subersach river and the 'Iferwies' granular aquifer (indirect evidence from tracer tests, hydrochemistry, flow measurements). Thus, the entire surface catchment of the upper Subersach river would be a part of the catchment of *Gb3*.

The catchment of Goldbach spring 1 (*Gb1*) is probably the slope and mountain ridge east of the spring which is characterised by mass movements. However, there is only an indirect evidence: The negative results of the tracer tests and the hydrochemical data show that the western Gottesacker, the Subersach river and the 'Iferwies' granular aquifer are not a part of the catchment. Goldbach spring 4 (*Gb4*) discharges the slope east of the spring.

The Kessleralp spring (*Ks*) to the north of the Gottesacker drains the western section of the syncline V/VI and the Lake Torsee.

In detail, the flow paths within that catchment are extremely complicated. One example for low water conditions: The karst water from the western Gottesacker is drained by the Rubach spring (*Rb*), sinks in a limestone bank within the Drusberg marl (IP14), comes out in a little lake, sinks again in the Schrattekalk limestone (IP15), comes out in the Schneckenlochbach spring (*Sl*), seeps in the bed of the Laublisbach stream (IP16), comes out in the springs *La1–4*, seeps in the Iferwies granular aquifer, flows to the Goldbach spring 3 (*Gb3*), seeps partially in the bed of the Goldbach stream and comes out in the karst spring (*Su*) at the Subersach river. Under high water conditions, there is a continuous stream from the Rubach spring down to the main river.

3.8.4 Hydraulic properties

Characteristic groundwater flow velocities are calculated by dividing the distance between the injection point and the spring by the travel time of the tracer. The *highest* velocity takes into account the time of the first arrival, the *dominant* velocity takes the time of the maximum concentration. Typical velocities for karst groundwater range between 18 and 360 m/h (MATTHEß & UBELL 1983). FORD & WILLIAMS (1989) give values between 4.5 and 1450 m/h.

The karst aquifer in the Hochifen-Gottesacker area is characterised by high flow velocities. The highest dominant velocities were found in the troughs of the large synclines (e.g. 247 m/h between IP2 and *Ev*) and in the Schwarzwasser valley (143 m/h, IP3–*Au*). On the limb of the synclines, the dominant flow velocities are significantly smaller (56 m/h, IP13–*Sl*). Lower velocities were found in the closed syncline north of the Gottesacker, where the catchment is smaller and partially covered by impervious rocks (60 m/h, IP11–*Ka*). The flow velocity in the limestone bank within the Drusberg marl is ten times lower than in the main karst aquifer but indicates significant karstification (23 m/h, IP14–*RS*). High velocities were found in the rockfall mass (81 m/h, IP8–*Ru*).

Tab. 3.5: Groundwater flow velocities in the Hochifen-Gottesacker area.

flow path	hydrologic conditions (discharge)	example	flow velocity	
			highest [m/h]	dominant [m/h]
trough of a large, open syncline	low-high*	IP9-Au	149	141
	moderate	IP2-Bü	331	233
trough of a small, covered syncline	low-high*	IP11-Ka	64	60
limb of a syncline	low-high*	IP13-Sl	56	56
karst groundwater collector in the Schwarzwasser valley	low-high*	IP7-Sb	98	66
	moderate	IP3-Au	160	143
	low	IP6-Au	147	85
		IP6-Sb	100	71
limestone bank in Drusberg marl	low-high*	IP14-Ls	25	23
rock fall mass	low-high*	IP8-Ru	113	81

* sudden change from low to high discharge due to storm rainfall

The determination of dispersion and other hydraulic properties by analytical modelling of breakthrough curves is not sensible for most of the experiments, as the hydrologic conditions and the resulting spring discharge rates were extremely variable, especially during the tracer test in September 1997 (IP7–16). Furthermore, the tracer was not always directly introduced into the groundwater via a swallow hole, but was often flushed through the unsaturated zone (IP4, 5, 9, 10, 13). The

preconditions for analytical modelling are consequently not fulfilled for the described injections.

The Uranine injection in the estavelle (IP6) in August 1997 was carried out under almost stable low to medium water conditions. The discharge rates were measured regularly using the salt-dilution method. Thus, it was possible to determine the hydraulic properties of the underground flow by analytical modelling using the computer programme TRACI 95 (WERNER 1998). Theoretical breakthrough curves were adapted to the measured concentrations using a best-fit method (Fig. 3.26).

The best results were obtained with a 1-D, non-standardised Single-Fissure-Dispersion-Model SFDM (MALOSZEWSKI et al. 1994). This model was originally made for fissured aquifers with a porous matrix. According to the SFDM, tracer transport is restricted on a single fissure or a series of parallel fissures. This implies that, if the mean transit time of water is sufficiently short, the tracer has no time to diffuse into the matrix deep enough to be affected by adjacent fissures. The model can also be applied for karst aquifers. In this case, the main conduits correspond to the „single fissure“ in the model. As the underground flow in the Hochifen-Gottesacker area is controlled by 1-D structures (syncline axes, valley axis), the application of a 1-D model is justified.

However, it was not possible to model the tailing of the breakthrough curves with only one tracer peak. Thus, a Multi-Dispersion-Model was applied (WERNER 1998). This model assumes that an injected tracer splits up into several tracer clouds which are transported simultaneously through spatially separated flow paths characterised by different flow velocities and dispersions. In the present case, the breakthrough curves can be modelled perfectly with two peaks. The first one corresponds to the fast main drainage network, while the second peak indicates the presence of a slower flow system. The longitudinal dispersivities range between 15.7 and 24.5 m – typical values for a karst system. The total recovery rate in the sampled springs (*Au*, *Bü*, *Ks*, *Sb*) is 91 %, the missing 9 % probably reached the bottom spring (*Bo*). An example for the modelling of a tracer breakthrough curve is given in Fig. 3.35, the complete results for the experiment are presented in Tab. 3.6.

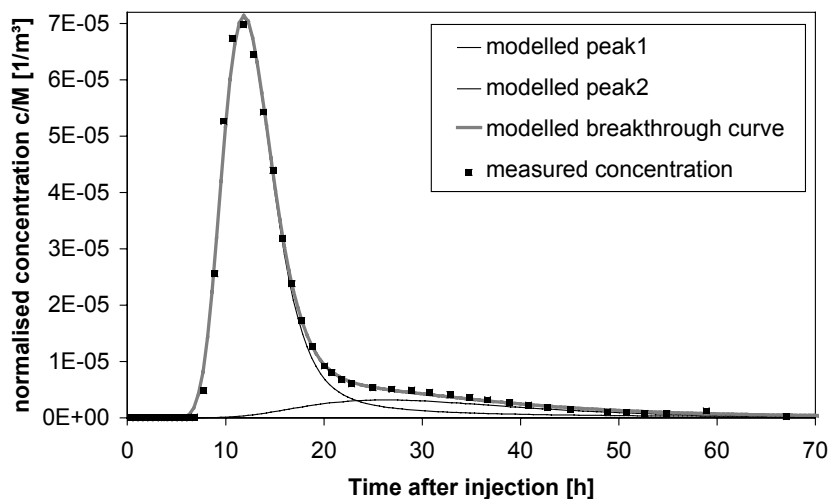


Fig. 3.35: The measures Uranine concentrations (sampling point Au, injection point IP6) can be modelled perfectly with Traci 95 (WERNER 1998) by superimposing two SFDM peaks.

Tab. 3.6: Determination of hydraulic properties of the karst aquifer on the basis of the tracer test IP6. Dispersivities and transit times were calculated by modelling the breakthrough curves with Traci 95 (Werner 1998).

property	spring				sum	unit
	Au	Bü	Ks	Sb		
distance to injection point IP6	1000	1325	1550	2225		m
time of first detection	6.8	7.8	8.8	22.2		h
time of maximum (peak) conc.	11.8	12.8	14.8	31.4		h
maximum concentration	14.0	13.6	12.2	6.1		µg/l
mean spring discharge rate	210	38	15	199	462	l/s
highest flow velocity	147	170	176	100		m/h
dominant (peak) flow velocity	85	103	105	71		m/h
tracer recovery rate	45.2	8.3	3.0	34.4	90.9	%
longitudinal dispersivity (1st peak)	20.9	24.5	23.0	15.7		m
longitudinal dispersivity (2nd peak)	80.5	164.8	135.3	55.2		m
mean transit time (1st peak)	12.2	13	15	31.7		h
mean transit time (2nd peak)	31.3	31.3	31.6	42.8		h

Unlike the above, hydrologic conditions were extremely variable during the experiment in September 1997. The day after the injection, a storm rainfall of 34.2 mm caused a sudden change from low to high water conditions. The discharge rates of all springs increased within hours,

the estavelle turned from a swallow hole into a spring. In the following weeks, there was almost no precipitation so that the discharge slowly decreased. For this experiment, it was consequently impossible to determine the recovery rate and the dispersivity. The breakthrough curves begin with an extremely steep increase in concentration. The first appearance of a tracer is often identical to its maximum concentration so that the maximum flow velocity is identical to the dominant velocity. After the following steep decrease, the concentrations stay almost constant on a relatively high level for several weeks (Fig. 3.36).

Due to the sudden increase of hydraulic pressure in the conduits and the rise of the water table, karst water – and tracers – penetrated the adjacent less karstified zones of the aquifer and the overlying unsaturated zone respectively. Later on, these zones were drained again by the conduits so that the temporary stored tracer left the system slowly.

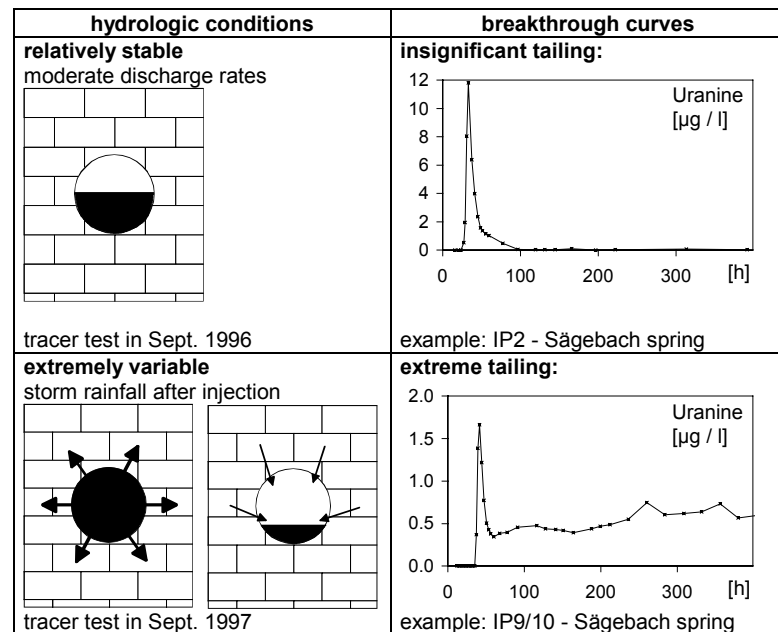


Fig. 3.36: Hydraulic interaction between karst conduits and the surrounding aquifer for different hydrologic conditions and the resulting breakthrough curves.

3.8.5 Hydrogeology of the rockfall mass

The groundwater in the rockfall mass is discharged by the following mechanisms: sink of the Schwarzwasser river, sink of several small streams from the southward bordering Flysch mountains, subsurface inflow from bordering scree slopes (above all from the north), direct infiltration from precipitation and, maybe, upwelling of water from the underlying karst aquifer under extreme high water conditions.

The rockfall mass is discharged by seepage into the underlying karst aquifer (about 70 l/s) and by two group of springs at the base of the rockfall mass. The tracer tests proved that the upper group of springs (*Ru*) is the resurgence of the sinking Schwarzwasser river while the lower one (*Rl*) is the resurgence of the streams from the Flysch mountains. Between the two directly neighbouring springs, there is a hydraulic barrier. However, water from the Schwarzwasser river can overflow this barrier under high water conditions and reach the lower spring.

Even though the rockfall mass is a granular aquifer, it shows many characteristic features of a karst aquifer (Tab. 3.7): There is no surface but only underground drainage, the flow velocities are very high (about 100 m/h), the springs are intermittent or show large discharge variations respectively, the flow is turbulent, turbidity is frequent in the springs, there are enlarged drains and the structure is heterogeneous and anisotrope (SINREICH et al. 2002).

Tab. 3.7: Hydrogeological characteristics of the rockfall mass compared with a typical karst and a typical granular aquifer.

characteristic	typical karst aquifer	rock fall mass in the Schwarzwasser valley	typical granular aquifer
rock type	hard rock	granular material	granular material
structure	anisotrope, heterogeneous	anisotrope, heterogeneous	± isotrope, ± homogenous
recharge	1. diffuse on area 2. concentrated	1. diffuse on area 2. concentrated	diffuse on area
drainage	underground	underground	surface and underground
porosity	1. fractures (and pores) 2. solutionally enlarged karst conduits	1. pores (and fractures) 2. erosionally enlarged drains	intergranular pores
process	karstification (chemical)	subsurface wash (physical)	-
groundwater flow velocity	high (10-1000 m/h)	high (≈ 100 m/h)	low (< 1 m/h)
spring discharge rate	high (m ³ /s)	high (m ³ /s)	low (l/s)
discharge variations	high (intermittent springs)	high (intermittent springs)	low (permanent springs)
turbidity in spring water	frequent	frequent	rare
hydraulic reaction	fast (h-d)	fast (h-d)	slow (d-m)
variations of groundwater table	high (m-100 m)	high (about 10 m)	low (cm-dm)

4 EXAMPLE: WINTERSTAUDE

4.1 Location, topography, climate

The community of Bezau is situated in an altitude of 650 m at the base of a 14 km long, W-E trending mountain chain in the centre of the Bregenzerwald Mountains in the West Austrian state of Vorarlberg (location see Fig. 2.1, Fig. 2.2, Fig. 3.3). The mountain chain is named after its highest summit, the 1877 m high Winterstaude (Fig. 4.1).



Fig. 4.1: Landscape impression of the Winterstaude area; Hochifen-Gottesacker area in the background.

Two springs at the base of the mountain chain serve as drinking water sources for Bezau. A hydrogeological research programme was set up in order to delineate the catchments of these springs and to suggest a scheme for drinking water supply and protection for the community of Bezau (NEUKUM 2001, WERZ 2001, GOLDSCHIEDER et al. 2001d, e).

The area of investigation includes the assumed catchment areas of all the relevant drinking water sources. The area is delimited by natural borders: the valley of the Bregenzerach river to the west, the crest of the Winterstaude mountain chain to the north, the topographic culmination to the east and the mountain ridge south of the Grebentobel valley

to the south. The southward bordering valley and mountain ridge was included in the investigation in order to get a comprehensive overview.

The climatic conditions are similar to those in the neighbouring Hochifenen-Gottesacker area (climatic diagram see there). The annual precipitations measured in the stations Bizau (681 m) and Andelsbuch (613 m), close to Bezau, range between 1800 and 2000 mm (1901–1970). The mean annual air temperature is 6.7 and 7.3 °C respectively.

4.2 Geology

4.2.1 Stratigraphy

The Winterstaude mountain chain is formed of the same tectonic-stratigraphic unit as the eastward bordering Hochifenen-Gottesacker area – the Helvetic Säntis nappe. However, there are significant differences in terms of tectonic structure and stratigraphy (lithology, thickness and chronostratigraphic age of the diachronous formations).

The Palfris formation (Berriasian) mainly consists of marl. According to WYSSLING (1986), the thickness ranges between 250 and 300 m but only 120 m were found in a tunnel through the Winterstaude mountain chain (NEUKUM 2001). The formation outcrops locally in the core of an anticline (Fig. 4.2, Fig. 4.3).

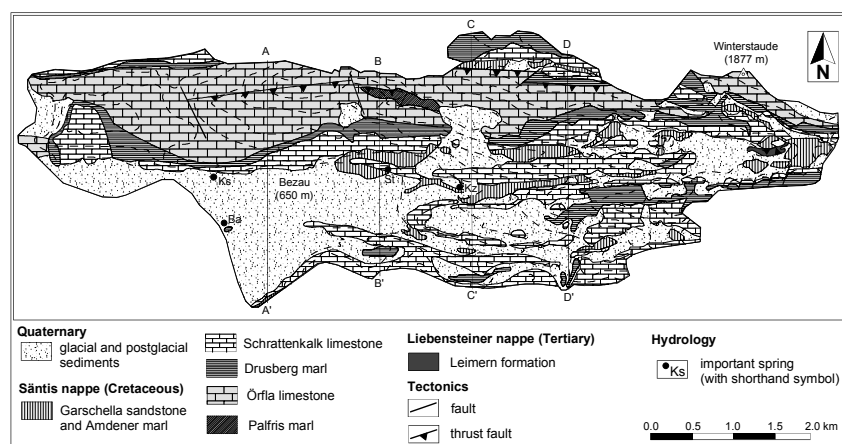


Fig. 4.2: Simplified geological map of the Winterstaude area and location of the sections in Fig. 4.3.

The Örfra formation (Berriasian–Lower Valanginian) is up to 160 m thick and consists of oolitic limestone with some interstratified thin banks of fine-grained sandstone and marl. It outcrops along the anticlines in large parts of the area and forms the entire crest of the mountain chain. A thin and discontinuous condensation zone (< 1m) was deposited in the Valanginian while the Hauterivian Kieselkalk formation – which is present in the neighbouring Hochifen-Gottesacker area – was not deposited in the Winterstaude area. Thus, the top of the Örfra formation forms a significant omission surface (WYSSLING 1986).

The Drusberg formation (Barremian) is highly heterochronous and consists of marl with interstratified thin limestone banks. The formation is about 60 m thick, much less than in the Hochifen-Gottesacker area. The Schratenkalk formation (Barremian–Aptian) is about 100 m thick and consists of pure limestone (ZACHER 1973, BOLLINGER 1988). The two formations outcrop in long, narrow strips along the fold limbs.

The Garschella formation (Aptian–Cenomanian) mainly consists of glauconitic quartz sandstone. The overlying Seewerkalk formation (Albian–Santonian) is characterised by thick bedded limestone. Both formations are only a few meters thick, discontinuous and outcrop locally.

The Amdener formation (Santonian–Campanian) consists of marl and shows strong cleavage. The total thickness is up to 400 m (FÖLLMI 1986), 70 m are preserved in the area along the cores of synclines (NEUKUM 2001). A small tectonic klippe of the Ultrahelvetic Liebensteiner nappe is preserved in the eastern part of the area.

Quaternary deposits cover the entire wide and flat valley floor of Bezau while the elevated areas are only locally covered with moraines, scree, rock fall material and moors (NEUKUM 2001, WERZ 2001).

4.2.2 Tectonics

4.2.2.1 Overview

In the Winterstaude area, tectonic constriction caused folding and thrusting. This is a significant difference to the Hochifen-Gottesacker area where thrust faults are absent. A major strike-slip fault zone (Ostergunten) separates both areas from each other (OBERHAUSER 1951). As the folding and faulting happened simultaneously, the degree of constriction and the resulting fold pattern is different on both sides of the fault zone, so that the folds can not be correlated. Another important fault zone follows the Bregenzerach valley to the west of the area.

4.2 Geology

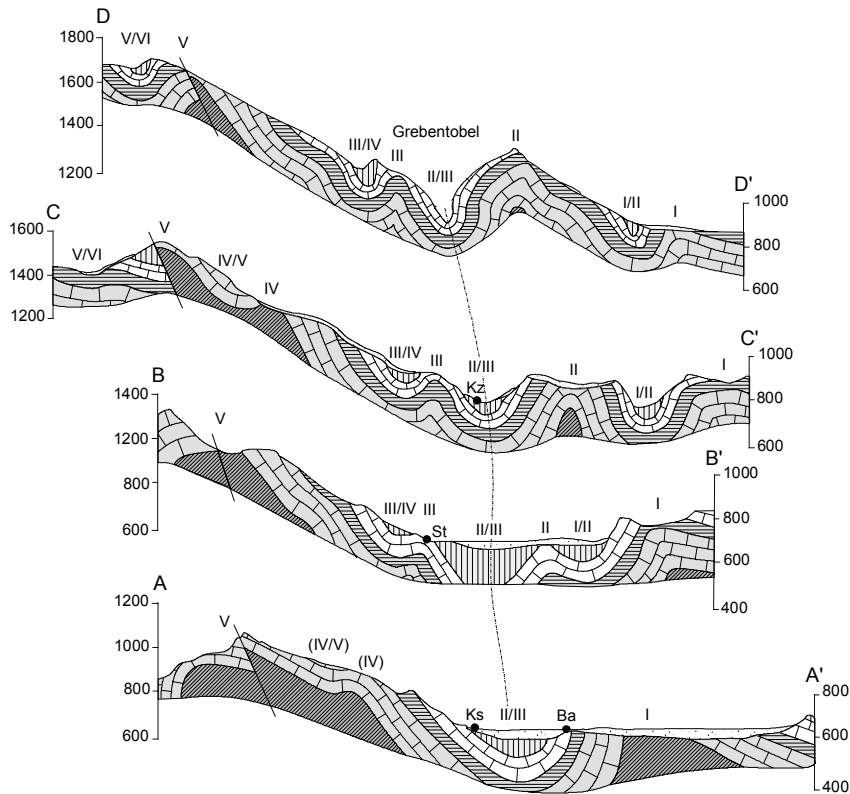


Fig. 4.3: Geological N-S-sections of the Winterstaude area (after NEUKUM 2001 and WERZ 2001). The springs were projected into the sections. Legend and location see Fig. 4.2.

4.2.2.2 Folds

The area is characterised by E-W trending, north-verging and often asymmetric flexural-shear folds (NEUKUM 2001). Both the wavelengths and the amplitudes range between a few hundred meters and about 1 km. The fold train of the Winterstaude mountain chain is both a culmination of fold axes and a narrow anticlinorium of only about 2 km width. The eastern border of the area of investigation is formed by the culmination of the main syncline which coincides with a topographic culmination. Thus, the fold axes predominantly plunge towards the west with about 8° within the area of investigation. Taken by and large, the topography coincides with the fold pattern: Anticlines often form

ridges while synclines form valleys. However, the topography is more gentle and evened out than the tectonics so that the dip of the fold limbs is usually steeper than the slopes.

Most of the folds are not continuous in their trend direction: They end at faults, split up into smaller folds, unify with neighbouring folds or are replaced by different fold structures respectively. NEUKUM (2001) mapped and described eight anticlines and seven synclines in the area. However, some of these folds can not be considered as independent structures so that only six anticlines and five synclines are described in the following. The anticlines are numbered from south to north and the synclines are numbered by combining the numerals of the bordering anticlines (Fig. 4.3 and Fig. 4.4).

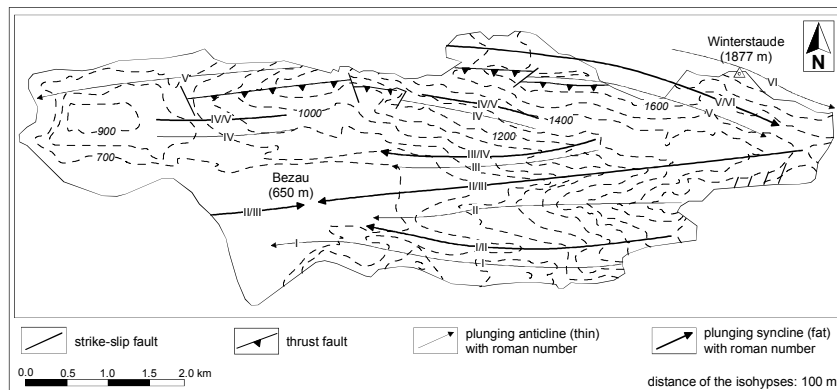


Fig. 4.4: Tectonical map of the Winterstaude area (NEUKUM 2001, GOLDSCHIEDER et al. 2001e).

Anticline VI trends WNW-ESE and plunges in ESE direction. It consists of Öfla limestone and forms the summit of Mt. Winterstaude. The southward bordering syncline V/VI is relatively small, discontinuous and displaced by strike slip faults which run across the fold. It plunges towards WNW in its western and towards ESE in its eastern section.

Anticline V is the main anticline of the area. It forms the crest of the mountain chain except from the Winterstaude summit. In the western section of the anticline, the axis trends W-E and plunges to the west. Along the middle section, a high-angle reverse fault cuts through the core of the anticline and thrusts the southern limb on top of the northern limb. In the eastern section, the axis turns and plunges towards ESE, where the anticline ends near the eastern border of the area.

The southward bordering syncline IV/V and anticline IV are not very distinct subordinate folds on the southern limb of the main anticline V. The fold pair has no significant topographic expression as well but forms the slope of the mountain chain. The only outcrop of the Palfris marl in the area is situated in the core of the anticline IV.

Syncline III/IV is 4 km long and forms a small valley parallel to the mountain chain. The syncline is nearly isoclinal in its eastern and tight in its western section. The fold axis plunges towards the west. Amdener marl is preserved in the core of the syncline. Its eastern end splits into high order folds (two synclines, one anticline). The bordering anticline III forms a low ridge made of Schrattekalk limestone.

Syncline II/III is the main syncline of the area. The pass at the eastern border of the area is formed by the culmination of its fold axis. To the west from the culmination, the syncline plunges with 8–10° under the valley floor of Bezau where it reaches an axial depression. Further to the west, below the Bregenzerach river, the axis rises up again. Along the trough of the syncline, the Schrattekalk limestone is covered with Amdener marl in many places.

Anticline II forms the distinct mountain ridge to the south of the Greben-tobel valley. The Schrattekalk limestone is eroded along the crest of the anticline, so that the older formations outcrop, often covered by moraines. The syncline I/II forms the southward bordering valley. Amdener marl is preserved along its core. Both the syncline and the anticline plunge under the valley floor of Bezau in western direction, where they end up or unify with the southward bordering anticline respectively. The anticline I forms a mountain ridge at the southern border of the area, consisting of Schrattekalk limestone and local outcrops of Drus-berg marl. In western direction it unifies with the anticline II.

The fold pattern becomes simpler in a western direction. In the eastern and central part of the area, there are six anticlines and five synclines side by side, while there are only two main anticlines and one syncline at the western border: Anticline V forms the western section of the Winterstaude mountain chain, while the syncline II/III and the anticline I are below the valley floor of Bezau, covered by Quaternary deposits.

4.2.3 Fault tectonics

The fault pattern is characterised by high-angle reverse faults that run parallel to the fold axes (E-W) and two systems of strike-slip faults that run across the folds. A significant high-angle reverse fault follows the

main anticline V. The southern limb of the anticline is thrust on top of its northern limb. The fault surface dips 60–70° to the south and the displacement is up to 500 m. The fault is subdivided into separate sections by strike-slip faults. A system of left-lateral strike slip faults with extensional component strikes approximately NE; the displacement often ranges between 40 and 70 m. A second system of NW faults with right-lateral displacement is less significant. The joint pattern is characterised by the predominant direction S-N, while SE-NW and NE-SW joints are less frequent (NEUKUM 2001, WERZ 2001).

4.3 Hydrogeology

In the Bezau-Winterstaude area, there are two karstifiable limestone formations – the Örfli and the Schrattenkalk limestone. The Örfli limestone is underlain by the Palfris marl, both limestone formations are separated from each other by the Drusberg marl and the Schrattenkalk limestone is locally covered by the Amdener marl (Fig. 4.3).

The Palfris formation consists of clayey marl which acts as an aquiclude and forms the base of karstification in the Winterstaude area.

The overlying Örfli formation predominantly consists of impure limestone which is intensively jointed and cut by faults. The joints are often enlarged by corrosion. However, the widening mostly extends to only a few centimetres. Thus, the Örfli limestone forms a moderately developed 160 m thick karst aquifer with interstratified layers of low permeability. There are few surface karst landforms. Only three dolines, two small shafts and some small karren were found in the entire area. Even though the slopes are often steep (30–40°), there is little surface runoff.

The Drusberg marl is generally of low permeability but includes some karstifiable limestone banks. It forms an aquiclude between the underlying and the overlying karst aquifer. However, the thickness of this formation is only about 60 m, that is in the same order of magnitude as the displacement of the faults that run across the folds. Consequently, hydraulic contact between the bordering karst aquifers is possible. In the Muotatal area, there are examples for hydraulic contact via faults between bordering karst aquifers which are separated by up to 400 m of marl (BÖGLI & HARUM 1981).

The Schrattenkalk limestone forms a well developed 100 m thick karst aquifer characterised by high flow velocities and fast hydraulic reactions to hydrologic events. The limestone is covered with shallow soil and overgrown with coniferous forest in many places. Karren are de-

4.4 Springs and surface waters

veloped below the soil and aligned dolines follow the troughs of the synclines and faults. In contrast to the bordering Hochifen-Gottesacker area, no important caves are known in the Winterstaude area. There is no surface runoff on Schrattenkalk limestone outcrops. Streams that inflow from bordering areas sink into the karst aquifer.

As both the Garschella and the Seewerkalk formation are discontinuous and only a few meters thick, they play no significant role in the hydrogeology of the area. WERZ (2001) observed slight karstification in the Seewerkalk limestone. The Amdener marl is impervious and acts as an aquiclude on top of the Schrattenkalk limestone karst aquifer. Outcrops of this formation always discharge by surface runoff.

The only significant aquifer in Quaternary deposits is below the wide and flat valley floor of Bezau. The sediments consist of sandy gravel and include some layers with silty sand. The depth to groundwater table ranges between a few meters and 22 m (NEUKUM 2001). Geological sections indicate an aquifer thickness of several tens of metres. The groundwater contour lines show a flow direction toward the SW which indicates recharge from the karst system in the NE (Fig. 4.5).

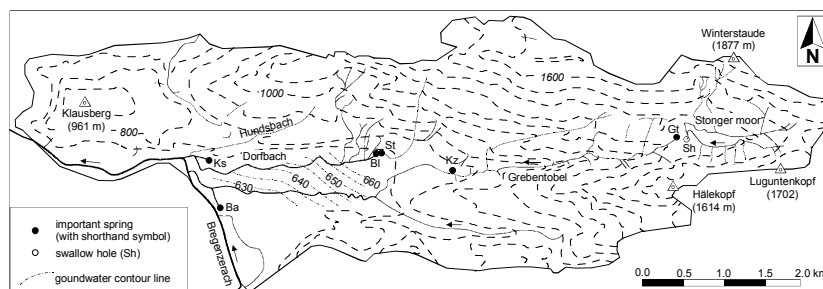


Fig. 4.5: Important springs and surface waters in the Winterstaude area and groundwater contour lines of the granular aquifer in the Bezau valley floor (compiled and modified after NEUKUM 2001).

4.4 Springs and surface waters

The Bregenzerach river acts as the receiving channel for the entire area and forms the base level of the karst system. As the area is formed by a folded sequence of impervious marl and karstified limestone, there is both surface and underground drainage which intensively interact. The water courses either flow in an E-W direction along the troughs of the plunging synclines, or flow in a N-S direction on the fold limbs (Fig. 4.5). All springs that are relevant for the drinking water

supply of Bezau are situated at the base of the mountain chain. In the elevated areas, there are several small springs which were all described by WERZ (2001) and NEUKUM (2001). Only the significant springs and surface waters are described in the following section.

The Grebentobel stream discharges the eastern part of the area. In its upper section, it follows the syncline II/III (Fig. 4.3). Several small springs around the Stonger moor at the eastern border of the area feed a stream that sinks via swallow holes in the karstified Schrattekalk limestone at the western margin of the moor. About 200 m to the west, there is a spring which discharges from karst conduits. This is the source of the Grebentobel stream (shorthand symbol in Fig. 4.5: *Gt*) which alternately flows on Schrattekalk limestone, Amdener marl or on gravel. Under low water conditions, the stream dries up in parts. Under high water conditions, there is a significant inflow from a stream that follows the northward bordering syncline. As this stream flows on Schrattekalk limestone in parts, it dries up frequently.

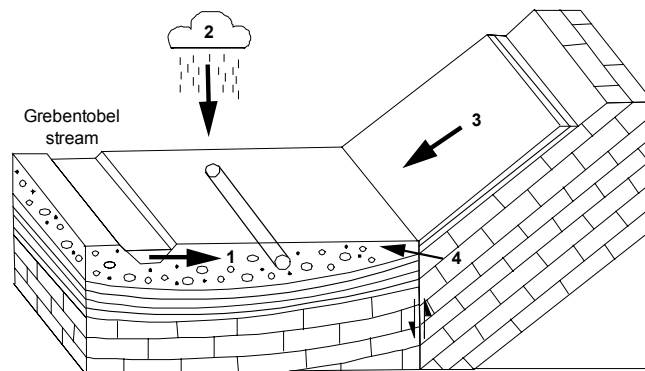


Fig. 4.6: Possible recharge mechanisms of the drainage tubes of the Kreuzboden spring; 1. infiltration from the Grebentobel stream, 2. direct infiltration of precipitation, 3. inflow from the adjacent slope, 4. inflow of karst water (WERZ 2001).

The main drinking water source of the community of Bezau is the Kreuzboden spring (*Kz*) at 770 m which is located at the right (N) side of the Grebentobel stream (Fig. 4.6). The water is extracted from alluvial sediments (gravel) by horizontal drainage tubes 2 m below the ground surface. In the surrounding, the Amdener marl outcrops. The

discharge rate usually ranges between 2 and 20 l/s. However, the spring almost dries up in long dry periods (WERZ 2001).

On the alluvial valley floor of Bezau, the Grebentobel stream loses water by seepage. The Grebentobel stream unites with a stream from the syncline I/II and flows into the Bregenzerach river near the western margin of the valley floor.

The second significant stream is the Dorfbach (*village stream*) which is fed by several tributaries coming down from the southern slope of the Winterstaude mountain chain. However, the main inflow comes from two neighbouring karst springs at 690 m near the base of the slope. The Stuole spring (*St*) is used for the drinking water supply of Bezau if the main source dries up. The spring discharges between about 10 and 100 l/s (Fig. 4.7). It discharges from the Schratenkalk limestone in anticline III (Fig. 4.3). The Bleile spring (*Bl*) shows very similar characteristics. Below these two springs, the karst aquifer plunges under the valley and is covered by Amdener marl.

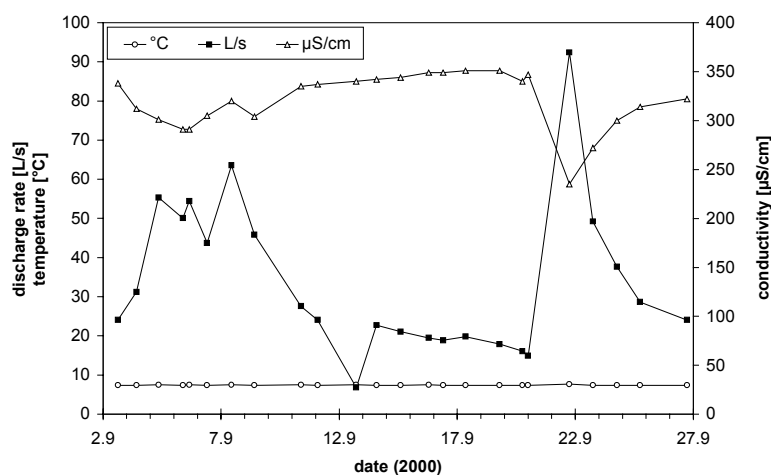


Fig. 4.7: Hydrograph of the Stuole spring (*St*) (NEUKUM 2001).

Another significant spring, the Kressbach spring (*Ks*), is situated at an altitude of 620 m on the flat valley floor directly below a Schratenkalk limestone rock face at the base of the mountain chain. The spring consists of several outlets and discharges about 30 to 300 l/s. Due to the sufficient quantity and the good quality, it is a promising future drinking water source. In autumn 2000, the *Landeswasserbauamt Bregenz*

installed a measuring station at the spring which records the water level, conductivity, water temperature and turbidity (Fig. 4.8). The stage discharge curve is not yet established, and so the discharge rate cannot be calculated on the basis of the measured water level. The temperature shows significant annual variations. The minimum monthly water temperature occurs in April (8.5 °C) and the maximum in October (9.6 °C), three months after the respective extreme values of the air temperature. This delay indicates storage in the granular aquifer of the valley floor. At the same time, the discharge rate of the spring, as well as the conductivity and temperature of the water show fast reactions on hydrologic events which indicates fast flow components (karst?).

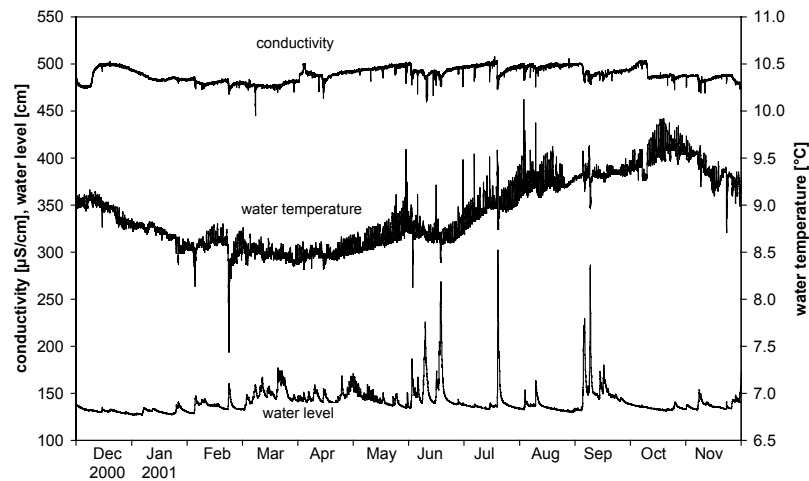


Fig. 4.8: Hydrograph of the Kressbach spring (Ks) (data source: *Landeswasserbauamt Bregenz*; stage discharge curve not yet established).

At the western margin of the Bezau valley floor, close to the right (E) bank of the Bregenzerach river and in the same altitude (617 m), there is a spring (*Ba*) that discharges between 40 and 500 l/s from gravel (Fig. 4.9). However, geological information indicates that the Schratenkalk limestone is present a few metres below the ground surface. Tectonically, it is the southern limb of the main syncline II/III (Fig. 4.3).

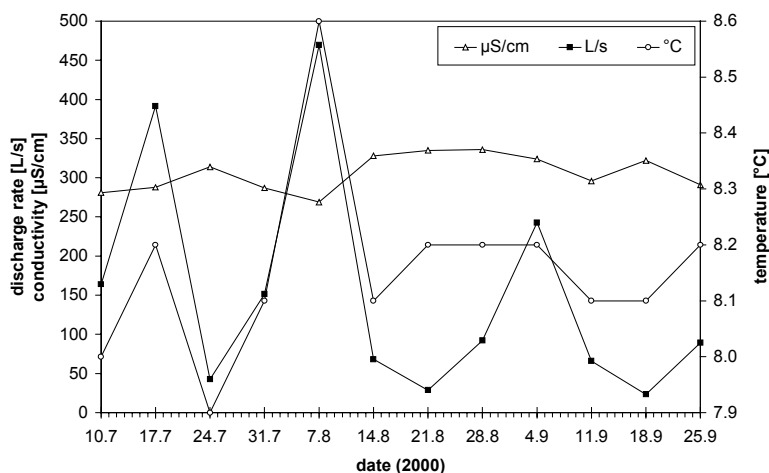


Fig. 4.9: Hydrograph of the spring near the Bregenzzerach (Ba) (NEUKUM 2001).

4.5 Hydrochemistry and microbiology

4.5.1 Overview

All 50 springs in the area were investigated in August 2000 under medium to low water conditions. The temperature, electrical conductivity, pH-value and discharge rate were determined at place, while the chemical and bacteriological parameters, as well as additional physical parameters, were measured at the *Umweltinstitut Vorarlberg* (environmental institute). The calcite saturation index was calculated for all springs on the basis of these data.

4.5.2 Hydrochemical characteristics of the springs

In most of the springs in the area, HCO_3^{2-} (131.2–491.1 mg/l) and Ca^{2+} (42.0–100.0 mg/l) are the dominant ions (Fig. 4.10). The contents of Mg^{2+} (0.6–20.0 mg/l) and SO_4^{2-} (2.0–170.0 mg/l) are highly variable; the highest contents were found in springs which drain the rockfall mass NE of the Stuole spring. NO_3^- , Na^+ and K^+ are always below 6.0 mg/l and NO_2^- , Cl^- , NH_4^+ , CO_3^{2-} , Fe^{2+} and Mn^{2+} are generally insignificant.

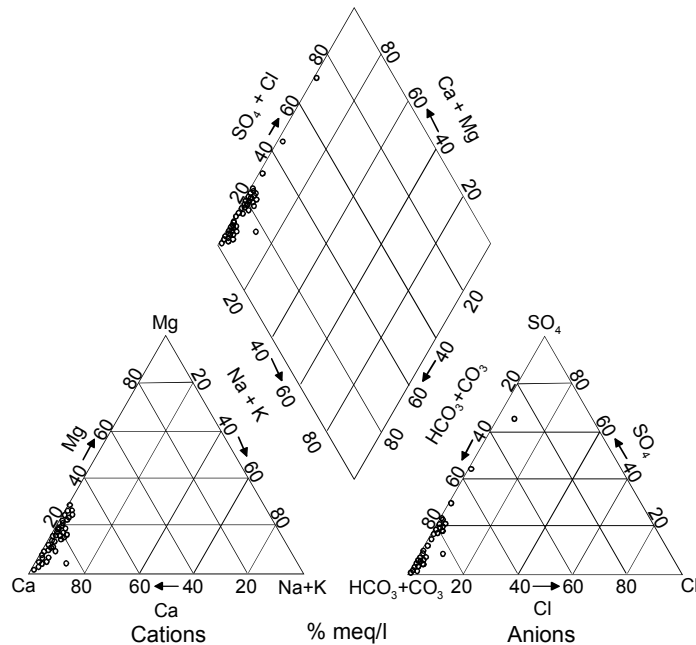


Fig. 4.10: PIPER-diagram of all springs in the area (data: NEUKUM 2001). Calcium and bicarbonate are dominant in most of the springs; exceptionally high contents of sulphate were found in springs which drain rockfall material.

Most of the spring waters are nearly saturated to significantly over-saturated with calcite ($-0.1 < SI < 1.0$). The highest over-saturation was detected in springs which drain rockfall material ($SI = 0.3-1.0$). Precipitation of calcite can be observed at a small waterfall below a spring near the Stuole spring ($SI = 0.6$). The Kressbach spring (*Ks*) and the spring near the Bregenzerach river (*Ba*) are moderately over-saturated ($SI = 0.2$). The Stuole and Bleile karst springs (*St*, *Bl*) are close to saturation ($SI = 0.0-0.1$). The Kreuzboden spring (*Kz*) is slightly under-saturated ($SI = -0.03$) which is unusual for groundwater from a porous aquifer; it indicates inflow from the bordering stream. The relatively high saturation indexes, compared to the Hochifen-Gottesacker area, reflect longer travel times in a generally less karstified and more complex system. Probably none of the springs in the Winterstaude area is fed only by karst water from the Schratenkalk aquifer. Direct or indirect inflow from the Örla karst aquifer, rockfall material, local granular aquifers and/or surface waters has to be expected for most of the springs.

The concentration of all inorganic dissolved solvents is significantly below the limits given in the Austrian drinking water ordinance (BGBI 1998). Consequently, all springs are suitable for drinking water supply in terms of hydrochemistry (but not in terms of microbiology).

The spring waters can be grouped on the basis of their hydrochemical properties (Fig. 4.11). The Stuole (*St*) and the neighbouring karst springs are characterised by moderated contents of HCO_3^{2-} , Ca^{2+} , Mg^{2+} and SO_4^{2-} . The Kressbach spring (*Ks*) shows higher concentrations of HCO_3^{2-} and Ca^{2+} ; its NO_3^- concentration (5.8 mg/l) is the highest of all springs but still far below the limit for drinking water (50 mg/l). The Kreuzboden spring (*Kz*) is characterised by low concentrations of Mg^{2+} and SO_4^{2-} and moderate concentrations of HCO_3^{2-} and Ca^{2+} .

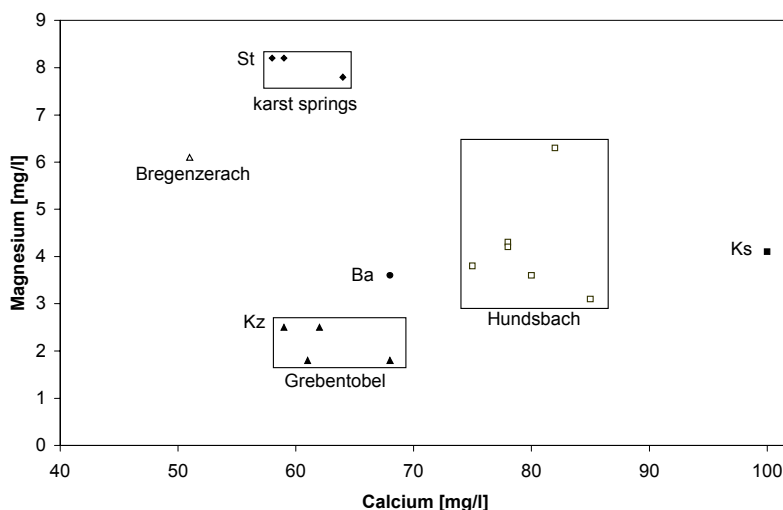


Fig. 4.11: Graphical presentation of the Ca^{2+} and Mg^{2+} concentrations of important springs in the Winterstaude area (data: NEUKUM 2001).

4.5.3 Microbiology

According to the Austrian drinking water law (BGBL 1998), the drinking water has to be free of disease-causing agents. The law prescribes that there must be no *Escherichia coli*, no *coliform* bacteria (at 37 and 44 °C) and no *Enterokokkes* in a water sample of 100 ml; these bacteria are indicators for faecal contamination. Furthermore, the total num-

ber of colony forming units in 1 ml must be less than 100 at 22 °C and less than 10 at 37 °C.

Most of the springs and surface waters that were sampled in August 2000 are rich in bacteria because almost the entire area is used as pasture for cattle. Of course a single analysis per spring can not give representative results but only an overview. Significant differences in bacteria content between the various springs were proved (Fig. 4.12).

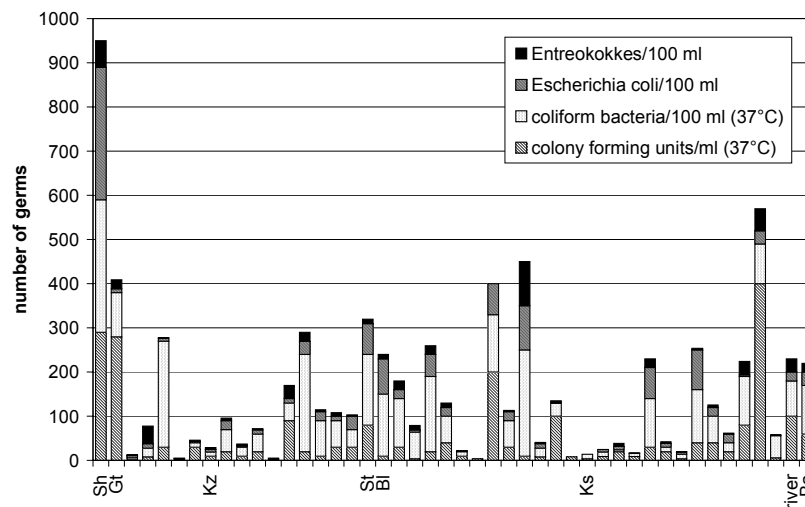


Fig. 4.12: Synopsis of the microbiological properties of all the springs in the area; abbreviations see text and Fig. 4.5 (data: NEUKUM 2001).

Among the springs that are relevant for the drinking water supply of Bezau, the Stuole spring (St) has the worst microbial water quality: 70 *E. coli*, 10 *Enterokokkes*, 160 (37 °C) and 40 (44 °C) *coliform* bacteria were detected in 100 ml of water; 500 (22 °C) and 80 (37 °C) colony forming units were found in 1 ml of water. All these bacteriological values are greatly high the limits. Of course, the spring water is disinfected before use while the samples were taken before the disinfecting.

The microbial water quality of the Kreuzboden spring (Kz) is significantly better: 6 *E. coli*, 1 *Enterokokke*, 9 (37 °C) and 0 (44 °C) *coliform* bacteria were found in 100 ml and the number of colony forming units is 90 (22 °C) and 10 (37 °C). These values are above or close below the limit respectively and disinfecting is necessary as well.

The best quality was found at the Kressbach spring (*Ks*) which is not yet used for drinking water supply: Neither *E. coli* nor *Enterokokkes* were detected in the spring water; 10 (37 °C) and 0 (44 °C) *coliform* bacteria were counted in 100 ml and the total number of colony forming units is 30 (22 °C) and 4 (37 °C) respectively. Thus, the content of coliform bacteria at 37 °C is above the limit while all other bacteriological data fulfil the limit and indicate a good drinking water quality.

Surface waters which are contaminated by human activity and which sink or seep underground are likely to endanger the groundwater quality (DREW & HÖTZL 1999b). These waters were consequently sampled as well: Very high contents of bacteria were detected in the sinking stream at the western margin of the Stonger moor and extreme microbial contamination was proved in waste water from the restaurants and farmhouses in Sonderdach that seeps into rock fall material. Both locations served as injection points during the multi tracer test and were proved to be situated within the catchment of the Stuole spring.

4.6 Tracer tests

4.6.1 Overview

In September 2000, a tracer test with seven injections was carried out in the Winterstaude area under medium to low water conditions. It was the first tracer test in that mountain chain. However, the experiences from the neighbouring Hochifen-Gottesacker system allowed planning both the required tracer masses and of a sensible sampling strategy.

The goal of the experiment was to characterise the hydraulic properties of the two karst aquifers and to determine their interaction, to investigate the influence of stratification and tectonics on the drainage pattern, to delineate the catchments of all karst springs and especially the drinking water springs, to obtain information on contaminant transport and to evaluate the risk potential resulting from existing hazards.

4.6.2 Selection of the injection points and the tracers, injection

Seven injection points (IP1–IP7) were selected in the area within the assumed catchment of the springs relevant for drinking water supply (Fig. 4.13, Tab. 4.1).

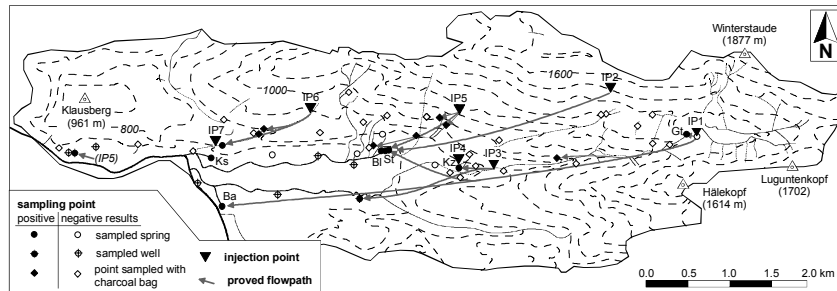


Fig. 4.13: Overview of the tracer tests in the Winterstaude area. Location of the injection points (IP), sampling points (important springs with shorthand symbol) and proved flow paths (after NEUKUM 2001, GOLDSCHIEDER et al. 2001e).

Tab. 4.1: Overview of the tracer injection points in the Winterstaude area.

no.	description	tracer	mass [kg]	flushing water
IP1	Swallow hole Stonger moor, Schrattenkalk limestone	Eosine	2	-
IP2	Karst shaft in Örflla limestone	Sulforh.	3	2000 l
IP3	Grebentobel stream upstream from Kreuzboden spring	Napht.	5	-
IP4	Meadow above Kreuzboden spring drainage tubes	Pyranine	0.1	2000 l
IP5	Waste water seepage Sonderdach (2 points)	Uranine	0.5 + 0.5	-
IP6	Sink of upper Hundsbach stream in Örflla limestone	Pyranine	2	-
IP7	Sink of lower Hundsbach stream in Schrattenkalk limestone	Napht.	1	-

The first injection point (IP1) was the swallow hole at the western margin of the Stonger moor at 1360 m, where a stream rich in faecal bacteria ($> 300 E. coli/100\text{ ml}$) sinks into the Schrattenkalk karst aquifer in the upper section of syncline II/III; 2 kg of Eosine were injected in IP1. The goal of this experiment was to characterise the hydrogeological function of the main syncline and to evaluate the impact of the microbial hazard on the springs.

A small karst shaft in the Örflla limestone at 1490 m that is used as the refrigerator of a mountain hut served as the injection point (IP2) for 3 kg of Sulforhodamine – probably the first tracer test in a refrigerator. 2000 l of flushing water were provided by the fire brigade. The goal of this injection was to obtain information on the hydraulic properties of the Örflla karst aquifer and to check for possible contacts with the Schrattenkalk karst aquifer.

The third injection point (IP3) was the Grebentobel stream 500 m upstream from the Kreuzboden spring at 810 m. Because of the low water conditions, the stream was seeping into gravel that covers Amdener marl downstream from the injection point. The goal of this experiment

was to check if the Kreuzboden spring gets inflow from surface water which is of major importance for drinking water protection. Thus, the UV fluorescent dye Naphthionate was selected as a tracer in order to avoid visible colouring in the drinking water. A relatively high amount of tracer (5 kg) was injected in order to obtain unambiguous results.

The water of the Kreuzboden spring (Kz) at 770 m is extracted from gravel by horizontal drainage tubes 2 m below a meadow. In order to check the protective function of the overlying layers above the tubes, 100 g of Pyranine was put directly on the ground surface over an area of $10\text{ m} \cdot 2\text{ m}$ (20 m^2) with a watering can (IP4). Afterwards, an artificial rainfall of 2000 l was produced by the fire brigade over an area of 60 m^2 in order to flush the tracer into the ground. The precipitation depth of 33 mm is typical for an average storm rainfall.

The waste water of a cable railway station, a restaurant and several farmhouses in the locality of Sonderdach (IP5) seeps into rock fall material that covers the Schrattekalk limestone on a steep slope directly above the two drinking water sources of Bezau. In order to evaluate the impact of this microbial hazard on the springs, each 0.5 kg of Uranine was injected into each of the two main waste water channels.

On the slope above the Kressbach spring, the intermittent Hundsbach stream follows approximately the narrow strip of outcropping Drusberg marl. In its upper section, the stream sinks into the northward bordering Öfla limestone under low water conditions; 2 kg of Pyranine was injected there (IP6). In the lower section, directly above the spring, the stream partially sinks into the southward bordering Schrattekalk limestone; 1 kg of Naphthionate was injected there (IP7). Both injections were intended to check for the inflow of karst groundwater from the two aquifers to the Kressbach spring (Ks).

Injections IP1–3 and IP5–7 were carried out on the 9th September 2001. The dye powder was put in plastic canisters of 10 to 20 l in the laboratory, dissolved with water on site and injected. Five of the injections were done in swallow holes, sinking and seeping streams so that no flushing water was required. Only for the injections IP2 and IP4 did flushing water have to be provided by the fire brigade. The injection IP4 was done two days later in order to reduce the risk of simultaneous visible colouring in both drinking water sources.

The tracers Pyranine and Naphthionate were used at each two different injection points: Pyranine was used at IP4 and IP6, Naphthionate at IP3 and IP7. However, interference is impossible as IP3 and IP4 are sur-

face injections within the catchment of the Kreuzboden spring which cannot reach one of the two karst aquifers, while IP6 and IP7 are injections into the two karst aquifers, directly above the Kressbach spring.

4.6.3 Sampling

All springs, streams and groundwater observation wells in the area were sampled for up to 68 days after the injection. Altogether, 51 sites were observed (Fig. 4.13). Water samples in 50 ml brown glass bottles were taken manually and with three automatic samplers in those sites where a breakthrough of tracers was considered to be likely and in sites of major interest (drinking water sources, large karst springs), while charcoal bags were installed in less important points and in points where the appearance of tracers was considered to be unlikely. In selected sampling points, both water samples and charcoal bags were used. The charcoal allows to detect concentrations that are below the detection limit in water samples, while water samples allow to determine the precise concentration at a given time.

4.7 Results

4.7.1 Overview

Positive results were obtained for six of the seven injected tracers. Only the Naphthionate injected in IP7 was not found again. An overview of the tracer test results is presented in Tab. 4.2 and Fig. 4.13.

4.7.2 Swallow hole Stonger moor (IP1)

The Eosine that was injected into the swallow hole at the western margin of the Stonger moor was detected at seven sampling points (Fig. 4.13). 45 h after the injection it was detected at the Stuole spring (*St*) and the neighbouring springs (Fig. 4.14). The maximum concentration of 70.1 µg/l was reached 60 h after the injection; the recovery rate was 131.6 g (6.58 %). These results prove that the Stuole spring discharges karst water from the Schrattenkalk aquifer in the syncline II/III and is endangered by contaminated surface water from the Stonger moor.

The Eosine also reached the spring of the Grebentobel stream (*Gt*) and another small karst spring at that stream. Three days after the injection, minor traces of Eosin were detected in two water samples of the Kreuzboden spring. As this spring is not a karst spring but fed by inflow

from the Grebentobel stream, it is probable that the tracer reached the spring indirectly, that is via the stream (Fig. 4.6).

Tab. 4.2: Overview of the tracer test results in the Winterstaude area for the important sampling points. The time of maximum concentration (t_m), normalised maximum concentration (c/M) and recovery rate (%) is given for each proved connection. White box: spring was analysed for the respective tracer; grey: not analysed, no connection (clear hydrogeological evidence); + connection proved with charcoal bags; - no connection.

spring no.	injection point							t_m c/M R
	IP1	IP2	IP3	IP4	IP5	IP6	IP7	
Gt	+	-						
Kz	77.2	-	9	0.33	-			h
	0.21		433	1161				$10^{-6}m^{-3}$
	0.0001		12.91	4.48				%
St	60.1	271.7			76.9	-		h
	35.1	6.62			1.34			$10^{-6}m^{-3}$
	6.58	6.25			1.66			%
Bl	60.2	271.0			77.0	-		h
	40.1	6.64			0.89			$10^{-6}m^{-3}$
	5.89	4.35			1.79			%
Ks	-	-			-	-	-	
Ba	211.3	-			-	-		h
	5.65							$10^{-6}m^{-3}$
	16.3							%

About 6 days after the injection, the Eosine reached the spring at the Bregenzerach river which is situated at the western margin of the wide, flat Bezau valley floor. Thus, this spring is a karst spring and the Schratenkalk limestone in the main syncline II/III forms a well developed connection between the alpine karst system and the spring.

4.7.3 Karst shaft in Örfli limestone (IP2)

The Sulforhodamine that was injected into the karst shaft in the Örfli limestone was detected in the Stuole spring (*St*), the Bleile spring (*Bl*) and the neighbouring karst springs which are all discharged from the Schratenkalk limestone (Fig. 4.13 and Fig. 4.14). In the Stuole spring, the tracer was first detected about 3 days after the injection and the maximum of 19.9 $\mu\text{g/l}$ was measured after 11 days. The recovery rate is 187 g (6.2 %). These results prove that there is a hydraulic connection between the Örfli and the Schratenkalk karst aquifer.

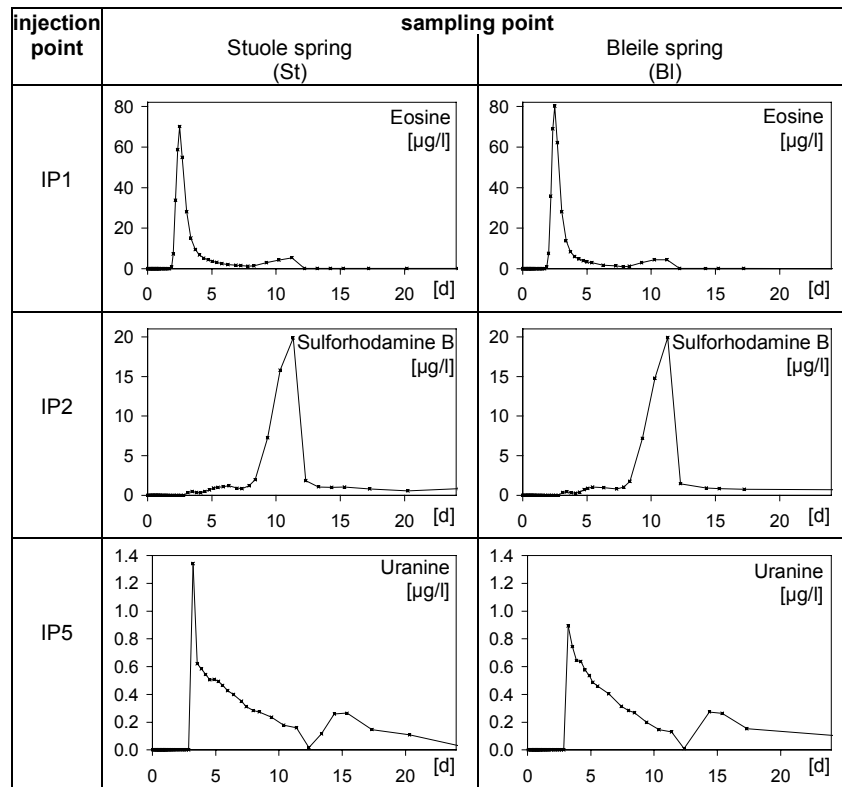


Fig. 4.14: Breakthrough curves for Eosine (injection IP1), Sulforhodamine (IP2) and Uranine (IP5) at the Stuole (St) and the neighbouring Bleile spring (Bl).

4.7.4 Grebentobel stream (IP3)

The Naphthionate that was injected in the Grebentobel stream arrived at the Kreuzboden spring (Kz) after 5 h and reached the maximum concentration of 2165.5 µg/l after 9 h. The recovery rate was 636 g (12.9 %). These results prove that the Kreuzboden spring gets significant inflow from the infiltrating surface water of the Grebentobel stream (Fig. 4.6). Naphthionate was also detected in one of the groundwater observation wells in the Bezau valley floor.

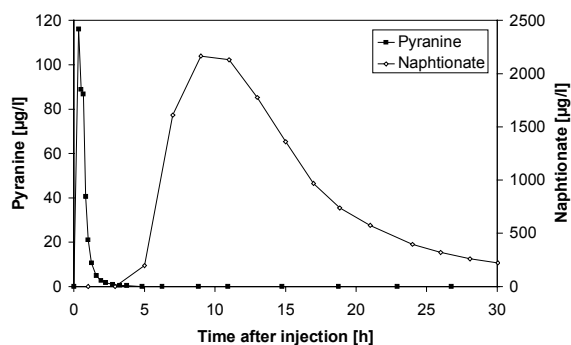


Fig. 4.15: Breakthrough curves for Naphthionate (IP3) and Pyranine (IP4) at the Kreuzboden spring.

4.7.5 Meadow above the Kreuzboden spring (IP4)

The Pyranine that was put on the ground surface directly above the drainage tubes of the Kreuzboden spring (Fig. 4.6) reached the spring within 5 minutes of the beginning of the artificial rainfall (Fig. 4.15). The total duration of the Pyranine breakthrough was only about 5 h and the recovery rate was 4.48 g (4.48 %). The results show that possible contaminants can reach the spring via preferential flow paths within minutes of a storm rainfall.

4.7.6 Waste water seepage at Sonderdach (IP5)

Uranine was injected in two waste water channels at Sonderdach seeping in rockfall material which covers the Schrätenkalk limestone. Uranine reached the Stuole spring (*St*) and the neighbouring karst springs (Fig. 4.13, Fig. 4.14). It was first detected at the Stuole spring three days after the injection with the maximum concentration of 1.34 µg/l. Traces were still detectable at the end of the 68 day sampling period; the recovery rate was 166 g (1.66 %). The results prove that the Stuole spring receives water from the syncline III/IV and that the water quality is endangered by seepage of waste water at Sonderdach.

Uranine was also detected in three small springs that discharge from rock fall material below Sonderdach, as well as in two groundwater observation wells at the western margin of the area (NEUKUM 2001).

4.7.7 Upper Hundsbach stream (IP6)

The Pyranine that was injected in the upper section of the Hundsbach stream did not reach the Kressbach spring (*Ks*). The tracer was detected in three small spring in the middle and lower section of the stream that were sampled with charcoal bags (Fig. 4.13). The negative results from the Kressbach spring indicated that it gets no significant inflow from the Örfra karst aquifer. However, Pyranine often fails in karst aquifers due to fast and complete decay (GOLDSCHIEDER et al. 2001b, c) so that negative results with Pyranine can be contested.

4.7.8 Lower Hundsbach stream (IP7)

The Naphthionate that was injected in the lower section of the Hundsbach stream was not detected in any sampling point, particularly not in the Kressbach spring (*Ks*). The negative results indicate that the Kressbach spring gets no inflow from the Schrattenkalk karst aquifer.

4.8 Conclusions

4.8.1 Fold tectonics and underground drainage pattern

The stratification, the fold and fault tectonics and the base level conditions are the main factors that control the underground drainage pattern of the Winterstaude alpine karst system.

There are two significant karst aquifers – the Örfra and the Schratenkalk limestone. The Örfra karst aquifer is about 160 m thick and underlain by marl that acts as an aquiclude. The 60 m thick Drusberg marl forms an aquiclude between the underlying Örfra and the overlying 100 m thick Schrattenkalk karst aquifer. Locally, along the synclines and in the valleys, the Schrattenkalk karst aquifer is overlain by impervious sandstone and marl aquicludes.

The Örfra limestone outcrops along the crest of the Winterstaude mountain chain and forms the core of the massive while the Schratenkalk limestone outcrops in the lower parts all around the mountain chain. Even though the outcrops of the Örfra aquifer form a large recharge area, all significant karst springs discharge from the Schratenkalk aquifer. Thus, it is evident that groundwater from the Örfra aquifer enters the Schrattenkalk aquifer via faults that cut through the Drusberg marl aquiclude. This hydraulic connection was proved by the

injection of a tracer into the Örfra aquifer (IP2) which reached several springs that discharge from the Schrattenkalk aquifer (Fig. 4.16).

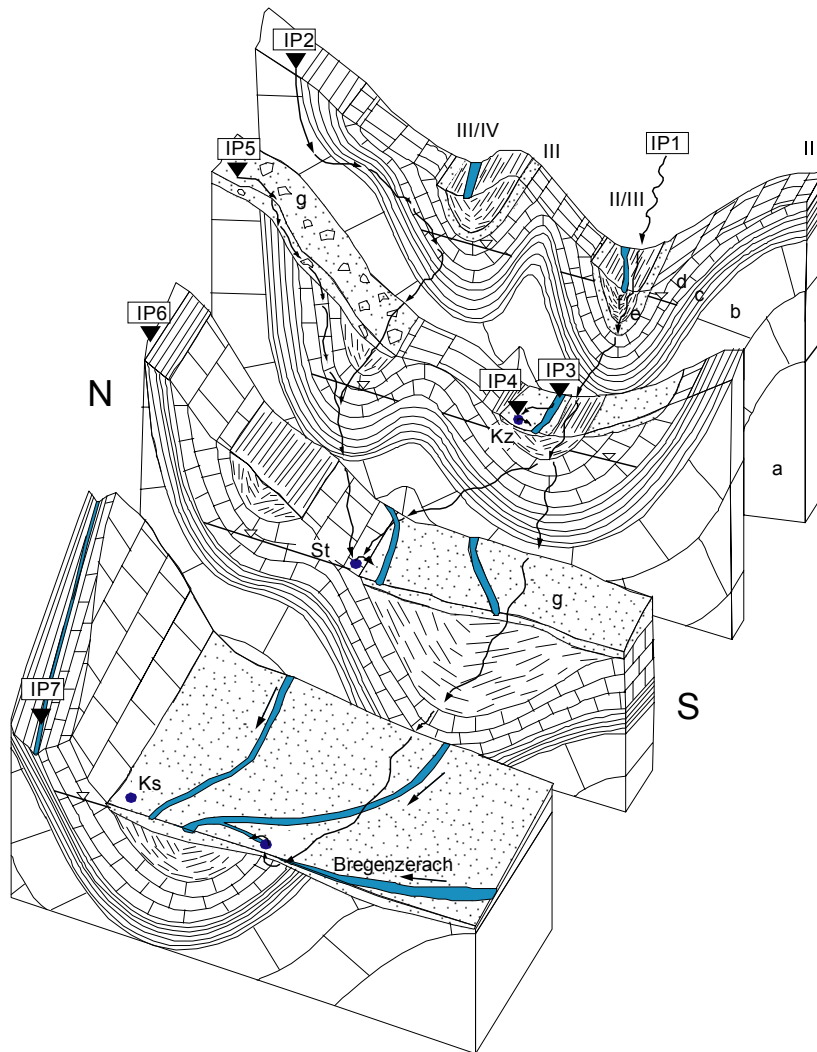


Fig. 4.16: Schematic hydrogeological block diagram of the Winterstaude area. Location of the injection points (IP1–IP7), the springs (with shorthand symbol) and the proved flow paths (NEUKUM 2001, slightly modified).

Due to the interstratification between marl aquicludes and karst aquifers, the underground flow is largely parallel to the stratification. The strong stratigraphic flow control leads to an effective tectonic flow control by the folds. In the elevated areas above the base level of the karst system, the troughs of the plunging synclines form the main flow paths for the karst groundwater. The crests of the anticlines form local watersheds and the culmination line of the folds at the eastern margin of the area forms a regional watershed. However, some of the folds are discontinuous and so their hydraulic function is limited.

Near the base level of the system, the groundwater often overflows the anticlines and so the waters from neighbouring synclines mix. For the same reason, the springs are usually not located in the troughs of the synclines but at the crests of anticlines or on the fold limbs: The Stuole spring is situated near the crest of anticline III and gets inflow from the bordering synclines and the spring at the Bregenzerach river is situated on the southern limb of the main syncline II/III which forms a karst water flow path below the valley floor.

The Winterstaude area is drained by four different mechanisms – surface runoff, shallow karst water flow, infiltration in the granular aquifer and deep karst water flow. There are various interactions between those mechanisms:

Surface runoff takes place on the outcrops of marl, that is along the cores of the synclines and on the limbs between the two limestone formations. The surface waters either run largely parallel to the axes of the synclines or go down the slopes formed by the fold limbs. Streams often seep or sink underground when they reach karstified limestone.

Shallow karst water flow takes place above the level of the valley floor. The alpine karst system is mainly discharged by the Stuole spring (*St*) and some neighbouring spring near the base of the mountain chain, between a few metres and some tens of metres above the valley floor. However, the waters from neighbouring synclines often mix so that the springs get water from several subsystems. Some small karst springs are situated in a higher position. The highest significant karst spring is the source of the Grebentobel stream (*Gt*) at 1350 m.

A portion of the water from the alpine karst system contributes to the recharge of the granular aquifer in the Bezau valley floor. The tracer tests, groundwater contour lines (NEUKUM 2001) and hydrological observations show that there is both seepage of surface streams and

direct inflow from karst groundwater into the granular aquifer. The Kressbach spring (*Ks*) discharges from that granular aquifer.

Deep karst water flow was proved by tracer test (IP1). The main syncline II/III continues below the Bezau valley floor and connects directly the alpine karst with the spring at the Bregenzerach river (*Ba*). Below the valley floor, the Schrattenkalk karst aquifer is covered with impervious Amdener marl and Quaternary deposits. Confined and (locally and temporary) artesian conditions are presumed in the deep karst.

4.8.2 Delineation of the catchments

The catchments of the drinking water sources and other significant springs were delineated on the basis of geological and hydrological information and tracer tests.

The Kreuzboden spring (*Kz*) gets no direct karst water inflow but discharges from a granular aquifer fed by infiltrating surface water from the Grebentobel stream. However, the stream gets karst water inflow from some small springs, and so there is indirect karst water influence. Thus, the catchment of the Grebentobel stream forms the catchment of the Kreuzboden spring.

The Stuole spring (*St*) and the neighbouring springs discharge from the Schrattenkalk karst aquifer but get inflow from the Örla karst aquifer as well. The springs are located at the anticline III and discharge the entire area between the anticlines II and V. The crest of the Winterstaude mountain chain (anticline V) is the northern border of their catchment; the culmination of the folds forms the eastern border and the crest of the mountain ridge (anticline II) south of the Grebentobel valley is the southern border. The western border cannot be precisely delineated. The injection point IP5 is inside the catchment while IP6 is outside, and so the border has to be in between.

The Kressbach spring (*Ks*) is situated at the base of the mountain chain on the Bezau valley floor. None of the tracers that were injected in the alpine karst system reached the spring. Probably, the Kressbach spring gets no direct inflow of karst water but is discharged from the granular aquifer in the valley floor. As there are intensive interactions between that granular aquifer and the alpine karst system, indirect inflow of karst water to the spring is expected and further research in the assumed catchment is suggested.

4.8.3 Hydraulic properties

The groundwater flow velocities were calculated on the basis of the tracer breakthrough curves and are moderate for an alpine karst system. Most of the proved flow paths are complicated and include passages in different aquifers.

The connection between the injection point IP1 and the Stuole spring (St) follows the trough of the main syncline II/III and is characteristic for the shallow Schrattenkalk karst aquifer. Here, the maximum flow velocity is 91 m/h and the dominant flow velocity is 73 m/h.

The deep Schrattenkalk karst aquifer below the valley floor can be characterised indirectly by comparing the breakthrough curves of the Stuole spring (shallow karst) and the spring at the Bregenzerach river (deep karst). The maximum flow velocity in the deep aquifer is 22 m/h.

The maximum and dominant flow velocities between the injection IP2 in the Örfli limestone and the Stuole spring are 41 m/h and 12 m/h respectively. As the flow path includes unsaturated and saturated flow in the Örfli aquifer, a passage through the Drusberg marl via a fault and subsequent flow in the Schrattenkalk aquifer, the calculated velocities are characteristic for the entire system but do not allow for the characterisation of the Örfli karst aquifer.

The maximum and the dominant flow velocity between the injection IP5 and the Stuole spring is 16 m/h (the maximum concentration was measured in the first positive sample). As the flow path consists of surface flow, seepage through rock fall material and karst water flow, the breakthrough curve is not characteristic for a particular aquifer.

Because of the described reasons, it is not possible to determine the hydraulic properties (e.g. dispersivity) of the Örfli and Schrattenkalk aquifer on the basis of the breakthrough curves.

5 EXAMPLE: ALPSPITZE

5.1 Location, topography, climate

The 2628 m high Alpspitze is a prominent summit of the Wettersteingebirge mountain range in the Northern Limestone Alps (location see Fig. 2.1, Fig. 2.2). The mountain range consists of three approximately W-E trending chains with two valleys in between. The northern and the central chain belong to Germany while the southern chain forms the Austrian border. To the west, the three chains unite and culminate in the 2962 m high Zugspitze, Germany's highest peak (Fig. 5.1).



Fig. 5.1: View from the Alpspitze to the Zugspitze.

The Alpspitze is situated in the eastern part of the central mountain chain. The bordering valleys form natural topographic and hydrologic boundaries: the Höllental valley (*hell valley*) with the Hammersbach river in the NW and the Reintal valley with the Partnach river in the south and east. Towards the NE, the karstified rocks end along a line which is followed by the two streams Bodenlaine and Graslaine. To the west, the central mountain chain connects Mt. Alpspitze with Mt. Zugspitze. As there is no clear natural boundary there, the limit of the area of investigation was set up arbitrarily along a N-S trending line.

There are two weather stations close to the Alpspitze. The first is situated in the community of Garmisch-Partenkirchen at 719 m and the second is on the summit of the Zugspitze at 2959 m. In Garmisch-Partenkirchen, the total annual precipitation is 1364 mm with a main maximum in summer (June-August), a secondary maximum in December and two minima in February and October. The mean annual air temperature is 6.7 °C with a minimum of -2.7 °C in January and a maximum of 15.9 °C in July. On the summit of Mt. Zugspitze, the total annual precipitation is 2003 mm. There is high precipitation all through the year except in the relatively dry months September and October. The mean annual air temperature is -4.8 °C with a minimum of -11.4 °C in February and a maximum of 2.2 °C in July and August (Fig. 5.2). Thus, the local vertical temperature gradient is 0.5 K/100 m.

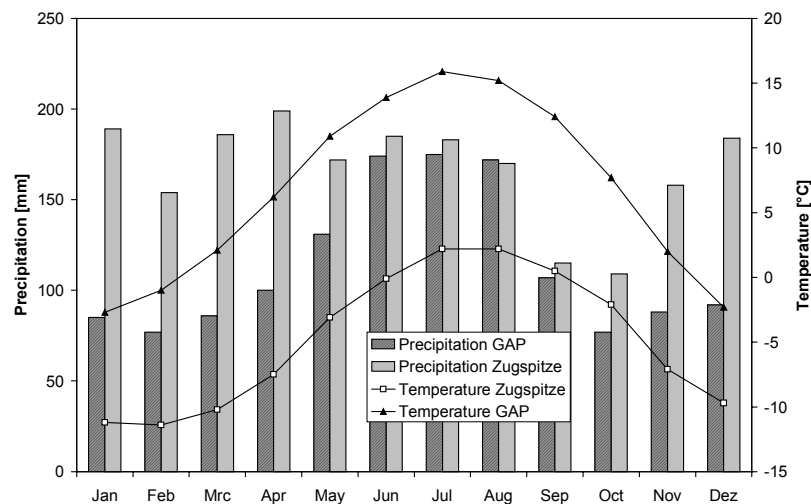


Fig. 5.2: Precipitation and air temperature in Garmisch-Partenkirchen (GAP) (719 m) and on the summit of the Zugspitze (2959 m). Data from the period 1961–1990.

5.2 Geology

5.2.1 Geological framework

The Wettersteingebirge mountain range is formed by the Lechtal nappe which belongs to the East Alpine (Austro-Alpine) system (TOLLMANN

1976). The area is predominantly made of Triassic sedimentary formations. The general thrust direction of the alpine nappes is largely toward the north, and so the thrust faults inside the Wettersteingebirge are north-verging. However, in a late stage of orogenesis, the massif was thrust on top of a southward bordering zone of younger sedimentary rocks (Rhaetian–Neocomian). Thus, the Wettersteingebirge is a large back thrust mass (MILLER 1962).

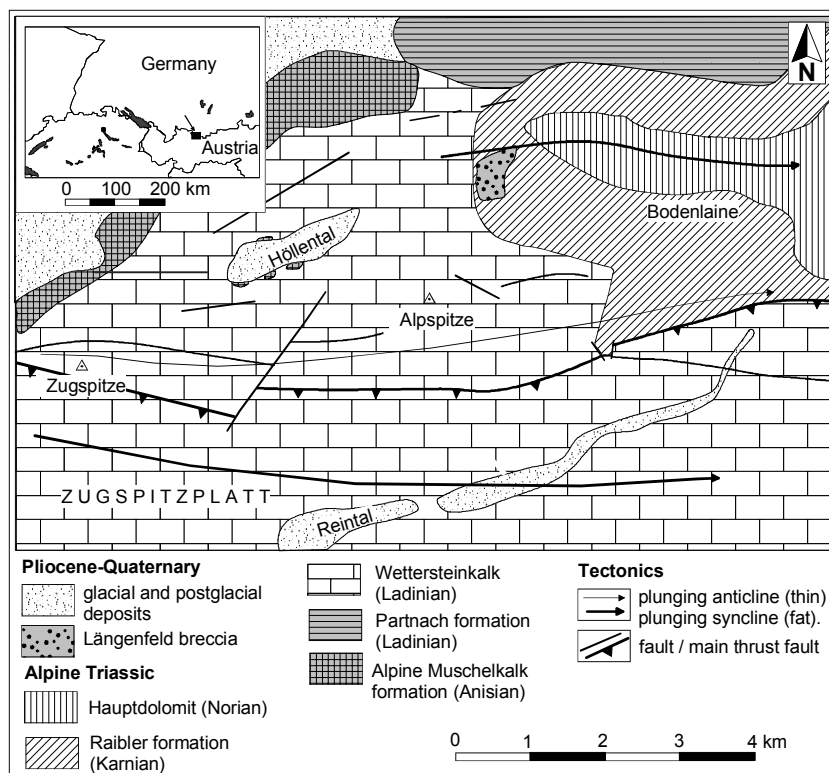


Fig. 5.3: Simplified geological map of the Alpspitze area (after MILLER 1962). Quaternary deposits outside the main valleys are not shown.

5.2.2 Stratigraphy

The Wettersteingebirge is made of sedimentary rock formations of the Alpine Triassic. The Anisian Alpine Muschelkalk is the oldest formation in the area. However, the term is misleading as the formation differs both in terms of time and lithology from the classical Germanic

Muschelkalk. The formation consists of reef and nodular limestone that outcrops at the base of north-face of the Wettersteingebirge and, locally, in the Höllental valley (Fig. 5.3).

The Ladinian Wettersteinkalk formation is named after the Wettersteingebirge, because it forms all summits in this mountain range and in many other parts of the Northern Limestone Alps. In the Alpspitze area, the formation is 800–1000 m thick. Towards the NE, the thickness decreases until the formation is laterally replaced by Partnach marl (VACHÉ 1960). The Wettersteinkalk formation represents different parts of a reef: the fore reef, the central reef and the lagoon (LINZER 1989). Consequently, the formation consists of massive limestone (reef) and well bedded limestone (lagoon) with characteristic algal mats; locally, the limestone underwent dolomitization (REIS 1911, MILLER 1962).

The Karnian Raibler formation outcrops in the NE of the area and can be subdivided in three members: The lowest member consists of sandstone, marl and shale. Its thickness increases from 20 m in the south to 150 m in the north. The middle member is up to 250 m thick and consists of massive, strongly fractured limestone and dolomite. The highest member is a highly heterogeneous evaporitic sequence of up to 250 m thickness. A portion of this sequence has been leached out, so that it is often represented by residual, cellular and cavernous limestone and dolomite which show bizarre weathering structures (REIS 1911, VACHÉ 1960, JERZ 1966). In the following, these three members will be called Raibler sandstone, limestone and cellular dolomite.

The highest formation in the Alpspitze area is the Norian Hauptdolomit (*main dolomite*). Only the lowest part of the originally 1000 m thick formation is preserved in the NE of the area. The formation consists of monotonous, strongly fractured dolomite which easily disintegrates into detritus. In other parts of the Northern Limestone Alps, the Hauptdolomit formation reaches a thickness of more than 2000 m and forms a lot of prominent summits.

The Längenfeld breccia probably formed in the Pliocene. It consists of detritus of the older formations with a carbonatic cement (REIS 1911, VACHÉ 1960, VIDAL 1953). Several cycles of graded bedding indicate the fluvial formation of the breccia. The breccia can be found in the north of the area in an altitude of 1600 to 1800 m – high above the current level of the surrounding valleys. This high topographic position indicates the young uplift of the mountain range and the fast erosion of

the surrounding valleys. The breccia probably represents the local base level of the Pliocene karstification (GOLDSCHIEDER et al. 1999a).

There are three types of moraines: The first type contains crystalline components from the central Alps indicating a far transport by glaciers in the Pleistocene. The second type consists of rock debris of the Triassic formations and is of local origin. East of Mt. Zugspitze, there are some remnants of glaciers. Thus, the third type of moraine is recent.

After deglaciation, several rockfalls took place, some of them in historical time. They often caused obstruction in the valleys (HIRTLREITER 1992, BROSEMER 1999, GOLDSCHIEDER et al. 1999a).

5.2.3 Tectonics

The strata are folded. The fold axes trend W-E and plunge towards the east (MILLER 1962, VACHÉ 1960). Within the area of investigation, there are two large synclines and one main anticline. The upper section of the Reintal valley south of Mt. Alpspitze follows a large syncline, the Reintal syncline. The northward bordering Wetterstein anticline forms the entire central mountain chain which connects Mt. Zugspitze and Mt. Alpspitze. The Wetterstein syncline in the north of the area plunges steeply (35°) in eastern direction towards the Reintal valley. In the core of this syncline, the younger formations above the Wettersteinkalk limestone are preserved (Fig. 5.3).

The most significant thrust fault within the area runs parallel to the main anticline. Here, the southern syncline is thrust in northern direction over the main anticline. The vertical displacement is 600 m, the constriction component is 800 m and the thrust is 1000 m (MILLER 1962); the strike-slip displacement is difficult to quantify. Additionally, the area is cut by a shear system of SW-NE trending left-lateral and SE-NW trending right lateral faults.

5.3 Hydrogeology

5.3.1 The Wettersteinkalk and Partnach formation

The limestone of the Wettersteinkalk formation is generally slightly to moderately karstified but extremely karstified locally. It is the main karst aquifer in the mountain range of the Wettersteingebirge. Most of the significant springs in the area are karst springs which are fed by this aquifer. The areas formed by limestone drain underground, at least under low water conditions. After storm rainfall, significant surface run-

off can be observed on steep slopes. In winter, the area is extremely endangered by avalanches. A significant portion of the total annual precipitation is consequently removed from the karst process (GOLDSCHIEDER et al. 1999a). However, this portion is hard to quantify.

Surface karst landforms are present in areas with gentle topography, above all in cirques. An impressive karst landscape is situated east of the Alpspitze around the lake Stuibensee (Fig. 5.4). The most prominent karst landscape in the entire mountain range is the *Zugspitzplatt* to the west of the Zugspitze. Karrenfields are the predominant exokarst features. Dolines and shafts, often filled with snow in summer, are frequent too, while caves are rare and small.

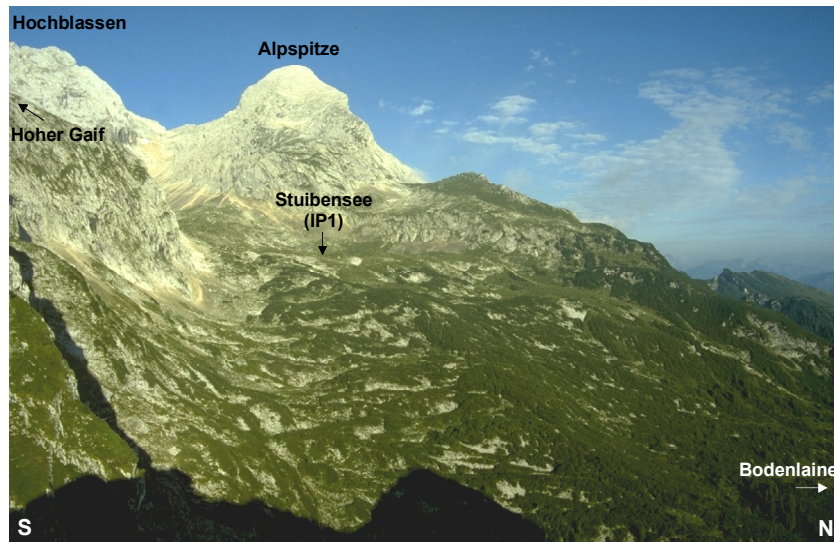


Fig. 5.4: View from the east on Mt. Alpspitze and the karstified cirque around the hidden lake Stuibensee. IP1: injection point of the tracer test.

On the summits, ridges and steep slopes, surface karst forms are rare, because the frost weathering exceeds the chemical dissolution. Furthermore, a large portion of the precipitation is removed from the karst process by surface runoff and avalanches. In the deep, steep and young valleys, there are also no significant exokarst features.

The Partnach formation predominantly consists of marl and acts as an aquiclude. The karst system consequently ends at the transition zone between the Wettersteinkalk limestone and the Partnach marl.

5.3.2 Raibler formation and Hauptdolomit formation

Generally, the Raibler formation acts as a confining layer for the underlying karst aquifer. However, the hydrogeological behaviour of this formation is more complex in detail: The Raibler sandstone (including marl and shale) is lowly permeable. It seals the top of the Wettersteinkalk karst aquifer and forms the base of karstification of the overlying Raibler limestone (and dolomite). Some fractures in this thin bedded limestone are enlarged by dissolution. As the outcrops of the limestone are small, it does not form a significant karst aquifer in the area of investigation. There is only one small spring (2 l/s) which directly discharges from solutionally enlarged fractures in the Raibler limestone (UMLAUF 1999). The Raibler cellular dolomite is extremely heterogeneous. In some parts, it behaves like a lowly permeable but highly porous soft rock (WROBEL 1970), in other parts, like a moderately karstified hard rock. One spring in the area (20 l/s) discharges from a karst conduit of the cellular dolomite (BROSEMER 1999).

In the area of investigation, the Hauptdolomit formation acts as an aquitard. As it consists of thin bedded (cm-dm) dolomites with a narrow joint spacing (cm-dm), the rock disintegrates into small pieces so that the infiltrating water is distributed through a large volume. Thus, the concentration of flow and the karstification are not significant. Furthermore, there are lowly permeable marl layers within the dolomite (BROSEMER 1999). However, in other parts of the Northern Limestone Alps, the Hauptdolomit forms significant alpine karst systems.

5.3.3 Quaternary deposits

As the composition and permeability of moraines is highly variable, they can either form an aquifer or an aquifuge. Highly permeable scree and coarse grained moraines can act as a groundwater store only if they are underlain by clayey glacial deposits or by the lowly permeable rocks of the Raibler formation. In the area of Mt. Alpspitze, some small springs within these local Quaternary aquifers are used for the water supply of mountain huts.

The rockfall masses in the valleys and the alluvial plains which formed upstream from these obstacles are the most significant granular aquifer systems. They consist of coarse-grained, highly permeable material and are drained mostly underground. Due to their large volume and their position in the valley, they can store large amounts of water, act as a buffer for flood waves and take away the sediment load.

5.3.4 Hydrogeological Zoning

The Wettersteinkalk limestone outcrops in about 70 % of the area. This is the zone of open karst with unconfined groundwater. In the Bodenglaine valley, the karst aquifer is covered by the lowly permeable Raibler formation in the Wetterstein syncline. This is the zone of confined karst; artesian groundwater can be expected locally.

The Alpspitze area cannot be subdivided unambiguously into zones of shallow and deep karst. The Höllental valley – the local base level of the karst system – is a hanging valley high above the Loisach valley which forms the definite base level of the area. In the Höllental valley, the basis of the karstifiable limestone is below the water course level (deep karst?). However, all large and permanent karst springs in the Höllental gorge are situated tens of meters above the river. This observation indicates that karstification could not keep abreast of the fast and deep Quaternary erosion of the gorge. The base of the active karst drainage network is consequently above the water course level (shallow karst?). However, the tracer tests (see section 5.6) proved one notable example for karst water flow below the gorge.

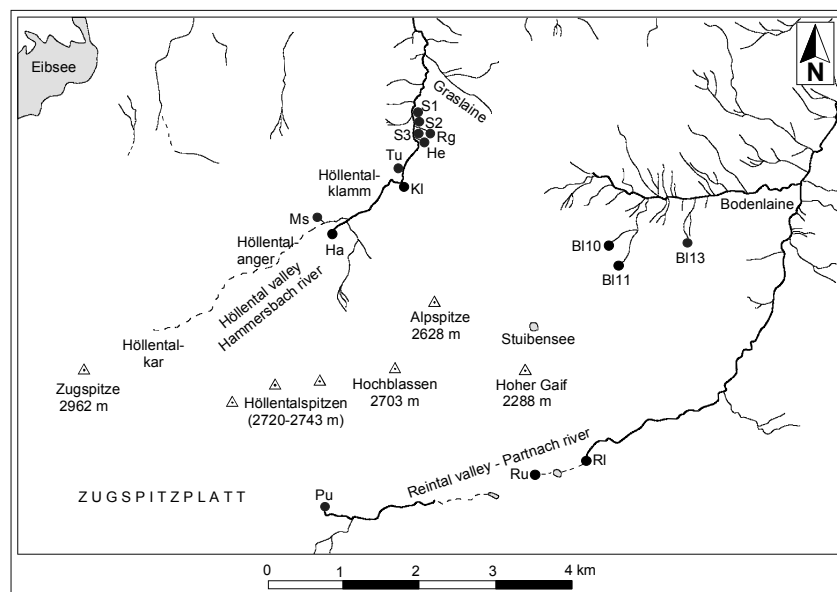


Fig. 5.5: Springs, surface waters and important locations in the Alpspitze area.

5.4 Springs and surface waters

5.4.1 Overview

The area around Mt. Alpspitze is drained by three receiving channels (confusingly, the valleys are not always named after the rivers): the Partnach river (Reintal valley) in the south and east, the Bodenlaine stream in the NE and the Hammersbach river (Höllental valley) in the NW (Fig. 5.5). Most of the springs are located in the valleys. The discharge of the springs and water courses was measured on a regular basis in summer 1998 using the salt-dilution method.

5.4.2 The Partnach river in the Reintal valley

The Partnach river in the Reintal valley has its source in an altitude of 1440 m in the so-called Partnachursprung (*Partnach origin*; *Pu* in Fig. 5.5), one of the largest karst springs in the German Alps. It discharges the most prominent karst landscape within the Wettersteingebirge, the Zugspitzplatt, a large karstified cirque west of Mt. Zugspitze (outside the area of investigation). The discharge of the spring ranges between 0.3 and 4 m³/s (ENDRES 1997). The spring reacts within hours on precipitation events (Fig. 5.6).

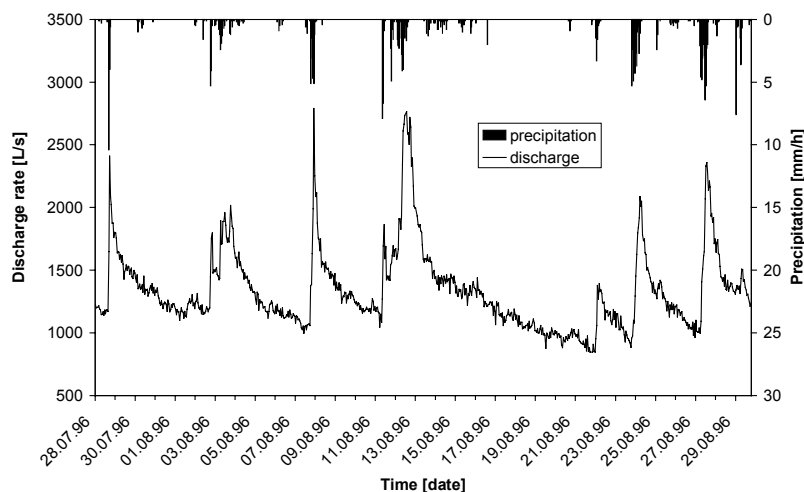


Fig. 5.6: Hydrograph of the Partnachursprung (*Pu*) (data: ENDRES 1997).

The upper section of the valley follows the Reintal syncline in eastern direction and is made of Wettersteinkalk limestone. Two rockfalls cause obstructions in the valley. As the rivers lose their sediment load at these obstacles, two alluvial plains formed upstream from the rockfalls. On each alluvial plain, there is an intermittent lake. Dependent on the hydrologic conditions, the Partnach river seeps at different locations upstream from the two rockfalls. Downstream from each rockfall, there is a resurgence. The upper resurgence (*Ru*) is intermittent, while the lower one (*RI*) is permanent. The system is highly variable (Fig. 5.7):

- Under low water conditions, the river seeps in the upper alluvial plain and reappears not before the lower resurgence, while the upper resurgence and the two lakes are dry.
- Under medium water conditions, the river seeps in the upper alluvial plain, reappears in the upper resurgence, seeps again in the lower alluvial plain and reappears in the lower resurgence. Both lakes are filled with groundwater but have no surface in- and outflow.
- Under high water conditions, the river sinks in the upper rockfall, reappears in the upper resurgence and does not sink again. The lower lake now has surface in- and outflow.

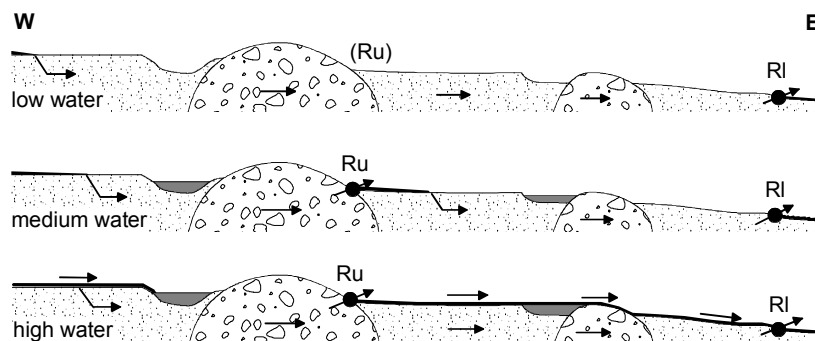


Fig. 5.7: Schematic hydrogeological section of the rockfalls in the Reintal valley (modified after BROSEMER 1999, out of scale, length 2 km).

In the upper section of the valley, there are only some small springs close to the river, most of them are situated at the bottom of steep scree slopes and debris cones.

The middle section of the valley trends NE, so that the river cuts the northward bordering anticline and syncline and flows over the sand-

stone, marl, shale, limestone and dolomite of the younger formations. In this section, the river receives inflow from several springs and streams on both sides of the valley. The area of investigation ends at the confluence of the Bodenlaine stream and the Partnach river. In the lower section of the valley, the river cuts through the Partnach marl, forming the famous Partnachklamm gorge.

5.4.3 The Bodenlaine stream

The Bodenlaine stream is tributary to the Partnach river. The Bodenlaine valley runs parallel to the axis of the Wetterstein syncline. The rocks of the Raibler and Hauptdolomit formation are preserved in the core of the syncline and are often covered with moraines, scree and rockfall material. The Bodenlaine stream is fed by many tributaries from both sides. Most of them have their source in small to medium permanent springs. The largest of them (*B/11*) discharges up to about 100 l/s. Another significant spring (*B/13*) discharges about 20 l/s from a karst conduit in the cellular dolomite of the Raibler formation.

5.4.4 The Hammersbach river and the Höllental valley

The Höllental (*hell valley*) runs in NE direction and can be subdivided in four sections: a cirque with a small remnant of a glacier (Höllentalkar), an alluvial plain (Höllentalanger), a famous gorge (Höllentalklamm) and the lower section of the valley. Almost the entire valley is formed by the Wettersteinkalk limestone.

The Höllental valley is extremely deep (1000 m), the slopes are extremely steep (average gradient 45°), and the gradient of the river is extremely high (16 %). On the bottom of the valley, the river formed a gorge which is 100 m deep and only a few meters wide. The gorge has undercut the bordering slopes so that a rockfall (one or several events) took place from the SE side of the valley. It blocked the upper part of the gorge which was consequently filled up by coarse-grained sediments forming an alluvial plain. A nameless stream which is fed by melting water of the glacier in the cirque often seeps into the alluvial plain. Below the rockfall mass, there is a permanent spring at 1270 m. This is the origin of the Hammersbach river (*Ha*). In the observation period, the spring discharged relatively constant about 300 l/s. Similar to the situation in the Reintal valley, the hydrologic behaviour of the system formed by the rockfall and the alluvial plain is highly variable:

- Under extremely low water conditions, the nameless stream dries up or sinks into the karstified limestone in the cirque without reaching the alluvial plain. Even though that the alluvial plain receives no surface inflow, the spring below the rockfall does not dry up.
- Under low to medium water conditions, the stream seeps into the plain. The location of the lowest seeping point depends on the discharge of the stream and shows a daily amplitude due to snow melt.
- Under high water conditions, the stream flows around the northern toe of the rockfall and falls down in the gorge downstream.

Several karst springs, e.g. the well-known Mariensprung (*Ms*), are situated near the rockfall on the NW side of the valley. The gorge of the Hammersbach river, the Höllentalklamm, begins downstream from the rockfall. It is formed by the Wettersteinkalk limestone and follows a SW-NE trending fault zone. There are several springs in the gorge, most of them inaccessible. The most spectacular one is the Klammquelle (*gorge spring, Kl*) at 1180 m, situated on the right (SE) side of the gorge, the side of Mt. Alpspitze. The water discharges from a karst conduit and falls down about 30 m directly into the river (Fig. 5.8). By measuring the discharge in the river up- and downstream from the spring, it was possible to determine the discharge of the spring. Within the observation period, it ranged between 150 and 200 l/s.

On the left (NW) side of the river, that is the opposite side of Mt. Alpspitze, a small karst spring with a discharge of about 5 l/s is situated in an altitude of 1100 in a tunnel of the footpath through the gorge, the so-called Tunnelquelle (*tunnel spring, Tu*).

Downstream from the gorge, at the beginning of the lower section of the valley, two karst springs are situated in an altitude of 1100 m in the rock face on the right (SE) side of the valley: The permanent spring *He* (Höllentaleingangquelle) discharges about 10–20 l/s and the intermittent spring *Rg* (Rotgraben) discharges 100 l/s after a storm rainfall and dries up after a few days without precipitation. At the base of the slope below this rock face, three springs (*S1–3*) are situated close to the Hammersbach river in an altitude of 910–950 m. They are used for the water supply of the community of Garmisch-Partenkirchen in case of emergency. In the lower section of the valley, several small tributaries flow into the Hammersbach river from both sides. The only relevant is the Graslaine stream which has its source at 1280 m. The stream forms the NE boundary of the area of investigation.

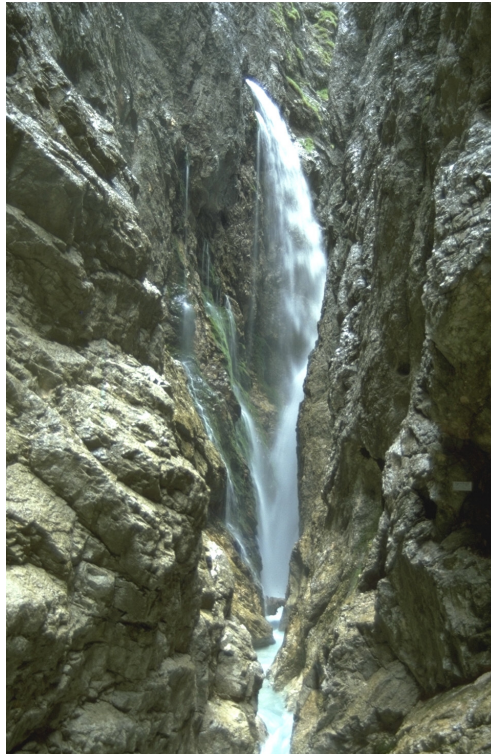


Fig. 5.8: The Klammsquelle (*gorge spring, KI*) discharges from a karst conduit in Wettersteinkalk limestone, around 30 m above the water course level.

5.4.5 The elevated areas

The elevated areas are mostly formed by the karstified Wettersteinkalk limestone and predominantly drain underground. However, significant surface runoff can be observed during storm rainfall. Several small springs are discharged from scree slopes and glacial deposits which overlay the Raibler formation. On the limestone areas, there are no relevant springs but some dripping points only (UMLAUF 1999). To the east of Mt. Alspitze, the lake Stuibensee (1921 m) is situated right in the middle of large karrenfields (Fig. 5.4). Obviously, the karstified limestone is locally sealed by lowly permeable glacial sediment. The lake has no surface in- and outflow (BROSEMER 1999).

5.5 Hydrochemistry

All springs ($n = 61$) of the Mt. Alpspitze area were sampled under medium to high water conditions in August 1998 and inorganic hydrochemical analyses were carried out. Selected springs in the Höllental valley were sampled in September and October 1998 under low water conditions. HCO_3^{2-} (85.4–262.3 mg/l) and Ca^{2+} (20.2–68.0 mg/l) are the dominant ions in all spring waters; Mg^{2+} (2.2–15.5 mg/l) and SO_4^{2-} (0.0–11.4 mg/l) are less important (Fig. 5.9); NO_3^- is below 8.4 mg/l and Na^+ and K^+ are below 1.0 mg/l in all springs; Cl^- , HPO_4^- , CO_3^{2-} , Fe^{2+} , Mn^{2+} and NH_4^+ are below the limit of detection in most of the springs. All spring waters are rich and sometimes over-saturated of dissolved oxygen (7.1–19.3 mg/l) due to turbulent flow, low temperatures and absence of oxygen consuming bacteria. All springs are suitable for drinking water supply with regard to their inorganic hydrochemical characteristics (UMLAUF 1999).

All springs which discharge from the Wettersteinkalk karst aquifer or from the rockfall masses in the Höllental and Reintal valley are characterised by calcite under-saturated water ($-0.26 < \text{SI} < -0.86$). Only a few springs which drain local granular aquifers are slightly over-saturated.

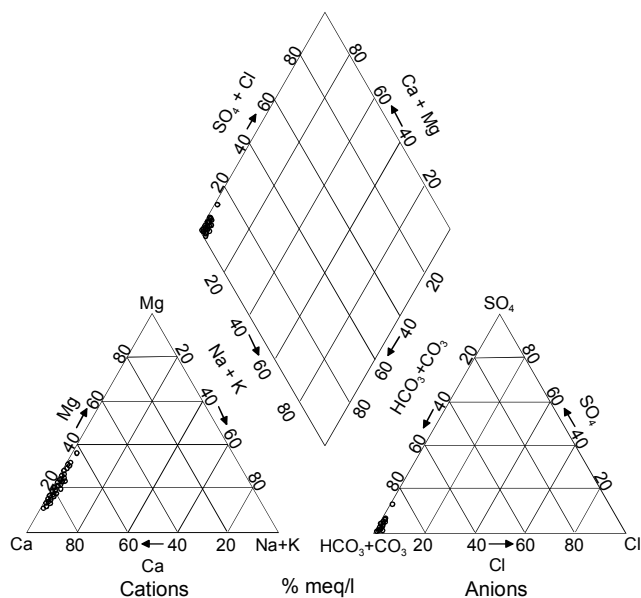


Fig. 5.9: PIPER diagram of all the springs in the area.

The mineralisation of the karst springs in the Wettersteinkalk limestone is generally low and the hydrochemical characteristics of the springs are similar to each other, while the mineralisation of the springs which are related to the Raibler and Hauptdolomit formation is generally higher and more variable.

5.6 Tracer tests

5.6.1 Overview

The Geological Survey of Bavaria carried out some tracer tests with fluorescent dyes in the Wettersteingebirge. A combined tracer test with three injections proved that the area NE of Mt. Alpspitze is drained by several karst springs in the bordering Höllental valley. Some springs in the Bodenlaine and Partnach valley were also sampled but no trace of the dyes was detected there (GLA 1977). Another tracer test was carried out in 1980 in the uppermost Reintal valley. The tracer was injected below Mt. Zugspitze and reappeared in the spring (*Pu*) of the Partnach river but in no other spring (ORTH 1984).

Within the framework of this thesis, a multi tracer test with three injections was carried out in the area of Mt. Alpspitze in 1998. The aim of this experiment was to get detailed information on the hydraulic characteristics of the Wettersteinkalk karst aquifer, to delineate the catchments of the karst springs, to locate the watersheds between the surrounding valleys, to investigate the relation between tectonic structures (folds, faults) and underground drainage pattern and to characterise the hydraulic function of the rockfall in the Höllental valley.

5.6.2 Selection of the injection points and the tracers, injections

Three injection points were selected. IP1 and 2 are situated in the centre of the Mt. Alpspitze area, IP3 is located in the upper Höllental valley (Fig. 5.10). The injections in IP1 and 2 were carried out at the 24.09.98, the injection in IP3 was done one day later.

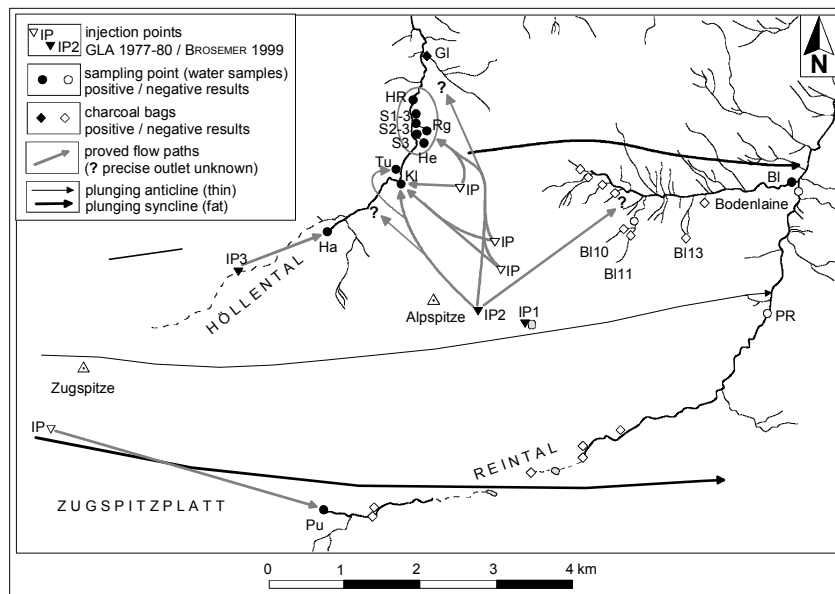


Fig. 5.10: Overview of the tracer tests in the Wettersteingeberge; location of the injection points (IP), the sampling points and the proved flow paths.

IP1 at 1927 m is a solutionally enlarged joint (a kluffkarren) 6 m above the lake Stuibensee; 2 kg of the fluorescent dye Eosine was injected and 600 l of water from the lake was used as flushing water.

IP2 is situated at 2200 m in the cirque to the east of Mt. Alpspitze where the water of a small intermittent spring sinks in the karstified limestone of the Wettersteinkalk formation. 2 kg of Uranine were injected a few meters below the spring which discharged about 0.2 l/s during the injection. Consequently, no flushing water was necessary.

IP3 is the point in the upper Höllental valley where the nameless stream coming down from the cirque seeps into the alluvial plain above the rockfall. Due to the relatively low discharge of the stream during the tracer test (about 4 l/s), it was sinking underground in the uppermost, southwestern edge of the alluvial plain at 1480 m, far up the valley from the rockfall. 10 kg of the UV fluorescent dye Naphthionate were used as tracer; no flushing water was necessary.

5.6.3 Sampling and Analyses

Due to the high alpine environment, the sampling strategy for this tracer test was a special challenge. The springs and rivers of the area were sampled from 25.09. to 04.11.98. Later on, sampling was no longer possible because of snow and avalanches. Water samples were taken manually and with two automatic samplers. Charcoal bags were installed in some remote springs. The sampling points are located in the three surrounding valleys.

The following points in the Höllental valley were sampled:

- As the access to the spring of the Hammersbach river (*Ha*) is dangerous, only a few water samples were taken directly at the spring. The only possible regular sampling point is about 1 km downstream in the gorge. This is not ideal because fluorescent dyes are sensitive to photolytical decay. Furthermore, several tributaries flow into the river between the spring and the sampling point. Two small springs below the rockfall were sampled occasionally.
- The Klammquelle (*gorge spring, Kl*) is situated in a rock face on the right (SE) side of the gorge. As direct sampling is impossible, samples were taken in the river up- and downstream from the spring.
- The Tunnelquelle (*tunnel spring, Tu*) is situated on the left (NE) side of the gorge, that is the opposite side to Mt. Alpspitze. Water samples were taken occasionally in order to check if the gorge forms an hydraulic boundary between the karst systems on its both sides.
- The springs at the entrance of the gorge (*He, Rg*) are situated in a rock face. Samples were taken in the streams below this rock face.

- The capture of the three springs of the community of Garmisch-Partenkirchen (*S1–3*) allows for direct sampling at *S3* only, but not at the two other springs. Thus, samples were taken from the overflows of the collector *S2–3* and *S1–3*.
- The Hammersbach river (*HR*) was sampled downstream from the gorge in order to calculate the total recovery rate of the injected tracers for all springs in the Höllental valley.
- Charcoal bags were installed in the Graslaine stream (*GI*).

In the Reintal valley, there are no significant, visible karst springs downstream from the Partnach origin (*Pu*). In order to detect and localise possible outflows of tracers in the Partnach river, the following sampling strategy was applied:

- Downstream from the point where the Partnach river cuts the karstified limestone of the Wettersteinkalk formation for the last time, an automatic sampler was installed in order to detect all possible tracer outflows in the Reintal valley (*PR*).
- Upstream from this point, charcoal bags were installed at six points in the river in order to localise possible outlets of the tracers.

Numerous small springs are situated in the Bodenglaine valley; most of them are not easily accessible. The following strategy was used:

- An automatic sampler was installed downstream from the confluence of the two streams which originate in the two largest, neighbouring springs (*BI10* and *BI11*). Charcoal bags were installed directly at the two springs.
- Charcoal bags were installed in all tributaries to the Bodenglaine stream.
- Water samples were taken at the point where the Bodenglaine stream (*BI*) flows into the Partnach river.

Altogether 508 water samples were taken and 43 charcoal bags were used. The fluorescence analyses were carried out at the AGK.

5.6.4 Hydrologic conditions during the tracer test

The weeks before the injection were rainy and in altitudes above 2000 m, there was snow. From the 19th to the 26th of September, it was dry and sunny, so that the snow was melting. Afterwards, there was

rain and snow almost every day. During the sampling, the discharge of most springs and rivers was medium to high and relatively constant. However, large discharge variations were observed at the spring *Rg*.

5.6.5 Results with Uranine

The Uranine which was injected in the cirque to the east of Mt. Alpitze reached the karst springs in the Höllental valley and the Bodenlaine creek. No trace of Uranine was detected in the Partnach river in the Reintal valley.

Uranine reached the Klammquelle (*gorge spring, Kl*) 184 h after the injection. The maximum concentration of 0.58 $\mu\text{g/l}$ was measured after 260 h in the river directly downstream from the inaccessible spring (Fig. 5.11). Upstream from the spring, the maximum concentration in the river was 0.02 $\mu\text{g/l}$. A simple mixing calculation using the discharge rates up- and downstream from the spring makes it possible to determine the maximum concentration in the spring water of about 1.98 $\mu\text{g/l}$. The recovery rate is 6 g (0.3 %) up- and 249 g (12.5 %) downstream from the spring. Thus, 243 g (12.2 %) of the tracer reached the spring.

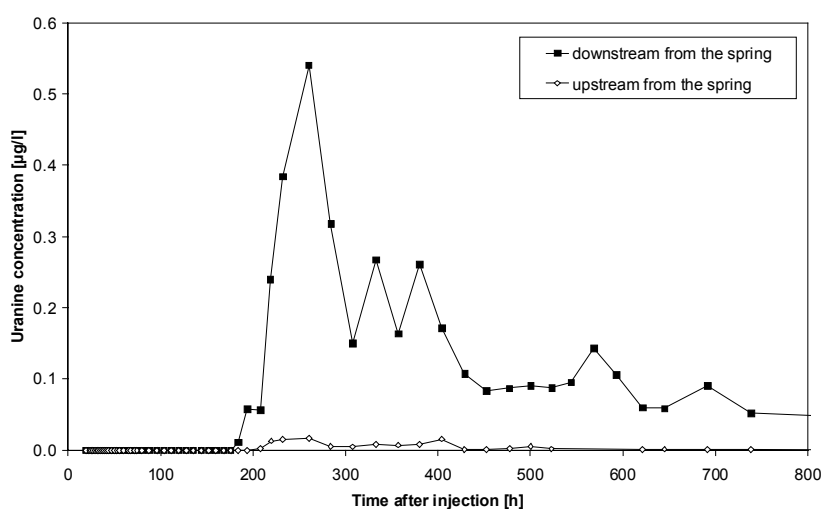


Fig. 5.11: Uranine breakthrough curve in the river up- and downstream from the Klammquelle (gorge spring, *Kl*).

Surprisingly, the Uranine reached the Tunnelquelle (*tunnel spring, Tu*). The highest concentration that was measured at the spring (1.00 $\mu\text{g/l}$)

is significantly higher than the maximum concentration in the Hammersbach river upstream from the spring ($0.58 \mu\text{g/l}$). Consequently, the spring is not a resurgence of seeping water from the river but there must be a direct hydraulic connection between the karst massif of Mt. Alpspitze on the right (SE) side and the spring on the left (NW) side of the gorge. Even though that the gorge cuts about 100 m deep into the karstified limestone on the bottom of a 1000 m deep valley, it seems not to be a totally effective hydraulic border. There is evidence from tracer experiments in other alpine karst systems that single karst drains may reach deep below the local base level (BÖGLI & HARUM 1981).

The tracer test allowed a more detailed characterisation of the two neighbouring karst springs *He* and *Rg* which are situated in the same altitude at the entrance of the gorge (Fig. 5.12). A continuous breakthrough curve was recorded at the permanent spring *He*. Unlike that, the intermittent spring *Re* acts as an highly variable overflow of the system. During the sampling period, it discharged up to 100 l/s after intensive rainfall but dried up three times in between. Thus, the breakthrough curve is discontinuous: The concentration increases when the discharge increases and decreases again, when the discharge decreases. Obviously, *Re* discharges two types of water: The Uranine-rich water comes from the karst aquifer which is also discharged by *He* and the other springs in the Höllental valley, while the Uranine-free water comes from an unknown, local origin.

5.6 Tracer tests

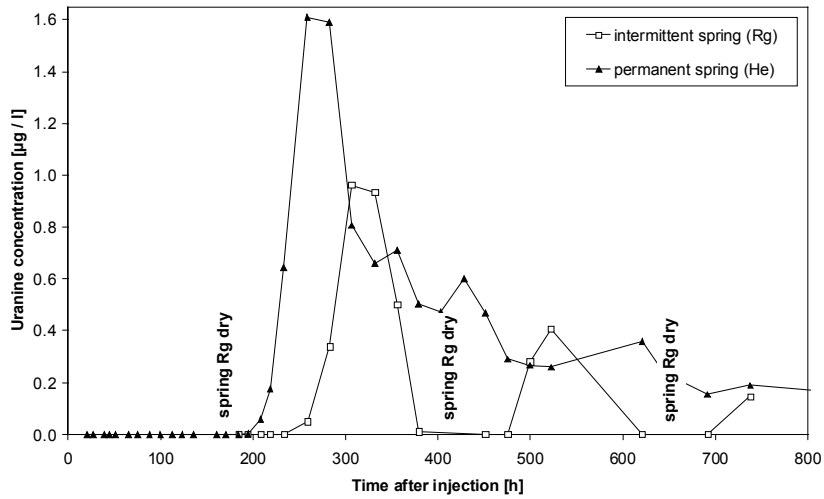


Fig. 5.12: Comparison of the Uranine breakthrough curves of the springs *He* and *Rg* at the entrance of the Höllental gorge.

The Uranine also reached the springs of the community of Garmisch-Partenkirchen (*S1–3*). The breakthrough curves of the spring *S3* and the collector *S2–3* are almost identical, indicating that *S2* and *S3* discharge the same karst water. The lower concentrations in the collector *S1–3* indicate that *S1* probably receives additional inflow from the scree slope above the spring (Fig. 5.13).

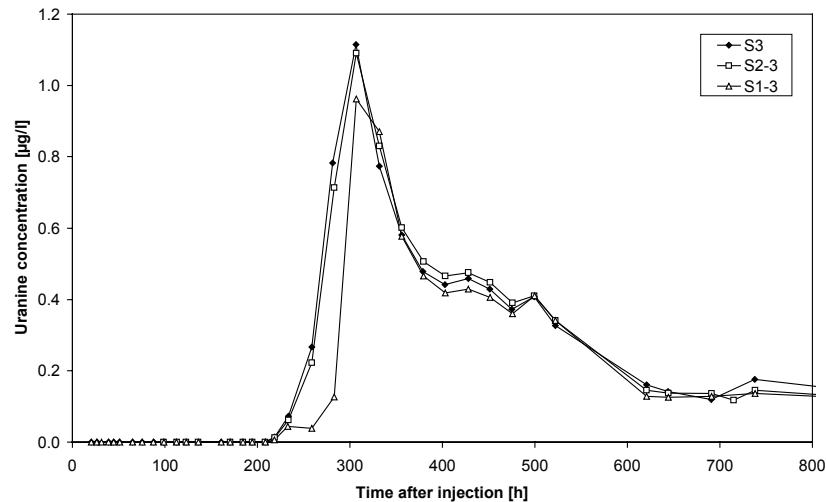


Fig. 5.13: Uranine breakthrough curves of the spring S3 and the collectors S1–3 and S2–3.

At the sampling point in the Hammersbach river (*HR*) downstream from the springs, a detailed breakthrough curve was recorded and the discharge was measured regularly using the salt dilution method. The discharge ranges between 673 and 849 l/s in the observation period (BROSEMER 1999). Thus, the total recovery rate of Uranine can be calculated: About 290 g of Uranine (14.5 %) reached the springs in the Höllental valley during the sampling period. However, the tracer breakthrough had not finished when snow and avalanches made it impossible to continue the sampling. Uranine was also detected in the charcoal bags that were installed in the Graslaine creek (*GI*).

In the Bodenglaine valley, an automatic sampler was installed at the two largest springs (*BI10* and *BI11*) and charcoal bags were installed in all the tributaries to the Bodenglaine stream. No trace of Uranine was detected in these sampling points. Surprisingly, concentrations of up to 0.74 µg/l were detected in water samples taken in the Bodenglaine stream (*BI*) directly upstream from the confluence with the Partnach river. The tracer must have reached an unknown spring in the valley, maybe a bottom spring. The discharge of the stream was measured only once during the observation period (100 l/s) and the breakthrough curve consists of five samples only. Thus, the calculated recovery of about 100 g (5 %) is just a rough estimation.

The total recovery of Uranine in all sampling points is about 390 g (19.5 %), of which 243 g (12.2 %) were found in the Klammsquelle (*gorge spring, Kl*). The mean value of the highest flow velocity (calculated from the time of first arrival) is 10.7 m/h and the mean value of the dominant flow velocity (calculated from the time of the maximum concentration) is 8.1 m/h. These are low velocities for an alpine karst system with an extremely high topographic gradient (about 0.5). However, the hydraulic gradient in the aquifer is much lower than the topographic gradient due to the large thickness of the unsaturated zone (several 100 metres). The low flow velocities indicate significant storage in the unsaturated zone and the aquifer.

5.6.6 Results with Eosine

The Eosine which was injected in the klufftkarren near the lake Stuibensee (IP1) disappeared completely. Thus, it is not possible to determine the direction of the underground discharge of this strongly karstified area. This failure indicates that the klufftkarren is not well connected with the underground karst drainage network so that the tracer was stored in the thick unsaturated zone.

5.6.7 Results with Naphthionate

The Naphthionate that was injected into the sink of the nameless stream into the alluvial plain in the upper Höllental valley (IP3) was detected after 176 h in the spring of the Hammersbach river (*Ha*) below the rockfall. The distance between the injection point and the sampling point is 1450 m and the maximum flow velocity is 8.2 m/h. At the end of the sampling period, 676 h after the injection, the maximum of the breakthrough curve was still not reached. Consequently, the dominant flow velocity can not be calculated but must be less than 2.1 m/h. The recovery until the end of the sampling was 1.1 kg (11 %).

The geometry of the granular aquifer formed by the rockfall and the alluvial plain is difficult to determine because it fills up the entire uppermost section of the gorge. Both the depth and the width of this buried gorge are unknown. The granular aquifer is probably up to 100 m thick. This large volume allows a significant storage of water and acts as a hydrologic buffer for the surface and underground inflow. During the observation period, the discharge of the spring *Ha* was relatively constant and ranged between 213 and 386 l/s even though that the hydrologic conditions were highly variable.

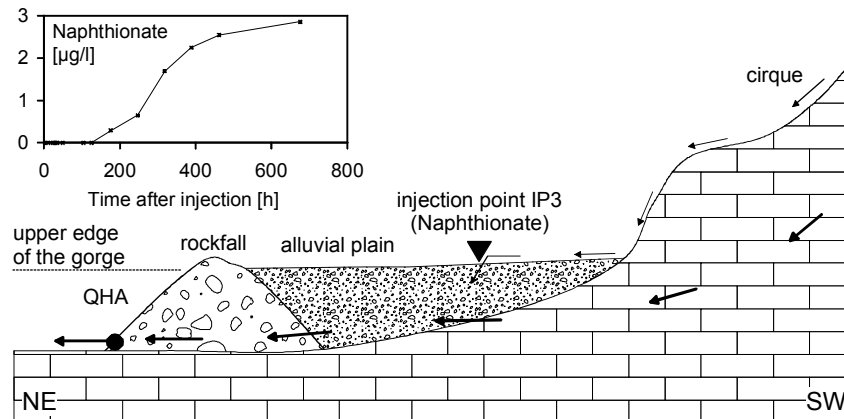


Fig. 5.14: Schematic hydrogeological section of the upper Höllental valley with the Naphthionate injection point (IP3) and the breakthrough curve of the Hammersbach spring (*Ha*). The granular aquifer formed by the rockfall mass and the alluvial plain collects the seeping surface water and the karst groundwater and is drained by the spring *Ha*.

5.7 Conceptual model of the karst system

The underground drainage pattern of the Mt. Alpspitze area is strongly influenced by the steep topography, the enormous thickness of the karstifiable carbonate rock and the fault tectonics (Fig. 5.15).

Almost the entire area consists of the about 1000 m thick Wettersteinkalk limestone. Locally, the thickness is even higher due to folding or thrusting. There are no interstratified low permeability layers and the underlying Anisian formation is below the level of the surrounding valleys in large parts of the area. As there is no significant stratigraphic flow control, the influence of the folds on the underground drainage pattern is limited as well. Instead of that, the karst groundwater flow is distributed to an extensive network of solutionally enlarged joints, fractures, faults and bedding planes which is mainly orientated towards the main receiving channel, the Hammerbach river in the Höllental gorge. The flow paths proved by the tracer tests cross the fold axes, some even run contrary to the plunge direction (Fig. 5.10).

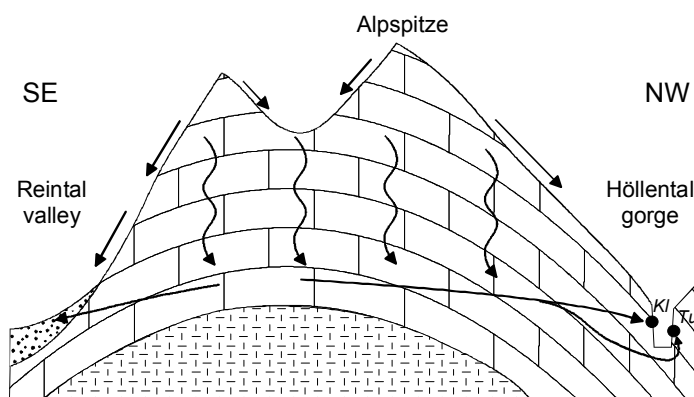


Fig. 5.15: Schematic graphical presentation of important factors controlling the hydrogeology of the Alpspitze area: steep topography, significant surface runoff during storm rainfall, large thickness of the karstifiable limestone, thick unsaturated zone, lack of low permeability layers, no significant stratigraphic flow control, underground flow crossing the folds.

This underground flow pattern differs significantly from the neighbouring karst system Zugspitzplatt which is formed by the same formations (ORTH 1984). In the Zugspitzplatt, the basis of the karstified Wettersteinkalk limestone outcrops towards the north, west and south, high above the surrounding valleys. Therefore, the underlying low permeability formation causes a stratigraphic flow control, and so the karst drainage follows the axis of the eastward plunging syncline towards the Partnachursprung spring *Pu* (Fig. 5.10).

All the tracers that were injected in the area of Mt. Alpspitze reached all the sampled karst springs in the Höllental gorge. Thus, the springs are discharged from the same groundwater body and their catchments are overlapping. However, the different discharge characteristics of neighbouring karst springs at the same altitude indicate that there is not an unified potentiometric surface but rather a system of moderately connected karst conduits.

As the karst springs in the Höllental gorge are situated in an altitude of 1100 to 1180 m while Mt. Alpspitze is 2628 m high, the unsaturated (vadose) zone is many hundreds of meters thick. Infiltrating water from precipitation or snow melt has to percolate vertically through this moderately karstified zone before reaching the drains of the phreatic zone which allow a lateral flow towards the springs. The relatively low discharge variations of the karst springs are an expression of the significant storage and buffering capacity provided by this system.

The groundwater table – if it exists at all – is far below the ground surface so that the effective hydraulic gradient in the aquifer is definitely significantly lower than the topographic gradient. The dominant flow velocities of only 8 about m/h are surprisingly low for an alpine karst system. Possible reasons are the significant storage both in the vadose and the phreatic zone, the absence of stratigraphic control of flow and the low hydraulic gradients.

Both the purity of the Wettersteinkalk limestone and the humid climate of the area favour intensive karstification. Nevertheless, both the geomorphic karst features and the underground karst network are poorly developed in large parts of the area and distributed very heterogeneously. The topographic gradient and the age of the landscape are the controlling factors for the spatial distribution of the karstification. Due to the fast uplift of the mountain range, there is a higher and older (Tertiary) generation of the karst landscape which shows gentle topography and well developed karstification, and a younger (Quaternary) generation with steep topography and initial karstification.

6 COMPARISON OF THE THREE TEST SITES – FOLD TECTONICS AND KARST DRAINAGE PATTERN

6.1 Introductory remark

The three alpine karst systems which were investigated within the framework of this thesis are formed of folded rock sequences. In the Hochifen-Gottesacker and Winterstaude area, the proved underground flow paths perfectly coincide with the fold pattern in the elevated areas (shallow karst), while flow across the folds was proved in the valleys. In the Alpspitze area, the underground drainage pattern seems to be largely independent from the fold pattern. The reasons for this notable difference are discussed in this chapter. The influence of stratigraphy, base level conditions, fold and fault tectonics on the underground drainage pattern of alpine karst systems is highlighted on the basis of the results from the three test sites and experiences from other karst systems described in the literature.

6.2 Rules of stratigraphic flow control

The necessary (but not sufficient) precondition for flow control provided by the folds is that the underground flow runs parallel to the stratification. It is consequently necessary to discuss the preconditions of stratigraphic flow control before highlighting the influence of fold tectonics on karst groundwater flow.

In alpine (and non-alpine) karst systems, there are many examples for groundwater flow parallel to the stratification (e.g. KRIEG 1988, ORTH 1992, RIEG 1994, LEIBUNDGUT 1995, GÖPPERT 2002), and some examples for flow across the stratification (e.g. MÜLLER & ZÖTL 1980, BÖGLI & HARUM 1981, ROSS et al. 2001). The evaluation of these examples and the results from the three test sites indicate that the degree of stratigraphic flow control depends on the contrast in hydraulic conductivity between the hydrostratigraphic units, on their contrast in thickness and on the degree of fault tectonics. The rules of stratigraphic flow control are the following (Fig. 6.1):

1. If the hydraulic conductivity contrast between a karst aquifer and a bordering aquitard is high, strong stratigraphic flow control has to be expected. This situation can be observed between a well karstified limestone and a clayey marl. In contrast to that, groundwater flow

across the stratification is possible, if the conductivity contrast is low, e.g. between a pure and an impure limestone.

2. A strong stratigraphic flow control can be observed if the karst aquifer is relatively thin while the bordering aquitards are thick. In contrast to that, the flow control is less significant if the aquifer is thick while the aquitards are thin and/or discontinuous.
3. The degree of stratigraphic flow control strongly depends on the faulting. Intensive faulting may allow for flow even through thick layers of low permeability, especially if the fault plains are vertical and open (extensional component). An aquitard between bordering karst aquifers can easily be bypassed if the displacement of the faults is of the same order of magnitude as the thickness of the aquitard.

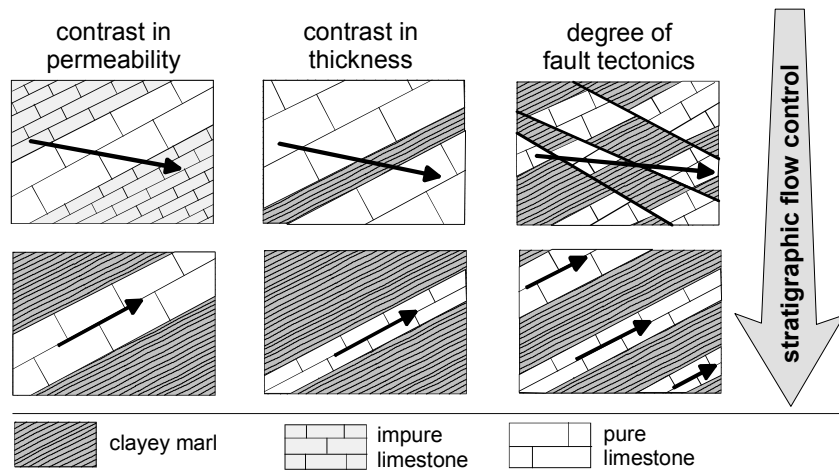


Fig. 6.1: Illustration of the three rules of stratigraphic flow control.

These rules explain the observed differences in the underground flow pattern of the three test sites and are consistent with examples described in the literature:

In the Hochifen-Gottesacker area, there is a large contrast in hydraulic conductivity between the Schratenkalk karst aquifer on the one hand, and the under- and overlying marl aquitards on the other hand. The karst aquifer is only about 100 m thick, while the thickness of the bordering aquitards is 250 and up to 400 m respectively. Even though the area is cut by faults, their displacement is in most cases significantly smaller than the thickness of the aquitards. As a consequence, this test

site is an excellent example of a strong stratigraphic flow control. There is no evidence for karst water flow running across the stratification.

The hydrostratigraphy and the resulting underground drainage pattern of the Winterstaude area are similar. However, there are two karst aquifers which are separated from each other by a marl aquiclude of 60 m thickness. This is in the same order of magnitude as the displacement of the faults. This leads to hydraulic contact between the two aquifers and, consequently, to karst water flow across the stratification.

In contrast to these two karst systems, the area of Mt. Alispitze is mainly formed by the 1000 m thick Wettersteinkalk limestone which contains no interstratified impervious layers. The entire system is cut by fault systems with relatively high displacement. Consequently, the stratigraphic flow control is present but limited and there are several evidences for karst groundwater flow across the stratification.

Two contrasting examples from the literature: The sub-alpine Molasse is characterised by a high contrast in permeability between karstified conglomerate banks and marl layers, the degree of faulting is very low and tracer tests proved underground flow parallel to the stratification (GÖPPERT 2002). The karst systems in the Muotatal area in central Switzerland are made of karst aquifers which are separated from each other by 400 m marl of low permeability. However, there is intensive fault tectonics and tracer tests proved flow paths which run across the stratification (BÖGLI & HARUM 1981).

6.3 Folded alpine karst systems with high stratigraphic flow control

6.3.1 Influence of the base level conditions

High stratigraphic flow control is the first, necessary precondition for flow control provided by the folds. The second, sufficient precondition is the presence of shallow karst. In the zone of shallow karst, the base of the karst aquifer is, by definition, above the base level of the system (BÖGLI 1978). The underground flow consequently takes place near the base of the karst aquifer. The flow consequently follows the attitude of the strata and is therefore controlled by the fold pattern.

This situation (high stratigraphic flow control and shallow karst) is present in the elevated parts of the test sites Hochifen-Gottesacker and Winterstaude. Several other examples are described in the literature: ORTH (1984) synthesises hydrogeological information from ten karst

areas in the Northern Alps, where the underground drainage pattern is controlled by fold and imbricate structures.

6.3.2 Flow pattern in the elevated areas (zone of shallow karst)

In the karst system Hochifen-Gottesacker, the karstifiable formation is relatively thin (100 m) compared to the difference in altitude between the elevated parts of the area and the surrounding valleys (1000 m). Almost the entire area consequently belongs to the zone of shallow karst, where the underground flow takes place near the base of the karst aquifer on top of the underlying marls. The troughs of the synclines consequently form the main flow paths and the flow direction is controlled by the plunge of the fold axes. The crests of the anticlines form local watersheds, and the axial culmination line forms the European watershed between Rhine and Danube. A similar flow pattern is present in the Winterstaude area and was also proved for alpine karst systems with comparable stratigraphic, tectonic and base level conditions, e.g. the Churfirften-Alvier and Säntis-Alpstein area in Switzerland (RIEG 1994, LEIBUNDGUT 1995).

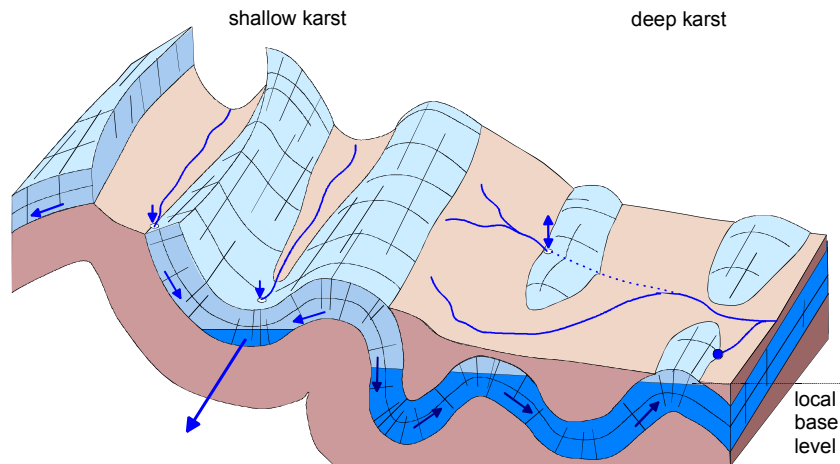


Fig. 6.2: Schematic illustration of the relation between fold tectonics, base level conditions, surface and underground drainage pattern in an alpine karst system with strong stratigraphic flow control. In the zone of shallow karst, synclines form the main flow paths; in the zone of deep karst, flow across the folds is possible.

If the strata are gently folded, the karstified carbonate formation often outcrops over large areas which drain underground. This situation is

present in the central Gottesacker and was also described for the Silberer area (YEANNIN et al. 1995). If the folds are close or isoclinal, the overlying impervious formation is often preserved along the synclines and the karstified formation is often eroded along the anticlines, so that the underlying aquiclude outcrops. Consequently, there is surface runoff parallel to the axes of the synclines and the anticlines. Surface streams sink in swallow holes as wherever the karstified formation reappears along strike (Fig. 6.2). This situation is present in the northern part of the Hochifen-Gottesacker area, in the Winterstaude area, and was also observed in the Säntis-Alpstein karst system (LEIBUNDGUT 1995).

6.3.3 Flow pattern in the valleys (deep or shallow karst)

The plunging synclines discharge into bordering valleys which run across or parallel to the folds. Valleys often follow geological structures: thrusts, strike-slip fault-zones, axial depressions or synclinoria.

Deep karst is present if the base of the karst aquifer is below the hydrologic base level (BÖGLI 1978). It is often debatable whether an alpine karst valley belongs to the zone of shallow or deep karst, even if the base of the karst aquifer is below the valley floor. Many alpine valleys are hanging glacial valleys high above a deeper level. Consequently, the deepest discharge point (the regional base level) is often much below the water course level of the hanging valley (local base level). The Schwarzwasser valley in the Hochifen-Gottesacker area is an example for that situation: The base of the karst aquifer is below the valley floor but the deepest discharge point is further down in the Breitach valley. In transversal sections (perpendicular to the valley axis), the valley consequently appears to be deep karst; in longitudinal sections (along the valley axis), it seems to be a zone of shallow karst.

A similar situation was described by BÖGLI & HARUM (1981) for the Swiss Muotatal valley, where the karst water table is deep below the valley floor. This proves the presence of a lower drainage point and makes it difficult to delimit the zones of deep and shallow karst.

The flow pattern in alpine karst valleys is more variable and more difficult to predict than in the elevated areas. Three possibilities were observed in the test sites under investigation:

If the valley runs across the folds and cuts through the karst aquifer in the anticlines, the synclines are separated from each other and the karst groundwater from the plunging synclines comes to the surface via

springs or inflows in alluvial sediments in the valley floors (e.g. Subersach valley in the western Hochifen-Gottesacker area). In this case, there is no significant underground flow system in the valley.

If the valley runs across the folds but does not cut through the karst aquifer in the anticlines, a continuous karstified limestone body is present in the valley and underground flow perpendicular to the fold axes can be observed. The groundwater fills up the synclines completely and overflows the anticlines. The synclines consequently lose their function as main flow paths, and the anticlines no longer act as effective watersheds (Fig. 6.2). The Schwarzwasser valley in the eastern Hochifen-Gottesacker area is an excellent example for this situation.

A third possibility can be observed if the valley runs parallel to the fold axes. In this case, the underground flow follows the synclines both in the elevated areas (shallow karst) and below the valley floor (deep karst). The continuous hydraulic connection along the main syncline of the Winterstaude area between the elevated areas and the spring near the Bregenzerach river is an example for this situation.

6.3.4 Position of the karst springs

The difference between the flow pattern in the elevated areas and in the valleys is reflected by the position of the springs. The elevated areas often form the main recharge area of the system, and so there are only a few springs. As the groundwater flows in the troughs of the synclines, the typical position of a spring is in a syncline which is cut through, so that the underlying aquiclude outcrops. The Rubach and the Kessleralp spring in the Hochifen-Gottesacker area are typical examples. ORTH (1992) describes springs of that type in the alpine karst systems Estergebirge and Laubenstein, Bavaria.

In the valleys, the springs are not confined to the synclines. The cores of the synclines are often covered by overlying impervious formations while the karst aquifer frequently outcrops in the anticlines. Thus, the karst springs in the valleys are often situated in the anticlines or on the fold limbs (Fig. 6.2). The karst springs in the Schwarzwasser valley belong to this type, as well as the springs at the base of the Winterstaude mountain chain and on the Bezau valley floor.

6.3.5 Delineation of the catchments

In folded alpine karst systems with high stratigraphic flow control, the fold pattern controls both the topography (synclines form valleys, anti-

clines form ridges) and the underground flow (synclines form flow paths, anticlines form watersheds). The two test sites Hochifen-Gottesacker and Winterstaude belong to that type, the Alpstein-Säntis area in Switzerland is another well-known example within the Helvetic zone (LEIBUNDGUT 1995). In these alpine karst systems, the catchment areas of springs can consequently be delineated much more precisely than in plateau-like karst systems. Indeed, all the hydraulic connections that were proved by tracer tests in the Hochifen-Gottesacker area coincide with the flow pattern predicted on the basis of fold tectonics.

6.4 Folded alpine karst systems with low stratigraphic flow control

In contrast to the karst systems described above, the flow control provided by the folds is limited if the stratigraphic flow control is low or absent. This is the case if the karstified formations are thick, while aquitards are thin, discontinuous or ineffective due to low permeability contrast and/or intensive fault tectonics. The flow control by the folds is nearly absent if the entire mountain massif is made of a thick karstified carbonate sequence without any effective aquitard above the base level of the system, so that the entire system belongs to the zone of deep karst. The Alpspitze area is an example for that type: The underground drainage pattern is mainly controlled by the base level conditions and by the fault tectonics. The tracer tests proved flow paths that run across the fold axes.

A precise delineation of catchment areas on the basis of geological and topographic criteria is difficult or even impossible for this type of karst systems. Variable underground watersheds have to be expected, similar to the situation in plateau-like karst systems (e.g. Tennengebirge plateau, TOUSSAINT 1971; Dachstein plateau, BAUER 1989).

7 THE CONCEPT OF GROUNDWATER VULNERABILITY

7.1 Background and definitions

The term „vulnerability of groundwater to contamination“ was introduced by MARGAT in 1968. The concept of groundwater vulnerability is based on the assumption that the physical environment provides some natural protection to groundwater against human impacts, especially with regard to contaminants entering the subsurface environment (VRBA & ZAPOROZEC 1994). The term „vulnerability to contamination“ is used in the opposite sense to the term „natural protection against contamination“ and the terms can be used alternatively (high vulnerability = low natural protection). The fundamental concept of groundwater vulnerability is that some areas are more vulnerable to contamination than others and the ultimate goal of a vulnerability map is the subdivision of an area into several units showing the different degree of vulnerability.

VRBA & ZAPOROZEC (1994) emphasise that vulnerability of groundwater is a relative, non-measurable, dimensionless property. They suggest to distinguish between intrinsic (natural) and specific vulnerability. The intrinsic vulnerability should only depend on the natural properties of an area, such as soil, aquifer properties and recharge. Specific vulnerability should additionally take into account the properties of the contaminant and the land-use practices. However, the latter is disputable.

Until now, there is no commonly agreed understanding of the term vulnerability. COST 65 (1995) presents an overview on the various definitions proposed by different authors. However, most of the suggested definitions are quite similar. The European COST Action 620 on „vulnerability and risk mapping for the protection of carbonate (karst) aquifers“ suggests the following definitions (DALY et al. 2002):

- **Intrinsic vulnerability** is the term used to define the vulnerability of groundwater to contaminants. It takes into account the geological, hydrological and hydrogeological characteristics of an area, but is independent of the nature of the contaminants.
- **Specific vulnerability** is the term used to define the vulnerability of groundwater to a particular contaminant or group of contaminants. It takes into account the properties of the contaminant(s) and its

(their) relationship(s) to the various aspects of the intrinsic vulnerability of the site.

According to the latter definition, the specific vulnerability is independent of the land-use practices, in contrast to the definition proposed by VRBA & ZAPOROZEC (1994). COST 620 suggests to show the aspects of land-use and possible sources of contamination on a separate „hazard map“. As this thesis has been developed within the framework of COST 620, it is based on the definitions and concepts that were proposed by COST 620.

Even though that most definitions and methods to mapping groundwater vulnerability aim on the qualitative aspects (contamination), there are also quantitative aspects of groundwater protection and vulnerability, such as over-exploration (VRBA & ZAPOROZEC 1994).

7.2 The origin-pathway-target model

COST 620 suggests that the concept of vulnerability mapping should be based on a origin-pathway-target model for environmental management (Fig. 7.1) (GOLDSCHIEDER et al. 2000b, DALY et al. 2002).

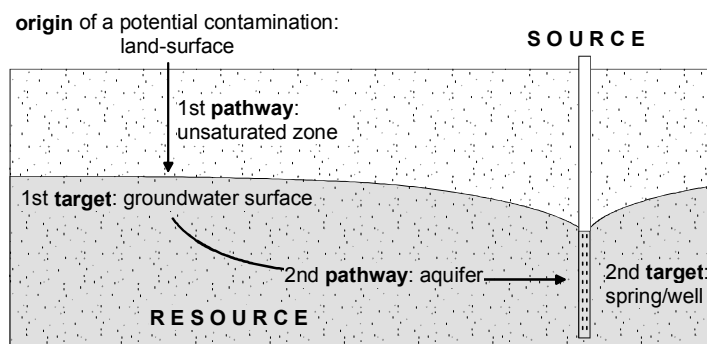


Fig. 7.1: The origin-pathway-target model for vulnerability assessment.

- **Origin** is the term used to describe the location of a potential contaminant release. COST 620 suggests to take the land surface as the origin. This refers to land-use practices like cattle pasture and spreading of pesticides. However, some contaminants are released below the ground surface, e.g. via leakages in sewerage systems.

- The **target** (receptor) is the water which has to be protected. For resource protection (see next section) the target is the groundwater surface, for source protection it is the water in the well or spring.
- The **pathway** includes everything between the origin and the target. For resource protection, the pathway consists of the mostly vertical passage within the protective cover, for source protection it also includes horizontal flow in the aquifer.

7.3 Resource and source protection

In Germany and in all other European countries, groundwater is considered to be a valuable resource which must be protected. Activities endangering its quality are forbidden by law (WHG 1996). The European Water Directive (2000) emphasises that water is not a commercial product like any other but a heritage which must be protected, defended and treated as such. Thus, the directive demands for the protection of ground- and surface water resources.

The highest priority is to protect the groundwater which is used for drinking water supply. Thus, there are special regulations in all European countries which aim on the protection of the drinking water sources (in Germany: DVGW 1995). The source might be a captured spring, a pumping well or any other groundwater abstraction point.

It is practicable to distinguish between resource and source protection (HÖTZL 1996), although both concepts are closely related to each other – it is impossible to protect a source without protecting the resource. However, it is essential to define the target precisely (Fig. 7.1): For resource protection, the groundwater surface is the target and the pathway consists of the mostly vertical passage through the layers above the groundwater surface (the unsaturated zone). For source protection, the water in the well or spring is the target and the pathway includes the mostly horizontal flow route in the aquifer (GOLDSCHIEDER et al. 2000b).

The Irish groundwater protection scheme shows how one vulnerability map can be used for both source and resource protection. According to this concept, the target is always the groundwater surface, and so the vulnerability map can be used for resource protection. However, if the map is intersected with the protection areas around a spring or well (the zone of contribution and the 100-day-line), it can also be used for source protection (GSI 1999).

COST 620 suggests a similar approach. It is proposed to prepare two intrinsic vulnerability maps: the resource and the source vulnerability map (DALY et al. 2002). The former takes into account the properties and thickness of the overlying layers, the latter additionally takes into account the properties of the aquifer and the distance to the source.

7.4 The special situation in karst

The concept of groundwater vulnerability is applicable for all types of aquifers – granular, fractured and karst. However, due to the special properties of karst, it is essential to develop a concept which takes into account the nature of karst. There are two possibilities to do so: develop a method which is specially dedicated to karst; develop a method that is applicable for all types of aquifers but provides some methodological tools for karst systems.

The second possibility is considered to be more applicable for the following reasons: Firstly, there are all kind of transitions between a purely fractured and an extremely karstified carbonate aquifer (HÖTZL 1996). Secondly, there are transitions between granular and karst aquifers, e.g. karstified carbonate gravel or intensively fractured dolomites that behave like a granular aquifer hydraulically (ANDREO 1997). Thirdly, there are often several types of aquifers in one area which interact in most cases, e.g. a granular aquifer overlying a karst aquifer.

The following special characteristics of karst systems are considered to be significant with respect to groundwater vulnerability and should consequently be taken into account (compiled from HÖTZL 1996, LEIBUNDGUT 1998, TRIMMEL 1998, DREW & HÖTZL 1999c):

- Each karst system has its individual characteristics and any generalisation is problematic. the detailed hydrogeological investigation of a karst system is an indispensable precondition for the application of any method to vulnerability mapping.
- Karst systems are highly heterogeneous and anisotropic. Interpolation and extrapolation of field data is problematic and the reliability of a vulnerability map is lower for karst than for other areas.
- Karst groundwater is recharged both by diffuse infiltration and by concentrated point recharge via dolines and swallow holes. The first case is considered to be less vulnerable than the second one.
- The overlying layers above the karst aquifer, such as soil, Quaternary deposits and non-karstifiable bedrock formations, provide

some degree of protection. However, surface or near-surface flow has to be expected in areas covered by such layers. These lateral flow components may be tributary to a stream sinking into the karst aquifer via a swallow hole.

- The presence of an epikarst zone has to be expected. The main functions of the epikarst are water storage and concentration of flow. The first process increases the natural protection of the system while the second process increases the vulnerability. The structure and the hydrologic function of the epikarst are difficult to assess. A large portion of the epikarst is not visible at the land surface.
- Karstic aquifers are characterised by a dual porosity due to fractures and solutional voids (conduits) and frequently by a triple porosity due to the additional presence of inter-granular pores (matrix). Groundwater storage takes place in the pores and fractures, while conduits act as drains. Consequently, there are both extremely fast and slow flow components within a karst system. Contaminants can be transported very fast or stored for a very long time.
- Karst systems are characterised by a fast and strong hydraulic reaction on hydrologic events. The temporal variations of the groundwater table often reach several tens of metres and sometimes more than 100 m. In many karst systems, the groundwater table is discontinuous and difficult to determine.
- Karst catchments are often extremely large and hydraulically connected over long distances. Watersheds are often difficult to determine and variable in time, dependent on the respective hydrologic conditions. The catchments of karst springs often overlap and the flow paths proved by tracer tests often cross each other.

7.5 Vulnerability and the European Water Directive

The European Water Directive (2000) aims to establish a framework for Community action in the field of water policy. The directive demands sustainable water use based on a long-term protection of available water resources (Article 1 b). The term „vulnerability“ is only used in relation to coastal aquatic ecosystems. However, the idea of groundwater vulnerability assessment is indirectly included in the directive.

Annex II 2 demands an initial characterisation of all groundwater bodies to assess their uses and the degree to which they are at risk. It is prescribed to identify the general character of the overlying strata in the

catchment area from which the groundwater body receives its recharge. Those groundwater bodies which have been identified as being at risk, shall be assessed more precisely. This characterisation shall include information on (shortened):

- geological and hydrogeological characteristics of the groundwater body, including hydraulic conductivity, porosity and confinement,
- characteristics of the superficial deposits and soils, including the thickness, porosity, hydraulic conductivity and absorptive properties,
- stratification of the groundwater body,
- an inventory of associated surface systems, including bodies of surface water, with which the groundwater is dynamically linked,
- estimates of the directions and rates of exchange of water between the groundwater body and associated surface systems,
- data to calculate the long-term annual average rate of recharge.

Although this is rather an inventory list to characterise a groundwater body, it can also be used as a list of data that should be included in an approach to mapping groundwater vulnerability.

8 OVERVIEW AND DISCUSSION ON EXISTING METHODS OF MAPPING VULNERABILITY

8.1 Classification of methods

8.1.1 Overview

Various methods of mapping groundwater vulnerability have been developed and applied. An overview and discussion of the different methods is presented by CIVITA (1993), VRBA & ZAPOROZEC (1994), COST 65 (1995), GOGU (2000) and GOGU & DASSARGUES (2000). MAGIERA (2000) describes and evaluates 69 methods to vulnerability mapping. The methods can be grouped in five types: hydrogeological complex and setting methods, index models and analogical relations, parametric system models, mathematical models and statistical methods. However, it is also possible to group the methods on the basis of other criteria, such as scale (local, regional, national) purpose (land-use planning, protection zoning, site assessment), type of definition (intrinsic or specific vulnerability) or target (source or resource vulnerability).

8.1.2 Hydrogeological Complex and Setting Methods

The hydrogeological complex and setting methods (HCS) are based on the assumption that two areas with comparable hydrogeological properties are characterised by a similar groundwater vulnerability (VRBA & ZAPOROZEC 1994). HCS methods take into account basic information presented on geological, hydrogeological and topographic maps, above all the lithology. These methods are applicable for small scale (often 1:1 million) and can be used for land-use planning and resource protection on a national to European scale. HCS methods refer to a general contaminant (intrinsic vulnerability), a validation is not possible. MAGIERA (2000) describes four different HCS methods, most of which are no longer used nowadays.

MARGAT (1968) and ALBINET & MARGAT (1970) prepared a vulnerability map at the scale 1:1 million for France using a HCS method based on the lithology. VIERHUFF et al. (1981) made a vulnerability map for West Germany at the same scale. The map shows two basic information: the vulnerability of the resource and the risk of lateral spreading of a contaminant in the aquifer. The vulnerability is determined on the basis of the properties of the overlying layers and the depth to groundwater

table. The risk of lateral contamination spreading depends on the type of the aquifer (granular, fractured, karst). Karst areas are characterised by a moderate to high vulnerability and a very high risk of lateral spreading of contaminants. Areas without significant groundwater resources are not considered on the map.

The DRASTIC method (ALLER et al. 1987) uses hydrogeological settings as well. However, the vulnerability (DRASTIC-Index) is calculated on the basis of a parametric system model.

8.1.3 Index Methods and Analogical Relations

The index methods (IM) and analogical relations (AR) are based on mathematical standard descriptions of hydrological and hydrogeological processes (e.g. transport equations) that are analogously used to assess the groundwater vulnerability. MAGIERA (2000) describes 13 methods of that type. Most of them are used for the evaluation of the specific vulnerability of groundwater to pesticides on a large to medium scale. The IM/AR methods take into account the properties of the overlying layers and the properties of the contaminant.

The attenuation factor (AF) was introduced by RAO et al. (1985) as one of the first index methods. It is used to describe the specific behaviour of pesticides in the soil. The AVI method (VAN STEMPVOORT et al. 1993) is a well-known index system used to assess intrinsic vulnerability.

8.1.4 Parametric System Models

The parametric system models are the most common approaches. MAGIERA (2000) counted 34 different methods. VRBA & ZAPOROZEC (1994) suggest to subdivide the parametric system models into matrix systems (MS), rating systems (RS) and point count system models (PCSM). However, the overall procedure for the various parametric systems is the same. The first step is the selection of factors (parameters) assumed to be significant for vulnerability. Each factor has a natural range which is subdivided into discrete intervals and each interval is assigned a value reflecting the relative degree of sensitivity to contamination. The vulnerability of an area is determined by putting together the values for the different factors using a matrix (MS), a rating system (RS) or a point count systems (PCSM).

A brief overview on some selected and important parametric system models is presented in the following sections. Most methods are

named with an acronym that is formed by the first letters of the factors that are taken into account (in bold capital letters).

The rating system GOD (FOSTER 1987) takes into account the **G**roundwater occurrence (e.g. none, confined, unconfined), the **O**verlying lithology (e.g. colluvial gravel, sandstone, limestone) and the **D**epth to groundwater table. Each factor is assigned a value between zero and one. The numeric value for vulnerability is obtained by multiplying the three factors and consequently ranges between 0.0 (negligible) and 1.0 (extreme). GOD is applicable for all types of aquifers; the special properties of karst are not considered. Due to the strong influence of the factor D, the vulnerability of a karst area is likely to be underestimated. For example: An unconfined karst aquifer with more than 100 m depth to groundwater table is assigned a moderate vulnerability (0.4).

The point count system DRASTIC (ALLER et al. 1987) calculates the vulnerability on the basis of the following factors: **D**epth to groundwater table, net **R**echarge, **A**quifer media, **S**oil media, **T**opography, **I**mpact of vadose zone and hydraulic **C**onductivity. DRASTIC provides two different weighting systems: one for normal conditions (intrinsic vulnerability), the other one for areas with intense agricultural activity and pesticide spreading (specific vulnerability). DRASTIC is applicable for all types of aquifers but does not take into account the special characteristics of karst landscapes. The Italian SINTACS method (CIVITA & DE MAIO 2000) uses the same seven factors as DRASTIC but the rating and weighting procedure is more flexible.

The EPIK method (DOERFLIGER 1996, DOERFLIGER & ZWAHLEN 1998) and an approach introduced by HÖLTING et al. (1995) form a basis of the PI method that was developed within the framework of this thesis (GOLDSCHIEDER et al. 2000a, b). Thus, these methods are described in detail in a separate section.

8.1.5 Mathematical Models

Even though there are a large number of mathematical (mostly numerical) flow and transport models for the unsaturated and saturated zone, models are rarely used for vulnerability mapping. Models are frequently used for operational purpose, e.g. in the management of water protection zones. MAGIERA (2000) describes nine examples for the application of mathematical models for specific vulnerability mapping on a large to medium scale. Those models take into account both the properties of

the contaminant (mostly nitrates and pesticides) and the properties of the overlying layers and are often verified.

GOGU & DASSARGUES (2000) point out that the set up of suitable mathematical models is a future challenge in vulnerability mapping. COST 620 suggests to use calibrated numerical simulations for the validation of vulnerability maps (DALY et al. 2002). BROUYERE et al. (2001) point out that models, which have a strong theoretical and physical background, allow to assess the consistency of methods to vulnerability mapping and propose to use the simple computed programme VULK (JEANNIN et al. 2001) for that purpose.

8.1.6 Statistical Methods

The physical processes that control the vulnerability of groundwater to contamination are often too complex to be described by taking into account only a selected number of parameters. Therefore, statistical and geostatistical approaches provide an applicable and scientifically based alternative to parametric system models and have been successfully used for specific vulnerability mapping on a small to medium scale (MAGIERA 2000). Statistical methods can always be verified and allow to take into account the reliability of the data.

The first step of a geostatistical vulnerability analysis is to map a selected number of influencing factors, such as depth to groundwater table, soil type, permeability and recharge. The second step is to map the spatial distribution of the concentration of a certain contaminant in the groundwater. The third step is to establish a correlation between the influencing factors and the contaminant concentration. This correlation can be used to map the specific vulnerability of groundwater to the selected contaminant (e.g. TESO et al. 1996).

The application of statistical methods of vulnerability mapping in karst aquifers is problematic. Due to fast lateral transport of contaminants in the aquifer, it is difficult to establish a correlation between the distributions of the influencing factors and the contaminant concentration.

8.2 Description and criticism of some basic methods

8.2.1 Introductory remark

The PI method which was developed within the framework of this thesis was influenced by three other methods: EPIK (DOERFLIGER 1996, DOERFLIGER & ZWAHLEN 1998), the Irish groundwater protection

schemes (GSI 1999) and, above all, the GLA method (HÖLTING et al. 1995). Thus, these methods are described in the following sections.

8.2.2 EPIK

The EPIK method (DOERFLIGER 1996, DOERFLIGER & ZWAHLEN 1998) is a multi-parameter approach to intrinsic vulnerability mapping in karst areas. In Switzerland, it is used for the delineation of source protection zones according to the Swiss Water Protection Ordinance (1998). The protection index F is calculated on the basis of four attributes which form the acronym: **E**pikarst, **P**rotective cover, **I**nfiltration and **K**arst network development. The index F is subdivided into four classes of vulnerability that are transformed into protection zones.

The epikarst (E) is a subsurface, highly fissured and karstified zone which can extend between decimetres and tens of metres. Its main functions are water storage and flow concentration. The degree of epikarst development is assessed on the basis of geomorphologic karst features. Three classes are distinguished:

- E₁: swallow holes, dolines, karrenfields
- E₂: intermediate zones between the aligned dolines, dry valleys
- E₃: the rest of the catchment

The protective cover (P) includes the soil and other non-karstic formations overlying the karst aquifer. Four categories are defined:

- P₁: 0–20 cm of soil and/or low permeability formations;
- P₂: 20–100 cm of soil and/or low permeability formations;
- P₃: more than 1 m of soil and/or low permeability formations;
- P₄: more than 8 m of low permeability formations, or more than 1 m of soil on 6 m of low permeability formations.

The infiltration conditions (I) take into account the type of recharge into the karst aquifer. Areas with diffuse infiltration are considered to be less vulnerable than areas that drain by concentrated recharge via a swallow hole. Four classes are distinguished:

- I₁: perennial or temporary swallow holes and sinking streams, including the beds and banks of the streams, as well as artificially drained sectors within the catchment of these streams;

- I₂: naturally drained areas inside the catchments of swallow holes or sinking streams with steep slopes (more than 10 % for arable areas, more than 25 % for meadows and pastures);
- I₃: areas inside the catchment of swallow holes or sinking streams with gentle slopes (less than 10 % or 25 % respectively); low lying areas outside such a catchment which collect runoff and steep slopes which generate this runoff;
- I₄: rest of the area.

The karst network development (K) is classified in the following way:

- K₁: moderate to well developed karst network with decimetres to metres wide conduits;
- K₂: poorly developed or blocked karst network;
- K₃: fissured non-karstic limestone aquifers and systems which infiltrate in porous media.

The protection index F is calculated with the formula:

$$F = 3 \cdot E + P + 3 \cdot I + 2 \cdot K$$

The values used to calculate the protection index are the following:

E ₁	E ₂	E ₃	P ₁	P ₂	P ₃	P ₄	I ₁	I ₂	I ₃	I ₄	K ₁	K ₂	K ₃
1	3	4	1	2	3	4	1	2	3	4	1	2	3

The protection factor ranges between 9 and 34. The vulnerability and the groundwater protection zones are determined according to the following matrix:

Vulnerability	Protection Factor	Protection /one
very high	$F \leq 19$	S1 (source protection)
high	$19 < F \leq 25$	S2 (inner protection zone)
moderate	$F > 25$	S3 (outer protection zone)
low	$F > 25, P = P_4, I = I_{3,4}$	rest of the catchment

8.2.3 Discussion on the EPIK method

The EPIK method is easily applicable and takes into account the special properties of karst. DOERFLIGER & ZWAHLEN (1998) describe several examples of the successful application of EPIK in different karst

systems in the Swiss Jura mountains and in the Alps. However, the method contains some inconsistencies. The main critical remarks concerning the EPIK-method are the following (GOLDSCHIEDER 1999):

- Some important factors are missing: The recharge and the thickness of the unsaturated zone (depth to water table) are not taken into account although most authors consider these factors to be of major importance (e.g. ALLER et al. 1987, FOSTER 1987, HÖLTING et al. 1995, MAGIERA 2000).
- The E factor is evaluated in an unreliable way: The epikarst is mapped on the basis of geomorphologic karst features (karren-fields, dolines, dry valleys). However, surface karst features are only one expression of epikarst, but most of it cannot be seen at the surface. Epikarst can be highly developed without visible karst features (DREW et al. 1999).
- The weighting system is contradictory: DOERFLIGER (1996) points out that the protective cover is very important for the natural protection and, vice versa, for the vulnerability of an aquifer, but the lowest weighting factor is assigned to the parameter P.
- The zero is missing: The minimum value of each attribute is 1 even if its effect on protection is zero. Together with the different weighting factors, this may lead to inconsistent results. For example: Both a swallow hole and a 5 m thick low permeability cover contribute 3 points to the protection index, although the cover provides some protection while the swallow hole is a point of extreme vulnerability.
- The EPIK formula is not always applicable: The protection index F is calculated by summing up the weighted values of the four factors. However, not all the factors always contribute to the protection of the system. For example: A thick low permeability formation (P = 4) is not protective if it produces surface runoff towards a swallow hole (I=2). Thus, it is inconsistent to sum up the values of P and I.
- EPIK is not defined for all hydrogeological settings: In some cases, it is impossible to define and quantify all the parameters. For example: E, P and K can not be defined for a non-karstic area that discharges into a bordering karst system by surface flow.
- The transformation of the vulnerability classes into source protection zones is disputable: The EPIK vulnerability classes are directly translated into source protection zones without using any additional

criteria such as travel time in the aquifer or distance to the source. However, for source protection zoning, the spring or well must be taken as the target. Thus, it is indispensable to take into account the pathway to the spring or well.

In some cases, the strict application of EPIK leads to inconsistent results (Fig. 8.1). However, experience has shown that sensible protection zones can be delineated if the method is applied in a flexible way and if the user is aware of the problems and limitation. EPIK was the background for several new methods of vulnerability mapping in karst areas, like the Slovakian REKS method (MALIK & SVASTA 1999).

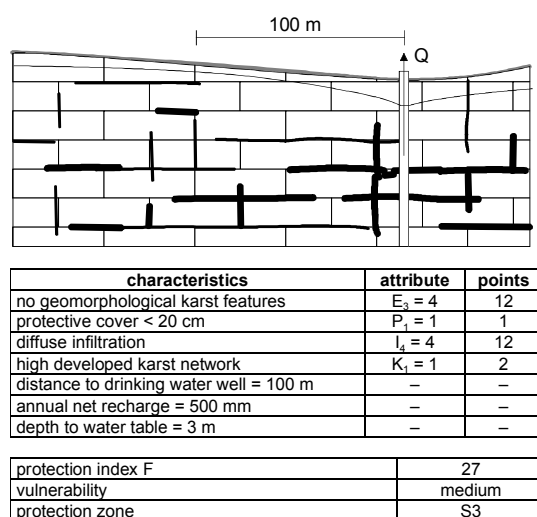


Fig. 8.1: Hypothetical example for an inconsistent vulnerability assessment when EPIK is applied strictly. The delineation as protection zone S3 would be insufficient in the described case.

8.2.4 The Irish groundwater protection scheme

In Ireland, the vulnerability map is not a stand-alone element, but an integrated component of a comprehensive groundwater protection scheme consisting of four elements (DALY & DREW 1998, GSI 1999):

1. The **aquifer map** shows the importance of the resource and its hydrogeological characteristics (e.g., Rk: Regionally important karst aquifer; Lg: Locally important sand/gravel aquifer; Pu: Poor aquifer, generally unproductive bedrock).

2. The **vulnerability map** is based mostly on the thickness and hydraulic conductivity of the subsoil. It takes the vertical movement of water and contaminants in the subsoil into consideration. An 'extreme vulnerability' is assigned to karst features (e.g. dolines).
3. The **source protection areas** take into account the lateral movement in the aquifer. The inner source protection area (SI) is delineated according to the 100-day line of travel time in the aquifer, the outer source protection area (SO) covers the entire catchment area (or the zone of contribution respectively).
4. The **protection responses** define clearly which kind of land-use is not acceptable or acceptable with or without further restrictions in the different protection zones (e.g., spreading of fertiliser is generally not acceptable in extremely and highly vulnerable areas within an inner source protection area).

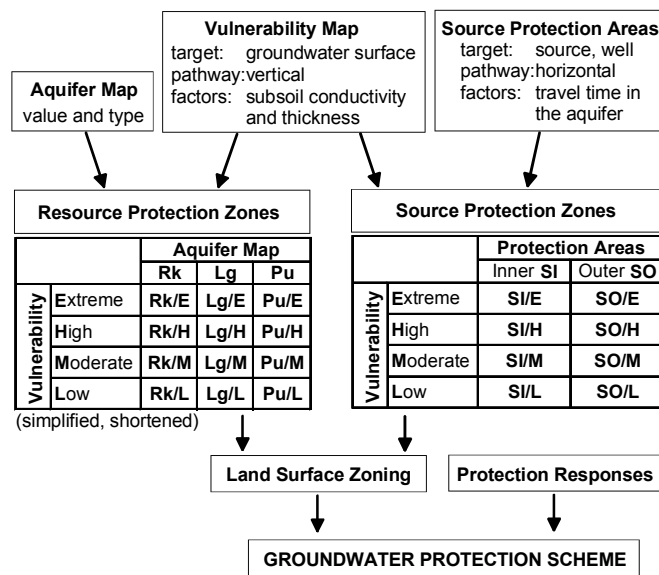


Fig. 8.2: Illustration of the Irish groundwater protection scheme. The vulnerability map can be used both for source and resource protection zoning (GSI 1999). Explanation of the abbreviations in the text.

Both source and resource protection zones can be obtained using the vulnerability map together with one of the other elements: For resource protection, the groundwater in the aquifer is the target. Consequently,

the resource protection zones are obtained by intersecting the aquifer map with the vulnerability map. For source protection, the spring or well is the target. Therefore, the source protection zones are obtained by a combination of the vulnerability map and the protection areas. For both resource and source protection zones, there are protection responses which define the land-use restrictions for each zone.

8.2.5 Discussion on the Irish system

The Irish system is an excellent example of the application of vulnerability maps within the framework of a comprehensive groundwater protection scheme that can be used for source protection, resource protection and land-use planning. The Irish scheme seems to largely fulfil the demands of the European Water Directive (2000) and could provide a model for other European countries.

However, according to the Irish method, the vulnerability of an area is assessed in a very simplistic way: Only the thickness and permeability of the subsoil (Quaternary deposits) and the presence of karst features are taken into account. All the other potential layers above the groundwater surface, that is the soil and the unsaturated zone of the bedrock, are assumed to be not protective and are consequently not taken into consideration. However, there are many possible hydrogeological settings, where these layers play an important role, e.g. a karst aquifer that is covered by tens of metres of marl.

8.2.6 The German or GLA method

In Germany, groundwater source protection zones are delineated on the basis of the DVGW Guideline W101 (1995). The main criterion for the delineation of the inner protection zone (zone II) is the 50-day line of travel time in the aquifer. However, groundwater protection must not be restricted on the catchments of drinking water captures. In order to provide a basis for land-use planning and groundwater resource protection, the German State Geological Surveys (German shorthand: GLA) and the Federal Institute of Geosciences and Natural Resources (BGR) worked out a concept to assess the protective function of the layers above the groundwater surface (HÖLTING et al. 1995). Although the German term for "vulnerability" is not used in the paper, the GLA method is an approach to resource vulnerability mapping according to the COST 620 definition (DALY et al. 2002). Together with the DVGW guideline (1995), it can also be used for a more detailed subdivision of drinking water source protection zones. The authors did not suggest an

official short name or acronym for this method. It is commonly known as the 'German', the 'GLA' or the 'HÖLTING' method. VON HOYER & SÖFNER (1998) translated the method into English.

The basic idea of the GLA method is that the effectiveness of all natural attenuation processes in the protective cover for reducing contaminant concentration is mainly dependent on the travel time. As a consequence, the protective function is dependent on the main factors controlling the travel time: the thickness of each stratum and the properties of the material. The protective cover includes all strata between the ground surface and the groundwater surface: the soil, the subsoil and the unsaturated (karstic and non-karstic) bedrock.

The protective function of the soil is assessed according to its effective field capacity (eFC). The subsoil, consisting of granular, non-lithified material (mostly Quaternary deposits), is the layer below the topsoil. Its protective function is calculated according to its grain-size distribution (GSD), which is also related to its cation exchange capacity (CEC). The protective function of the unsaturated part of the bedrock is calculated taking into account the type of rock and structural features like fracturing and degree of karstification.

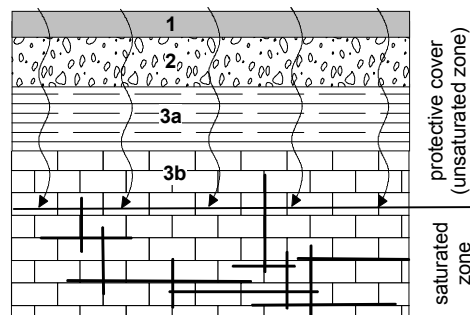


Fig. 8.3: Illustration of the GLA concept (HÖLTING et al. 1995) to assess the protective function of the layers above the groundwater surface: 1. topsoil, 2. subsoil, 3. unsaturated bedrock (a. non-karstic, b. karstic).

The total protective function of the cover is obtained as follows: The value for the protective function of each stratum is multiplied by the thickness of that stratum in metres (M). The resulting values are added and multiplied by a factor reflecting the amount of recharge. An additional protective function term is included for artesian conditions and for perched aquifers above the aquifer in question. The total score of the protective function P_{TS} (in German: Gesamtschutzfunktion S_G) can be

any positive value. The range of possible values is subdivided into five classes: very high, high, medium, low and very low.

8.2.7 Discussion on the GLA method

The concept of the GLA method is logical and applicable. It can be used for resource protection and land-use planning for all types of aquifers. The GLA method can also be used for source protection together with the DVGW guidelines W101 (1995). According to these guidelines, the main criterion for the delineation of source protection zones is the travel time in the aquifer. However, the guidelines allow a reduction in the size of the zones if the overlying layers are sufficiently protective and the GLA method can be used for that evaluation.

Even though the GLA method is in principle applicable for all types of aquifers, it does not sufficiently take into account the special properties of karst. The basic assumption of the GLA method is that infiltration occurs diffusely and all the infiltrating water slowly percolates vertically through the unsaturated zone towards the groundwater table. In non-karstic areas with permeable soils and gentle topography, this assumption is generally fulfilled. However, especially in karst areas and in mountainous landscapes, lateral concentration of flow occurs frequently at or near the surface and these flow components often sink into the karst aquifer via swallow holes. This process can bypass the protective cover partially or completely. In this case, the GLA method is not applicable. This is the starting point for the PI method, which takes into account the lateral concentration of flow via the I factor.

Furthermore, the ranges of the five classes of protective function are too narrow to take into account the extremely wide range of natural conditions. For example, overlying layers that consist of less than 20 m of sand are considered to provide a „very low“ degree of protection (very high vulnerability), while more than 8 m of clay are considered to provide a very high degree of protection (very low vulnerability).

9 THE PI METHOD

9.1 Background and Overview

The PI method was developed within a project funded by the Federal Institute for Geosciences and Natural Resources (BGR) and is a part of the German contribution to the COST action 620 on vulnerability and risk mapping for the protection of carbonate (karst) aquifers. The complete results of the project were reported by GOLDSCHIEDER et al. (2000a); the PI method was published by GOLDSCHIEDER et al. (2000b).

The first step of the project was to compare the Swiss EPIK method (DOERFLIGER & ZWAHLEN 1998) with the German GLA method (HÖLTING et al. 1995) in the test site „Engen“ in the Swabian Alb, SW Germany. The GLA method had already been applied there manually and using a GIS (DICKEL et al. 1993a, b). On the basis of these studies, STURM (1999) and KLUTE (2000) applied EPIK in the same area.

The comparison and evaluation of the two maps showed that both were not completely satisfactory: The GLA map considers the protective cover in a sensible and logical way, but the method doesn't allow to take into account the infiltration conditions which are, however, very significant for the vulnerability of a karst area. In contrast, the EPIK map takes into account the infiltration conditions and especially the presence of swallow holes and sinking streams, but the protective cover is not considered sufficiently.

Therefore, the second step of the project was to develop a new method that takes into account both the protective cover (P) and the infiltration conditions (I) in a sensible and reliable way. The P factor is calculated according to a slightly modified GLA method. The I factor was influenced by the EPIK method but strongly modified. The new method was called the PI method. It was first applied in the test site „Engen“ by STURM (1999) and KLUTE (2000). An excellent GIS data base was available for this area. Later on, a COST 620 task group (DALY et al. 2000a) worked out suggestions to modify PI method, especially the P factor, in order to make it more flexibly applicable for areas with a less extensive data base (see section 9.6). Until now, the „original“ and the „modified“ PI method have been successfully applied in eight karstic test sites in four European countries:

- Engen, Swabian Alb, Germany (see chapter 10);

- Hochifen-Gottesacker, Alps, Germany/Austria (see chapter 11);
- Winterstaude, Alps, Austria (see chapter 12);
- Albiztur unit, Basque county, Spain (MUGUERZA 2001)
- Veldensteiner Mulde, Franconian Alb, Germany (SCHMIDT 2001);
- Hydrogeological unit of Mt. Cornacchia and Mt. della Meta, Latium, Italy (COVIELLO 2001);
- Mühlthalquellen, Thuringia, Germany (SAUTER et al. 2001);
- Sierra de Libar, Andalusia, Spain (Brenchenmacher 2002).

COST 620 outlined the main concepts of an “European Approach” for (karst) groundwater vulnerability assessment and mapping (DALY et al. 2002). It is suggested to use an O factor (overlying layers) and a C factor (concentration of flow) which are similar to the P factor (protective cover) and the I factor (infiltration conditions) of the PI method. Additionally, COST 620 has introduced a K factor (karstic network) and a P factor (precipitation regime) (see chapter 13.3).

9.2 General Concept of the PI Method

The PI Method is a GIS-based approach to mapping groundwater vulnerability for all types of aquifers but with special consideration of karst. It is based on a origin-pathway-target model: The land surface is taken as the origin of a potential contamination, the groundwater table in the uppermost aquifer is the target, and the pathway includes all layers between the ground surface and the groundwater table. Similar to the Irish scheme, the PI vulnerability map can be used for resource protection and, together with an aquifer map, for source protection.

The acronym PI stands for the two factors protective cover (P factor) and infiltration conditions (I factor) (Fig. 9.1). The P factor describes the effectiveness of the protective cover resulting mainly from the thickness and hydraulic properties of all the strata between the ground surface and the groundwater table – the soil, the subsoil, the non-karstic bedrock and the unsaturated zone of the karstic bedrock. The P factor is calculated according to a slightly modified version of the GLA method (HÖLTING et al. 1995) and divided into five classes. Form P = 1 for an extremely low degree of protection to P = 5 for very thick and protective overlying layers. The distribution of the P factor is shown on the P map.

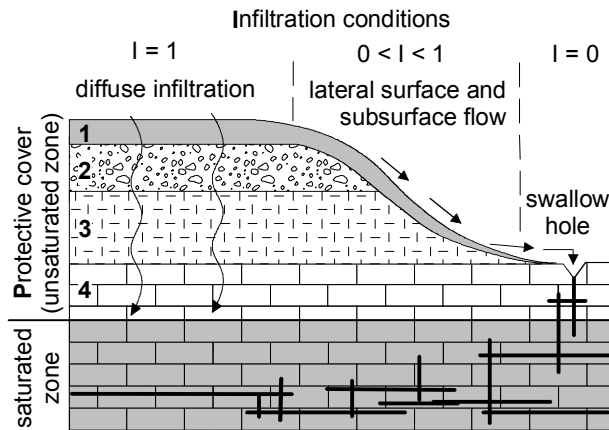


Fig. 9.1: Illustration of the PI method: The P factor takes into account the effectiveness of the protective cover (1. topsoil, 2. subsoil, 3. non-karstic bedrock, 4. unsaturated karstic bedrock). The I factor expresses the degree to which the protective cover is bypassed by lateral surface and subsurface flow, especially within the catchments of sinking streams.

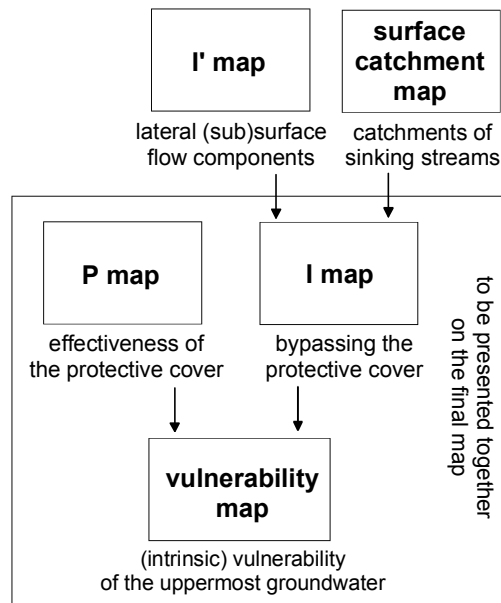


Fig. 9.2: Simplified flow chart for the PI method.

The I factor describes the infiltration conditions, particularly the degree to which the protective cover is bypassed as a result of lateral surface and subsurface flow. The I factor is 1 if the infiltration occurs diffusely, e.g. on a flat, highly permeable and free draining surface. In contrast, the protective cover is completely bypassed by a swallow hole, through which surface water may pass directly into the karst aquifer. In such a case, the I factor is 0. The catchment of a sinking stream is assigned a value between 0 and 1, depending on proportion of lateral flow components. The I map shows the spatial distribution of the I factor.

The final protection factor π is the product of P and I. It is subdivided into five classes. A protective factor of $\pi \leq 1$ indicates a very low degree of protection and an extreme vulnerability to contamination; $\pi = 5$ indicates a high degree of protection and a very low vulnerability. The spatial distribution of the π factor is shown on the vulnerability map. Small I and P maps should be printed as insets on this map, so that it can be distinguished how the vulnerability of a particular area is influenced by the two independent factors (Fig. 9.2).

9.3 Protective Cover (P factor)

The P factor indicates the effectiveness of the protective cover and is calculated using a modified version of the GLA method (HÖLTING et al. 1995). The calculation and assessment scheme is shown in Fig. 9.3. Please note: All the original letter symbols of the GLA method have been changed for the English translation.

The score B for the bedrock is obtained by multiplying the factor L for the lithology and the factor F for the degree of fracturing and karstification. The F factor was modified in order to describe the development of the epikarst and its influence on groundwater vulnerability.

The epikarst is defined as the uppermost zone of karstified rock outcrops, in which permeability due to fissuring and karstification is substantially higher and more uniformly distributed than in the rock below (KLIMCHOUK 1997). Its thickness ranges between a few decimetres and tens of metres. The possible functions of epikarst are storage and concentration of flow (FORD & WILLIAMS 1989). If the epikarst is developed in a way that leads to extreme concentration of flow, e.g., a bare karrenfield connected with hidden, karstic shafts, the structural factor is assigned a value of zero, expressing that the protective cover of the unsaturated zone below this epikarst is completely bypassed (Fig. 9.4).

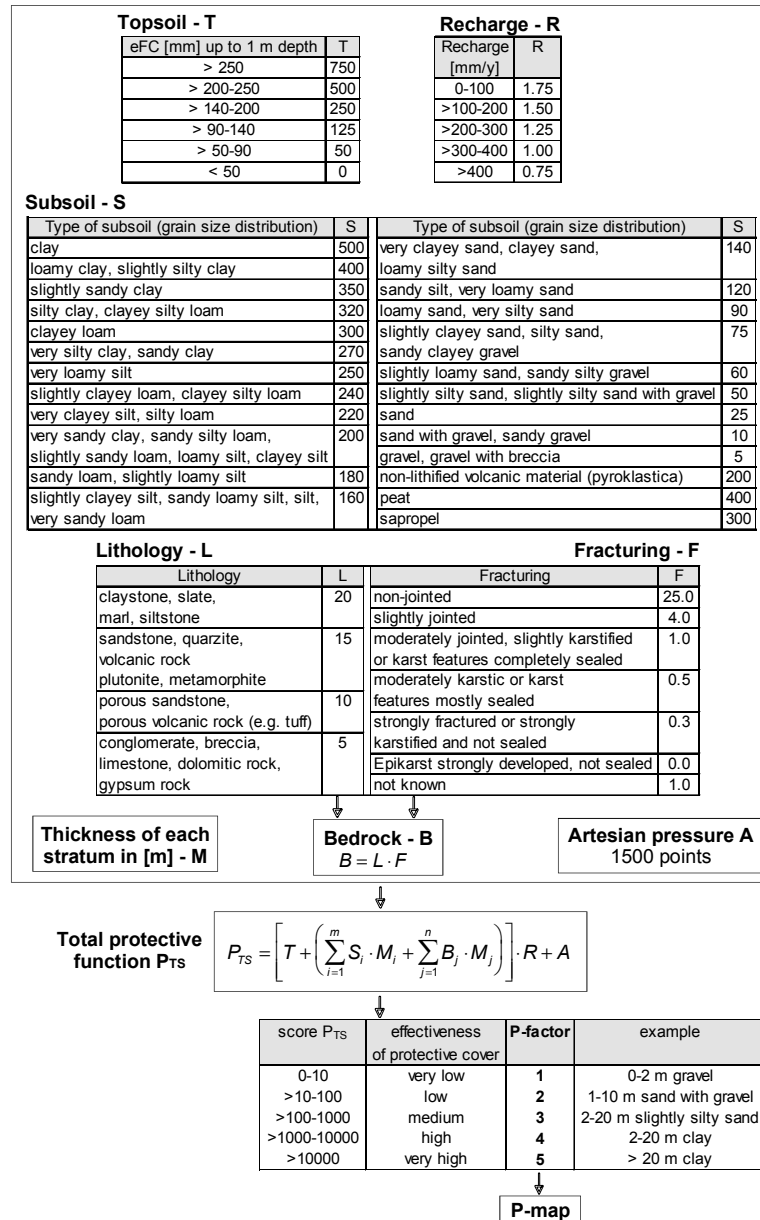


Fig. 9.3: Determination of the P factor (modified after HÖLTING et al. 1995).

Surface karst features (exokarst) are only one expression of epikarst, but most of it cannot be seen at the surface. The epikarst zone can be highly developed without any visible karst features. As a consequence, it is assumed that epikarst is present (even if it is not visible) if there are conditions that are favourable for epikarst development, such as pure limestone with widely spaced fractures, or if there are geomorphological indicators of extensive development of epikarst, such as dolines and karrenfields (DREW et al. 1999).

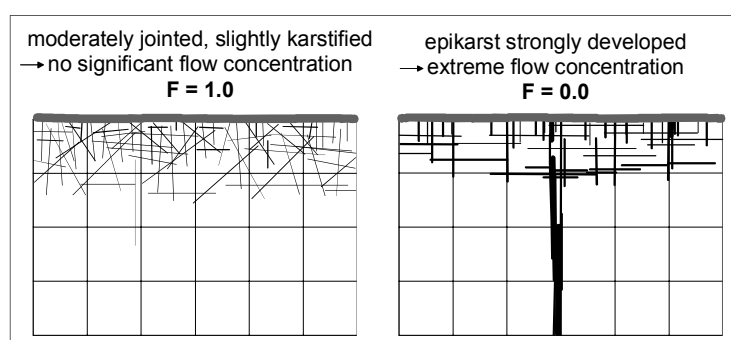


Fig. 9.4: Epikarst and protective function: a) The unsaturated karstic bedrock may provide a protective function if the epikarst is slightly developed so that water storage is the dominant process. b) Concentration of flow in a highly developed epikarst decreases the protective function.

It can be misleading to assign a low vulnerability to an area where the aquifer under consideration is overlain by a higher aquifer – in this case, the higher aquifer needs protection. Therefore, the PI method always takes the groundwater table in the uppermost aquifer as the target. As a consequence, a higher aquifer is not considered to be protection for the underlying aquifer, in contrast to the GLA method. Consideration of artesian pressure in the aquifer by an additional score of $A = 1500$ points was not modified.

The scores for the subsoil and the bedrock are multiplied by the respective thickness in m (factor M). Thin, low permeability strata can be bypassed if they are not laterally extensive, but occur in form of lenses. As a consequence, the lateral continuity of each layer should be taken into account in order to avoid overestimation of the protective function (DALY et al. 2000b). The score for the total effectiveness of the protective cover P_{TS} is calculated according to a formula similar to the one used in the GLA method (HÖLTING et al. 1995).

The range of possible scores for the total protective function P_{TS} is subdivided into five classes, which are the final P factors in the PI method. Each class covers a score range of one magnitude. The classes are much wider than those in the original GLA method, allowing a better description of the high natural variation of protective cover: $P_{TS} \leq 10$ (e.g., < 2 m of gravel) is considered to provide a very low degree of protection and to be extremely vulnerable ($P = 1$), while a very high degree of natural protection and a very low vulnerability ($P = 5$) is assigned to $P_{TS} > 10000$ (e.g., > 20 m of clay). The spatial distribution of the P factor is shown on a P map. For flat areas with a high infiltration capacity, the P factor is multiplied by an I factor of 1. Consequently, the final vulnerability map will be identical to the P map for this area.

A P factor of 5 is assigned to areas outside the considered aquifer from which recharge enters the aquifer by surface and lateral surface or subsurface flow; these areas can be subdivided and classified according to different I values (see next chapter).

9.4 Infiltration Conditions (I factor)

9.4.1 General Concept

The overlying layers can protect the groundwater only if the precipitation infiltrates directly into the ground without significant concentration of flow. However, the disappearance of a surface stream into a swallow hole is common in karst areas. In this case, the protective cover is completely bypassed at the swallow hole and bypassed in part by the surface runoff in the catchment area of the sinking stream.

Therefore, the I factor was introduced. It expresses the degree to which the protective cover is bypassed as a result of lateral, surface and subsurface concentration of flow, especially within the catchment of a sinking stream. If the infiltration occurs directly on a flat surface without significant lateral flow, the I factor is 1, indicating that the protective cover is not bypassed and 100 % effective. On the other hand, the protective cover is completely bypassed by a swallow hole through which surface water directly enters the karst aquifer. In this case, the I factor is 0. The catchment area of a sinking stream is assigned a value between 0 and 1 according to the extent of lateral (sub)surface flow.

It has to be emphasised that the I factor can not be precisely defined in terms of hydrology. It is a semi-quantitative tool to express the vulnerability of groundwater resulting from bypassing of the protective cover

by surface and lateral subsurface flow. The I factor is used for further GIS operations to generate the vulnerability map.

9.4.2 Hydrological Basis

The vulnerability of an area to groundwater contamination is dependent on the pathway of a possible contaminant from the ground surface to the groundwater table. As contaminants are usually transported in water, it is necessary to describe the possible flow paths of the water. We can distinguish between three relevant processes: infiltration with subsequent percolation, surface flow, and subsurface flow. Which of these processes predominates depends on both the properties of the site and the characteristics of the rainfall event, as well as the previous precipitation history and the degree of saturation of the soil.

Diffuse infiltration of rain water from the surface into the soil and the subsequent downward percolation through the soil is the dominant hydrological process if the rainfall intensity is less than the capacity of the soil to absorb the water and if the hydraulic conductivity of the total soil profile is high enough to allow downward movement of the water. Gentle slopes, dense vegetation – especially forest cover – and coarse-textured soils with thick organic horizons and stable pedes favour infiltration (DYCK & PESCHKE 1995).

Surface flow occurs when not all of the rain water is able to penetrate the soil surface. There are two main types: Hortonian runoff and saturated surface flow.

Hortonian runoff occurs when the intensity of a rainfall event exceeds the infiltration capacity of the topsoil and the surplus rain water flows away on the surface. The necessary condition for Hortonian runoff is that the intensity of the rain is significantly higher than the hydraulic conductivity of the topsoil. The amount (depth) of surplus water which is sufficient to produce surface runoff is dependent on the slope of ground surface (PESCHKE et al. 1999).

Saturated surface flow occurs when a rainfall event is sufficiently long and intense to saturate the soil and exhaust its throughflow capacity or if the soil was saturated due to previous precipitation and the additional precipitation cannot infiltrate but flows away on the surface. This process is favoured when lower permeability layers are present below thin, relatively highly permeable topsoil. The necessary condition for this type of flow is that the total amount of precipitation is more than the effective porosity; similar to Hortonian runoff, the amount of surplus

water that is sufficiently high to produce surface runoff depends on the ground surface gradient (MERZ 1996).

Subsurface flow occurs when the hydraulic conductivity of the topsoil is high enough for the infiltration of rain water while lower permeability layers in or below the soil do not allow the further downward percolation to continue. In this case, the layers above the low permeability zone become temporarily saturated, allowing movement parallel to the slope. The velocity of the subsurface flow is strongly dependent on the slope gradient, the hydraulic conductivity of the topsoil, and on preferential flow paths. We can distinguish between two relevant types:

Subsurface storm water flow in diffuse pathways is a fast flow process, which occurs in very highly permeable soils. The flow velocity depends on the hydraulic conductivity and the slope gradient (ZUIDEMA 1985).

Subsurface storm water flow in preferential pathways is another fast flow process. Soil pipes, desiccation fissures, worm holes and mouse holes are usually dry but become filled with water during intensive rain events, enabling very fast flow (LEHNHARDT 1984).

9.4.3 The I Factor

The I factor expresses the degree to which the protective cover is bypassed by lateral surface and subsurface flow. The distribution of the I factor is shown on the I map. Such flow is considered to be especially dangerous within the catchment area of a sinking stream because contaminants can directly enter the karst groundwater. Therefore, the I factor (the I map) is obtained using the following components:

The I' factor expresses the estimated direct infiltration relative to surface and lateral subsurface flow. The controlling factors are soil properties, slope and vegetation. The spatial distribution of the I' factor is shown on the I' map.

The 'surface catchment map' shows the surface catchment areas of sinking streams disappearing into a swallow hole and buffer zones of 10 m and 100 m on both sides of the sinking streams.

The assessment scheme for the I factor is presented in Fig. 9.5 and explained in detail in the following sections.

1st Step: Determination of the dominant flow process

		Depth to low permeability layer		
		< 30 cm	30-100 cm	> 100 cm
Saturated hydraulic conductivity [m/s]	> 10 ⁻⁴	Type D	Type C	Type A
	> 10 ⁻⁵ -10 ⁻⁴		Type B	
	> 10 ⁻⁶ -10 ⁻⁵	Type E		
	< 10 ⁻⁶	Type F		

2nd Step: Determination of the I'-factor

Forest				
dominant flow process		Slope		
		< 3.5 %	3.5 - 27 %	> 27 %
infiltration	Type A	1.0	1.0	1.0
	Type B	1.0	0.8	0.6
subsurface flow	Type C	1.0	0.6	0.6
	Type D	0.8	0.6	0.4
surface flow	Type E	1.0	0.6	0.4
	Type F	0.8	0.4	0.2

Field/Meadow/Pature				
dominant flow process		Slope		
		< 3.5 %	3.5 - 27 %	> 27 %
infiltration	Type A	1.0	1.0	0.8
	Type B	1.0	0.6	0.4
subsurface flow	Type C	1.0	0.4	0.2
	Type D	0.6	0.4	0.2
surface flow	Type E	0.8	0.4	0.2
	Type F	0.6	0.2	0.0

3^d Step: Determination of the I-factor

Surface Catchment Map		I' factor					
		0.0	0.2	0.4	0.6	0.8	1.0
a	swallow hole, sinking stream and 10 m buffer	0.0	0.0	0.0	0.0	0.0	0.0
b	100 m buffer on both sides of sinking stream	0.0	0.2	0.4	0.6	0.8	1.0
c	catchment of sinking stream	0.2	0.4	0.6	0.8	1.0	1.0
d	area discharging inside karst area	0.4	0.6	0.8	1.0	1.0	1.0
e	area discharging out of the karst area	1.0	1.0	1.0	1.0	1.0	1.0



Fig. 9.5: Determination of the I factor. If it is impossible to distinguish six different flow processes, it is sufficient to distinguish between infiltration (white), subsurface (light grey) and surface flow (dark grey). In this case, the bold numbers can be used to determine the I' factor (2nd step).

The amount of surface and subsurface flow is dependent on rainfall intensity and site properties. Characteristics of single events, like precipitation rate, cannot be included in the concept of vulnerability – otherwise we would have to draw a different vulnerability map for each rain event. Therefore, the proportion of surface and subsurface flow is estimated only on the basis of the site properties and assuming average storm rainfall, which might occur several times per year.

On the basis of the hydrological concepts described in the previous section, KLUTE (2000) worked out a system to deduce the dominant flow process from the hydraulic conductivity and depth of lower permeability layers within or below the soil (Fig. 9.6). The critical values for hydraulic conductivity and thickness were calculated using data and theoretical approaches from the hydrological literature, mainly from ZUIDEMA (1985), DYCK & PESCHKE (1995) and PESCHKE et al. (1999).

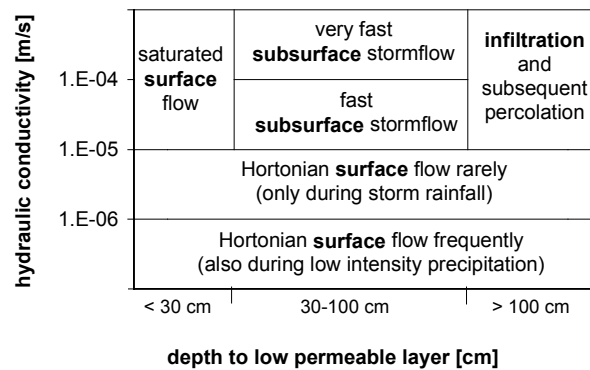


Fig. 9.6: Determination of the predominant flow process as a function of the saturated hydraulic conductivity and the depth to low permeability layers. If it is not possible to distinguish all six processes, it is often sufficient to differentiate between infiltration, subsurface and surface flow. This can be done on the basis of direct field observations and geological data.

- Infiltration is the dominant process when the hydraulic conductivity of the topsoil is greater than 10^{-5} m/s and the thickness is more than 100 cm.
- Fast subsurface storm-water flow is the dominant process when the thickness is 30–100 cm and the conductivity is greater than 10^{-5} m/s; if it exceeds 10^{-4} m/s, very fast subsurface flow of more

than 50 m/d is to be expected. Macropores favour subsurface storm-water flow.

- Saturated overland flow is the dominant process if we find low permeable layers at depths of less than 30 cm and if the conductivity of the topsoil is greater than 10^{-5} m/s.
- Hortonian flow occurs rarely (rainfall intensity of 30 mm/h on steep slopes and 50 mm/h on gentle slopes) if the conductivity of the topsoil is between 10^{-5} and 10^{-6} m/s.
- Hortonian flow occurs frequently (rainfall intensity of 3 mm/h on steep slopes and 30 mm/h on gentle slopes) if the conductivity of the topsoil is less than 10^{-5} m/s.

This system makes it possible to delineate areas with different flow processes predominate. However, there are often not enough detailed data to distinguish between the six different processes described above. In this case it is sufficient to differentiate between the three processes infiltration, subsurface and surface flow. This can often be done on the basis of geological data, information on the soil type and/or direct field observations. For example: Infiltration has to be expected on highly permeable rendzina soil on karst rocks; subsurface flow predominates on coarse rock debris covering low permeability formations; surface flow takes place on outcrops of marl and claystone formations.

The proportion of each of these flow processes depends on the factors vegetation (land use) and slope of the ground surface. In general, forest cover favours infiltration, whereas agricultural areas are more likely to produce surface runoff. The flow velocity of subsurface flow can be estimated using the Darcy equation (except for preferential flow) and is directly proportional to the slope gradient. Hortonian runoff and saturated flow can occur even on very gentle slopes if the precipitation exceeds infiltration or if the topsoil is saturated, but steep slopes favour surface flow and increase its flow velocity.

A system to assess the proportion of lateral surface and subsurface flow was developed, based on the dominant flow process and the factors vegetation and slope. The slope was done using the divisions of the German soil mapping guidelines (AG Boden 1996). The proportion of lateral flow is expressed by the so-called I' factor. Its spatial distribution is shown on the I' map. However, for vulnerability mapping in karst areas, it is indispensable to distinguish whether this flow occurs inside or outside the catchment area of a sinking stream as well as to take

into account the distance of the evaluated site to the stream. With respect to groundwater vulnerability, the most dangerous situation is lateral flow close to a swallow hole or sinking stream, while the least dangerous situation is flow that leaves the system under consideration without sinking or seeping underground. Therefore, the final I map is obtained by intersection of the I' map with a map showing the catchment areas of sinking streams (Fig. 9.7).

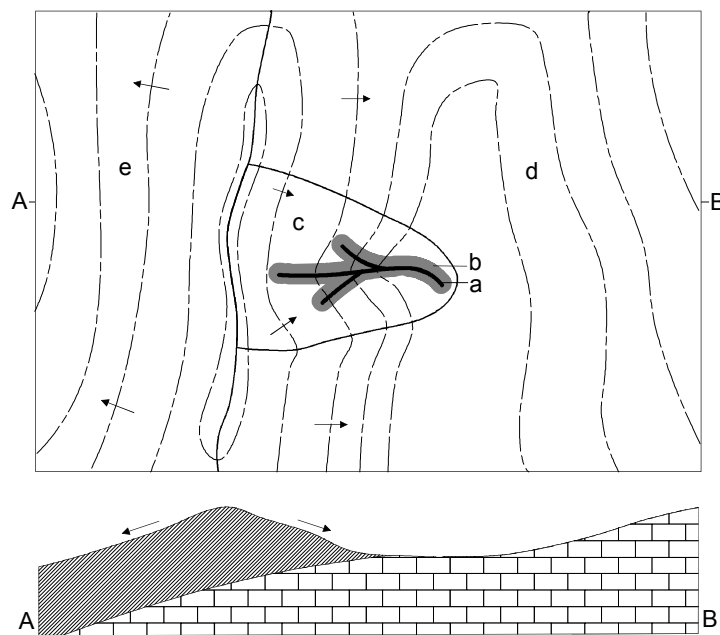


Fig. 9.7: Topographic sketch and geological profile illustrating the five different zones of the „surface catchment map“ in the order of decreasing risk: a) sinking stream with 10 m buffer, b) 100 m buffer, c) catchment of sinking stream, d) rest of the area draining into the karst, e) area draining out of the karst. The arrows indicate lateral (sub)surface flow.

Five zones are delineated on this „surface catchment map“ in order of decreasing risk.

- a) Swallow holes, sinking streams and a 10 m buffer zones on both sides of these streams.
- b) 100 m buffer zones on both sides of the sinking streams.
- c) The rest of the surface catchment areas of the sinking streams.

- d) Areas outside the catchment areas of sinking streams but inside the topographic catchment of the (karst) system under consideration. In that zone, surface and subsurface flow can not enter a swallow hole but can infiltrate somewhere else, e.g. at the base of a slope or in a closed depression.
- e) Areas that drain by surface or subsurface flow out of the (karst) system under consideration. In this zone, surface and subsurface flow can never reach the groundwater.

The I map is obtained by intersecting the I' map and the map of the surface catchment area according to the scheme presented in Fig. 9.5.

9.5 Construction of the Vulnerability Map

The vulnerability map shows the intrinsic vulnerability and, vice versa, the natural protection of the groundwater in the uppermost aquifer. The map shows the spatial distribution of the protection factor π , which is obtained by multiplying the P and I factors:

$$\pi = P \cdot I$$

The π factor ranges between 0.0 and 5.0, with high values representing a high degree of natural protection and low vulnerability. Small maps of the protective cover and the infiltration conditions are also printed as insets on the vulnerability map. The areas on each of the three maps are assigned to one of five classes, symbolised by five colours: from red for high risk to blue for low risk. One legend can thus be used for the three maps (Tab. 9.1).

Tab. 9.1: Legend for the vulnerability map, the P and the I map.

	vulnerability map		P-map		I-map	
	description	π -factor	description	P-factor	description	I-factor
red	extreme	0-1	very low	1	very high	0.0-0.2
orange	high	>1-2	low	2	high	0.4
yellow	moderate	>2-3	moderate	3	moderate	0.6
green	low	>3-4	high	4	low	0.8
blue	very low	>4-5	very high	5	very low	1.0

As the information on the vulnerability map is always for the uppermost groundwater, aquifers above the main groundwater body under consideration are indicated graphically by a thick line.

Dolines that are too small to be classified using the P and I factors are given special treatment: An extreme vulnerability is assigned both to active ponor dolines and to dry dolines that are not filled by sediments. A high vulnerability is assigned to partially filled dolines. In any case, the existence of dolines serves as an indicator for extensively developed epikarst and for a low degree of protection provided by the unsaturated karstic bedrock. Dolines should be shown on the vulnerability map with the customary symbols.

9.6 Modified assessment scheme for the P factor

9.6.1 Background

The PI method was presented to Working Group 1 of COST 620 on the 6th meeting in Cardiff in April 2000. The method was found to be consistent with the concepts that had been developed by task groups of COST 620 (e.g. DREW et al. 1999, 2000; DALY et al. 2000a). The method was considered to provide a basis for the development of a COST 620 approach („European Approach“) to vulnerability mapping.

A task group met in Karlsruhe in June 2000 in order to outline such an approach (DALY et al. 2000b). Based on the suggestions given by this task group, the PI method was modified, particularly the P factor. In order to test the preliminary COST 620 concept, the *modified* PI method was applied in the alpine test sites Hochifen-Gottesacker and Winterstaude (see chapter 11 and 12).

On the 9th meeting of COST 620 in Besançon in September 2001, it was decided to use the *original* PI method as one possibility for mapping and assessing intrinsic groundwater vulnerability within the framework of a rather general „European Approach“. Consequently, the *original* PI method was used for all further applications in different test sites (e.g. SCHMIDT 2001, COVIELLO 2001, BRECHENMACHER 2002).

9.6.2 Modified assessment scheme

DALY et al. 2000b suggest to assess the protective function [points] of the overlaying layers (topsoil, subsoil, non-karstic bedrock and unsaturated karstic bedrock) on the basis of the protective properties of the

respective substrate [points/m] multiplied by its thickness [m]. They suggest to use the permeability as a means to evaluate the protective properties. HÖLTING et al. (1995) established a qualitative relationship between the grain size distribution (GSD) and the protective properties of subsoil material (German/GLA method, see page 150). As there is also a close relationship between the GSD of subsoil material and the permeability, DALY et al. (2002) suggest to use the tables of HÖLTING et al. (1995) as a basis to establish a qualitative relationship between the permeability of any substrate and its protective properties. In the standard hydrogeological literature, there are extensive data on the permeability of different geological materials. These data were compiled by KUNOTH (2000) and used to establish a modified assessment scheme for the P factor (Fig. 9.8). As intergranular pores increase the protective function of fractured and karstified bedrock (e.g. SEILER et al. 1991, KOCH 1999), the presence or absence of such pores is used as a modifying factor for the non-karstic and karstic bedrock (layer 3 and 4).

As it is extremely time consuming to measure the permeability of each layer by field or laboratory experiments, it is often sufficient to assess the thickness and type of layers on the basis of geological maps, soil maps and field investigations, and then use the given tables in Fig. 9.8 to calculate the protective function of each layer. Of course, the tables can easily be extended using permeability data for different soil, subsoil and bedrock types from the standard literature.

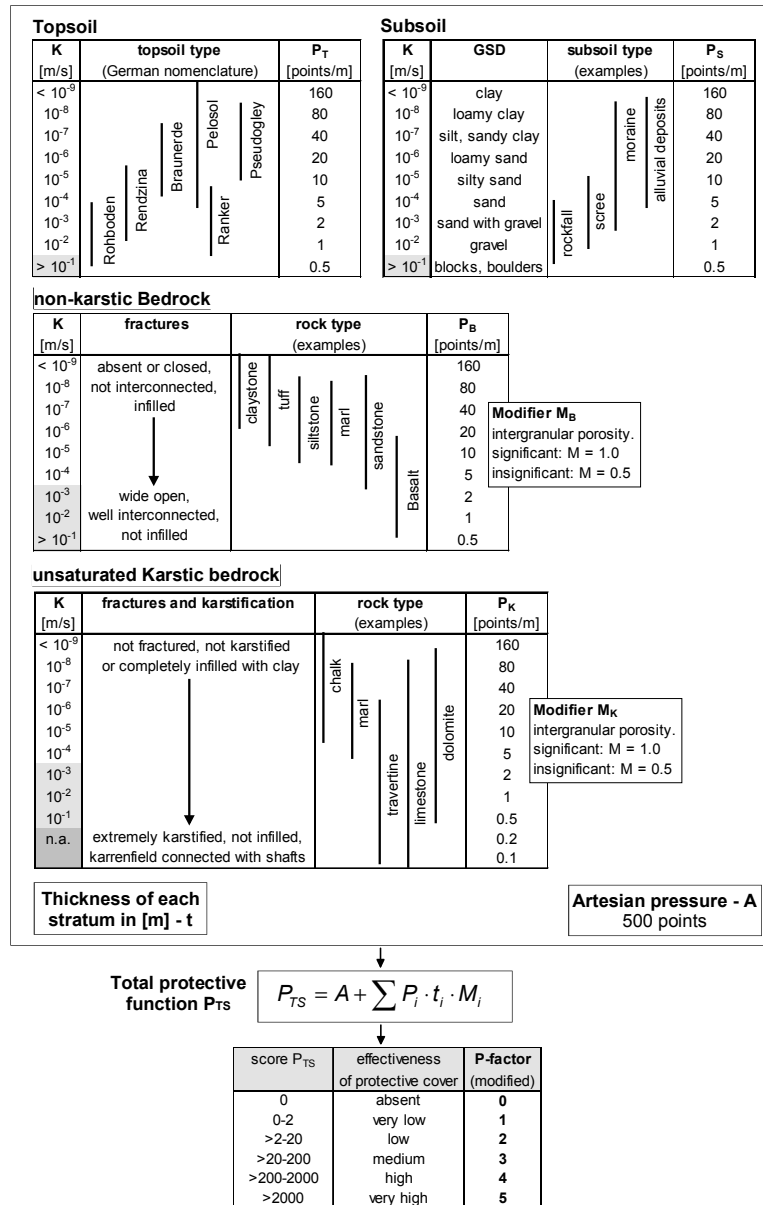


Fig. 9.8: Determination of the “modified” P factor (after DALY et al. 2000b). Grey colours symbolise the limitation of Darcy’s law and the K value.

10 COMPARATIVE APPLICATION OF THE PI METHOD IN THE TEST SITE ENGEN

10.1 The test site Engen

10.1.1 Location, Topography, Climate

The test site is a drinking water protection area of the city of Engen and neighbouring communities. It is located in the German state Baden-Württemberg and covers an area of 36 km². The area belongs to the *Hegau* landscape in the south-western Swabian Alb. The altitude ranges between 470 m in the southern lowlands and 690 m in the karstified plateau in the north. 50 % of the area is covered with forest, 44 % is used as field, meadow or pasture and 6 % are settlements (Fig. 10.1). The mean annual air temperature is 8,1°C (478 m), the precipitation is 740 to 895 mm per year (DICKEL 1993).

10.1.2 Geology

The geological description of the area is based on the work of SCHREINER (1976, 1992, 1993, 1997), SCHREINER & LUTERBACHER (1999), SCHWEIGERT (1995) and SZENKLER & BOCK (1999). The description of the stratigraphy follows the new nomenclature of the Geological Survey of Baden-Württemberg (GLA 1995).

The Hegau landscape is located within the transition zone of the Swabian Alb, which is formed by Upper Jurassic (Malm) carbonate rocks, and the Tertiary Molasse foreland basin of the Alps. The Engen area is formed by slightly SE-dipping Upper Jurassic formations that are partially overlain by Oligo- to Miocene Molasse sediments and, locally, volcanites. Glacial deposits of alpine origin and alluvial sediments cover large parts of the area (Fig. 10.2).

The carbonate rocks of the Upper Jurassic Malm reach a total thickness of 300 to 400 m. The Oxfordian (ox1–2), as well as most part of the Kimmeridgian (ki1–3) marl and limestone formations do not outcrop in the area. Beginning with the ki2, all formations are present both in bedded and massive facies. The latter consists sponge and stromatholitic reefs which may cross all stratigraphic units up to the uppermost Jurassic strata. The reefs often outcrop as up to 40 m high rock towers along the valleys. The bedded limestone of the ki4 is the oldest formation that outcrops. The bedded facies of the ki5 consists of a 70 m thick

interstratification of marl and limestone and can be subdivided in a lower, middle and upper member. The pure limestone of the Tithonian 1 (ti1) is the uppermost Jurassic formation in the Swabian Alb. About 50 m of the original thickness are still preserved. The bedded facies of the ti1 outcrops in the Engen area.

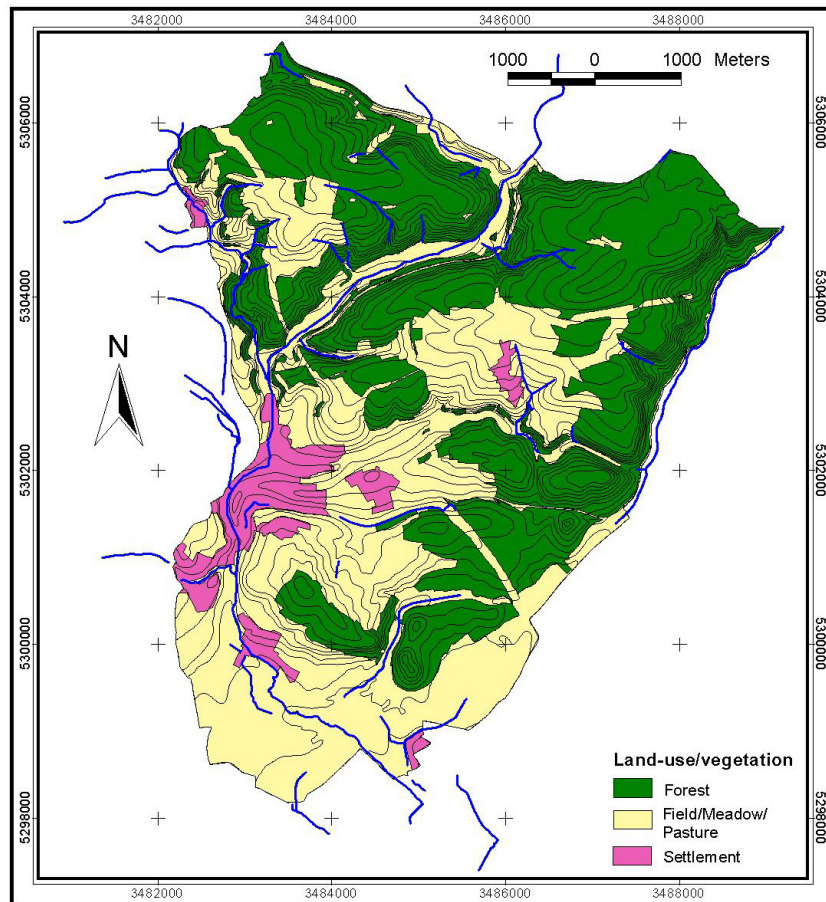


Fig. 10.1: Overview of the Engen area (data base: LGRB 1999).

In the Cretaceous and Tertiary, SW Germany emerged above the sea-level and suffered weathering, karstification and erosion. The only remain of this period is brown to red residual bean iron ore loam that is preserved in dolines and other karst features.

The northern foreland basin of the Alps formed in the Oligo- and Miocene and is filled with Molasse sediments mostly originating from the Alps. The sediments are coarse-grained near the Alps in the south of the basin and become finer toward the north. However, some sediments near the northern margin of the basin originate from the SW German cuesta landscape. They contain pebbles from Jurassic carbonate rocks and are called „Jura-Nagelfluh“. Several periods with marine, freshwater and brackish conditions can be distinguished: the Lower Marine Molasse (UMM), the Lower Freshwater Molasse (USM), the Upper Marine Molasse (OMM), the Brackish Water Molasse (BM) and the Upper Freshwater Molasse (OSM).

In the Engen area, the Lower Jura-Nagelfluh (J1) replaces the UMM. This formation was deposited in channels and consists of fluvial sandy marl with pebbles of Jurassic rocks. Large parts of the OMM have been eroded but some deposits remain: the Randengrobkalk (MR), a 10 m thick sandy limestone rich of fossil detritus; the fine-grained Deck-schichten sandstone (MD) and the Krusten- und Knollenkalk (KK), a calcrete which formed in a subtropic climate. The Kirchberger formation (Ki) belongs to the BM and consist of silty, sandy or clayey sediments. The Upper Jura-Nagelfluh (J2) replaces the OSM in the Engen area. Analogous to the J1 formation, it can often be found in channels, but in contrast to the older deposits, the J2 sediments contain material both from Triassic and Jurassic rocks.

Glacial and fluvio-glacial deposits of the Riss Ice Age (R) cover large parts of the elevated areas in the north, while sediments of the Würm Ice Age (W) predominate in the south. Four types of deposits can be mapped: alluvial gravel terraces (Rgt/Wgt), glacial gravel (Rg/Wg), ground moraine (Rm/Gm) and end moraine (Re/We). In the Holocene, detritus (qu) formed on slopes while alluvial sediments (hl) were deposited in the valleys. Large areas in the south of Engen have been modified by gravel mining and other human activities (y).

The Jurassic strata dip gently towards the S to SE (towards the foreland basin of the Alps) at about 2–3° and are cut by faults with a displacement of tens of meters. There are three predominant fault directions: N-S, WNW-ESE and W-E. The faults are important for the drainage pattern of the karst aquifer (BATSCHKE et al. 1970) and control the direction of several dry valleys (VOGELSSANG & VILLINGER 1987).

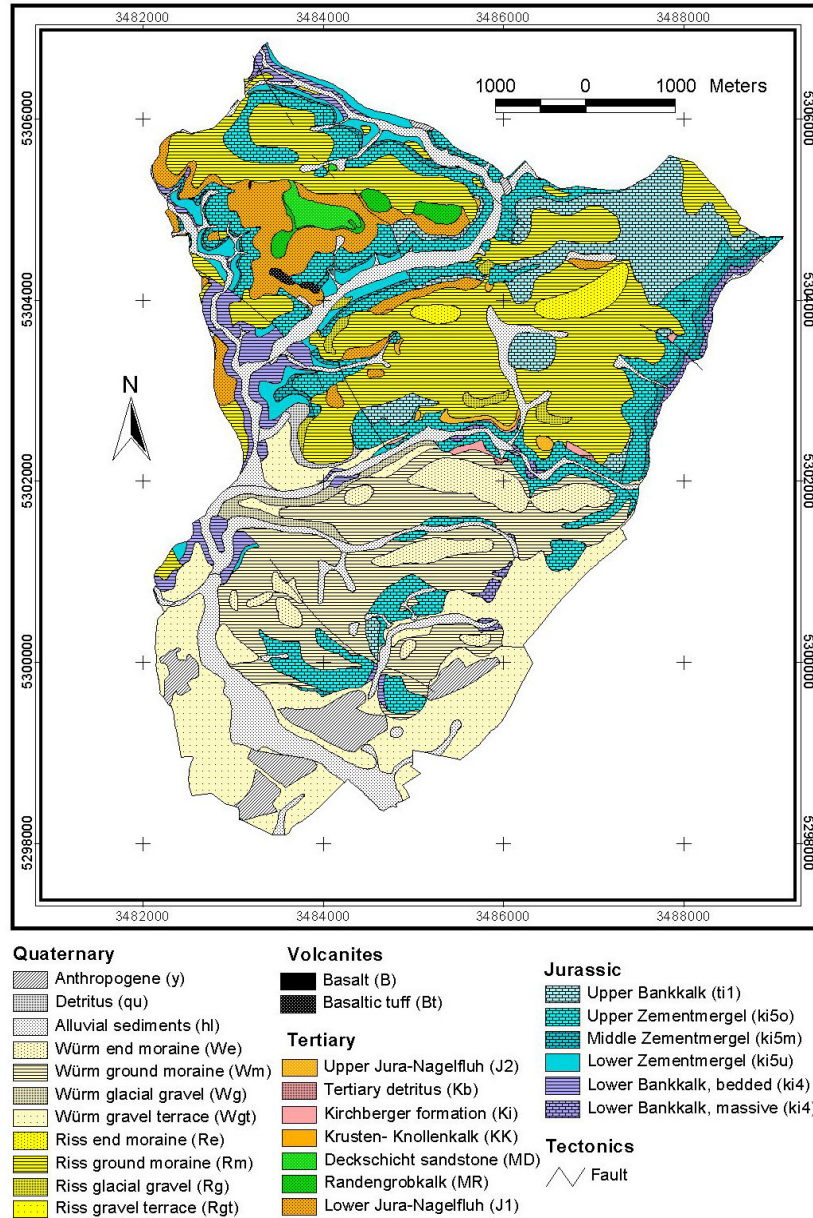


Fig. 10.2: Geology of the Engen area (data: LGRB 1999, nomenclature GLA 1995).

10.1.3 Karstification and hydrogeology

In large parts of the area, the karstified rocks are covered with sediments and soils. Exokarst features like dolines and karren are rare and often not noticeable. The only relevant geomorphologic karst landforms are dry valleys. However, due to the widespread low permeability sediments, there are many surface waters. Consequently, most of the valleys are not permanently dry but the water courses sink or seep underground in different places, dependent on the hydrologic conditions.

In quarries, a large variety of cavities is visible: corrosional enlarged bedding planes, joints and cracks, shafts, conduits and caves. Most of the cavities are filled with bean iron ore loam, indicating that they formed during the Cretaceous and Tertiary. In the Pliocene and Quaternary, some of the old karst conduits were reactivated and a younger, active karst generation was formed – the Danube-Aach-System.

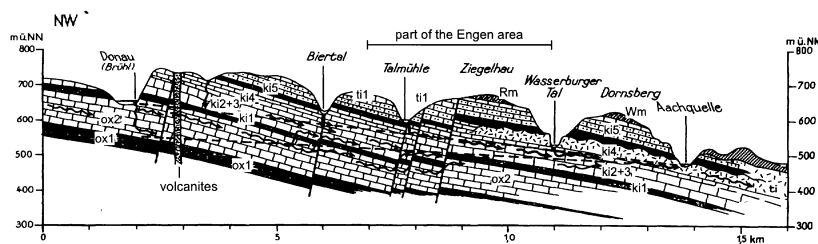


Fig. 10.3: Hydrogeological profile of the Danube-Aach system (SCHREINER 1992, new stratigraphic nomenclature GLA 1995).

The Oxfordian and Kimmeridgian carbonate rocks form the main aquifer system which has been studied in great detail within the framework of the investigation of the famous Danube-Aach-System (KÄSS 1969, BATSCHKE et al. 1970, HÖTZL 1971, HÖTZL 1973, KÄSS & HÖTZL 1973, VILLINGER 1977, VOGELSANG & VILLINGER 1987). Water from the Danube river sinks in several swallow holes into Oxfordian limestone (ox2) and flows 10 to 20 km southward to several springs that are tributary to the Rhine river. The main outlet of the system is the Aach spring with an average discharge of 8.5 m³/s. As the dip of the strata is steeper than the dip of the land surface, the karst water rises up across the stratification on its way to the Aach spring which discharges from Kimmeridgian limestone (ki4) (Fig. 10.3). Tracer tests proved flow velocities of up to 250 m/h, indicating the presence of a well developed and

connected system of wide and open conduits. Some of the dyes reached the wells and springs of the Engen area.

Locally, there are higher groundwater bodies above the main karst aquifer. The Tithonian limestone (ti1) often forms a perched aquifer while the underlying marl (ki5) acts as an aquiclude. Small springs are frequent at the boundary between the two formations. Furthermore, there are fractured aquifers in Tertiary rocks (SCHREINER 1997).

In the south of the Engen area, the karst aquifer is covered by 30–50 m thick glacial sand and gravel deposits with an interstratified layer of clayey sediments. Tracer tests proved that the karst water is rising up into the granular aquifers. Consequently, the springs in the south of the area discharge a mixture between karst water and groundwater from the granular aquifer (HÖTZL in BATSCHKE et al. 1970, SCHREINER 1997).

10.1.4 Soils

GIS-data on the soils were provided by the Geological Survey of Baden-Württemberg on a CD-ROM (LGRB 1999). Additional information were taken from the explanations to the soil map (KÖSEL & WEINZIERL 1993). The soil map (Fig. 10.4) is based on the German mapping instructions (AG Boden 1996) and a legend suggested by the Geological Survey of Baden-Württemberg (GLA 1995). For a better understanding, the approximate FAO equivalents to the German soil names are given in brackets (FAO-UNESCO 1974). A detailed description of the soils is presented by STURM (1999) and GOLDSCHIEDER et al. (2000a).

Four main landscape units can be distinguished: Upper Jurassic carbonate rocks, old glacial deposits (Riss), young glacial deposits (Würm) and alluvial sediments.

The typical soils on Jurassic carbonate rocks are *Braunerde-Terra fusca* (Chromic-Cambisol) and *Rendzina*. Both types are characterised by a low to medium effective field capacity (eFC) (50–140 mm) and a high saturated hydraulic conductivity (40–300 cm/d).

On the old glacial deposits (Riss) there are a large variety of deep, loamy soils, such as *Pararendzina* (Calcaric Regosol, Calcaric Ranker, Phaeozem), *Parabraunerde* (Luvisol, Acrisol) and *Pseudogley* (Stagnic Gleyosols). The eFC of these soils is medium to high (90–200 mm) and the conductivity of the subsoil is often very low (< 1 cm/d).

The soils on the young glacial deposits (Würm) in the south of the area had less time to develop and are consequently less deep than the soils

10.1 The test site Engen

on the older deposits. However, there are similar soil types – *Parabraunerde* and *Pararendzina*. The hydraulic properties of the soils are favourable: medium to high eFC (90–200 mm) and moderate conductivity (10–40 cm/d).

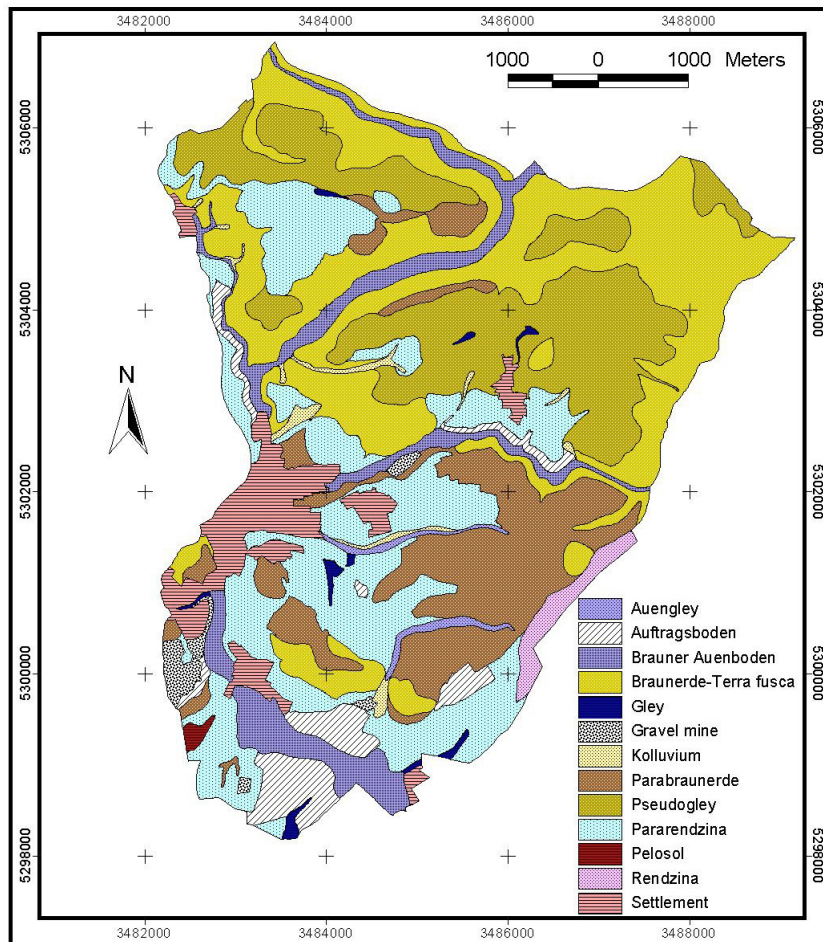


Fig. 10.4: Soil map of the Engen area (data: LGRB 1999, German nomenclature).

In areas with shallow depth to groundwater table, there are hydromorphic soils, such as *Gley* (Gleysol). *Pelosol* soils (Vertisol or Regosol) developed locally on clayey sediments. In the areas which were influenced by gravel mining, the soil type *Auftragsboden* (Anthrosol) was

mapped. All soils on sand and gravel are characterised by a low to medium eFC (50–140 mm) and a very high saturated hydraulic conductivity (> 300 cm/d).

At the base of slopes, there are often deep and carbonate rich colluvial deposits. On the alluvial sediments in the valleys, the characteristic soil types are *Auengley* and *Brauner Auenboden* which both belong to the Fluvisols according to the FAO nomenclature.

10.2 Application of the EPIK method

10.2.1 Introductory remark

The EPIK method (DOERFLIGER 1996, DOERFLIGER & ZWAHLEN 1998, see p. 145) was applied in the Engen area by GOLDSCHIEDER et al. (2000a). STURM (1999) contributed to the evaluation of the protective cover (P) and karst network development (K), KLUTE (2000) mapped the epikarst (E) and the infiltration conditions (I).

10.2.2 Epikarst (E factor)

The epikarst was assessed on the basis of topographic maps (1:25.000; sheet 8118/19) and mapping in the field. Aerial photographs (1:10.000) were used as well but were found to be not useful because 50 % of the area is covered with forest (KLUTE 2000).

Due to widespread soils and sediments, there are few karst features visible. Thus, the class E_1 is present on very small areas: two single dolines, one group of dolines and one outcrop of highly fractured limestone. The class E_2 was assigned for the dry valleys. However, the delineation of the dry valleys is ambiguous, as there is often no clear topographic boundary between the valleys and the bordering elevated areas. The rest of the area was classified as E_3 .

10.2.3 Protective cover (P factor)

As the GLA method (HÖLTING et al. 1995) had already been applied in the Engen area by DICKEL et al. (1993a, b), detailed data on the overlying layers were available on a CD-ROM (LGRB 1999) and in the explanations to the soil map (KÖSEL & WEINZIERL 1993). However, EPIK demands relatively simple information on the protective cover, so that the detailed database had to be generalised in order to determine the P factor. EPIK takes into account the layers *above* the top of the carbon-

ate rock, and so the marl formations within the Upper Jurassic stratigraphy were not considered to be a part of the protective cover.

As a first step, the test site was subdivided into areas with or without low permeability formations. The Riss ground moraines, the Würm end and ground moraines, alluvial loam, the Jura-Nagelfluh, the Kirchberger formation and marly scree slopes are of low permeability (STURM 1999). As a second step, the thickness of these formations was determined using GIS operations on the basis of GRID data, while the soil thickness was taken from the soil map. As a last step, the information on the soil and the low permeability formations were re-classed on the basis of the EPIK classification.

As large parts of the area are covered with Tertiary sedimentary rocks, Quaternary deposits and soils, the class P_4 predominates by far, above all in the elevated areas and in the lowlands in the south of the test site. The classes P_{2-3} are present in the valleys and on the bordering slopes. Areas with settlements (cities, towns, villages) are not considered in the EPIK method. However, for the Engen test site, it was decided to classify settlements on areas without low permeability layers as P_1 , because the soils are assumed to be highly disturbed and not protective there (GOLDSCHIEDER et al. 2000a).

10.2.4 Infiltration conditions (I factor)

The I factor takes into consideration the presence of swallow holes, sinking streams and their catchments, as well as the slope gradient and the land-use (DOERFLIGER & ZWAHLEN 1998). The required information were determined on the basis of topographic maps, digital elevation models, digital data on land-use and vegetation (LGRB 1999) and field observations. DICKEL (1993) proved that all the streams in the northern and central part of the area infiltrate into the karstified underground. KLUTE (2000) distinguished three types: permanent total sink, temporary total sink and permanent partial sink. Consequently, the river network in the entire area except from the southern lowland was classified as sinking streams (I_1). Swallow holes in quarries and ponds without surface outflow were put in the same class.

The delineation of the catchments of the sinking streams is problematic: Formally, almost the entire area is inside the topographic catchment of a sinking stream. However, large areas never produce any runoff and are consequently not part of the hydrologic catchment, e.g. areas with plateau-like topography and high permeability soils. Thus,

KLUTE (2000) created a polygon coverage showing the effective catchments of the sinking streams.

A coverage showing the slope angle (<10 %, 10–25 %, >25 %) was created using the digital elevation model which had to be transformed from a GRID into the TIN format in order to obtain more precision (KLUTE 2000). Another coverage shows the type of land-use. EPIK distinguishes between arable areas on the one hand and meadows/pastures on the other hand, but does not take into account forests and settlements. However, 56 % of the Engen area are forest or settlement and some areas are used as meadow/pasture in one year but used as arable land in the following year. Thus, the method was slightly modified and the area was classified into forest and non-forest areas (meadow, pasture, arable land, settlements). The critical slope angle is 25 % for forest areas and 10 % for the rest of the area.

The classification into I_{2-4} was done by intersecting the coverages showing the catchments, the slopes and the land-use. The map showing the distribution of the I factor consists of numerous very small areas and had to be generalised.

10.2.5 Karst network development (K factor)

As the Engen area is a (subsidiary) part of the Danube-Aach-System, there is clear evidence for the existence of a well developed and connected karst network: visible open conduits and shafts in quarries (SCHREINER 1993); flow velocities of up to 250 m/h proved by tracer tests (KÄSS 1969, BATSCHKE et al. 1970, KÄSS & HÖTZL 1973); electromagnetic investigations of hydraulically active faults (VOGELSANG & VILLINGER 1987); speleological observations (HASENMEYER 1972). Consequently, the entire area was classified as K_1 (STURM 1999).

10.2.6 The EPIK vulnerability map

The EPIK vulnerability map (Fig. 10.5) was created by intersecting the four coverages and calculating the protection index F on the basis of the given formula. Large areas are classified as moderately vulnerable; the dry valleys and the bordering slopes are zones of high to very high vulnerability (dependent on the gradient and land-use); the sinking streams are very highly vulnerable. Altogether, this is a sensible and plausible distribution of vulnerability zones.

However, all areas without visible epikarst features and without concentrated infiltration are classified as moderately vulnerable. Consequently, the EPIK map shows no difference between areas that

10.2 Application of the EPIK method

quently, the EPIK map shows no difference between areas that are characterised by a high depth to groundwater table and by the presence of low permeability layers on the one hand, and areas with a shallow depth to groundwater table and without any low permeability layers on the other hand.

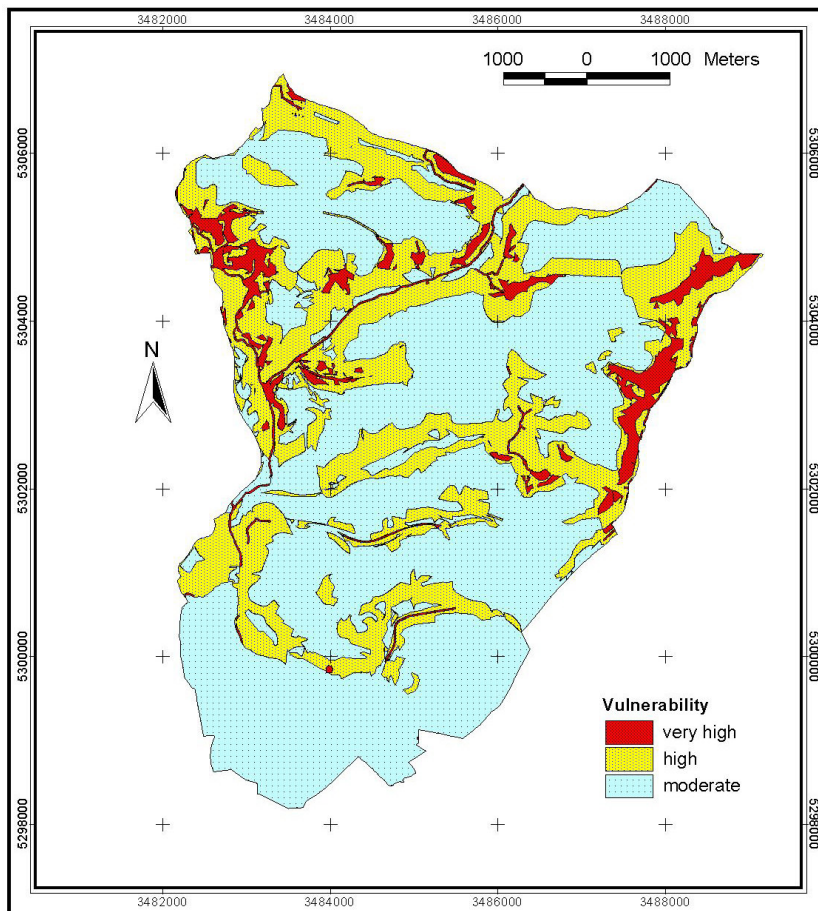


Fig. 10.5: EPIK vulnerability map of the Engen area.

10.3 Application of the GLA method

The GLA method (HÖLTING et al. 1995) had already been applied in the test site manually and using a GIS (DICKEL et al. 1993a, b) (Fig. 10.6).

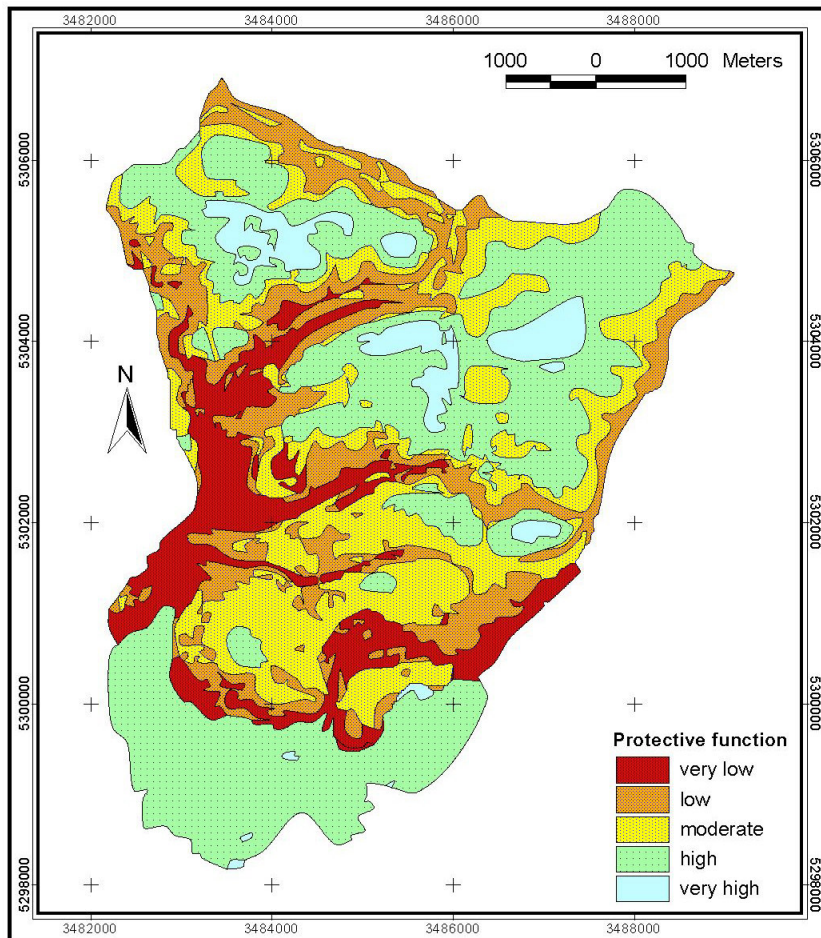


Fig. 10.6: Map of the protective function of the layers above the groundwater surface ("vulnerability map") after the GLA method (Dickel et al. 1993a, b; LGRB 1999).

The GLA method is a starting point for the PI method and the data base that was created for the application of the GLA method was later

used, modified and supplemented, for the PI method (STURM 1999, KLUTE 2000, GOLDSCHIEDER et al. 2000a). Thus, the application of the GLA method will be briefly described in this section.

The GLA map for the Engen area shows the natural protection (and vice versa the vulnerability) of the groundwater in the Upper Jurassic karst aquifer. Thus, perched aquifers are considered to protect the underlying karst aquifer. In the southern lowlands, artesian pressure was proved in the karst aquifer which is overlain by a sand and gravel aquifer system. Thus, these lowlands are considered to be an area of high protective function (low vulnerability), though the groundwater in the granular aquifer is slightly protected.

Information on the effective field capacity of the soils were taken from the soil map (KÖSEL & WEINZIERL 1993). The grain size distribution of the subsoils and the fracturing of the bedrocks was assessed on the basis of the geological map, field observations and lab-analyses. The thickness and distribution of the layers was determined by intersecting the geological map, the digital elevation model and the groundwater contour lines.

On the final map, the zone of artesian pressure in the karst aquifer in the southern lowlands, the areas with perched aquifers and the elevated areas in the north are characterised by a high to very high protective function (low to very low vulnerability). A very low to moderate protective function (very high to moderate vulnerability) was calculated for most of the valleys.

Altogether, the GLA map is consistent. However, swallow holes, sinking streams and their catchments are not taken into account, and so some areas with thick low permeability layers are considered to provide a very high protection, even though they frequently produce surface runoff towards a near swallow hole.

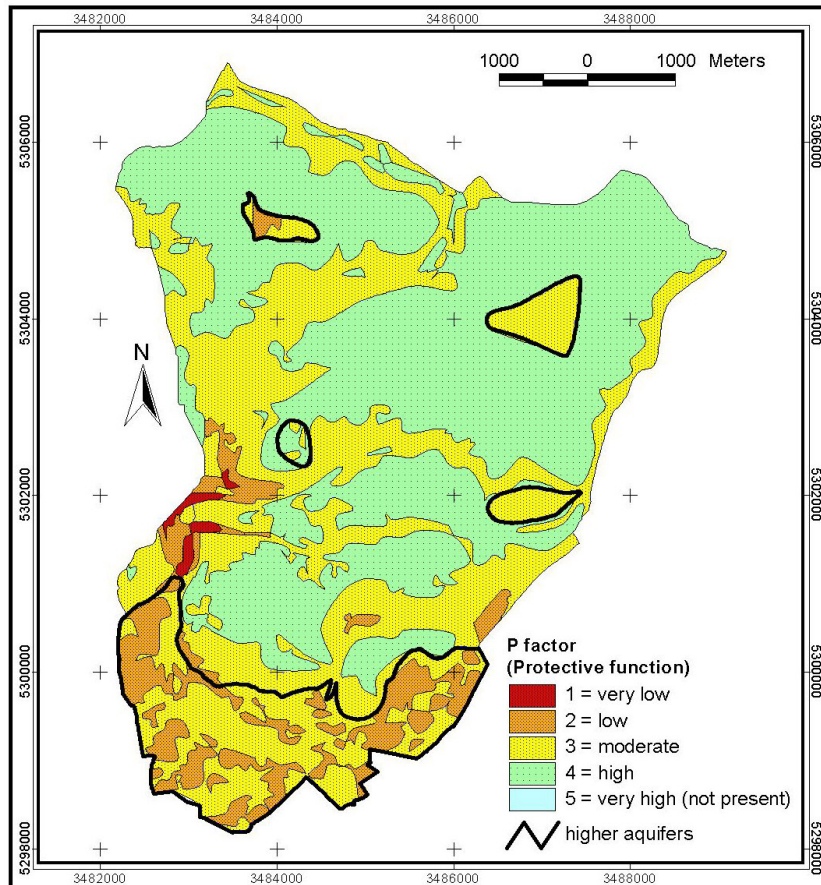


Fig. 10.7: Map of the protective cover (P map) after the PI method.

10.4 Application of the PI method

10.4.1 Determination of the P factor

As the P factor of the (original) PI method is calculated using a slightly modified version of the GLA method (HÖLTING et al. 1995), it was possible to use the detailed digital database of the LGRB (1999) that was available for the test site Engen. Two significant changes were made:

- The score ranges of the total protective function are much wider in the PI than in the GLA method. As a consequence, the areas of very high natural protection disappear completely on the P map and the areas with very low protection become smaller (Fig. 10.7).
- In contrast to the GLA method, the PI approach always takes the groundwater surface of the uppermost aquifer as the target. Therefore, all areas with higher groundwater bodies above the karst aquifer had to be re-evaluated – the four perched aquifers in the central and northern part of the area and the granular aquifer in the southern lowlands. According to the GLA method, this lowland is characterised by a high natural protection, because of the artesian pressure in the karst aquifer. According to the PI method, it is considered to be low to moderately protected because the groundwater in the sand and gravel is taken as the target (STRUM 1999, using data by WEINZIERL 1993 and SCHREINER 1997).

10.4.2 Determination of the I factor

The following steps were carried out in order to determine the I factor:

- 1st step: determination of the dominant flow process

The dominant flow process is assessed on the basis of topsoil permeability and the presence or absence of low permeability layers ($k < 10^{-6}$ m/s). Surface flow predominates on low permeability soils; subsurface flow takes place in highly permeable soils with low permeability layers; infiltration predominates if low permeability layers are absent.

The tabular explanations to the soil map (KÖSEL & WEINZIERL 1993) and the digital soil map (LGRB 1999) contain data on the permeability (saturated hydraulic conductivity) of the soils in different depths (0–30, 30–60, 60–100 cm) and the underlying bedrock.

One coverage was created showing the permeability of the topsoil, another coverage shows the depth to low permeability layers inside or below the soil. The dominant flow process (Fig. 10.8) was determined by intersecting the two coverages.

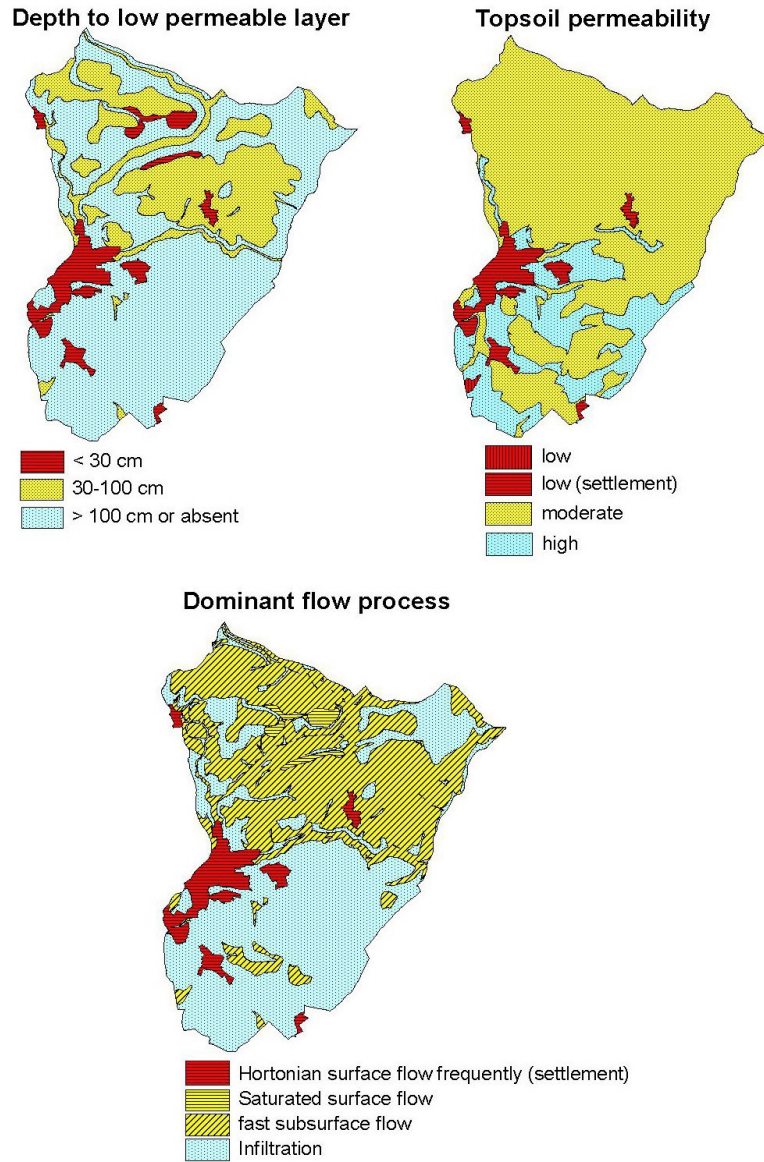


Fig. 10.8: Determination of the dominant flow process by intersecting the coverage *depth to low permeability layers* with the coverage *topsoil permeability*.

- 2nd step: determination of the I' factor

The intensity of lateral surface and subsurface flow depends on the slope gradient and the land-use/vegetation (Fig. 10.1). Gentle slopes and forests favour infiltration, steep slopes and agricultural land-use favour lateral flow. The I' factor is determined by intersecting the coverages on the dominant flow process, the vegetation and the slope gradient. In the Engen area, significant surface or subsurface flow has to be expected in villages and in the northern part of the area, above all on steep slopes bordering the valleys and on areas made of ground moraine and Jura-Nagelfluh.

- 3rd step: determination of the I factor

Lateral surface and subsurface flow is relevant for groundwater vulnerability only if the water and possible contaminants enter the underground at another place, e.g. via a swallow hole. Consequently, the I map (showing the degree to which the protective cover is bypassed) is obtained by intersecting the I' map (showing the intensity of lateral flow) with the surface catchment map (showing the sinking streams and their catchments) (Fig. 10.9).

The surface catchment map was created on the basis of a digital map with all the swallow holes and sinking streams. The 10 m and the 100 m zone was created with the ArcInfo command „buffer“ and the catchments of the sinking streams and swallow holes were delineated automatically from the digital elevation model (KLUTE 2000).

The I map of the Engen area shows that lateral flow components which bypass the protective cover have to be expected along the valleys in the northern part of the area, while the protective cover is not likely to be bypassed in the southern part of the area.

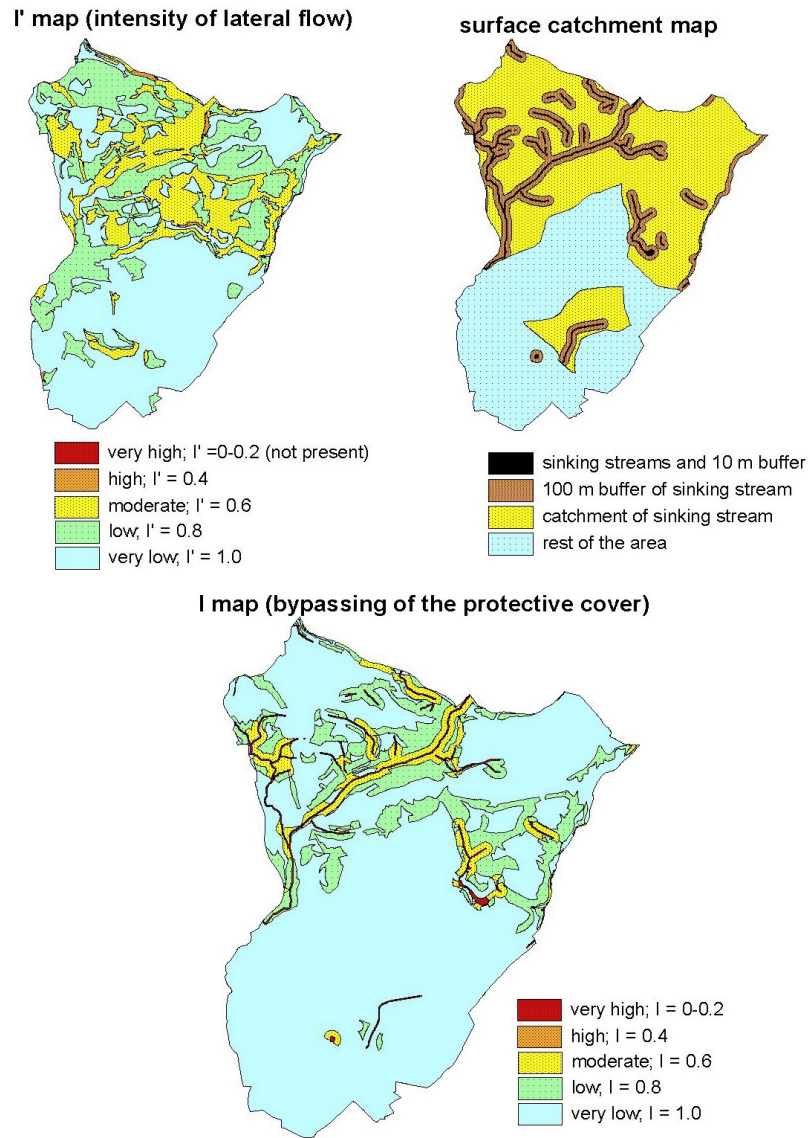


Fig. 10.9: Determination of the I map (showing the degree to which the protective cover is bypassed) by intersecting the I' map (intensity of lateral flow) and the surface catchment map (sinking streams and their catchments).

10.4.3 The PI vulnerability map

The final PI vulnerability map (Fig. 10.10) is obtained by intersecting the P and the I map; the protection factor π is calculated by multiplying the P and the I factor. The range of possible values for π is subdivided in five classes of natural protection and vulnerability respectively.

Insets of the P and the I map were printed on the 1:10.000 vulnerability map (GOLDSCHIEDER et al. 2000a), so that the end-user can easily see, if the vulnerability of a particular area is controlled rather by the protective cover or by the infiltration conditions.

On the PI vulnerability map for the Engen area, most areas range between high and low vulnerability. Only the swallow holes, sinking streams and some small areas turn out to be extremely vulnerable. A high to moderate vulnerability was assigned to large parts of the valleys, the perched aquifers and the granular aquifer in the southern lowlands. The elevated areas which are covered by glacial deposits and Tertiary sediments are characterised by low vulnerability. The class „very low vulnerability“ is not present in the area.

10.5 Comparison and discussion of the maps

Comparing the vulnerability maps that were created using the GLA (DICKEL et al. 1993a, b) the EPIK, and the PI method (STURM 1999, KLUTE 2000, GOLDSCHIEDER et al. 2000a), it is noticeable that the valleys are always assessed to be more vulnerable than the bordering elevated areas. However, there are different reasons for that common result: On the EPIK map, the valleys are vulnerable because they are epikarst features (E factor) and form the catchments of sinking streams (I factor). On the GLA map, the valleys are vulnerable because the thickness of the layers above the groundwater surface is significantly reduced there. On the PI map, both the reduced thickness (P factor) and the concentrated infiltration (I factor) are taken into account.

In detail, there are significant differences between the three maps. On the EPIK map, flat areas outside the catchments of sinking streams (high I factor) and without epikarst features (high E factor) are evaluated to be moderately vulnerable, even if the layers above the groundwater surface are thin and highly permeable. On the GLA map, the vulnerability of the same areas appears to be very high (very low protective function), and on the PI map, they are classified as highly vulnerable (low P, high I factor). The catchments of sinking streams are highly to extremely vulnerable according to the EPIK and PI method,

which is consistent. However, parts of the catchments are formed by thick layers of low permeability and are classified as areas of moderate to low vulnerability according to the GLA method, which is inconsistent.

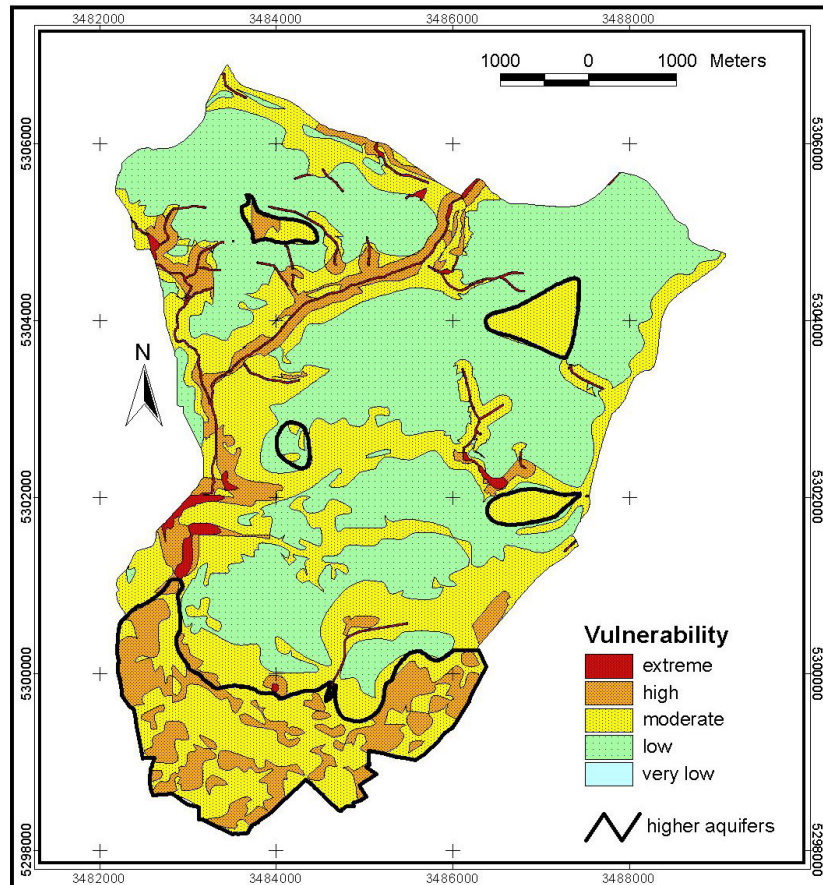


Fig. 10.10: PI vulnerability map of the Engen area.

Comparing the GLA and the PI map, it is noticeable that on the one hand, the GLA map shows much more extremely vulnerable areas than the PI map, and on the other hand, there are zones of very low vulnerability on the GLA map but not on the PI map. This is mainly due to the different classification schemes (examples see Tab. 10.1).

10.5 Comparison and discussion of the maps

Tab. 10.1: Comparison of the different classification schemes for the protective cover after the PI and the GLA method.

PI method		evaluation of the protective function	GLA method	
score	example		example	score
< 10	0-2 m gravel	very low	0-100 m gravel	< 500
10-100	1-10 m sand + gravel	low	50-100 m sand + gravel	500-1000
100-1000	2-20 m silty sand	moderate	20-40 m silty sand	1000-2000
1000-10000	2-20 m clay	high	4-8 m clay	2000-4000
>10000	> 20 m clay	very high	> 8 m clay	> 4000

A further difference between the PI and the GLA map is that the PI map shows the vulnerability of the highest groundwater body, while the GLA map always shows the vulnerability of the main karst aquifer. As a consequence, the southern lowlands are a zone of high to moderate groundwater vulnerability according to the PI method, because the sand and gravel aquifer in that area is very slightly protected. Unlike that, the GLA method shows the vulnerability of the karst aquifer which is highly protected by the artesian pressure and the overlying sand and gravel aquifer. The EPIK method can only be applied for karst aquifers and so it is impossible to assess the vulnerability of the granular aquifer, even though it is interacting with the underlying karst aquifer.

11 APPLICATION OF THE PI METHOD IN THE HOCHIFEN-GOTTESACKER AREA

11.1 Overview

The hydrogeology of the alpine karst system Hochifen-Gottesacker was described in great detail in chapter 3. The area is an interesting test site for the application of the modified PI method. The geology, hydrogeology and topography of the area is relatively complicated and the data base is not extensive. There are no boreholes and no precise data on permeability, field capacity and grain size distribution. However, the hydrogeology of the area is well understood, there are detailed recent large-scale geological and topographic maps and at least some information on the soils (34 profiles). The modified PI method is mostly based on topographic, geological and hydrogeological information. It should consequently be applicable in such a test site.

There is a great variety of different rock types and Quaternary deposits in the area and there is intensive interaction between the surface drainage network and the karst groundwater flow. Thus, the area is characterised by large variations of both the P and the I factor.

11.2 Definition of the target

The karstified Schratenkalk limestone forms the most important aquifer in the area, and so the groundwater surface in this karst aquifer was taken as the target for vulnerability mapping. However, there are three areas where a significant granular aquifer is present (Fig. 11.1). There, the groundwater table in the granular aquifer was taken as the target:

1. the rockfall mass in the upper section of the Schwarzwasser valley;
2. the alluvial plain 'Iferwies' in the Subersach valley;
3. the 'Ifenmulde' cirque NE of Mt. Hochifen.

A special situation is present in the upper section of the Subersach valley. In this area, the limestone is completely eroded and there are no other significant groundwater bodies present. The area is drained by the Subersach river which flows out of the karst system. However, flow measurements proved that water from the river infiltrates into the Iferwies granular aquifer and hydrochemical data indicate that the Goldbach karst spring (Gb3) gets inflow from this granular aquifer (Fig.

11.2 Definition of the target

11.1). The upper Subersach valley is consequently not a part of the karst system but belongs to the catchment of one significant karst spring. Thus, the area was not considered for resource vulnerability mapping. However, if the spring was used for drinking water supply, it was essential to delineate this area as a protection zone.

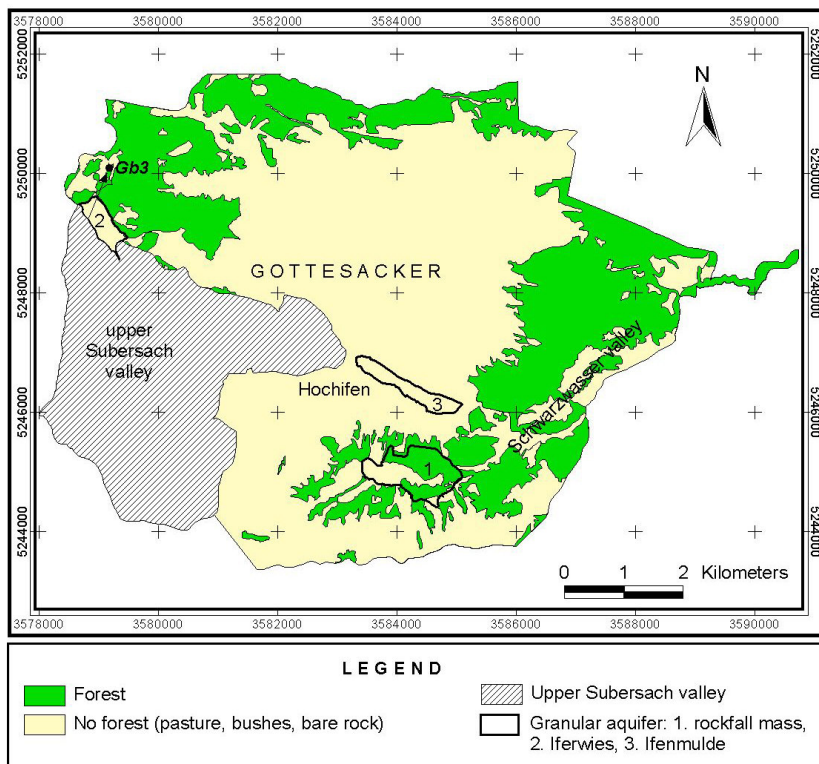


Fig. 11.1: Overview of the Hochfien-Gottesacker area. The groundwater in the karst aquifer was taken as the target for vulnerability mapping. In three areas, the groundwater in a local granular aquifer was taken as the target. The upper Subersach valley is not part of the karst system. However, river water infiltrates into the aquifer 2 and reaches the karst spring Gb3.

11.3 Protective cover (modified P factor)

11.3.1 The topsoil (layer 1)

The topsoil map was compiled by KUNOTH (2000) using the descriptions of 34 soil profiles (unpublished field data by GOLDSCHIEDER 1996) together with geological (GOLDSCHIEDER 1997, TOMSU 1998, SINREICH 1998, HUTH 1998) and topographic maps. The ArcInfo attribute table consists of four columns: the topsoil type, the protective properties [points/m], the thickness [m] and the protective function [points]. In large parts of the area, the topsoil is absent or patchy and does not contribute to the natural protection of the system (Fig. 11.2).

11.3.2 The subsoil (layer 2)

The type and the spatial distribution of the subsoils (Quaternary deposits) can be derived directly from the geological maps. As there are no drillings, the thickness must be estimated on the basis of geomorphological, geological and topographic information. The permeability was estimated on the basis of field observations (drainage density) and grain size analyses (unpublished field data by GOLDSCHIEDER 1996). Similar to the topsoil, the attribute table consists of four columns: the subsoil type, the protective properties, the thickness and the protective function. In large parts of the area, the subsoil layer is absent. In other parts of the area, above all in the valley, the subsoil contributes 150 points to the total protective function (Fig. 11.2).

11.3.3 The non-karstic bedrock (layer 3)

The distribution of the non-karstic bedrock can not be derived directly from a geological map as Quaternary deposits often hide the boundaries between different bedrock units. Thus, a bedrock map was created (KUNOTH 2000). Four situations can be distinguished on the basis of this map and additional hydrogeological information:

1. if there is a significant granular aquifer above the bedrock, the presence of layer 3 is not relevant for vulnerability mapping as the target is always the uppermost groundwater;
2. if the karst aquifer has been eroded so that the underlying marl formation outcrops, the target (groundwater surface in karst aquifer) is absent and the thickness of layer 3 can not be defined;

3. if the bedrock map shows Schratenkalk limestone (which may be covered by Quaternary deposits), layer 3 is absent;
4. if the limestone is covered by younger bedrock formations, there is a layer 3 above the karst aquifer, and so the next step is to assess the protective function of this layer.

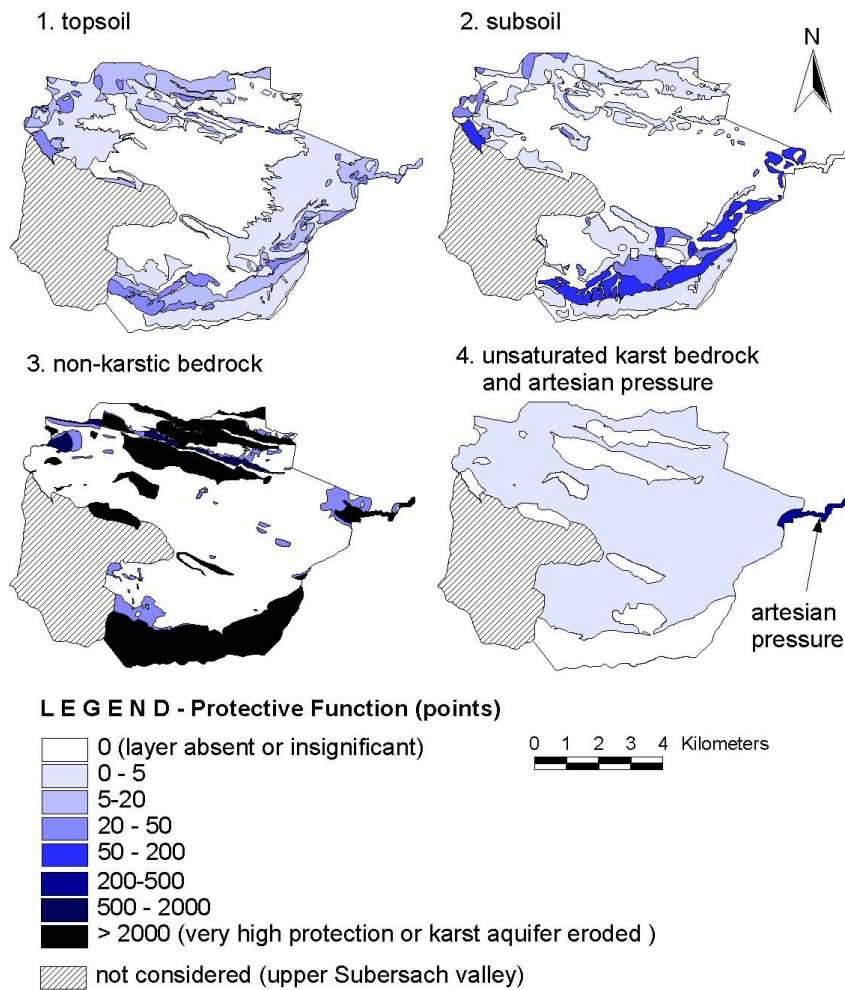


Fig. 11.2: Protective function of the topsoil, subsoil, non-karstic bedrock and unsaturated karst bedrock; artesian pressure in the aquifer.

The permeability of the bedrock formations was estimated on the basis of the lithology, the fracturing and data from the literature (compiled by KUNOTH 2000). The thickness was determined on the basis of geological information, mainly geological cross sections.

11.3.4 The unsaturated karstic bedrock (layer 4)

The bedrock map and hydrogeological information were used to create a map of the unsaturated karstic bedrock. Three situations were distinguished:

1. if a granular aquifer is present, the groundwater surface in this aquifer was taken as the target and layer 4 is consequently not relevant;
2. if the Schratenkalk limestone was eroded, layer 4 is absent;
3. if the bedrock map shows Schratenkalk limestone, an unsaturated karstic bedrock layer is present, unless the aquifer is confined.

There is clear evidence for the extreme karstification of the Schratenkalk limestone in the entire area: there are many caves both in the valleys and in the elevated areas, epikarst features are widely distributed (karrenfields, dolines, shafts) and outcrops of Schratenkalk always drain underground. The intergranular porosity is negligible. Thus, the lowest possible value for the protective properties (0.05 points/m) was assigned to the unsaturated karstic bedrock.

In the zone of shallow karst, the underground flow takes place near the base of the karstified limestone which is 75–125 m thick. This is consequently the maximum possible thickness of the unsaturated zone. However, the upper part of the formation was eroded in large parts of the area. In the valleys, the groundwater table may be tens of metres above the basis of the aquifer. As there are no observation wells in the area, the depth to groundwater table can only be estimated on the basis of geological and hydrogeological information (sections, maps, topographic position and characteristics of springs and swallow holes) and observations in caves. An average thickness of the unsaturated zone of 30 m was estimated, which is a conservative assumption (KUNOTH 2000). As the layer 4 is not a sensitive parameter for the determination of the total protective function – it contributes only 1.5 points –, a rough estimation of the thickness is sufficient. In the lowest section of the Schwarzwasser valley and below the Flysch zone, there is no unsaturated zone, as the top of the aquifer is below the water course level (confined conditions).

11.3.5 Artesian pressure

In the lowest section of the Schwarzwasser valley, there is a local artesian system (GOLDSCHIEDER 1997). The artesian pressure protects the groundwater very well from contamination, and so an additional score of 500 points was assigned to that zone (Fig. 11.2).

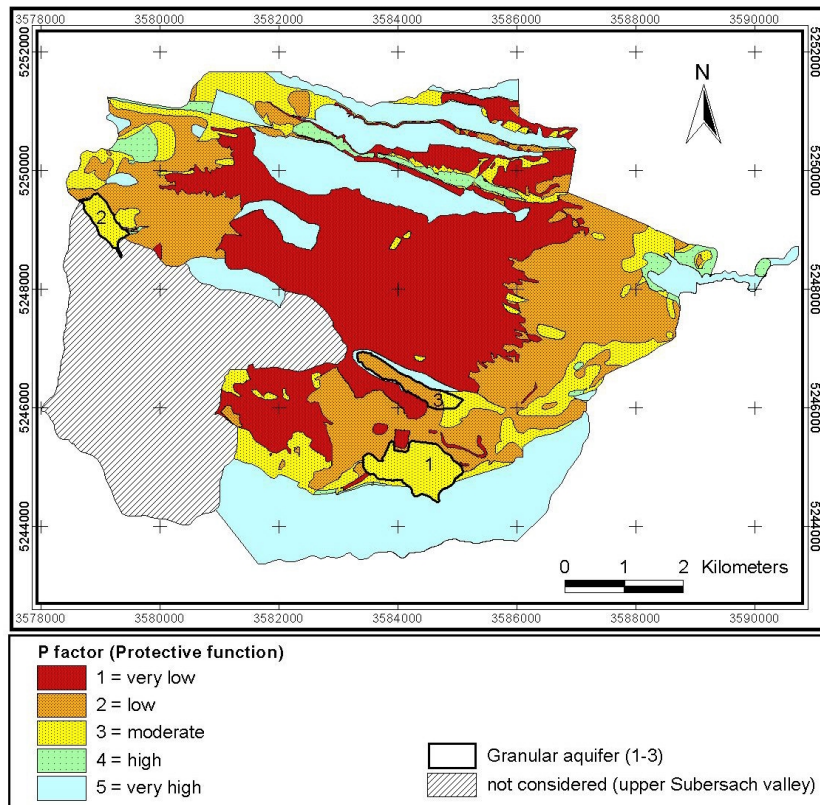


Fig. 11.3: The P map of the Hochifen-Gottesacker area (after KUNOTH 2000).

11.3.6 The map of the protective cover (P map)

The score of the total protective function of the overlying layers was calculated by adding up the scores for the four layers. The P factor was determined by subdividing the score range into five classes (P = 1–5). The P map shows the spatial distribution of the P factor (Fig. 11.3).

All outcrops of Schrattenkalk limestone without soil or with discontinuous, thin rendzina soils were evaluated to provide a very low protective function ($P = 1$). If a continuous topsoil layer is present, the protective function is low ($P = 2$). A moderate to high protective function ($P = 3-4$) was assigned to areas where the Schrattenkalk limestone is covered by Quaternary deposits and/or bedrock formations.

A very high protective function ($P = 5$) is present in areas where the karst aquifer is covered by thick layers of the Amdener marl and/or Flysch (e.g. on the SE side of the Schwarzwasser valley). In areas where the karst aquifer is absent (e.g. along the cores of the anticlines), the P factor is 5 by definition.

The overlying layers in the three granular aquifers are characterised by a low to moderate protective function ($P = 2-3$).

Altogether, the P map is plausible and sensible. However, it cannot be used as a vulnerability map, because many of the areas with a relatively high protective function drain laterally by surface runoff into the karst system. This phenomenon is taken into account via the I factor.

11.4 Infiltration conditions (I factor)

11.4.1 Determination of the dominant flow process

The dominant flow processes in the Hochifen-Gottesacker area were assessed on the basis of geological information, soil data and direct field observations (STRATHOFF 2000). It was possible to distinguish between the following situations (Fig. 11.4):

- Direct infiltration into the karst aquifer takes place on outcrops of karstified limestone, with or without topsoil cover (rendzina).
- Diffuse infiltration with subsequent percolation takes place on areas of highly permeable subsoils (Quaternary deposits).
- Surface runoff predominates on outcrops of low permeability bedrock (Drusberg marl, Amdener marl, Flysch) with or without shallow topsoil cover. A more detailed subdivision into different types of surface runoff is not applicable in the test site.
- Very fast subsurface flow has to be expected on coarse-grained, highly permeable material covering low permeability formations.

11.4 Infiltration conditions (I factor)

- Fast subsurface flow takes is characteristic for fine-grained, moderately permeable rock debris on low permeability formations.

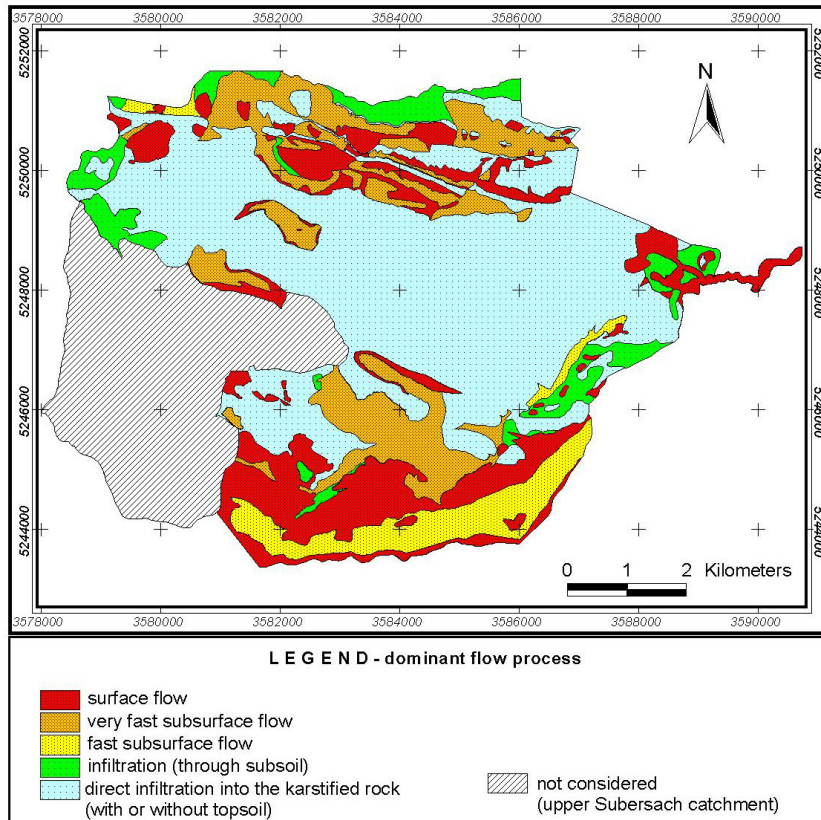


Fig. 11.4: Map of the dominant flow process (after STRATHOFF 2000).

The map of the dominant flow process shows that infiltration predominates in areas made of limestone and moraine (most of the moraines in the area are made of coarse-grained, highly permeable material which drains underground), while lateral surface and subsurface flow predominate on areas formed by non-karstic bedrock. Field observations during storm rainfall proved this analysis.

The coverage showing the dominant flow process was intersected with the coverages showing the slope gradient and the vegetation/land-use in order to obtain the I' map (see assessment scheme Fig. 9.5).

11.4.2 Determination of the I factor

Lateral surface and subsurface flow components are relevant for groundwater vulnerability only if the water and possible contaminants enter the aquifer at another place, for example via a swallow hole. Therefore, the I map (showing the degree to which the protective cover is bypassed) was created by intersecting the I' map (showing the intensity of lateral flow) with the surface catchment map (showing the sinking streams and their catchments) (Fig. 11.5).

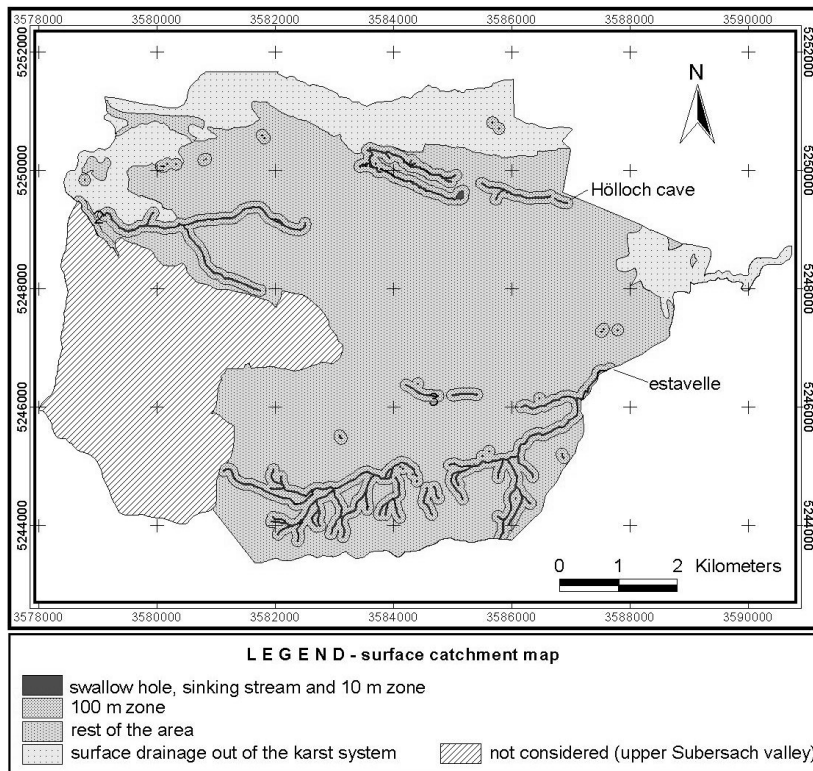


Fig. 11.5: Surface catchment map of the Hochifen-Gottesacker area.

The I map of the Hochifen-Gottesacker area reflects the hydrogeological variability of this alpine karst system (Fig. 11.6). Some examples: The lower section of the Schwarzwasser valley is formed by marl and drains by lateral surface flow out of the karst system; here, the I factor

11.4 Infiltration conditions (I factor)

is 1.0. The SE side of the upper and middle Schwarzwasser valley is formed by Flysch and drains by surface flow towards a sinking stream; here, the I factor often ranges between 0.0 and 0.4, dependent on the slope gradient and vegetation. On all outcrops of karstified limestone, there is never any lateral surface flow and all the precipitation infiltrates directly into the karst aquifer; here the I factor is 1.0.

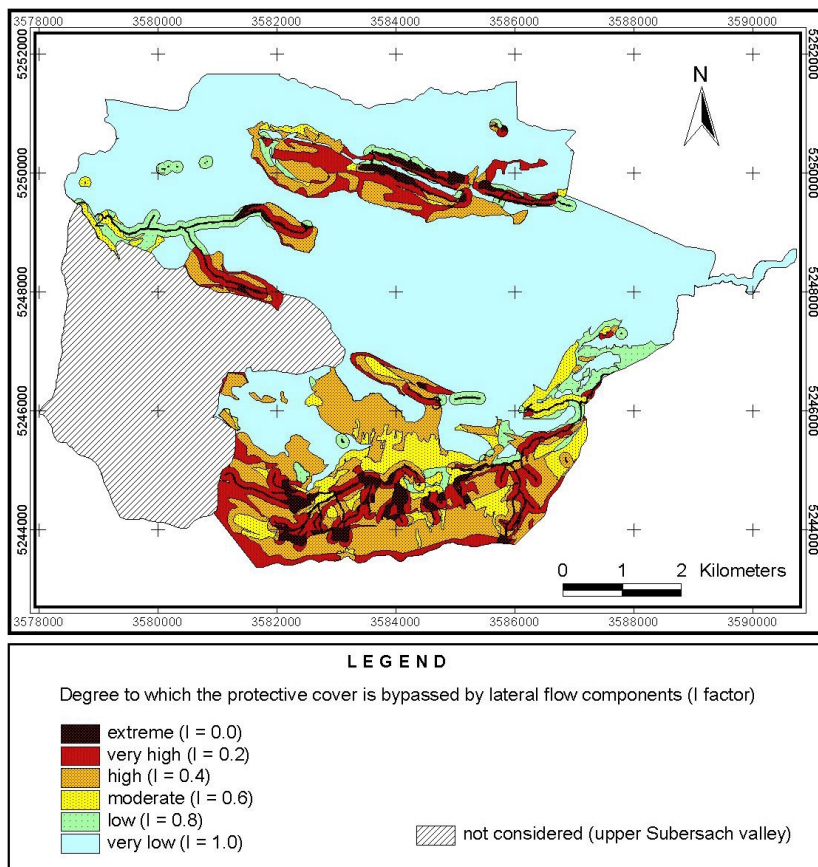


Fig. 11.6: The I map shows the degree to which the protective cover is bypassed by lateral (sub)surface flow which enters the karst aquifer at another point.

11.5 The PI vulnerability map

The PI vulnerability map is obtained by overlaying the P and I map and multiplying the P and I factor (Fig. 11.7). The legend for the vulnerability map was extended following the suggestions of DALY et al. (2002), so that the class “extreme vulnerability” is restricted to swallow holes and sinking streams ($\pi = 0.0$), while karrenfields are classified as “very highly vulnerable” ($0 < \pi < 1$). However, in many cases it may be more practicable to unify these two classes.

On the P, I and PI map, warm colours indicate a dangerous setting (low protective function, concentrated infiltration, high vulnerability), while cold colours indicate a favourable situation (high protective function, diffuse infiltration, low vulnerability).

The P and the I map of the area show a contrasting picture:

On areas formed by Schraffenkalk limestone, warm colours predominate on the P map, as the protective function of the overlying layers is very low there. Unlike that, cold colours predominate on the I map because there is no lateral surface or subsurface flow.

The situation is the other way round in areas formed by marl and Flysch formations. Here, the cold colours predominate on the P map as the protective function of the bedrock formations is very high. However, these areas often drain by lateral surface and subsurface flow into the karst system, and so the warm colours predominate on the I map.

As a consequence, the vulnerability map shows warm colours almost for the entire Hochifen-Gottesacker area: In areas made of karstified limestone, the groundwater is vulnerable to contamination because the protective function of the overlying layers is very low (low P factor); and areas formed by marl are vulnerable because they drain laterally into the karst system (low I factor).

A low to very low vulnerability is present only if the karstified limestone is covered by thick marl formations (high P factor) which drain laterally out of the area by surface flow (high I factor). This situation is present in the lower section of the Schwarzwasser valley and in some areas near the northern margin of the karst system, where the limestone is eroded in the anticlines or covered by thick marl in the synclines.

11.5 The PI vulnerability map

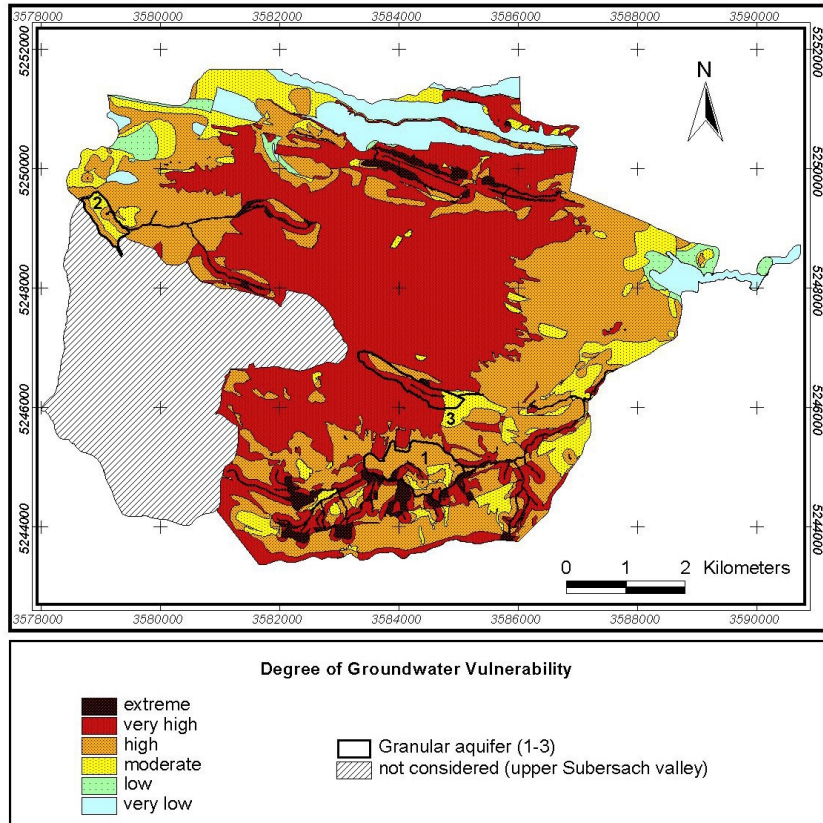


Fig. 11.7: PI vulnerability map of the Hochifen-Gottesacker area.

12 APPLICATION OF THE PI METHOD IN THE WINTERSTAUDE AREA

12.1 Overview and definition of the target

The geology and hydrogeology of the Winterstaude area was described in chapter 4. The vulnerability mapping using the modified PI method was part of an applied research project for the community of Bezau which aimed at protection zoning for the *Kreuzboden* and *Stuole* drinking water sources. The PI method was created for resource protection and not for source protection. However, if the PI vulnerability map is used together with information on the groundwater flow in the aquifer (catchment boundaries, travel time in the aquifer), it can provide a basis for the delineation of source protection zones. The combined tracer test in the area provided these information (see chapter 4).

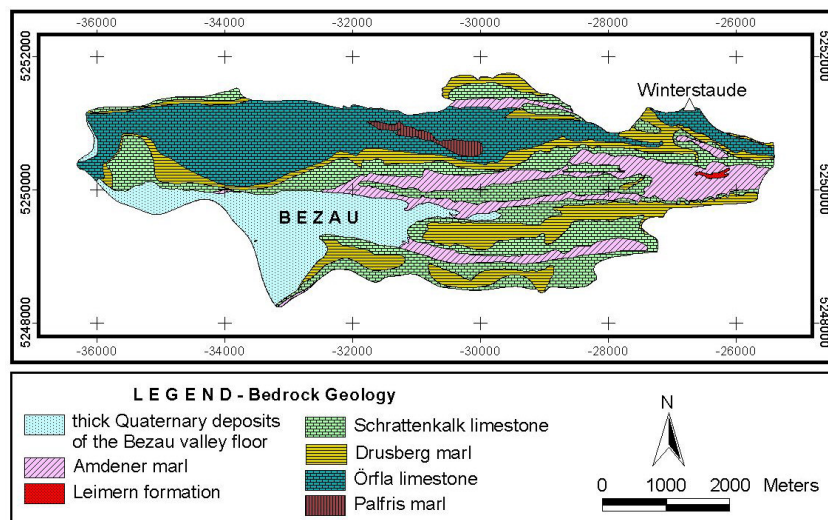


Fig. 12.1: Bedrock geology map of the Winterstaude area (after Werz 2001). There are two interacting karst aquifers – Örfli and Schrattenkalk limestone. The target for vulnerability mapping is the groundwater in the respective uppermost aquifer. The granular aquifer of the valley floor and the southern strip of the area was not considered for vulnerability mapping.

The definition of the target is a crucial point, as there are two karst aquifers – the Örfli and Schrattenkalk aquifer (Fig. 12.1). Tracer tests

proved that the two aquifers are hydraulically connected. Most of the recharge into the Örfra limestone flows quickly (within days) into the Schrattenkalk limestone via faults and is drained by several karst springs (NEUKUM 2001). Therefore, the groundwater surface in the respective uppermost karst aquifer – Örfra or Schrattenkalk – was taken as the target for vulnerability mapping (WERZ 2001).

The Stuole spring drains these two interacting karst aquifers. As a consequence, the vulnerability map is applicable for the delineation of protection zones for this spring. The map cannot be used for the Kreuzboden spring which discharges from a granular aquifer fed by infiltrating stream water and is thus independent from the karst system.

The only significant granular aquifer in the area is the sand and gravel in the Bezau valley floor which was not investigated in detail.

12.2 Protective cover (P factor)

12.2.1 The topsoil (layer 1)

WERZ (2001) created a (top)soil map for the area. The type and distribution of the soils is controlled by the geology. Thin and patchy rendzina soils predominate on Schrattenkalk, while the Örfra limestone is often covered with about 50 cm of loamy soil. The protective properties of the topsoils [points/m] were assessed on the basis of permeability (data: SEIJMONSBERGEN & VAN WESTEN 1987). The protective function [points] was calculated by multiplying the score for the protective properties with the thickness. The protective function of the topsoil is significant in areas formed of marl and Örfra limestone, while it is very low or absent in areas made of Schrattenkalk (Fig. 12.2).

12.2.2 The subsoil (layer 2)

The subsoil map was derived from information on Quaternary deposits shown on the geological map. As there are no drillings, the thickness of the subsoil was estimated on the basis of field observations and geological sections. Subsoils are not widely distributed and contribute only locally to the protection of the groundwater (Fig. 12.2).

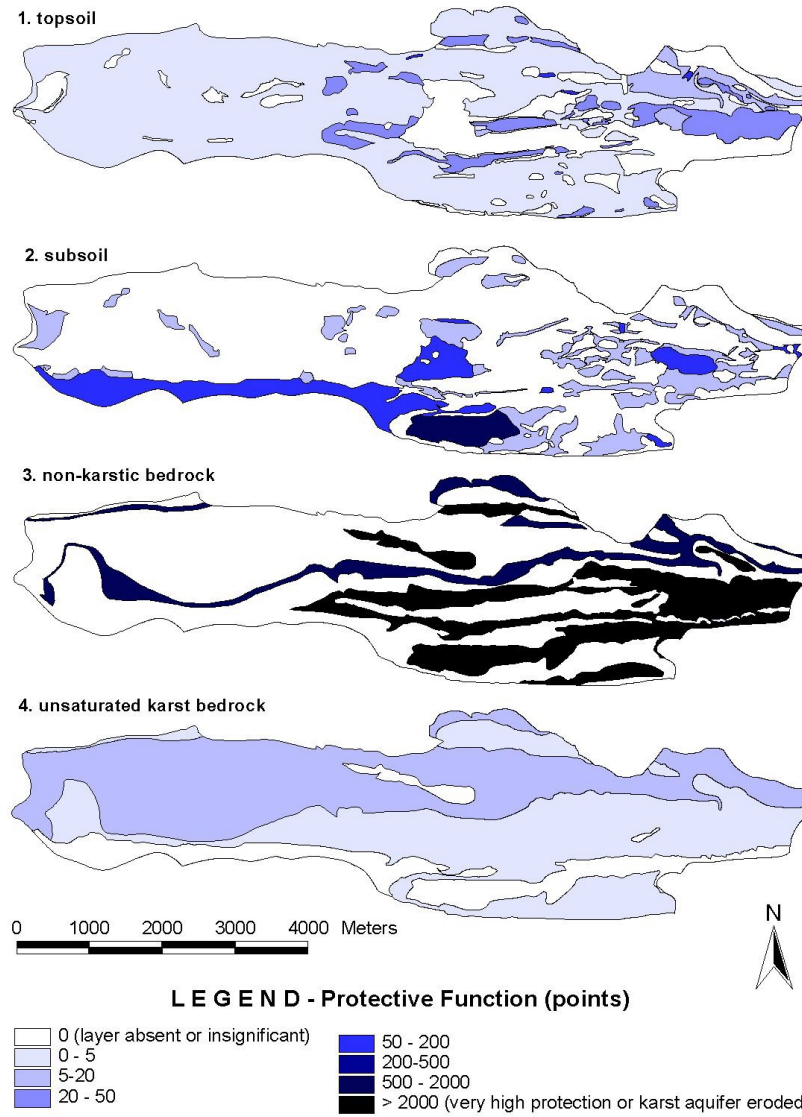


Fig. 12.2: Protective function of the topsoil, the subsoil, the non-karstic bedrock and the unsaturated karst (modified after Werz 2001).

12.2.3 The non-karstic bedrock (layer 3)

On the bedrock geology map, five situations can be distinguished:

1. if the Örfra limestone has been eroded so that the Palfris marl is the uppermost bedrock layer, the target (the karst groundwater surface) is absent and layer 3 can not be defined;
2. if the Örfra limestone is the uppermost bedrock, layer 3 is absent;
3. if the bedrock map shows Drusberg marl, the groundwater surface in the Örfra aquifer is the target and the marl is the layer 3;
4. if the bedrock map shows Schrattenkalk limestone, layer 3 is absent (similar to situation 2);
5. if the bedrock map shows younger formations (e.g. Amdener marl), the groundwater surface in the Schrattenkalk karst aquifer is the target and the younger formations are the layer 3.

For situations 3 and 5, the thickness of the non-karstic bedrock was estimated on the basis of geological information (total thickness of the formation, geological sections). Data on the permeability were taken from the literature (SEIJMONSBERGEN & VAN WESTEN 1987). The layer 3 contributes significantly to the total protective function (Fig. 12.2).

12.2.4 The unsaturated karstic bedrock (layer 4)

The unsaturated karstic bedrock either consists of Örfra or Schrattenkalk limestone. The two formations have no significant intergranular porosity. The Örfra limestone is up to 160 m thick and moderately karstified (rare and poorly developed epikarst features). The estimated average thickness of the unsaturated zone is 60 m and the calculated protective function is 15 points. The Schrattenkalk limestone is up to 100 m thick and extremely karstified (karrenfields, dolines, caves). The average thickness of the unsaturated zone is around 30 m and the resulting protective function is only 1.5 points (WERZ 2001) (Fig. 12.2).

12.2.5 The map of the protective cover (P map)

The P factor was determined by adding up the scores of the four layers and subdividing the score range into five classes (P = 1, 2, 3, 4, 5). The map of the protective cover (P map) is strongly influenced by the bedrock geology (compare Fig. 12.1 and Fig. 12.3).

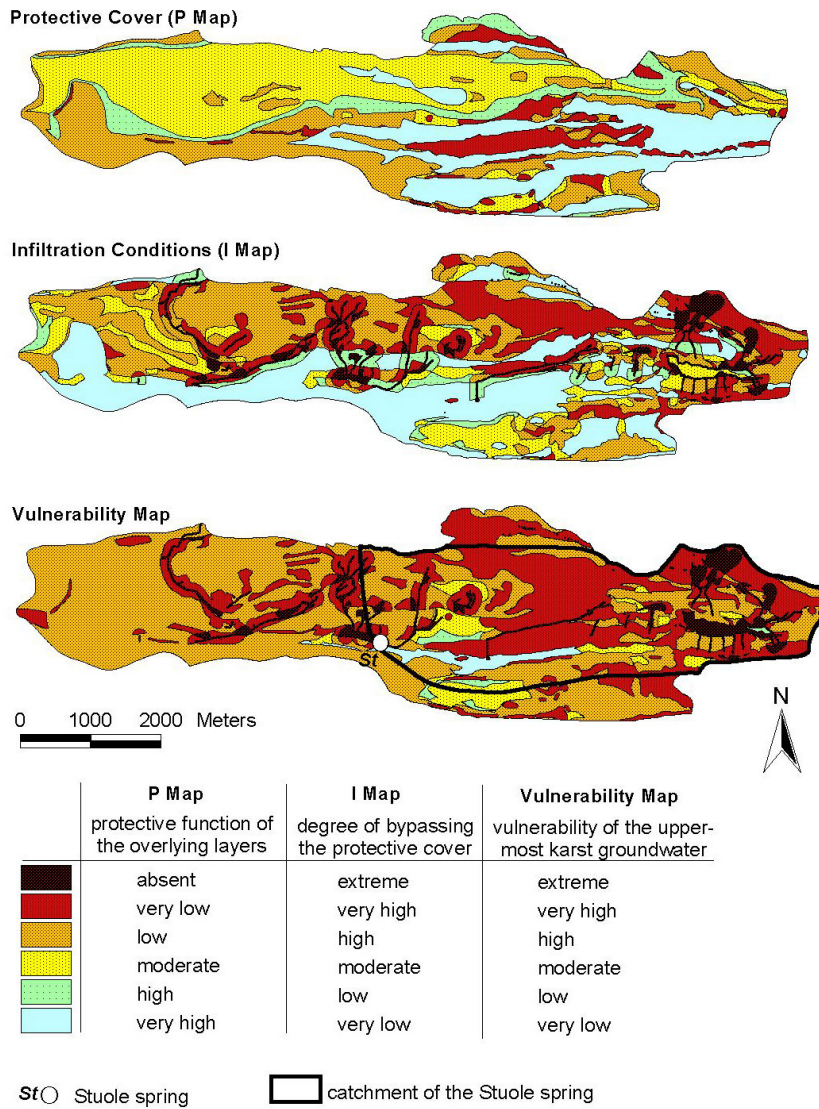


Fig. 12.3: The vulnerability map was made by intersecting the P and the I map.

A very low protective function (P = 1) was assigned to all areas made of Schratenkalk limestone with or without thin and patchy rendzina

soils. If the limestone is covered by a significant layer of top- or subsoil, the protective function is low ($P = 2$).

The areas formed of Örfra limestone are characterised by a low to moderate protective function ($P = 2-3$), dependent on the properties of the topsoil layer. The Drusberg marl provides a high to very high protection ($P = 4-5$) to the underlying Örfra karst aquifer.

A very high protective function ($P = 5$) was assigned to areas where the Schrattenkalk limestone is covered by the thick and nearly impervious Amdener marl and, by definition, to all areas where the Örfra karst aquifer was eroded so that the underlying Palfris marl outcrops.

The P map is consistent and reliable. However, there is significant lateral surface flow and there are many swallow holes, and so it is essential to take into account the infiltration conditions as a next step.

12.3 Infiltration conditions

12.3.1 Determination of the dominant flow process

It was possible to distinguish between seven dominant flow processes on the basis of direct field observations, geological and pedological information (WERZ 2000):

- Direct infiltration into the karst aquifer takes place on areas with highly permeable soils on karstic limestone (all areas made of Schrattenkalk limestone or Örfra limestone without loamy topsoil).
- Diffuse infiltration with subsequent percolation predominates on highly permeable soils covering Quaternary deposits.
- Fast subsurface flow takes place on low permeability bedrock (marl) covered by moderately permeable fine-grained rock debris.
- Very fast subsurface flow predominates on low permeability bedrock covered with very highly permeable material.
- Saturated overland flow occurs on wetland areas and moors.
- Surface runoff takes place frequently on outcrops of marl if the topsoils are absent, thin or of low permeability.
- Surface runoff takes place rarely on Örfra limestone with loamy soil.

The I' map was created by overlaying the coverage of the dominant flow process with the coverage of the slope gradient and the vegeta-

tion/land-use. Forest predominates in the lower parts (< 1400 m), while the higher parts of the area, which are often formed by Örfli limestone, are used as alpine pasture. Steep slopes (> 27 %) predominate by far.

12.3.2 Determination of the I factor

The I map (Fig. 12.3) was created by overlaying the I' map and the surface catchment map. The I map shows the degree to which the protective cover is bypassed by lateral surface and subsurface flow components entering the karst aquifer at another place. Areas made of Schrattekalk limestone are characterised by diffuse infiltration through highly permeable soils. There is no lateral surface flow and the I factor is consequently 1.0 in most cases. Unlike that, the Örfli limestone is often covered by loamy soils. Significant lateral surface flow takes place during storm rainfall and the I factor often ranges between 0.0 (on steep slopes without forest) and 0.6 (on gentle slopes with forest).

Areas formed by marl frequently produce surface runoff, and so the I factor often ranges between 0.0 and 0.4. An I factor of 1.0 was assigned to those parts of the area that produce surface runoff flowing out of the aquifer system under consideration.

12.4 The PI vulnerability map

The vulnerability map was created by overlaying the P and the I map and multiplying the P and the I factor (Fig. 12.3). In the Winterstaude area, the degree of vulnerability predominantly ranges between high and very high. Extreme vulnerability is present on small areas around swallow holes and along sinking streams. The vulnerability is moderate to low in areas with thick Quaternary deposits. A very low vulnerability was assigned to the Grebentobel valley, because the valley is formed by the impervious Amdener marl and the stream flows out of the karst system. However, the Kreuzboden spring which is used for the drinking water supply of Bezau receives significant inflow from this stream!

12.5 Consequences for source protection

The vulnerability map together with the results of the tracer test form the scientific basis for a source protection scheme for the community of Bezau which is in progress at present (GOLDSCHIEDER et al. 2001d, e).

The Stuole spring discharges from the Schrattekalk karst aquifer which gets inflow from the Örfli karst aquifer. The catchment of the

spring comprises the eastern part of the area between the crests of the anticlines II and V (Fig. 12.3). The three tracers that have been injected inside the catchment arrived at the spring within days. The Austrian guidelines for source protection zoning take the 60 day-line of travel time as the main criterion for the delineation of the inner source protection zone (zone II), and so the entire area should be zone II if these guidelines were strictly applied. This would be favourable from the point of view of drinking water protection but unacceptable because of the resulting land-use restrictions. Almost the entire area is used as cattle pasture. The vulnerability map can help to find a compromise between drinking water protection and land-use. At least all areas with a very high to extreme vulnerability should be delineated as zone II. The final decision on the protection zones is not a scientific but a political one.

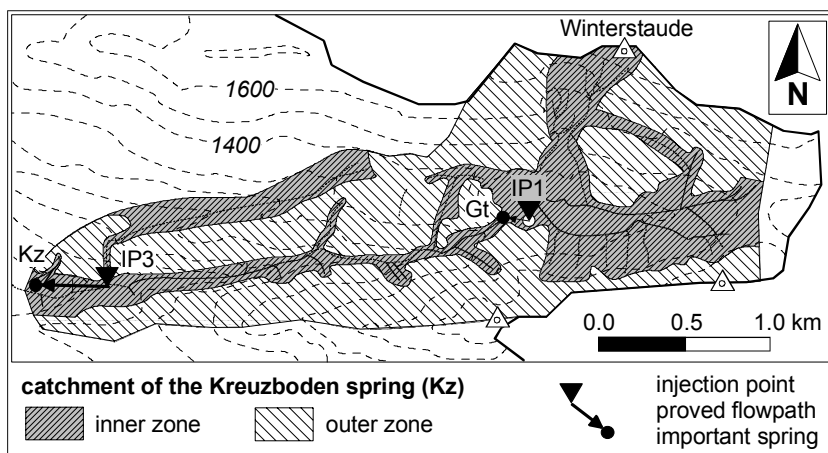


Fig. 12.4: The catchment of the Kreuzboden spring is identical to the surface catchment of the Grebentobel stream. It can be subdivided in an inner (low permeability formations, frequent surface runoff) and outer zone (high permeability formations, rare surface runoff) (after WERZ 2001).

The Kreuzboden spring is not a karst spring but is mainly fed by infiltrating surface water from the Grebentobel stream. Thus, the vulnerability map (which takes the karst groundwater as the target) cannot be used for the delineation of source protection zones for this spring. In order to protect the Kreuzboden spring, it is indispensable to protect the topographic catchment of the Grebentobel stream which can be subdivided into two zones (Fig. 12.4):

1. The stream itself and all areas within its topographic catchment which are formed by marl and consequently drain by surface runoff should be the inner protection zone;
2. all areas within the catchment made of highly permeable formations which hardly ever produce any surface runoff should be the outer source protection zone.

None of the tracers injected in the Winterstaude area reached the Kressbach spring. The spring probably discharges from the granular aquifer in the Bezau valley floor, and so the vulnerability map (which takes the karst groundwater as the target) cannot be used as a basis for protection zoning. Indirect inflow of karst water has to be expected but was not proved. If this spring should be used for drinking water supply, further research was necessary.

13 CONCLUSIONS, DISCUSSION AND OUTLOOK

13.1 The problem of definition

Since the late 1960s, groundwater vulnerability maps have played an increasingly important role in bringing an interest in groundwater to the attention of decision makers in the planning process. Vulnerability maps have become a means of presenting various complex hydrogeological parameters in the form of an easily understood term „vulnerability“ (HÖTZL et al. 1995). The definition of (intrinsic) vulnerability suggested by ALBINET & MARGAT (1970) and further developed by many authors (e.g. FOSTER 1987, DOERFLIGER 1996, GSI 1999, CIVITA & DE MAIO 2000) is a purely descriptive one. VRBA & ZAPOROZEC (1994) point out that vulnerability is a „relative, non-measurable, dimensionless property“. According to the definition suggested by COST 620 (DALY et al. 2002), intrinsic vulnerability is the term used to describe the vulnerability of groundwater to contaminants generated by human activities; it takes into account the inherent geological, hydrological, and hydrogeological characteristics of an area, but is independent of the nature of the contaminants.

Some authors criticise that such a purely descriptive definition, which is not quantitatively defined in terms of physics, may be the source of misinterpretations. ANDERSEN & GOSK 1989 point out that it is impossible to create a „general“ vulnerability map which expresses in a comparable way recuperable (i.e. permanent) protective properties (e.g. microbial activity) and depletable properties (e.g. buffer capacity) of an area. They emphasise that a vulnerability map cannot at the same time be applicable for both conservative and reactive contaminants, for both instantaneous and long-term, and for both point and diffuse contamination scenarios. They consequently demand that vulnerability maps should be prepared for well defined specific situations only.

Obviously, it is debatable if a descriptive, general definition and the lack of physical precision in vulnerability concepts should be considered as an advantage or as a disadvantage.

The advantage of a descriptive definition is that the term vulnerability is often intuitively understood, particularly by decision-makers in the planning process (HÖTZL et al. 1995). A vulnerability map showing areas of different colour symbolising different degrees of vulnerability (or natural protection respectively) is easily to interpret and can be a practical and

applicable tool for land-use planning, protection zoning and risk assessment. In many countries (e.g. Switzerland, Ireland, Italy), vulnerability maps are successfully used as an integrated part of an overall groundwater protection scheme – although a purely descriptive definition of the term vulnerability is used.

There are also disadvantages to a purely descriptive definition. A property which is not precisely defined in terms of physics cannot be derived unambiguously from measurable physical quantities. Therefore, every method of vulnerability mapping is based on the individual point of view and experience of the person who developed it and is thus subjective. It is difficult to compare different vulnerability methods or maps and to decide which one is best. If different methods are tested in one area, the resulting maps are always different and sometimes contradictory (e.g. GOGU 2000). Nevertheless, it is possible to decide whether a method (or map) is plausible, practical and applicable, or not. Another important consequence of the lack of a physical definition is, that it is difficult to validate (verify or negate) a vulnerability assessment or mapping (BROUYÈRE et al. 2001).

However, even if the term vulnerability is not defined in a physically precise way, it is possible to base the concept on sensible and applicable physical assumptions. The PI method and the concept suggested by COST 620 are based on the assumption that intrinsic vulnerability depends on three attributes: the travel time of water (and contaminants), the relative quantity of water (and contaminants) that can reach the target and the physical attenuation by dispersion (GOLDSCHIEDER et al. 2000b, DALY et al. 2002). If a contaminant which is released in a given area reaches the target (groundwater surface or spring) quickly, completely (100 % recovery rate) and at high concentration, the area is evaluated to be highly vulnerable. The vulnerability of an area is low if a released contaminant reaches the target with a long delay, in a small proportion and with low concentrations.

Particularly in karst areas, there is an additional attribute which is difficult to handle – the temporal variability. A contaminant which is accidentally released during a storm rainfall might reach the groundwater quickly and in high concentrations via surface runoff towards a swallow hole, while it might reach the target much later and in lower concentrations if the same accident occurred on the same area under low water conditions. The vulnerability of the given area is consequently dependent on the particular hydrologic conditions. However, it is not practical to create different vulnerability maps for different hydrologic conditions,

and so the temporal variability (in this case of surface runoff) was included in the PI method. Areas within the catchment of a sinking stream which produce surface flow frequently are evaluated to be more vulnerable than areas which produce surface flow only during storm rainfall.

BROUYERE et al. (2001) suggest that the three practical questions to which a vulnerability assessment has to answer are the following: If a pollution occurs, when will it reach the target, at which concentration level and for how long will the target be polluted? It is suggested to use a so-called „vulnerability cube“. The three axes of the cube are the transfer time, the maximum concentration and the duration of a contamination. Vulnerability mapping should be based on assessing all the intrinsic properties which control the impulse response of the system to a DIRAC-type input of a conservative contaminant.

At present, the vulnerability cube is a promising concept but has not yet been worked out in detail and applied in reality. However, the basic idea of the vulnerability cube is consistent to the concept of the PI method and the suggestions given by DALY et al. (2000a, 2002) which take into account the three attributes travel time, relative quantity and physical attenuation.

13.2 The problem of „intrinsic“ vulnerability

The intrinsic vulnerability of groundwater to contamination takes into account the inherent properties of an area but is, by definition, independent of the nature and specific properties of a contaminant. However, the transport of any contaminant always depends on the interaction between the specific properties of the area and the specific properties of the contaminant: the transport of pesticides depends on (amongst others) the type and content of organic matter; the retention of heavy metals is controlled by the cation exchange capacity; the transport and mortality of bacteria depends on the pore size and the residence time; and the behaviour of nitrates is influenced by the redox potential. There is no such thing as a general contaminant, and there is no property of a hydrogeological system which is in the same way effective for all types of contaminants. Therefore, it is debatable which properties of the area should be taken into account for intrinsic vulnerability mapping.

One possibility is to take into account those properties of an area which are relevant for the attenuation of the most significant, frequent and

problematic contaminants, for example for organic solvents, nitrates, pesticides, heavy metals and bacteria. A vulnerability map based on this concept would have to take into consideration, amongst others, the type and content of clay minerals and organic matter, the redox potential and the effective pore size. Such a vulnerability map can give a general impression of the self purification capacity of the system.

COST 620 has chosen another possibility. Intrinsic vulnerability is assessed on the basis of properties controlling the transport of a conservative contaminant which behaves like the water molecule itself (DALY et al. 2002). The most important attributes are advective transit time, physical attenuation by dispersion and dilution, and relative quantity of contaminants that can reach the target – a portion of contaminants may leave the area via surface runoff. The factors to be mapped in the field are consequently the permeability and thickness. Factors relevant only for specific contaminants (e.g. redox potential, type and content of clay minerals and organic matter) are not considered for intrinsic vulnerability mapping, but for specific vulnerability mapping.

This second possibility may be criticised, because most contaminants are not conservative, and for a conservative contaminant, it makes no difference if it reaches the groundwater after twenty years instead of two days (ANDERSEN & GOSK 1989). This criticism is partially justified. However, most natural attenuation processes are directly or indirectly related to the travel time and most of the factors controlling the travel time are also relevant for the various processes of contaminant attenuation. For example: A high content of fine-grained material (e.g. clay) in the overlying layers increases the travel time (intrinsic), the heavy metals adsorption (specific), and the retention of bacteria (specific). Furthermore, a long travel time also means a long time to react on an accidental pollution. The travel time of a conservative contaminant can consequently be used as an indirect and practicable means to describe the vulnerability of a hydrogeological system to contamination generated by human activities, although most hazardous substances are not conservative ones.

13.3 The COST 620 approach to intrinsic vulnerability mapping

COST 620 outlines a flexible and comprehensive approach to intrinsic vulnerability mapping (DALY et al. 2002). This „European Approach“ is rather a general framework than a prescriptive method; a detailed as-

assessment scheme with tables and formulas is not given. Four factors are considered: overlying layers (O), concentration of flow (C), precipitation regime (P) and karstic network (K) (Fig. 13.1).

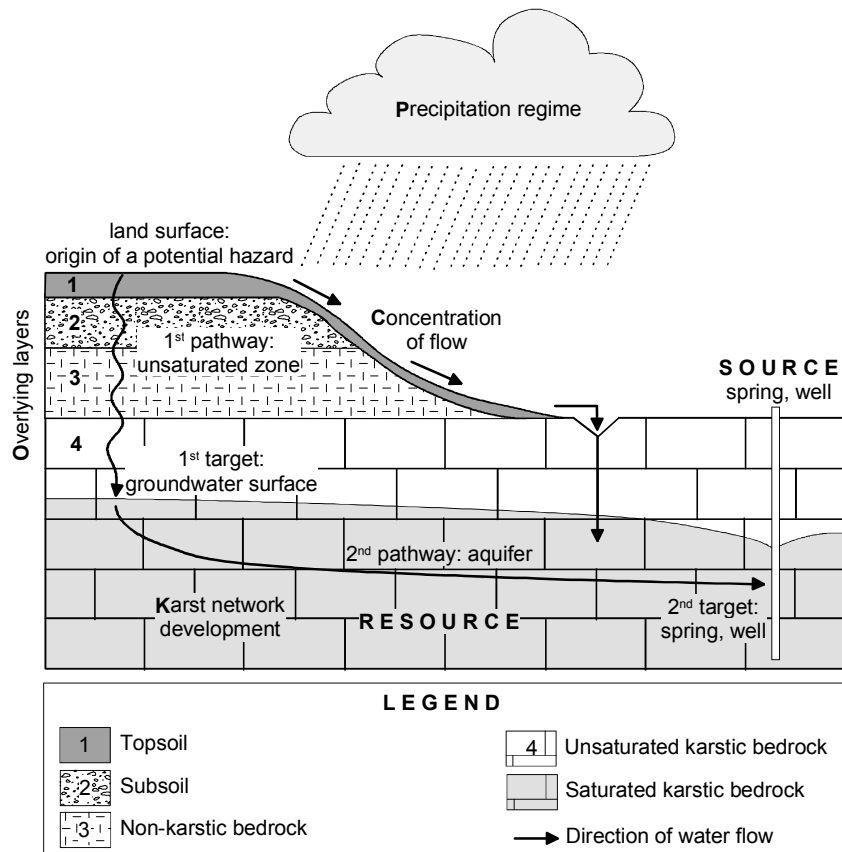


Fig. 13.1: Conceptual model of the European Approach (DALY et al. 2002; Graphics: N. Goldscheider).

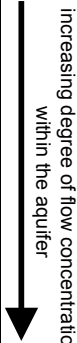
The overlying layers are those located between the land surface and the groundwater surface. They can consist of up to four types of layers: topsoil, subsoil, non-karstic bedrock and unsaturated karstic bedrock. The main data which should be used to assess the O factor are the layer thickness, hydraulic conductivity, effective porosity, macroporosity, fissuring, fracturing and karstification; these main data can also be assessed indirectly on the basis of grain-size distribution, lithol-

ogy, soil type, vegetation indicators and drainage density. The O factor is largely identical to the P factor of the PI method.

The C factor represents the degree to which precipitation is concentrated towards places where fast infiltration can occur. If infiltration occurs diffusely without significant concentration of flow, the C factor is not an issue as the overlying layers are not bypassed. On the other hand, precipitation can be concentrated at or near the surface of the ground, and the overlying layers can be completely bypassed via a swallow hole through which surface water and contaminants directly enter the karst aquifer. In such a case, the C factor is a significant issue in determining vulnerability. The degree of flow concentration depends on the presence of features which allow for concentrated infiltration (swallow holes) and the parameters that control runoff, like slope, vegetation and soil properties. The C factor is almost identical to the I factor of the PI method.

Tab. 13.1: suggested COST 620 classification of carbonate aquifers (modified after DALY et al. 2002).

network	intergranular porosity	type of carbonate aquifer
absent	no	(no aquifer)
absent	low-high	intergranular aquifer
fractures	high	fractured aquifer
	low	
solutionally enlarged fractures	high	karst aquifer
	low	
	no	
slow active conduit network	high	
	low	
fast active conduit network	high	
	low	
	no	


 increasing degree of flow concentration within the aquifer

The K factor represents the degree of karst network development in the saturated zone of the aquifer. It is based on a general description of the bedrock, giving a range of possibilities from non-karstified carbonate rocks with only intergranular porosity to karst aquifers with fast active conduit systems (Tab. 13.1). This K factor is similar to the one used in the EPIK method (DOERFLIGER & ZWAHLEN 1998). In the PI method, the horizontal flow in the karst aquifer is not considered as this method was made for resource vulnerability mapping and consequently takes the groundwater surface as the target.

The P factor reflects not only the total quantity of annual precipitation, but also the frequency, duration, and intensity of extreme events, which can have a major influence on the type and quantity of infiltration. In many cases, there is no large variation of the precipitation regime within one catchment, but there may be large differences between different test sites in different climatic zones. Thus, the precipitation factor may not be an issue on the catchment scale, but it is relevant on a national or European scale. In the PI method, there is no independent factor for the precipitation. However, the precipitation is indirectly included: The protective cover factor takes into account the total annual recharge dependent on the annual precipitation, and the infiltration conditions factor takes into consideration the predominant flow process which depends both on the properties of the area and the precipitation regime, i.e. the time distribution of precipitation. The generation of surface runoff is also influenced by antecedent conditions (e.g. soil moisture) which are, however, difficult to include into vulnerability concepts.

The factors O, C and K represent the internal characteristics of the system, while the P (precipitation) factor is an external stress applied to the system.

The PI method is consistent with this concept. The COST 620 group consequently suggests to use the PI method within the framework of the „European Approach“.

13.4 Application of vulnerability maps for source and resource protection zoning

The four factors of the COST 620 approach can be combined in order to create resource and source vulnerability maps (DALY et al. 2002). For resource vulnerability, the groundwater surface is the target and the horizontal flow in the aquifer is not considered. Thus, the resource vulnerability map takes into account the O, C and P factor (Fig. 13.2). For source vulnerability, the drinking water spring or well is the target, and the horizontal flow in the aquifer has to be considered. The source vulnerability map can therefore be obtained by a combination of the factors O, C, P and K. The source and resource vulnerability map can be used as a basis for the delineation of source and resource protection zones respectively.

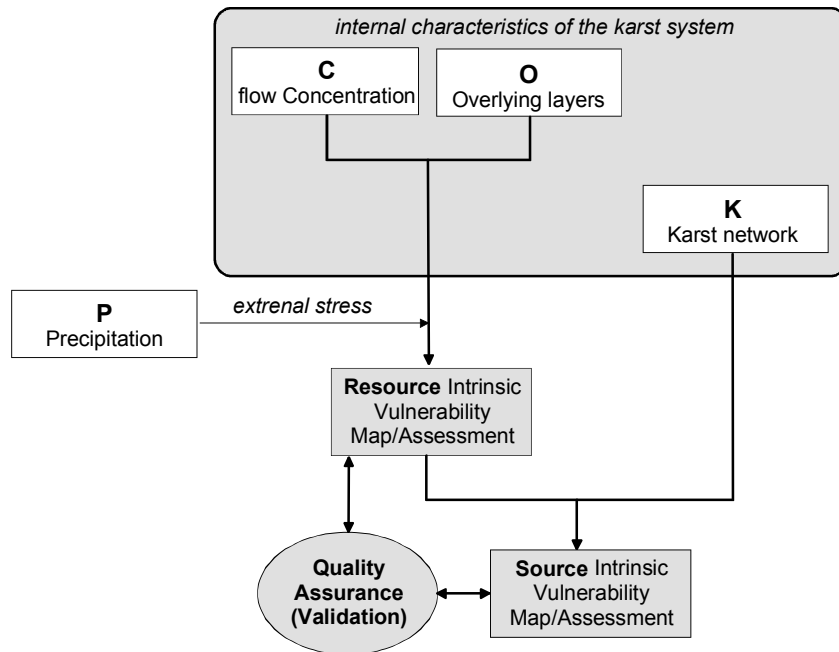


Fig. 13.2: Creation of resource and source vulnerability maps by a combination of the factors O, C, P and K (after Daly et al. 2002).

The Irish groundwater protection scheme provides an example of how vulnerability maps can be used both for resource and source protection zoning (Fig. 13.3). Irish resource protection zones are delineated on the basis of an intrinsic resource vulnerability map which takes into consideration the thickness and properties of the overlying layers and the presence of karst features. Source protection zones are delineated by overlaying the resource vulnerability map with a map showing the inner and outer source protection areas which generally correspond to the 100 day-line of travel time in the aquifer and the rest of the zone of contribution respectively (GSI 1999). Thus, the Irish system is consistent with the approach suggested by COST 620 although the nomenclature is slightly different.

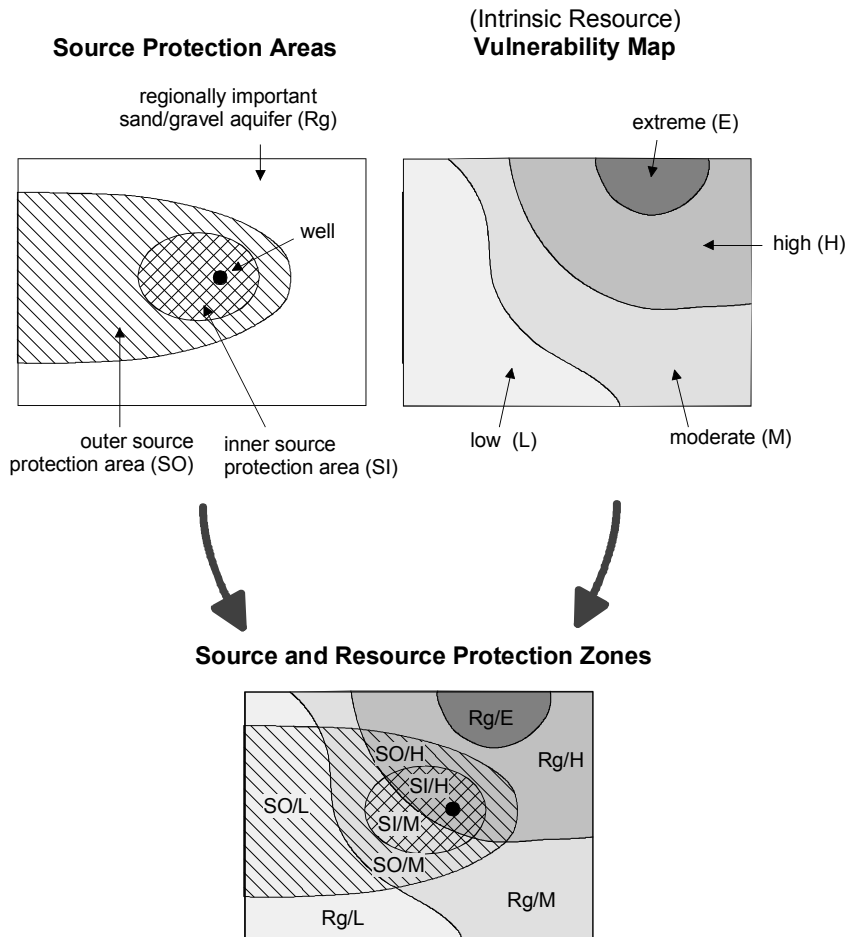


Fig. 13.3: The Irish groundwater protection scheme provides an example of how vulnerability maps can be used as a basis for resource and source protection. The scheme is not restricted on karst but applicable for all types of aquifers, in this case a sand/gravel aquifer (modified after GSI 1999). The PI method and the COST 620 concept follows this logic but uses a slightly different nomenclature.

13.5 The COST 620 approach to specific vulnerability mapping

Methods of specific vulnerability mapping have previously been developed by RAO et al. (1985), ALLER et al. (1987), TESO et al. (1996) and others (see MAGIERA 2000).

According to the COST 620 definition, specific vulnerability is the term used to describe the vulnerability of groundwater to a particular contaminant or group of contaminants. It takes into account the properties of the contaminant(s) and its (their) relationship(s) to the various aspects of the intrinsic vulnerability of the site. Specific vulnerability maps can be prepared for organic solvents, heavy metals, nitrates, pesticides or bacteria. Specific vulnerability maps can be created on the basis of information presented on the intrinsic vulnerability map, together with additional information on subsurface processes relevant for specific contaminant attenuation, such as cation exchange, bioegradation, oxidation, reduction, complexation, hydrolysis, precipitation, filtration, sedimentation, volatilization and decay.

13.6 Validation of vulnerability maps

Until now, there has been no generally accepted validation procedure for vulnerability maps. COST 620 suggests a validation using the following methods: (a) hydrographs, chemographs, bacteriology; (b) tracer techniques; (c) water balance; (d) calibrated numerical simulations; (e) analogy studies (DALY et al. 2002).

The requirements of a validation procedure by means of tracer tests can be directly derived from the concept of vulnerability assessment suggested by COST 620. Three aspects have to be considered in order to quantify intrinsic vulnerability: travel time of a (conservative) contaminant from the origin to the target, relative quantity of the contaminant that can reach the target, and physical attenuation. For source vulnerability, the ground surface is taken as the origin of a contamination, the spring is the target. For the validation of an intrinsic source vulnerability map, a conservative tracer should thus be injected on the ground surface, the samples should be taken at the spring.

Based on this concept, an EPIK vulnerability map for the karstic catchment of a drinking water source in the Swiss Jura mountains was validated by means of combined tracer tests (GOLDSCHIEDER et al. 2001a). Seven tracers were injected at seven different locations. Six of

them were injected at the land surface on rectangles of 10 m x 1 m with a watering can. An artificial rainfall of 20 mm was simulated after each injection. The seventh tracer was injected in a swallow hole. Four of the seven tracers arrived at the drinking water source. The tracer break-through curves were evaluated. Three criteria were taken into account: the normalised maximum concentration c/M , the travel time which corresponds to the maximum concentration and the recovery rate of the tracer. The experiments proved a correlation of the EPIK vulnerability with the normalised maximum concentration and the recovery rate, while the differences in travel time were insignificant – all tracers arrived within days.

It is a future challenge to develop applicable validation techniques for intrinsic and specific source and resource vulnerability maps.

13.7 The importance/value of groundwater

Many people will agree that a highly vulnerable groundwater body needs more protection (stricter land-use restrictions) than a lowly vulnerable one. However, vulnerability by itself is not a sufficient criterion for the required protection (Fig. 13.4). The importance or value (economic, ecological, social) of the groundwater body should be taken into account as an additional criterion (DREW & HÖTZL 1999a, COMMITTEE ON VALUING GROUND WATER 1997).

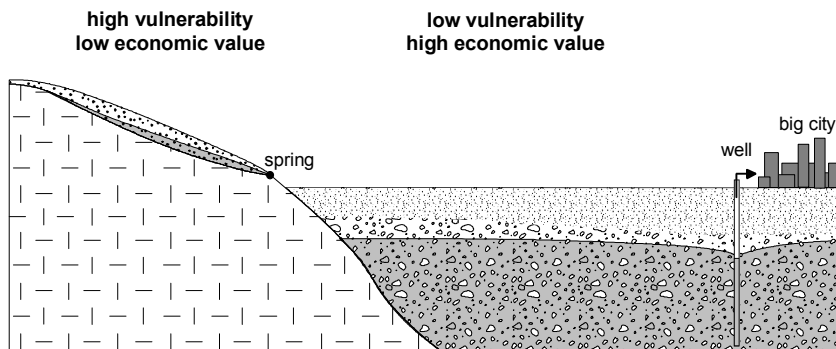


Fig. 13.4: Vulnerability by itself is not a sufficient criterion for protection zoning. Thus, the Irish groundwater protection schemes additionally take into account the value/importance of the groundwater.

According to the Irish groundwater protection scheme, aquifers of regional importance are considered to be more valuable than poor aquifers. The required protection and the resulting land-use restrictions

depend on both the vulnerability and the importance of the groundwater body. The highest protection and the most strict land-use restrictions are required on extremely vulnerable zones within a regionally important aquifer (or within the inner source protection area of a spring or well respectively). Extremely vulnerable zones within a generally unproductive aquifer require less protection (GSI 1999).

The German water protection ordinance (WHG 1996) emphasises that all groundwater is valuable and has to be protected from contamination. Also the European Water Directive (2000) emphasises that ground (and surface) water is a heritage which must be protected. There is nothing to say against that evaluation. Nevertheless, the value of the groundwater is taken into consideration implicitly within all existing groundwater protection schemes. In all national regulations, the highest protection and the strictest land-use restrictions are demanded for those groundwater bodies which are actually used for drinking water supply – which is an economic criterion independent from vulnerability.

13.8 Vulnerability maps within the framework of risk assessment

Vulnerability maps can be used together with hazard maps in order to prepare risk maps which provide a tool for land-use planning and groundwater management. The vulnerability map (source or resource, intrinsic or specific) shows the sensitivity of an area to groundwater contamination generated by human activities. The hazard map shows the presence of potential sources of groundwater contamination. Hazards have been grouped into three categories: infrastructure development, industrial activities, livestock and agriculture (COST 620, 2001). Hazards are evaluated on the basis of a so-called hazard index which takes into account the „harmfulness“ of a hazard to groundwater, the quantity of relevant substances which can be released in case of an accident, and the probability for a contamination event to occur.

Risk map can be created by overlaying vulnerability and hazard maps. The risk map consequently shows the probability of groundwater to be actually contaminated by human activities. The value of the source or resource can also be included within the framework of risk assessment. The highest risk is present in situations where a dangerous hazard (high probability of large quantities of harmful substances to be released) is located in a highly vulnerable zone of an area which holds a valuable groundwater body. If the risk of a specific contamination is to

be shown, e.g. the risk of groundwater contamination with pesticides, the hazard map should be combined with a specific, in this case pesticide-specific, vulnerability map. The intrinsic vulnerability map can be used within the framework of a more general risk assessment. The risk map consequently shows area, where an engineering, political, legislative and/or management response is required (DREW & HÖTZL 1999a).

13.9 Concluding comment

In terms of groundwater protection, any kind of contamination is problematic and should be avoided. At the same time, almost all human activities and land-use practices cause some contamination. Therefore, it is necessary to find a compromise between land-use on the one hand and groundwater protection on the other hand. The vulnerability map can help to find such a compromise and is consequently a useful tool.

There are still many scientific problems concerning the concept of vulnerability which have been discussed in great detail in the previous sections, as well as within the meetings of the COST 620 group. However, one should not forget that the concept of vulnerability mapping was not developed to satisfy scientists but to help land-use planners and decision makers. Consequently, vulnerability concepts should be kept as simple and applicable as possible.

At the same time, the problems and limitations of vulnerability mapping should be clarified. Vulnerability maps should be made for a well defined purpose and can only be used for that purpose. A vulnerability map cannot give an answer to all questions of groundwater protection and contamination. Consequently, a vulnerability map should not be a stand-alone element but an integrated part of an overall groundwater protection scheme which must always be based on a detailed geological and hydrogeological understanding of the area under investigation.

14 REFERENCES

- AG BODEN (1996): *Bodenkundliche Kartieranleitung*: 392 p.; Hannover.
- ALBINET, M. & MARGAT, J. (1970): Cartographie de la vulnérabilité à la pollution des nappes d'eau souterraines. – Bull. BRGM, 2ème série, 3(4): 13-22.
- ALLER, L., BENNETT, T., LEHR, J.H., PETTY, R.J. (1987): DRASTIC: A Standardized System for Evaluating Ground Water Pollution Potential Using Hydrogeological Settings. – U.S. Environmental Protection Agency, Oklahoma.
- ANDERSEN, L. J. & GOSK, E. (1989): Applicability of Vulnerability Maps. – Environ. Geol. Water Sci., 13/1: 39-43; New York.
- ANDREO, B. (1997): Hidrogeología de acuíferos carbonatados en las Sierras Blanca y Mijas (Cordillera Bética, Sur de España). – University of Malaga: 489 p.
- AUDRA, P. (1994): Karsts alpins. Genèse de grands réseaux souterrains: Exemples le Tennenengebirge (Autriche), l'Île de Crémieux, la Chartreuse et le Vercors (France). – Karstologia Mémoires, 5: 280 p.
- BATSCHKE, H., BAUER, F., BEHRENS, H., BUCHTELA, K., DOMBROWSKI, H. J., GEISLER, R., GEYH, M. A., HÖTZL, H., HRIBAR, F., KÄSS, W., MAIRHOFER, J., MAURIN, V., MOSER, H., NEUMAIER, F., SCHMITZ, J., SCHNITZER, W. A., SCHREINER, A., VOGG, H. & ZÖTL, J. (1970): Kombinierte Karstwasseruntersuchungen im Gebiet der Donauversickerung (Baden-Württemberg) in den Jahren 1967-1969. – Steir. Beitr. z. Hydrogeol., 22: 1-165; Graz.
- BÄTZING, W. (1997): Kleines Alpen-Lexikon - Umwelt, Wirtschaft, Kultur: 320 p.; München (Beck).
- BAUER, F. (1989): Die unterirdischen Abflußverhältnisse im Dachsteingebiet und ihre Bedeutung für den Karstwasserschutz. – Report, UBA-89-028: 73 p.; Umweltbundesamt Wien.
- BEHRENS, H. (1982): Verfahren zum qualitativen und quantitativen Nachweis von nebeneinander vorliegenden Fluoreszenztracern. – Beitr. z. Geologie der Schweiz, 28: 39-50; Bern.
- BEHRENS, H., BENISCHKE, R., BRICELJ, M., HARUM, T., KÄSS, W., KOSI, G., LEDITZKY, H.P., LEIBUNDGUT, CH., MALOSZEWSKI, P., MAURIN, V., RAJNER, V., RANK, D., REICHER, B., STADLER, H., STICHLER, W., TRIMBORN, P., ZOJER, H. & ZUPAN, M. (1992): Investigations with Natural and Artificial Tracers in the Karst Aquifer of the Lurbach System (Peggau-Tanneben-Semirach, Austria). – Steir. Beitr. z. Hydrogeologie, 43: 9-158; Graz.
- BGBL (BUNDESGESETZBLATT) (1998): Verordnung des Bundesministeriums für Frauenangelegenheiten und Verbraucherschutz über die Qualität von Wasser für den menschlichen Gebrauch. N. 235; Vienna (Österr. Staatsdruckerei).
- BÖGLI, A. (1978): Karsthydrographie und physische Speläologie. – 292 p.; Berlin, Heidelberg, New York (Springer).
- BÖGLI, A. & HARUM, T. [eds.] (1981): Hydrogeologische Untersuchungen im Karst des hinteren Muotatales (Schweiz). – Steir. Beitr. Hydrogeol., 33: 125-264; Graz.
- BOLLINGER, D. (1988): Die Entwicklung des distalen Osthelvetischen Schelfs im Barremian und Früh-Aptian (Drusberg-, Mittagsspitzen- und Schratzenkalk-Fm.). – Mitteilungen aus dem geologischen Institut der Eidg. Technischen Hochschule der Universität Zürich, Neue Folge, 259a: 136 p.; Zürich.
- BORSATO, A., FRISA, S., CORRADINI, F., LONGINELLI, A., ARTIOLI, G., CASAGRANDE, S., DELL'EVA, I., SANTULIANA, E., GIALANELLA, S., SELMO, E., ANGELLI, P., LUTTEROTTI, L., LAURO, C. & AVANZINI, M. (2000): Acquiferi carsici in Trentino:

14 References

- caratteristiche chimicofisiche, vulnerabilità e inquinamento. Rapporto Interno Provincia Autonoma di Trento, Dipartimento dell'Ambiente: 280 p.
- BRECHENMACHER, J. (2002): Vulnerability mapping in the karst system Sierra de Libar, Andalusia. – Master thesis Univ. Karlsruhe; Karlsruhe (in prep.).
- BROSEMER, M. (1999): Hydrogeologische Untersuchungen im Wettersteingebirge (Bayerische Alpen). – Master thesis Univ. Karlsruhe: 83 p.; Karlsruhe (unpubl.).
- BROUYÈRE, S., JEANNIN, P.-Y., DASSARGUES, A., GOLDSCHIEDER, N., POPESCU, I.-C., SAUTER, M., VADILLO, I. & ZWAHLEN, F. (2001) Evaluation and validation of vulnerability concepts using a physically based approach. – 7th Conference on Limestone Hydrology and Fissured Media, Besançon 20–22 Sep. 2001, Sci. Tech. Envir., Mém. H. S., 13: 67-72.
- CIVITA, M. (1993): Ground water vulnerability maps: a review. – Proc. IX Symp. on Pesticide Chemistry *Degradation and Mobility of Xenobiotics*, Piacenza, Italy, 11-13 Oct. 1993: 587-631; Lucca (Biagini).
- CIVITA, M. & DE MAIO, M. (2000): Valutazione e cartografia automatica della vulnerabilità degli acquiferi all'inquinamento con il systema parametrico SINTACS R5. – 248 p; Bologna (Pitagora Editrice).
- COMMITTEE ON VALUING GROUND WATER (1997): Valuing Ground Water. Economic Concepts and Approaches: 123 p.; Washington D.C. (National Academic Press).
- COST 65 (1995): Hydrogeological aspects of groundwater protection in karstic areas, Final report (COST action 65). – European Commission, Directorate-General XII Science, Research and Development, Report EUR 16547 EN: 446 p.; Brüssel, Luxemburg.
- COST 620 (2001): Guidelines for Hazard Mapping and GIS Techniques. – Internal Report of COST Action 620, Working Group III: 8 p.; (unpublished).
- COVIELLO, M. T. (2001): 'Vulnerabilità' del Bacino di Alimentazione delle Sorgenti die Posta Fibreno (FR). – Master thesis, Università degli Studi di Roma, D.I.T.S.; Roma (unpubl.).
- COWARD, M. & DIETRICH, D. (1989): Alpine tectonics – an overview. – In: COWARD, M.P., DIETRICH, D. & PARK, R.G. (eds.), Alpine Tectonics, Geological Society Special Publication, 45, 1-29; Oxford (Blackwell).
- COXON, C. (1999): Agriculturally induced impacts. – In: DREW, D. & HÖTZL, H. [eds.] (1999): Karst Hydrogeology and Human Activities. Impacts, Consequences and Implications. – International Contributions to hydrogeology (IAH), 20: 37-80.; Rotterdam/Brookfield (Balkema).
- CRAMER, K. (1959): Die Geologie des Mahdtales und der Karst des Gottesackergebietes. – Master thesis TH Munich: 80p.; Munich (unpubl.).
- DALY, D., DASSARGUES, A., DREW, D., DUNNE, S., GOLDSCHIEDER, N., NEALE, S., POPESCU, I.C. & ZWAHLEN, F. (2002): Main concepts of the European Approach for (karst) groundwater vulnerability assessment and mapping. – Hydrogeology Journal (in press).
- DALY, D. & DREW, D. (1998): The Role of Karst and Karst Vulnerability in the Irish Groundwater Protection Scheme. – Vulnérabilité et protection des eaux karstiques, Workshop 18.-20. Mai 1998: 4 p.; Neuchâtel.
- DALY, D., DREW, D., GOLDSCHIEDER, N. & HÖTZL, H. (2000a): Suggested Outline of an European Approach to Mapping Groundwater Vulnerability, Recommendations to Working Group 1 of COST 620. Results of the Task Group Meeting „European Approach“, Karlsruhe, 1-3 June 2000: 6 p; Karlsruhe (unpubl.).
- DALY, D., GOLDSCHIEDER, N., KRALIK, M., SÖFNER, B., SUASTA, J. (2000b): Role of Protective Cover in Assessing and Mapping Groundwater Vulnerability, Recommendations to COST 620. – Results of the WG-Meeting „Protective Cover“, Hannover, 21-22 Jan. 2000: 7 p; Hannover (unpubl.).

- DEWEY, J. F., PITMAN, W.C. III, RYAN, W. B. F. & BONNIN, K. (1973): Plate tectonics and the evolution of the alpine system. – *Geol. Soc. Am. Bull.*, **84**: 3137-3180.
- DICKEL, T. (1993): Schutzfunktion der Grundwasserüberdeckung unter Berücksichtigung der punktuellen Gefährdung von infiltrierenden Oberflächengewässern, Testanwendung im geplanten Wasserschutzgebiet der Stadt Engen, der Gemeinde Mühlhausen-Ehingen und der Stadt Singen. – Master thesis Univ. Freiburg: 118 p.; Freiburg (unpubl.).
- DICKEL, T., SOKOL, G., WATZEL, R. & WEINZIERL, W. (1993a): GIS-gestützte Bewertung der Schutzfunktion der Grundwasserüberdeckung am Beispiel des Wasserschutzgebietes „Engen“, Landkreis Konstanz. – FAW Ulm und Geol. Landesamt Bad.-Württ., FAW-TR-93010; Ulm, Freiburg (unpubl.).
- DICKEL, T., WEINZIERL, W. & VILLINGER, E. (1993b): Karte der Gesamtschutzfunktion der Grundwasserüberdeckung des Karstaquifers im Malm im Bereich des geplanten Wasserschutzgebietes „Engen“ der Stadt Engen, der Gemeinde Mühlhausen-Ehingen und der Stadt Singen, Landkreis Konstanz, 1:10.000. – GLA Baden-Württemberg, Freiburg.
- DIN 38404 (1993): Physikalische und physikalisch-chemische Stoffkenngrößen (Gruppe C), Calcitsättigung eines Wassers. – DIN 38404 Teil 10.
- DOERFLIGER, N. & ZWAHLEN, F. (1998): Practical Guide, Groundwater Vulnerability Mapping in Karstic Regions (EPIK). – Swiss Agency for the Environment, Forests and Landscape (SAEFL): 56 p.; Bern.
- DOERFLIGER, N. (1996): Advances in Karst Groundwater Protection Strategy using Artificial Tracer Tests Analysis and Multiattribute Vulnerability Mapping (EPIK method). – Ph.D. thesis Univ. Neuchâtel: 308 p.; Neuchâtel.
- DREW, D., GOLDSCHIEDER, N. & PUECH, V. (1999): Epikarst and Groundwater Vulnerability, Recommendations to COST 620. – Results of the WG Meeting „Epikarst“, Neuchâtel, 8-11 Sept. 1999; Neuchâtel (unpubl.).
- DREW, D. & HÖTZL, H. (1999a): Conservation of karst terrains and karst waters: the future. – In: DREW, D. & HÖTZL, H. [eds.] (1999): Karst Hydrogeology and Human Activities. Impacts, Consequences and Implications. – International Contributions to hydrogeology (IAH), **20**: 275-280 p.; Rotterdam/Brookfield (Balkema).
- DREW, D. & HÖTZL, H. [eds.] (1999b): Karst Hydrogeology and Human Activities. Impacts, Consequences and Implications. – International Contributions to hydrogeology (IAH), **20**: 322 p.; Rotterdam/Brookfield (Balkema).
- DREW, D. & HÖTZL, H. (1999c): The management of karst environments. – In: DREW, D. & HÖTZL, H. [eds.] (1999): Karst Hydrogeology and Human Activities. Impacts, Consequences and Implications. – International Contributions to hydrogeology (IAH), **20**: 259-272 p.; Rotterdam/Brookfield (Balkema).
- DREYBRODT, W. (2000): Equilibrium Chemistry of Karst Waters in Limestone Terranes. – In: KLIMCHOUK, A., FORD, D.C., PALMER, A.N., DREYBRODT, W. (eds.): Speleogenesis, Evolution of Karst Aquifers: 126-135; Huntsville, Alabama, USA (National Speleological Society, Inc.).
- DVGW (1995): Richtlinien für Trinkwasserschutzgebiete, I. Teil: Schutzgebiete für Grundwasser. – Deutscher Verein des Gas- und Wasserfaches e.V., DVGW-Regelwerk, Arbeitsblatt W101: 23 p.; Eschborn.
- DYCK, S. & PESCHKE, G. (1995): Grundlagen der Hydrologie. – 536 p.; Berlin (Verlag für Bauwesen).
- ECKERT, M. (1902): Das Gottesackerplateau, ein Karrenfeld im Allgäu. Studien zur Lösung des Karrenproblems. – Wissenschaftl. Ergänzungshefte zur Zeitschr. d. D. u. Ö. Alpenvereins, **1(3)**; Innsbruck.

14 References

- EISBACHER, G.H. (1996): Einführung in die Tektonik, 2. Auflage: 374 p.; Stuttgart (Enke).
- ENDRES, C. (1997): Hydrogeologie des Parthachursprungs. – Master thesis LMU Munich: 54 p.; Munich (unpubl.).
- EUROPEAN WATER DIRECTIVE (2000): Directive 2000/60/EC of the European Parliament and of the Council of 23 October 2000 establishing a framework for Community action in the field of water policy.
- FAO-UNESCO (1974): Map of the World, Vol. 1, Legend. Paris.
- FERNÁNDEZ-GIBERT, E., CALAFORRA, J. M. & ROSSI, C. (2000): Speleogenesis in the Picos de Europa Massif, Northern Spain. – In: KLIMCHOUK, A. B., FORD, D. C., PALMER, A. N. & DREYBRODT, W. (eds.): Speleogenesis. Evolution of Karst Aquifers: 352-357; National Speleological Society.
- FÖLLMI, K.B., (1986): Die Garschella- und Seewer Kalk-Formation (Aptian-Santonian) im Vorarlberger Helvetikum und Ultrahelvetikum. - Mitteilungen aus dem geologischen Institut der Eidg. Technischen Hochschule und der Universität Zürich, Neue Folge, 262: 391 p.; Zürich.
- FÖLLMI, K. B. & OUWEHAND, P. J. (1987): Garschella-Formation und Götzis-Schichten (Aptian-Coniacian): Neue stratigraphische Daten aus dem Helvetikum der Ostschweiz und des Vorarlbergs. - *Eclogae geol. Helv.*, 80: 141-191; Basel.
- FORD, D. & WILLIAMS, D. W. (1989): Karst Geomorphology and Hydrology. – 601 p.; Boston (Unwin Hyman).
- FOSTER, S. S. D. (1987): Fundamental Concepts in Aquifer Vulnerability, Pollution Risk and Protection Strategy. – In: VAN DUJIEVENBODEN, W. & VAN WAEGENINGH, H. G. [eds.]: Vulnerability of Soil and Groundwater to Pollutants, TNO Committee on Hydrogeological Research, Proceedings and Information, 38: 69-86; The Hague.
- FRISCH, W. (1981): Plate motions in the Alpine region and their correlation to the opening of the Atlantic ocean. – *Geol. Rdsch.*, 70: 402-411.
- FUMY, R., MAMMEL, F., NIGGEMANN, S., ORTH, J.-P., ROSENDAHL, W., SCHAFROTH, J., VATER, K. & WOLF, A. (2000): Die Höhlen des Gottesacker-Hochiften-Gebietes. – In: Hochiften und Gottesacker, eine Karstlandschaft zwischen Bregenzer Wald und Allgäuer Alpen. Karst und Höhle, 2000/2001: 89-157; Munich.
- GLA (Bayerisches Geol. Landesamt) (1977): Bericht des Bayerischen Geologischen Landesamtes über den Markierungsversuch im Osterfelder-Gebiet bei Garmisch-Partenkirchen im August/September 1977 [WROBEL, J. P.]. – Report no. 318-IV/2a-1931: 7 p.; (unpubl.).
- GLA (Geol. Landesamt Baden-Württemberg) (1995): Symbolschlüssel Geologie (Teil 1) und Bodenkunde Baden-Württemberg. – Informationen (Geolog. Landesamt Baden-Württemberg), 5/95: 67 p.; Freiburg.
- GOGU, R. C. (2000): Advances in groundwater protection strategy using vulnerability mapping and hydrogeological GIS databases. – Ph.D. thesis University of Liège: 153 p.; Liège.
- GOGU, R. C. & DASSARGUES, A. (2000): Current trends and future challenges in groundwater vulnerability assessment using overlay and index methods. – *Environmental Geology*, 39(6): 549-559.
- GOLDSCHIEDER, N. (1997): Hydrogeologische Untersuchungen im alpinen Karstgebiet Gottesacker und Schwarzwassertal (Allgäu/Vorarlberg). – Master thesis Univ. Karlsruhe: 128p.; Karlsruhe (unpubl.)
- GOLDSCHIEDER, N. (1998a): Hydrogeologische Untersuchungen im alpinen Karstgebiet Gottesacker und Schwarzwassertal (Allgäu/Vorarlberg). – *Vorarlberger Naturschau*, 4: 247-294; Dornbirn.
- GOLDSCHIEDER, N. (1998b): Der Ladstattschacht – tracerhydrologische Untersuchung einer organischen Alltlast im alpinen Karst. – In: CZURDA, K., HÖTZL, H. & EIS-

- WIRTH, M. (eds.): Natürliche und anthropogene Umweltgefährdungen, Forschungsergebnisse aus dem Lehrstuhl für Angewandte Geologie, Schr. Angew. Geol. Karlsruhe, 50: 155-172; Karlsruhe.
- GOLDSCHIEDER, N. (1999): Critical remarks on the applicability of EPIK under special karst conditions. – 5th MC and WG meeting of COST 620, St. Veit/Glan, Austria, 22-24 Apr. 1999: 13 p.; (unpubl.).
- GOLDSCHIEDER, N. (2000): Von der Zerstörung einer Höhle und den Folgen fürs Karstwasser. – In: Hochiften und Gottesacker – eine Karstlandschaft zwischen Bregenzer Wald und Allgäuer Alpen. Karst und Höhle, 2000/2001: 51-82; München.
- GOLDSCHIEDER, N., BROSEMER, M., UMLAUF, N. & HÖTZL, H. (1999a): Karstentwässerung im Gebiet der Alpspitze (Wettersteingebirge, Bayerische Kalkhochalpen). – Laichinger Höhlenfreund, 34(2): 47-68; Laichingen.
- GOLDSCHIEDER, N. & HÖTZL, H. (1999): Hydrogeological characteristics of folded alpine karst systems exemplified by the Gottesacker Plateau (German-Austrian Alps). – Acta Carsologica, 28(1): 87-103; Ljubljana.
- GOLDSCHIEDER, N. & HÖTZL, H. (2000): Tektonik und Karstentwässerung. – In: Hochiften und Gottesacker - eine Karstlandschaft zwischen Bregenzer Wald und Allgäuer Alpen. Karst und Höhle, 2000/2001: 51-82; München.
- GOLDSCHIEDER, N., HÖTZL, H., FRIES, W. & JORDAN, P. (2001a): Validation of a vulnerability map (EPIK) with tracer tests. – 7th Conference on Limestone Hydrology and Fissured Media, Besançon 20–22 Sep. 2001, Sci. Tech. Envir., Mém. H. S., 13: 167-170.
- GOLDSCHIEDER, N., HÖTZL, H. & KÄSS, W. (2001b): Comparative Tracer Test in the Alpine Karst System Hochiften-Gottesacker, German-Austrian Alps – Beitr. z. Hydrogeologie, 52: 145-158; Graz.
- GOLDSCHIEDER, N., HÖTZL, H., KÄSS, W., KOTTKE, K. & UFRICHT, W. (2001c): Kombinierte Markierungsversuche im Stuttgarter Talkessel zur Klärung der hydrogeologischen Verhältnisse und zur Abschätzung des Gefährdungspotenzials im Mineralwasseraquifer Oberer Muschelkalk, Stadtgebiet Stuttgart. – Schriftenreihe des Amtes für Umweltschutz. Stuttgart, 1/2001: 5-80; Stuttgart.
- GOLDSCHIEDER, N., HÖTZL, H., NEUKUM, CH. & WERZ, H. (2001d): Tracer tests and vulnerability mapping (PI method) in the alpine karst system Winterstaude as the scientific basis of a drinking water protection strategy for the community of Bezau (Austria). – 7th Conference on Limestone Hydrology and Fissured Media, Besançon 20–22 Sep. 2001, Sci. Tech. Envir., Mém. H. S., 13: 171-174.
- GOLDSCHIEDER, N., KLUTE, M., STURM, S. & HÖTZL, H. (2000a): Kartierung der Grundwasserverschmutzungsempfindlichkeit eines ausgesuchten Karstgebietes bei Engen, Baden-Württemberg. – Final report: 83 p; Karlsruhe (unpubl.).
- GOLDSCHIEDER, N., KLUTE, M., STURM, S. & HÖTZL, H. (2000b): The PI method – a GIS-based approach to mapping groundwater vulnerability with special consideration of karst aquifers. – Z. angew. Geol., 46 (2000) 3: 157-166; Hannover.
- GOLDSCHIEDER, N., NEUKUM, C. & WERZ, H. (2001e): Hydrogeologie und Trinkwasserschutz im alpinen Karstsystem der Winterstaude (Marktgemeinde Bezau, Bregenzerwald). – Vorarlberger Naturschau; Dornbirn (in press).
- GOLDSCHIEDER, N., NIGGEMANN, S. & ROSENDAHL, W. (2000c): Überlegungen zur Speläogenese im Gebiet von Hochiften und Gottesacker. – In: Hochiften und Gottesacker - eine Karstlandschaft zwischen Bregenzer Wald und Allgäuer Alpen. Karst und Höhle, 2000/2001: 159-164; Munich.
- GOLDSCHIEDER, N., ORTH, J.-P., VATER, K. & HÖTZL, H. (1999b): Die Schwarzwasserhöhle – eine hydrogeologisch bedeutsame Estavelle im alpinen Karstgebiet

14 References

- Hochifen-Gottesacker (Kleinwalsertal, Vorarlberg, Österreich). – Laichinger Höhlenfreund, 34(2): 69-96; Laichingen.
- GÖPPERT, N. (2002): Karsterscheinungen und Hydrogeologie karbonatischer Konglomerate der subalpinen Molasse im Gebiet Nagelfluhkette-Lecknertal (Bayern/Vorarlberg). – Master thesis Univ. Karlsruhe (in prep.).
- GSI (1999): Groundwater Protection Schemes. – Department of the Environmental and Local Government, Environmental Protection Agency and Geological Survey of Ireland: 24 p.; Dublin.
- HÄCKEL, H. (1990): Meteorologie (3rd edition). – 402 p.; Stuttgart (Ulmer).
- HASENMAYER, J. (1972): Tauchabstiege in die Quelhöhle der Aach, Geol. Jb., C 2: 351-357; Hannover.
- HIRTLEITER, G. (1992): Spät- und postglaziale Gletscherschwankungen im Wettersteingebirge und seiner Umgebung. – Münchener Geographische Abhandlungen, B 15: 153 p.; Munich.
- HÖLTING, B., HAERTLE, T., HOHBERGER, K.-H., NACHTIGALL, K. H., VILLINGER, E., WEINZIERL, W. & WROBEL, J.-P. (1995): Konzept zur Ermittlung der Schutzfunktion der Grundwasserüberdeckung. – Geol. Jb., C 63: 5-24; Hannover.
- HOMEWOOD, P. & CARON, C. (1982): Flysch of the Western Alps. – In: HSÜ, K. J. (ed.), Mountain Building Processes: 157-168; London (Acad. Press).
- HÖPFNER, B. (1970): Stratigraphie und Faziesverteilung der südhelvetischen Kreide-Tertiär-Grenzschichten des mittleren Allgäu und ein Vergleich nach Osten und Westen. – Ph.D. thesis Univ. Munich: 139 p.; Munich.
- HÖTZL, H. (1971): Zur Hydrogeologie des Einzugsgebietes der Donau oberhalb von Sigmaringen. – Habil. Univ. Karlsruhe: 294 p.; Karlsruhe.
- HÖTZL, H. (1973): Die Hydrogeologie und Hydrochemie des Einzugsgebietes der oberen Donau. – Steir. Beitr. z. Hydrogeol., 25: 5-102; Graz.
- HÖTZL, H. (1992): Karstgrundwasser. – In: KÄSS, W. (1992): Geohydrologische Markierungstechnik, Lehrb. d. Hydrogeol., 9: 374-406.; Berlin, Stuttgart (Gebrüder Bornträger).
- HÖTZL, H. (1996): Grundwasserschutz in Karstgebieten. – Grundwasser, 1/1: 5-11.
- HÖTZL, H., ADAMS, B., ALDWELL, R., DALY, D., HERLICKSKA, H., HUMER, G., DE KETELARE, D., SILVA, M.L., SINDLER, M. & TRIPET, J.P. (1995): Regulations. – In: COST 65 (1995): Hydrogeological aspects of groundwater protection in karstic areas, Final report (COST action 65). European Commission, Directorate-General XII Science, Research and Development, Report EUR 16547 EN: 403-434; Brüssel, Luxemburg.
- HUTH, J. (1998): Geologisch-tektonische Kartierung und hydrochemische Untersuchungen im nordwestlichen Gottesackergebiet (Vorarlberg/Bayern). – Master thesis Univ. Karlsruhe: 105 p.; Karlsruhe (unpubl.).
- JEANNIN, P.-Y., CORNATON, F., ZWAHLEN, F. & PERROCHET, P. (2001): VULK: a tool for intrinsic vulnerability assessment and validation. – 7th Conference on Limestone Hydrology and Fissured Media, Besançon 20–22 Sep. 2001, Sci. Tech. Envir., Mém. H. S., 13: 185-190.
- JERZ, H. (1966): Untersuchungen über Stoffbestand, Bildungsbedingungen und Paläogeographie der Raibler Schichten zwischen Lech und Inn (Nördliche Kalkalpen). – Geol. Bav., 56: 3–102; Munich.
- KÄSS, W. (1969): Schrifttum zur Versickerung der oberen Donau zwischen Immendingen und Friedingen (Südwestdeutschland), Steir. Beitr. z. Hydrogeol.: 215-246; Graz.
- KÄSS, W. & HÖTZL, H. (1973): Weitere Untersuchungen im Raum Donauversickerung-Aachquelle (Baden-Württemberg), Steir. Beitr. z. Hydrogeol., 25: 103-116; Graz.

- KÄSS, W. (1992): Geohydrologische Markierungstechnik. – In: MATTHESS, G. [eds.], Lehrbuch der Hydrogeologie, 9: 520 p.; Stuttgart (Borntraeger).
- KLIMCHOUK, A. (1997): The nature and principal characteristics of epikarst. Proceedings of the 12th Internat. Congr. of Speleol., vol.1, La Chaux-de-Fonds, Switzerland, 10–17.08.1997.
- KLUTE, M. (2000.): GIS-gestützte Anwendung und Entwicklung von Methoden zur Vulnerabilitätskartierung unter besonderer Berücksichtigung der Infiltrationsbedingungen am Beispiel eines Karstgebietes bei Engen (Hegau, Baden-Württemberg). – Master thesis Univ. Karlsruhe: 130 p; Karlsruhe (unpubl.).
- KÖSEL, M. & WEINZIERL, W. (1993): Bodenübersichtskarte 1:25.000 (Geplantes Wasserschutzgebiet der Stadt Engen, der Gemeinde Mühlhausen-Ehingen und der Stadt Singen, Landkreis Konstanz).- mit tabellarischen Erläuterungen (Az.: 1353.01 / 93 - 4765) (unpubl.), Freiburg.
- KRALIK, M. (2001): Strategie zum Schutz der Karstwassergebiete in Österreich. – Umweltbundesamt GmbH, BE-189: 99 p.; Vienna.
- KRIEG, W. (ed.) (1988): Karst und Höhlen in Vorarlberg. – Karst- und Höhlenkundlicher Ausschuß des Vorarlberger Landesmuseumsvereins: 84 p.; Dornbirn.
- KUNOTH, K. (2000): GIS-gestützte Vulnerabilitätskartierung als Beitrag zur Entwicklung der Europäischen Methode unter besonderer Berücksichtigung der Schutzfunktion der Grundwasserüberdeckung am Beispiel des alpinen Karstgebietes Gottesacker-Hochfifen (Vorarlberg, Bayern). – Master thesis Univ. Karlsruhe: 94 p.; Karlsruhe (unpubl.).
- KUSCER, I. & KUSCER, D. (1964): Observations on brackish karst sources and sea swallow-holes on the jugoslav coast. – Int. Assoc. Hydrogeol. Mem., 5: 344–353; Athen.
- LAUBSCHER, H.P. (1989): The tectonics of the southern Alps and the Austro-Alpine nappes: a comparison. – In: COWARD, M.P., DIETRICH, D. & PARK, R.G. (eds.), Alpine Tectonics, Geological Society Special Publication, 45: 1-29; Oxford (Blackwell).
- LEHNHARDT, F. (1985): Einfluß morho-pedologischer Eigenschaften auf Infiltration von Waldstandorten. – In: DVWK-Schriften, 71: 231-260; Bonn (Parey).
- LEIBUNDGUT, CH. (ed.) (1995): Zur Hydrologie des Alpsteins Hydrologische Untersuchungen im Karstgebiet des Alpsteins Kanton Appenzell (Hrsg.). – Innerrhoder Schriften; Appenzell (CH).
- LEIBUNDGUT, CH. (1998): Vulnerability of karst aquifers (keynote paper) IAHS Publ., 247: 45-60.
- LGRB (1999): Schutzfunktion der Grundwasserüberdeckung am Beispiel des Wasserschutzgebietes Engen, Baden-Württemberg, nach der GLA-Methode. – GIS data on CD-ROM (unpubl.).
- LINZER, H.-G. (1989): Ausgeglichenes Profil und Kinematik der zentralen Lechtal- und Inntaldecke, Tirol. - Ph.D. thesis Univ. Karlsruhe: 119 p.; Karlsruhe.
- MAGIERA, P. (2000): Methoden zur Abschätzung der Verschmutzungsempfindlichkeit des Grundwassers. – Grundwasser 3/2000: 103-114.
- MALIK, P. & SVASTA, J. (1999): REKS - an alternative method of karst groundwater vulnerability estimation. – Geological Survey of Slovak Republik; Bratislava (unpubl.).
- MALOSZEWSKI, P. (1994): Mathematical modelling of tracer experiments in fissured rocks with porous matrix. – J. Hydrol., 79: 333-358.
- MALOSZEWSKI, P., BENISCHKE, R. & HARUM, T. (1992): Mathematical modelling of tracer experiments in the karst of Lurbach-System. – Steir. Beitr. Z Hydrogeologie, 43: 116-136; Graz.

14 References

- MARGAT, J. (1968): Vulnérabilité des nappes d'eau souterraine à la pollution. – BRGM-Publication 68 SGL 198 HYD; Orléans.
- MATTHEß, G. (1994): Die Beschaffenheit des Grundwassers (3rd edition). – Lehrbuch der Hydrogeologie, 2: 499 p.; Berlin, Stuttgart (Bornträger).
- MATTHEß, G. & UBELL, K. (1983): Allgemeine Hydrogeologie-Grundwasserhaushalt. – Lehrbuch der Hydrogeologie, 1: 438 p.; Berlin, Stuttgart (Bornträger).
- MAURIN, V. & ZÖTL, J. (1959): Die Untersuchung der Zusammenhänge unterirdischer Wässer mit besonderer Berücksichtigung der Karstverhältnisse: Großversuche im nordostalpinen Karst (Hochschneeberg, Niederösterreich). – Steir. Beitr. z. Hydrogeol., 1/2: 50-55; Graz.
- MERZ, B. (1996): Modellierung des Niederschlags-Abfluß-Vorgangs in kleinen Einzugsgebieten unter Berücksichtigung der natürlichen Variabilität. – Ph.D. thesis, Mitt. des Instituts für Hydrologie und Wasserwirtschaft (IHW), 56: 215 p.; Karlsruhe.
- MILLER, H. (1962): Zur Geologie des westlichen Wetterstein- und Mieminger Gebirges (Tirol). – Ph.D. thesis LMU Munich: 118 p.; Munich.
- MUGUERZA, I. (2001): Estudio hidrogeológico de la Unidad Hidrogeológico Kárstica de Albiztur (Gipuzkoa). (Establecimiento de una metodología para la evaluación y cartografía de la vulnerabilidad intrínseca en acuíferos kársticos). – Ph.D. thesis, University of Basque Country; Bilbao.
- MÜLLER, I. & ZÖTL, J. G. (eds.) (1980): Karsthydrologische Untersuchungen mit natürlichen und künstlichen Tracern im Neuenburger Jura (Schweiz). – Steir. Beitr. z. Hydrogeologie, 32: 5-100; Graz.
- NEUKUM, CH. (2001): Tektonik und Karstentwässerung im Gebirgsmassiv der Winterstaude (Marktgemeinde Bezau, Vorarlberg, Österreich). – Master thesis Univ. Karlsruhe: 104 p.; (unpubl.).
- OBERHAUSER, R. (1951): Zur Geologie des Gebietes zwischen Canisfluh und Hohem Ifen (Bregenzerwald). – Ph.D. thesis Univ. Innsbruck: 45 p.; Innsbruck.
- ORTH, J.P. (1984): Entwässerung synklinaler Karstkörper in den Bayerischen Alpen. – Akten 7. nat. Kongr. Höhlenforsch. Schwyz 1982 (Suppl. no.11 à „Stalactite“): 185-204; Genève.
- ORTH, J. P. (1992): Falten- und Schuppenstrukturen als Leitelemente der Karstentwässerung in den Bayerischen Alpen. – Laichinger Höhlenfreund, 27 (1): 23–39; Laichingen.
- PESCHKE, G.; ETZENBERG, C.; MÜLLER, G.; TÖPFER, J. & ZIMMERMANN, S. (1999): Das wissensbasierte Sytem FLAB, ein Instrument zur rechnergestützten Bestimmung von Landschaftseinheiten gleicher Abflußbildung. – IHI-Schriften, 10: 122 p.; Zittau.
- PREY, S. (1978): Rekonstruktionsversuch der alpidischen Entwicklung der Ostalpen. – Mitt. österr. geol. Ges., 69: 1-25.
- RAO, P., HORNSBY, A. & JESSUP, R. (1985): Indices for ranking the potential for pesticide contamination of groundwater. – Proc. Soil Crop Sci. Soc. Florida, 44: 1-8.
- REIS, O. M. (1911): Erläuterungen zur Geologischen Karte des Wettersteingebirges. – Geogn. Jh., 23: 61-114; Munich.
- RICHTER, D. (1984): Allgäuer Alpen (3rd edition). – Slg. geol. Führer, 77: 253 p.; Berlin, Stuttgart (Borntraeger).
- RIEG, A. (1994): Zur Hydrologie im Karstgebiet Churfürsten–Alvier. – PhD thesis Institute of Hydrology, University of Freiburg: 213 p.; Freiburg.
- ROSENDAHL, W. (2000): Die Formen des Oberflächenkarstes (Exokarst) im Gebiet Hochifen-Gottesackerplateau (Kleinwalsertal). – In: Hochifen und Gottesacker - eine Karstlandschaft zwischen Bregenzer Wald und Allgäuer Alpen. Karst und Höhle 2000/2001: 83-88; Munich.

- ROSENDAHL, W. & GRUNER (1995): Karrenkunde und Karrenformen am Beispiel des Gottesackerplateaus. – Jahresheft der ArGe Höhle und Karst Grabenstetten: 62-69; Grabenstetten.
- ROSS J. H., RIEG A. & LEIBUNDGUT CH. (2001): Tracer study on the tectonic controll of the drainage system in the contact karst zone of lake Voralp (Swiss Alps). – *Acta carsologica* 30/2: 203-213; Ljubljana.
- SAUTER, M., HERCH, A., JUNGSTAND, P., SIEBERT, C. & KOCH, C. (2001): Kartierung der Grundwasserverschmutzungsempfindlichkeit im Muschelkalkaquifer am Beispiel des Einzugsgebietes der Mühltalquellen bei Jena, Thüringen. – Final report (unpubl.).
- SCHLOZ, W. (1994): Geohydrologische Kriterien bei der Ausweisung von Grundwasserschutzgebieten, dargelegt an Fallbeispielen für Festgesteins- und Karstgrundwasserleiter. – *DVGW-Schriftenreihe Wasser*, 84: 113-126.
- SCHMID, S.M., AEBLI, H.R., HELLER, F. & ZINGG, A. (1989): The role of the Periadriatic line in the tectonic evolution of the Alps. – In: COWARD, M.P., DIETRICH, D. & PARK, R.G. (eds.), *Alpine Tectonics*, Geological Society Special Publication, 45: 1-29; Oxford (Blackwell).
- SCHMIDT, F. (2001): Bewertung der Verletzlichkeit (Vulnerabilität) des Karstgrundwassers in der Veldensteiner Mulde (Nördliche Frankenalb) nach der PI-Methode. – Master thesis Univ. Karlsruhe: 105 p.; Karlsruhe.
- SCHMIDT-THOMÉ, P. (1960): Zur Geologie und Morphologie des Ifengebirgsstockes (Allgäu). Erläuterungen zur topographisch-morphologischen Kartenprobe VI 3: Alpiner Karst und Bergsturz. – *Erdkunde*, 14 (3): 181–195; Bonn.
- SCHOLZ, H. (1995): Bau und Werden der Allgäuer Landschaft (2nd edition): 305 p.; Stuttgart (Schweizerbart).
- SCHOLZ, H. & STROHMENGER, M. (1999): Dolinenartige Sackungsstrukturen in den Molassebergen des südwestbayerischen Alpenvorlandes. – *Jber. Mitt. oberrhein. geol. Ver.*, 81: 275-283; Stuttgart.
- SCHÖNENBERG, R. & NEUGEBAUER, J. (1997): Einführung in die Geologie Europas (7th edition): 385 p.; Rombach (Freiburg).
- SCHREINER, A. (1976): Hegau und westlicher Bodensee. – *Slg. geol. Führer*, 62: 93 p.; Berlin, Stuttgart (Borntraeger).
- SCHREINER, A. (1992): Erläuterungen zu Blatt Hegau und westlicher Bodensee. *Geol. Karte 1:50.000 Baden-Württemberg*: 290 p.; Freiburg, Stuttgart.
- SCHREINER, A. (1993): Erläuterungen zu Blatt 8119 Eigeltingen. *Geol. Karte 1:25.000 Baden-Württemberg*: 86 p.; Freiburg, Stuttgart.
- SCHREINER, A. (1997): Erläuterungen zu Blatt 8118 Engen. *Geol. Karte 1:25.000 Baden-Württemberg*: 184 p.; Freiburg.
- SCHREINER, A. & LUTERBACHER, H. (1999): Die Molasse zwischen Blumberg und Überlingen. – *Jber. Mitt. oberrhein. geol. Ver.*, 81: 171-180; Stuttgart.
- SCHWEIGERT, G. (1995): Neues zur Stratigraphie des Schwäbischen Jura. – *Laichinger Höhlenfreund*, 30(2): 49-60; Laichingen.
- SCHWERD, K (1996): Erläuterungen zur Geologischen Karte von Bayern 1:500.000. – *Bayerisches Geologisches Landesamt*: 329 p.; Munich.
- SEIJMONSBERGEN, A.C. & VAN WESTEN, C.J. (1987): Geomorphological-, geotechnical- and natural hazard maps of the 'Hintere Bregenzerwald' area (Vorarlberg, Austria). Part I: Text. – Report, Alpine Geomorphology Research Group, University of Amsterdam: 176 p.; Amsterdam (unpubl.).
- SINREICH, M. (1998): Hydrogeologische Untersuchungen im oberen Schwarzwassertal (Vorarlberg). Wechselwirkungen zwischen Bergsturzmasse, Karstgrundwas-

14 References

- serleiter und Flyschgebiet. – Master thesis Univ. Karlsruhe: 118 p.; Karlsruhe (unpubl.).
- SINREICH, M. (2000): Paläokarst am Gottesacker-Hochiften und seine Bedeutung für Paläogeographie und Karstentwässerung. – In: Hochiften und Gottesacker - eine Karstlandschaft zwischen Bregenzer Wald und Allgäuer Alpen. Karst und Höhle 2000/2001: 167-173; Munich.
- SINREICH, S., GOLDSCHIEDER, N. & HÖTZL, H. (2002): Hydrogeologie einer alpinen Bergsturzmasse (Schwarzwassertal, Vorarlberg). – Beitr. z. Hydrogeologie; Graz (in press).
- SMART, C. C. (1983): Hydrology of a glacierised alpine karst. – PhD Thesis McMaster University.
- SPÖCKER, R. G. (1950): Das obere Pegnitz-Gebiet, die geologischen und hydrogeologischen Voraussetzungen für eine Wassererschließung im fränkischen Karst. – Sonderbeilage zu den Mitteilungen der Deutschen Gesellschaft für Karstforschung: 205 p.; Nürnberg.
- SPÖCKER, R. G. (1961): Das Hölloch als geographisches Element. – In: SCHMIDT-THOMÉ, P. [Red.]: Das Hölloch bei Riezern im Kleinen Walsertal (Allgäu-Vorarlberg) – eine karstkundliche Monographie. – Wiss. Alpenvereinsh., 18: 33-53; Innsbruck (Wagner).
- STRATHOFF, M. (2000): GIS-gestützte Vulnerabilitätskartierung als Beitrag zur Entwicklung der Europäischen Methode unter besonderer Berücksichtigung der Abflusskonzentration im Alpen Karstgebiet Hoher Ifen-Gottesacker (Bayern / Vorarlberg). – Master thesis Univ. Karlsruhe: 83 p.; (unpubl.).
- STURM, S. (1999): GIS-gestützte Anwendung und Entwicklung von Methoden zur Vulnerabilitätskartierung am Beispiel eines Karstgebietes bei Engen (Hegau, Baden-Württemberg) unter besonderer Berücksichtigung der Schutzfunktion der Grundwasserüberdeckung. – Master thesis Univ. Karlsruhe: 97 p.; Karlsruhe.
- SWISS WATER PROTECTION ORDINANCE (1998): Water Protection Ordinance of October 28th, 1998 (814.201).
- SZENKLER, C. & BOCK, H. (1999): Quartärgeologie und Rohstoffgeologie im Singener Beckenkomplex - Westliches Rheingletschergebiet (Hegau, Landkreis Konstanz) (Exkursion K am 9. April 1999).- Jber. Mitt. oberrhein. geol. Ver., 81: 183-216; Stuttgart.
- TESO, R., POE, M., YOUNGLOVE, T. & MCCOOL, P. (1996): Use of logistic regression and GIS modelling to predict groundwater vulnerability to pesticides. – J. Environ. Qual., 25: 425-432.
- TOLLMANN, A. (1976 b): Der Bau der Nördlichen Kalkalpen, orogene Stellung und regionale Tektonik. – In: Monographie der Nördlichen Kalkalpen, Teil 3: 449 p.; Wien (Deuticke).
- TOMSU, C. (1998): Zur Hydrogeologie des Karstes zwischen Hochiften und Subersach, Hinterer Bregenzerwald, Vorarlberg. – Master thesis Univ. Karlsruhe: 90 p.; Karlsruhe (unpubl.).
- TOUSSAINT, B. (1971): Hydrogeologie und Karstgenese des Tennengebirges (Salzburger Kalkalpen). – Steir. Beitr. z. Hydrogeologie, 23: 5-115; Graz.
- TRIMMEL, H. [ed.] (1998): Die Karstlandschaften der österreichischen Alpen und der Schutz ihres Lebensraumes und ihrer natürlichen Ressourcen. – Fachausschuß Karst, CIPRA-Österreich: 119 p.; Vienna.
- TRÜMPY, R. (1985): Die Plattentektonik und die Entstehung der Alpen. – Veröff. Naturf. Ges. Zürich, 129: 5-47.
- UHLIG, H. (1954): Die Altformen des Wettersteingebirges mit Vergleichen in den Allgäuer und Lechtaler Alpen. – Forsch. dt. Landeskd., 79: 104 p.; Remagen (Bundesanst. Landeskd.).

- UMLAUF, N. (1999): Hydrogeologische und hydrochemische Untersuchungen im Alp-spitzgebiet (Wettersteingebirge). – Master thesis Univ. Karlsruhe: 106 p.; Karlsruhe (unpubl.).
- VACHÉ, R. (1960): Geologie und Lagerstätten des mittleren Wettersteingebirges zwi-schen Hammersbach und Partnach. – Diplomarbeit Univ. München: 68 S.; München (unpubl.).
- VAM STEMPVOORT, D., EWERT, L. & WASSENAAR, L. (1993): Aquifer vulnerability index: A GIS-compatible method for groundwater vulnerability mapping. – *Canad. Wa-ter Res. J.*, 18/1: 25-37.
- VIDAL, H. (1953): Neue Ergebnisse zur Stratigraphie und Tektonik des nordwestlichen Wettersteingebirges und seines nördlichen Vorlandes. – *Geologica Bavaria*, 17: 56-88; Munich.
- VIERHUFF, H., WAGNER, W. & AUST, H. (1981): Die Grundwasservorkommen in der Bundesrepublik Deutschland. – *Geol. Jb.*, C30: 3-110.
- VILLINGER, E. (1977): Über Potentialverteilung und Störungssysteme im Karstwasser der Schwäbischen Alb (Oberer Jura, SW-Deutschland), *Geol. Jb.* C18: 3-93; Han-nover.
- VOGELSANG, D. & VILLINGER, E. (1987): Elektromagnetische und hydrogeologische Erkundung des Donau-Aach-Karstsystems (Schwäbische Alb), *Geol. Jb.*, C49: 3-33, 8 Abb., 1 Tab., 3 Taf., Hannover.
- VON HOYER, M. & SÖFNER, B. (1998): Groundwater vulnerability mapping in carbonate (karst) areas of Germany. – BGR Hannover, Archive Nr. 117 854, unpubl. re-port for EC-project COST Action 620; 38 p.
- VRBA, J. & ZOPOROZEC, A. [eds.] (1994): Guidebook on Mapping Groundwater Vulner-ability. – *International Contributions to Hydrogeology (IAH)*, 16: 131 p.; Han-nover.
- WAGNER, G. (1950): Rund um Hochfien und Gottesackergebiet. Eine Einführung in die Erd- und Landschaftsgeschichte des Gebietes zwischen Iller und Bregenzer Ach: 116 p.; Öhringen (Rau).
- WEINZIERL, W. (1993): Bodenkundliche und geologische Untersuchungen im geplanten Wasserschutzgebiet der Stadt Engen, der Gemeinde Mülhausen-Ehingen und der Stadt Singen. – unpubl. final report GLA Freiburg, Az 1353.01/91-4765 Wz/Gg: 19 p.
- WYSSLING, G. (1986): Der frühkretazische Schelf in Vorarlberg und im Allgäu – Stra-tigraphie, Sedimentologie und Paläogeographie. – *Jb. Geol. B.-Anst.*, 129 (1): 161-265; Vienna.
- WERNER, A. (1998): Hydraulische Charakterisierung von Karstsystemen mit künstlichen Tracern. – Ph.D. thesis Univ. Karlsruhe, *Schr. Angew. Geol. Karlsruhe*, 51: 169 p.; Karlsruhe.
- WERZ, H. 2001. Kartierung der Geologie, Hydrogeologie und Vulnerabilität im alpinen Karst als Grundlage eines Konzeptes zum Trinkwasserschutz für die Gemein-de Bezau (Bregenzer Wald, Österreich). – Master thesis Univ. Karlsruhe: 120 p.; Karlsruhe (unpubl.).
- WHG (1996): Gesetz zur Ordnung des Wasserhaushalts (Wasserhaushaltsgesetz). – BGI; Bonn.
- WHITE, W. B. (1969): Conceptual models for carbonate aquifers. – *Ground Water* 7(3): 15-21.
- WILHELMY, H. (1992): Geomorphologie in Stichworten – III Exogene Morphodynamik: 176 p.; Berlin, Stuttgart (Hirt).
- WINDLEY, B. F. (1995): *The evolving continents*. – 3rd edition: 526 p.; Wiley (Chichester).

14 References

- WROBEL, J. P. (1970): Hydrogeologische Untersuchungen im Einzugsgebiet der Loisach zwischen Garmisch-Partenkirchen und Eschenlohe/obb - Beitrag zur hydrogeologischen Dekade der UNESCO. – Inaugural-Diss.: 87 p.; Munich.
- YEANNIN, P.-Y., WILDBERGER, A. & ROSSI, P. (1995): Multitracing-Versuche 1992 und 1993 im Karstgebiet der Silberer (Muotatal und Klöntal, Zentralschweiz). – Beitr. z. Hydrogeologie, 46: 43-88; Graz.
- ZACHER, W. (1973): Das Helvetikum zwischen Rhein und Iller (Allgäu-Vorarlberg). Tektonische, paläogeographische und sedimentologische Untersuchungen. – Geotekt. Forsch., 44: 1-74; Stuttgart.
- ZACHER, W. (1985): Geologische Karte von Bayern 1:100 000, Blatt 670 Oberstdorf. – Bayerisches Geologisches Landesamt, Munich.
- ZOJER, H. (1999): Impacts from tourism. – In: Drew, D. & Hötzl, H. [eds.] (1999): Karst Hydrogeology and Human Activities. Impacts, Consequences and Implications. – International Contributions to hydrogeology (IAH), 20: 124-136 p.; Rotterdam/Brookfield (Balkema).
- ZÖTL, J. (1961): Die Hydrographie des nordalpinen Karstes. – Steir. Beitr. Hydrogeol., 1960/61: 163p.; Graz.
- ZÖTL, J. (1974): Karsthydrogeologie: 291 p.; Springer (Vienna).
- ZUIDEMA, P. K. (1985): Hydraulik der Abflußbildung während Starkniederschlägen. – Mitt. der Versuchsanstalt für Wasserbau, Hydrologie und Glaziologie, TH Zurich, 79: 150 p.; Zurich.

ANHANG: LEBENS LAUF

Persönliche Daten

Name: Andreas Nicola Goldscheider
Geburtsort und -datum: Karlsruhe, 22.10.1969
Staatsbürgerschaft: Deutsch
Eltern: Erika (Lehrerin, Hausfrau) und
Michael Goldscheider (Dr. Bauingenieur)



Schule, Zivildienst, Studium

1976-1980 Grundschule in Waldbronn.
1980–1989 Gymnasium Karlsbad; LK Mathe u. Physik; Abitur 1,3.
1989-1990 Zivildienst in einem Altenpflegeheim in Ettlingen.
1991-1997 Studium der Geoökologie (ab 1990) u. Geologie (ab 1991)
an der Uni Karlsruhe; gefördert von der Studienstiftung;
1993 Vordiplom in Geologie u. Geoökologie (sehr gut);
1994 Preis der Jubiläums-Staatsstiftung für Vordiplom.
Hauptdiplom: Hydrogeologie, Allgemeine/Regionale Geo-
logie, Geophysik, Geochemie, Landschaftsökologie, Bo-
denkunde/Mineralogie; Diplomarbeit bei Prof. Hötzl; Geo-
logie-Diplom *mit Auszeichnung bestanden*; 1998 Umwelt-
preis der Sparkasse Karlsruhe.

Beruflicher Werdegang und wissenschaftliche Tätigkeit

1997-2002 Wissenschaftlicher Mitarbeiter und Doktorand von Prof.
Hötzl am Lehrstuhl für Angewandte Geologie Karlsruhe.

Arbeitsgebiete: Regionale Hydrogeologie, alpiner Karst, Markierungs-
versuche, Grundwasserschutz, Vulnerabilitätskartierung (GIS).

Mitgliedschaft: International Association of Hydrogeology, Association
of Tracer Hydrology, Fachsektion Hydrogeologie der Deutschen Geol.
Ges.; *Permanent Expert* in der EU COST Action 620 *vulnerability and
risk mapping for the protection of carbonate (karst) aquifers*;

Projekte, Konferenzen u. wissenschaftliche Aufenthalte in Österreich,
Belgien, Frankreich, Großbritannien, Irland, Rumänien, Slowakei, Slo-
wenien, Spanien, Schweiz; 20 **Publikationen** (siehe *References*).